

UNCLASSIFIED

SECURITY CLASSIFICATION OF THIS PAGE (When Data Entered)

| REPORT DOCUMENTATION PAGE | | READ INSTRUCTIONS BEFORE COMPLETING FORM |
|---|-----------------------|--|
| 1. REPORT NUMBER NAVENVPREDRSCHFAC Technical Report TR 79-06 | 2. GOVT ACCESSION NO. | 3. RECIPIENT'S CATALOG NUMBER |
| 4. TITLE (and Subtitle) Winter Shamal in the Persian Gulf | | 5. TYPE OF REPORT & PERIOD COVERED Final |
| | | 6. PERFORMING ORG. REPORT NUMBER |
| 7. AUTHOR(s) Thomas J. Perrone | | 8. CONTRACT OR GRANT NUMBER(s) |
| 9. PERFORMING ORGANIZATION NAME AND ADDRESS Naval Environmental Prediction Research Facility, Monterey, CA 93940 | | 10. PROGRAM ELEMENT, PROJECT, TASK AREA & WORK UNIT NUMBERS PE 63207N PN 7W0513 TA CC00 NEPRF WU 6.3-11 |
| 11. CONTROLLING OFFICE NAME AND ADDRESS Naval Air Systems Command Department of the Navy Washington, DC 20361 | | 12. REPORT DATE August 1979 |
| | | 13. NUMBER OF PAGES 180 |
| 14. MONITORING AGENCY NAME & ADDRESS (if different from Controlling Office) | | 15. SECURITY CLASS. (of this report) UNCLASSIFIED |
| | | 15a. DECLASSIFICATION/DOWNGRADING SCHEDULE |
| 16. DISTRIBUTION STATEMENT (of this Report) Approved for public release; distribution unlimited. | | |
| 17. DISTRIBUTION STATEMENT (of the abstract entered in Block 20, if different from Report) | | |
| 18. SUPPLEMENTARY NOTES | | |
| 19. KEY WORDS (Continue on reverse side if necessary and identify by block number) Shamal Defense Meteorological Satellite Program (DMSP) Regional winds Jet streams Persian Gulf Kaus Wind climatology Satellite meteorology | | |
| 20. ABSTRACT (Continue on reverse side if necessary and identify by block number) Occurrence and air/sea effects of the winter shamal, a sub-synoptic-scale wind phenomenon in the Persian Gulf region, are examined by means of a conceptual model which relates upper air and surface features to mesoscale weather events and conditions. Two case studies based on surface data and satellite imagery are presented to illustrate the model. A regional wind climatology and a collection of rules of thumb for shamal forecasting are provided. | | |

AN (1) AD-A077 727
FG (2) 040200
FG (2) 080300
CI (3) (U)
CA (5) NAVAL ENVIRONMENTAL PREDICTION RESEARCH FACILITY
MONTEREY CA
TI (6) Winter Shamal in the Persian Gulf.
TC (8) (U)
DN (9) Final rept.,
AU (10) Perrone, Thomas J.
RD (11) Aug 1979
PG (12) 178p
R3 (14) NEPRF-TR-79-06
PJ (16) W0513
TN (17) W0513
RC (20) Unclassified report
DE (23) *Wind, *Air water interactions, Meteorological data,
Persian Gulf, Winter, Cold fronts, Climate, Jet
streams, Atmosphere models, Weather forecasting, Ocean
waves, Ocean surface, Upper atmosphere, Turbulence,
Storms, Sea states, Photographic images, Infrared
images, Visibility, Meteorological satellites,
Department of Defense
DC (24) (U)
ID (25) Mesometeorology, Shamal, WU6311, PE63207N
IC (26) (U)
AB (27) Occurrence and air/sea effects of the winter shamal, a
subsynoptic-scale wind phenomenon in the Persian Gulf
region, are examined by means of a conceptual model
which relates upper air and surface features to
mesoscale weather events and conditions. Two case
studies based on surface data and satellite imagery are
presented to illustrate the model. A regional wind
climatology and a collection of rules of thumb for
shamal forecasting are provided. (Author)
AC (28) (U)
DL (33) 01
SE (34) F
CC (35) 407279



NAVENVPREDRSCHFAC TR 79-06

LIBRARY
RESEARCH REPORTS DIVISION
NAVAL POSTGRADUATE SCHOOL
MONTEREY, CALIFORNIA 93940

NAVENVPREDRSCHFAC
TECHNICAL REPORT
TR 79-06

WINTER SHAMAL IN THE PERSIAN GULF

Thomas J. Perrone

Naval Environmental Prediction Research Facility

AUGUST 1979

APPROVED FOR PUBLIC RELEASE
DISTRIBUTION UNLIMITED



NAVAL ENVIRONMENTAL PREDICTION RESEARCH FACILITY
MONTEREY, CALIFORNIA 93940

QUALIFIED REQUESTORS MAY OBTAIN ADDITIONAL COPIES
FROM THE DEFENSE TECHNICAL INFORMATION CENTER.
ALL OTHERS SHOULD APPLY TO THE NATIONAL TECHNICAL
INFORMATION SERVICE.

Fig 2-1

CONTENTS

| | |
|--|-------|
| Preface | iii |
| Acknowledgments | iv |
| 1. INTRODUCTION | 1-1 |
| 1.1 General Description | 1-1 |
| 1.2 Report Organization | 1-1 |
| 1.3 Order of Presentation | 1-2 |
| 2. THE PERSIAN GULF REGION | 2-1 |
| 2.1 General Description | 2-1 |
| 2.2 Effect of Topography on Air Flow | 2-1 |
| 3. SHAMAL CHARACTERISTICS AND ASSOCIATED WEATHER PHENOMENA | 3-1 |
| 3.1 Typical Synoptic Sequences | 3-1 |
| 3.1.1 Shamal Lasting 3-5 Days. | 3-1 |
| 3.1.2 Shamal Lasting 24-36 Hours. | 3-5 |
| 3.2 Variations in Typical Synoptic Sequence. | 3-5 |
| 3.3 Onset | 3-6 |
| 3.3.1 Conditions Prior to Onset | 3-6 |
| 3.3.2 Onset in Different Parts of the Gulf | 3-8 |
| 3.3.3 Difficulties in Forecasting Onset | 3-11 |
| 3.4 Duration | 3-14 |
| 3.5 Significant Mesoscale Weather Phenomena. | 3-15 |
| 3.6 Surface Winds | 3-16 |
| 3.6.1 Areas of Stronger Than Normal Shamal Winds | 3-17 |
| 3.6.2 Diurnal Variations in Surface Winds. | 3-18 |
| 3.7 Seas/Swell | 3-18 |
| 3.7.1 Seas (Combined Sea Height). | 3-18 |
| 3.7.2 Residual Swell. | 3-20 |
| 3.8 Turbulence | 3-20 |
| 3.8.1 Low Level Turbulence. | 3-20 |
| 3.8.2 Upper Level Turbulence | 3-22 |
| References | Ref-1 |
| APPENDIX A - CASE STUDY 1 | |
| TYPICAL SYNOPTIC SEQUENCE OF THE 24-36 HOUR SHAMAL | A-1 |
| A.1 Step One | A-2 |
| A.2 Step Two | A-11 |
| A.3 Step Three. | A-15 |
| A.4 Step Four | A-35 |
| A.5 Step Five | A-50 |
| A.6 Summary. | A-64 |

CONTENTS (Continued)

APPENDIX B - CASE STUDY 2

| | |
|---|------|
| TYPICAL SYNOPTIC SEQUENCE OF THE 3-5 DAY SHAMAL | B-1 |
| B.1 Introduction | B-1 |
| B.2 15 January 1973 | B-3 |
| B.3 16 January 1973 | B-3 |
| B.4 17 January 1973 | B-24 |
| B.5 18 January 1973 | B-32 |
| B.6 19 January 1973 | B-41 |
| B.7 20 and 21 January 1973 | B-50 |
| B.8 Summary | B-59 |

APPENDIX C

| | |
|---|-----|
| WIND CLIMATOLOGY OF THE WINTER SHAMAL | C-1 |
|---|-----|

APPENDIX D

| | |
|--|------|
| FORECAST GUIDANCE | D-1 |
| D.1 Rule 1: Onset | D-1 |
| D.2 Rule 2: Onset Intensity (Nov-Feb) | D-5 |
| D.3 Rule 3: Duration (Nov-Feb). | D-6 |
| D.4 Rule 4: Cessation. | D-6 |
| D.5 Rule 5: Typical Sea Heights (Nov-Feb) | D-7 |
| D.6 Rule 6: Late-Season Special Cases | D-7 |
| D.7 Rule 7: Swell Decay | D-7 |
| D.8 Rule 8: Higher-Winds Special Cases | D-8 |
| D.9 Rule 9: Thunderstorms, Rainshowers | D-8 |
| D.10 Rule 10: Reduced Visibility in Blowing Dust | D-9 |
| D.11 Rule 11: Low Level Turbulence. | D-9 |
| D.12 Rule 12: Upper Level Turbulence | D-10 |

PREFACE

The Persian Gulf and surrounding land areas comprise a region of strategic importance in international affairs. Yet only in recent years have the region's general climate and specific weather phenomena been studied closely from a modern meteorological point of view.

This report^{*} examines the winter shamal, a subsynoptic scale wind phenomenon that occurs in the Persian Gulf region with sufficient effect and frequency to make it an operationally significant event.

The study uses a conceptual model to relate upper air and surface features to mesoscale weather events; variations in the model and associated weather conditions are addressed. Wind and sea-state patterns produced by the shamal are described; related conditions such as thunderstorms, reduced visibilities due to blowing sand dust, turbulence, and sea/swell are discussed.

Two detailed case studies are presented as appendices to illustrate the conceptual model. Both cases are based on actual surface data collected from a network of oil rigs and shore stations, plus visible and infrared satellite imagery from the Defense Meteorological Satellite Program (DMSP). Two additional appendices provide a regional wind climatology and a collection of rules of thumb for forecasting various stages of shamal occurrence.

This report is designed to meet several needs. Written primarily for the operational forecaster, it provides a conceptual framework for understanding and forecasting the shamal. The case studies demonstrate the usefulness of DMSP satellite imagery in the regional analysis/prediction process. For the military planner, the study provides an overview of some of the operationally significant weather and wind climatology in this part of the world. For atmospheric scientists, particularly mesoscale modelers, the study details a mesoscale-synoptic scale interaction that involves cyclogenesis; this information can be useful as input to models of the region's atmospheric processes.

*The author, research meteorologist Thomas J. Perrone, served for two years as a meteorologist/forecaster for commercial oil operations in the Persian Gulf region.

ACKNOWLEDGMENTS

The contributions of three organizations that supplied observational data for this study are gratefully acknowledged: the Oil Companies Weather Coordination Scheme, an association of companies operating in the Persian Gulf, and IMCOS Marine, Ltd., London, a private forecasting firm, which jointly provided detailed weather and sea-state observations from oil rigs and shore stations; and the Space Science and Engineering Center, University of Wisconsin, which provided satellite imagery from the Defense Meteorological Satellite Program.

Appreciation is expressed to the following individuals for their guidance and constructive comments during the development of the study: Mr. Robert Fett, Mr. Robin Brody, LCDR Martin Nestor, RN, and LCDR Ronald Englebretson of the Naval Environmental Prediction Research Facility; and Professors Russell Elsberry and Richard Anthes (visiting) of the Naval Postgraduate School at Monterey, California.

The services of the following NAVENVPREDRSCHFAC personnel in the production of this publication are appreciated: Stephen Bishop, editorial; Russell Chambers, meteorological laboratory; AG1 James Carlson, graphics; Dennis Daigle, photography; and Winona Carlisle and Susan Tilley, word processing. Figures were prepared by Publishers Art Service, Monterey, CA.

1. INTRODUCTION

1.1 GENERAL DESCRIPTION

"Shamal," an Arabic word meaning "north," is also the name given to seasonal northwesterly winds that occur during the winter and summer in the Persian Gulf region. The characteristics of the two seasons' shamals are markedly different, so any discussion of these phenomena must recognize their differences.

The winter shamal, which occurs chiefly from November through March, is associated with mid-latitude disturbances that progress from west to east. It occurs following cold frontal passages and is characterized by strong northwesterly winds -- most prominently in December, January, and February -- accompanied by such adverse weather conditions as thunderstorms, turbulence, low visibilities, and high seas.

Although the winter shamal is a relatively rare event -- winds at most Gulf locations exceed 20 kt less than 5% of the time during the season -- it can not be considered operationally insignificant. The winter shamal sets in with such abruptness and force, that its irregularly occurring gale strength winds stand out in bold relief against a background of more common, lighter wind conditions.

The summer shamal generally occurs with little interruption from early June through mid-July. Its occurrence, which is associated with the relative strengths of the Indian and Arabian thermal lows, is usually much less significant than that of the winter shamal in terms of wind strength and accompanying weather conditions.

Because of its greater potential for adverse operational effects, only the winter shamal is examined in this study. Unless otherwise specified, the term "shamal" hereafter is understood to mean the winter event.

1.2 REPORT ORGANIZATION

Shamals can be characterized as being of two general types, based on duration: those which last 24-36 hours, and those which last for a typically longer period of 3-5 days. The differences between these two duration-types are cited in text and illustrations where appropriate.

Section 2 of this report describes the geography and topography of the Gulf region in which the shamals occur.

Section 3 discusses eight aspects of shamal occurrence:

- (1) Typical synoptic sequences of both duration-types
- (2) Variations from these typical sequences
- (3) Conditions related to onset
- (4) Duration of occurrence
- (5) Significant mesoscale weather phenomena
- (6) Wind structure
- (7) Sea and swell structure under shamal conditions
- (8) Associated atmospheric turbulence

Four appendices follow the main text, providing two case studies, a wind climatology, and forecast guidance.

Appendix A, a detailed case study of a typical 24-36 hr shamal, illustrates the concepts developed in the main text by presenting a series of surface analyses, upper air charts, DMSP visible and infrared satellite imagery, and discussions in text. The wide scope of the data in this case study provides an in-depth, analytic view of shamal occurrence that might not otherwise be available to the field observer working under operational conditions.

Appendix B examines the longer 3-5 day shamal. The available data is less, however, providing a level of information that would more likely be generally available to the operational forecaster.

Appendices C and D present a wind climatology and a series of forecasting rules-of-thumb, respectively.

1.3 ORDER OF PRESENTATION

In Section 3.1, which describes typical synoptic sequences, the 3-5 day shamal is discussed first, and the 24-36 hr shamal, second. In the appendices, by contrast, case study 1 (Appendix A) is the 24-36 hr event and case study 2 (Appendix B) is the 3-5 day event.

The order of presentation in the main text was selected because, from the standpoint of meteorological dynamics, the 24-36 hr sequence of events is contained within the 3-5 day sequence. Thus it is logical to discuss the longer and more inclusive sequence first and contrast the shorter one with it.

A reversal of this order was indicated in the case studies, simply because there is more information available for the short-duration shamal than for the longer one, and because the 24-36 hr event occurs more frequently. It is anticipated that the more detailed data given in Appendix A will enable the user to better understand the related, though less detailed, discussions of conditions and events given in Appendix B.

2. THE PERSIAN GULF REGION

2.1 GENERAL DESCRIPTION

The shamal occurs in a region comprising low-lying central areas encircled by mountains. At low elevations are the Persian Gulf, its immediate shoreline, and the Tigris-Euphrates valley. The bordering mountain ranges are the Taurus family of mountains in southern Turkey, the Pontic Mountains in northeast Turkey, the Caucasus Mountains of Georgian Russia, the Zagros Mountains of Iran, and the Hajar and Hejaz Mountains of the Arabian Peninsula. Regional geography and topography are shown in Figure 2-1.

The highest peaks of the Taurus chain in Turkey rise to 9000 ft (2743 m). The general elevation in the Eastern Taurus and Pontic Mountains is 9000-12,000 ft (2743-3658 m). The ridge heights of the Caucasus chain are generally 9000-12,000 ft (2743-3658 m), but some peaks exceed 12,000 ft (3658 m). The Zagros Mountains of Iran have a general elevation of 6000-9000 ft (1829-2743 m); some isolated peaks in the central part of the country are higher. The Hajar and Hejaz Mountains of the Arabian Peninsula are somewhat lower than in Iran or Turkey, with a general elevation of 3000-6000 ft (914-1829 m); in the southwest Arabian Peninsula, isolated peaks rise to 6000-9000 ft (1829-2743 m).

2.2 EFFECT OF TOPOGRAPHY ON AIR FLOW

The incursion of cold air into the Persian Gulf region from the north precedes the more intense winter shamals. The mountains of Turkey, Georgia, and Iran provide an effective barrier to all but the most intense of these incursions. Cold air can also reach the region by means of a less direct route, however: via the Aegean Sea or over the less impenetrable mountain barrier of western Turkey, thence across the eastern Mediterranean Sea, then over or around the relatively low mountains (3000-6000 ft/914-1829 m) of Syria and Lebanon, and into the upper Tigris-Euphrates valley.

The configuration of the topography also affects air flows within the Persian Gulf. The basin-like contours of the region, with sharply rising mountains to the north and east and more gradual upsloping terrain to the west and southwest, tend to direct the low-level air flow in a general northwest-southeast orientation.

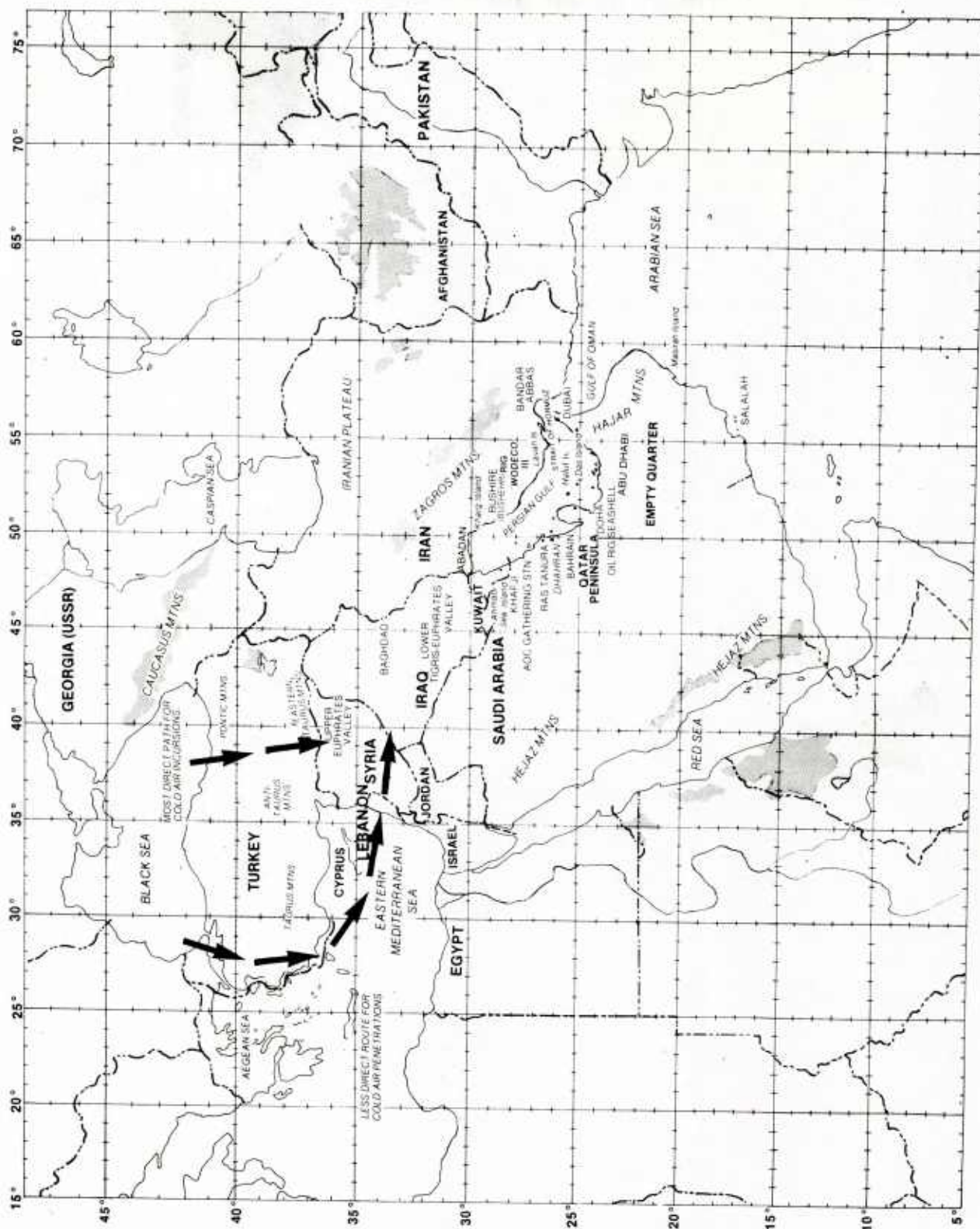


Figure 2-1. Locator map for the Persian Gulf region. Paths of cold air incursions into upper Euphrates valley are indicated by arrows.

3. SHAMAL CHARACTERISTICS AND ASSOCIATED WEATHER PHENOMENA

3.1 TYPICAL SYNOPTIC SEQUENCES

3.1.1 Shamal Lasting 3-5 Days

Figures 3-1a through 3-1f depict a typical synoptic sequence for the 3-5 day shamal.

a. Figure 3-1a. An upper trough is reflected in a surface low advected over Syria from the eastern Mediterranean area.

b. Figure 3-1b. The upper trough and associated surface low move eastward. A surface cold front extends south, then west, from the low. A second low moves eastward across Saudi Arabia from the Red Sea. The Kaus, a southeasterly wind, occurs in the Gulf.

c. Figure 3-1c. The upper trough moves eastward; a new low forms on the front in the general area as far north as the southern Tigris-Euphrates valley and as far south as the central Persian Gulf. The original low fills over northern Iraq or retains some surface identity as it is advected with the upper trough to the northeast toward the Caspian Sea. Subsidence in the lower troposphere induces a surface high pressure area over northern Saudi Arabia.

A strong but shallow northwesterly airstream sets in, west of the new surface low. This is the winter shamal which produces gale force winds, raises a short-period steep sea, sets off thunderstorms, and advects dust and sand over the Persian Gulf to sharply reduce visibilities.

d. Figure 3-1d. The surface low (formed in Fig. 3-1c) becomes fully developed. It is advected by, and ahead of, the upper trough to eastern Iran. The associated cold front has swept down the Gulf and into the Arabian Sea. Subsidence continues in the lower troposphere over northern Saudi Arabia to the west of the upper trough. The surface pressure over Saudi Arabia increases. The pressure gradient between the Saudi Arabian high and the lower pressure in the Gulf of Oman sustains the gale force shamal. The weather elements described in the preceding paragraph tend to continue. Thunderstorms may or may not occur after frontal passage, depending upon how soon after frontal passage wide area subsidence occurs. The sooner the subsidence occurs after frontal passage, the sooner thunderstorm activity is inhibited.

e. Figure 3-1e. The upper air trough "stalls" over the Strait of Hormuz (or moves through the southern Persian Gulf region very slowly) while the surface low moves away to the northeast. A second, terrain-induced low forms

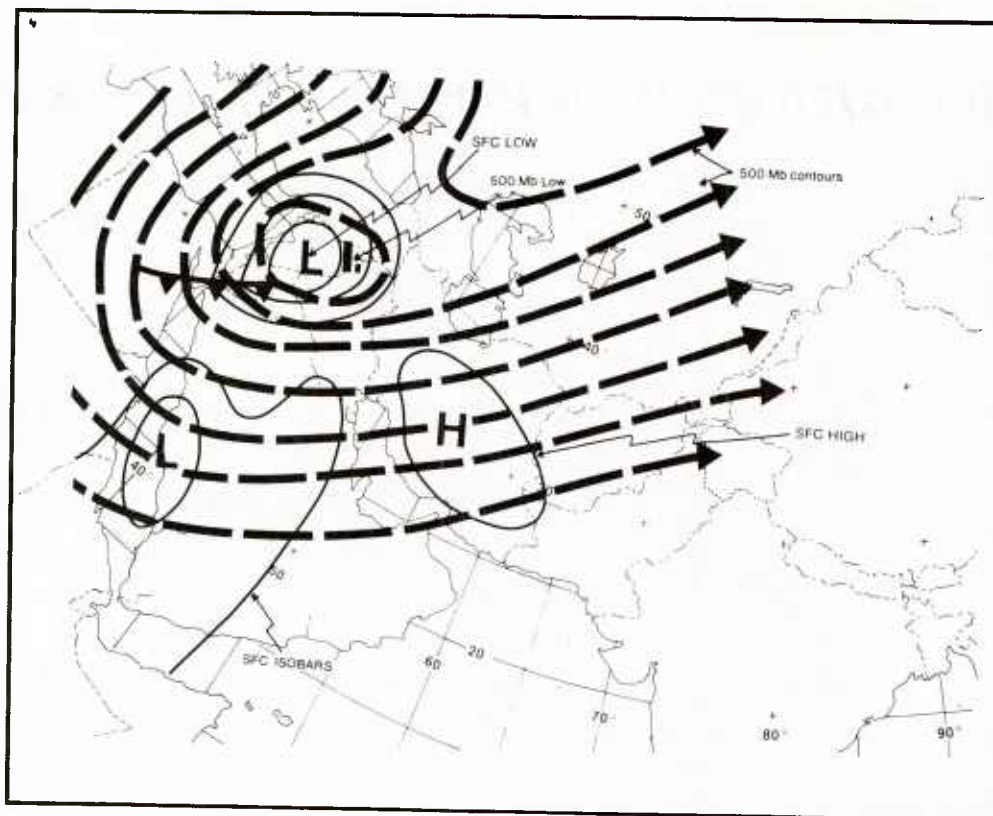


Figure 3-1a. Typical shamal synoptic sequence.

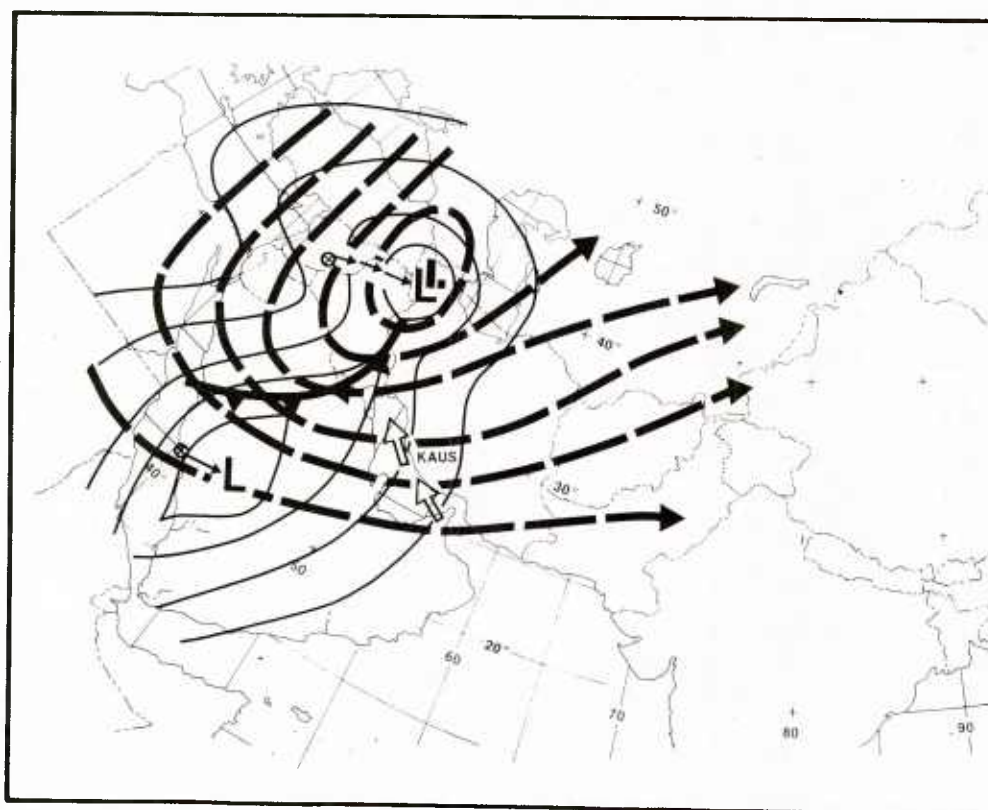


Figure 3-1b. Continued.

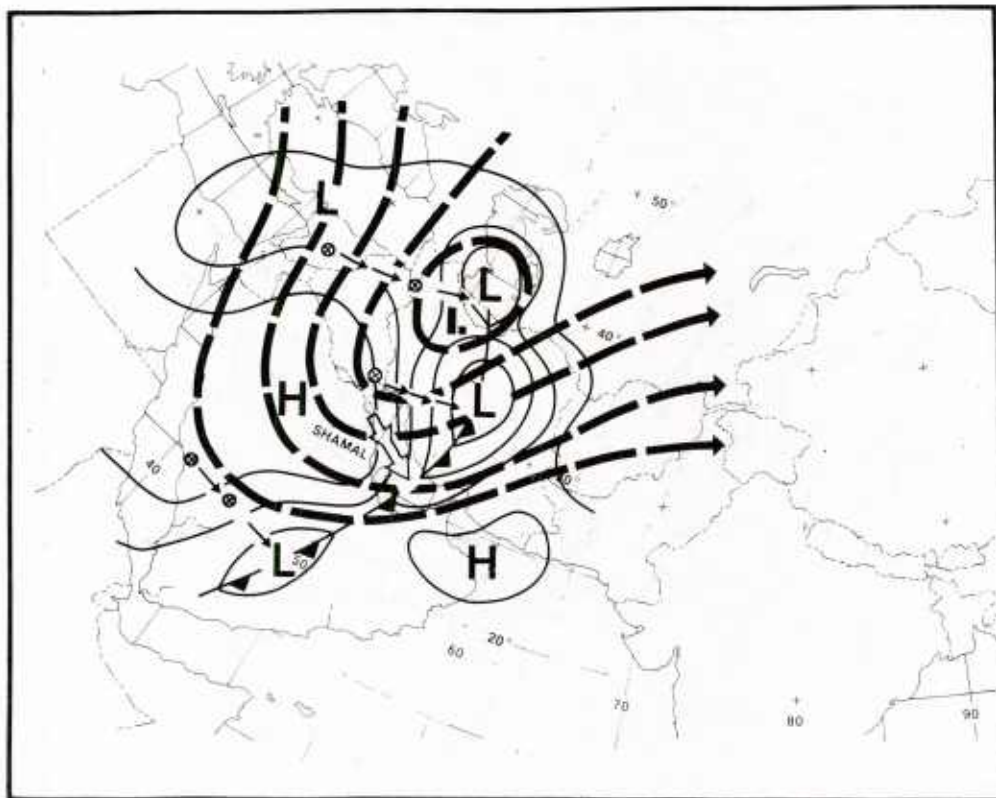


Figure 3-1c. Continued.

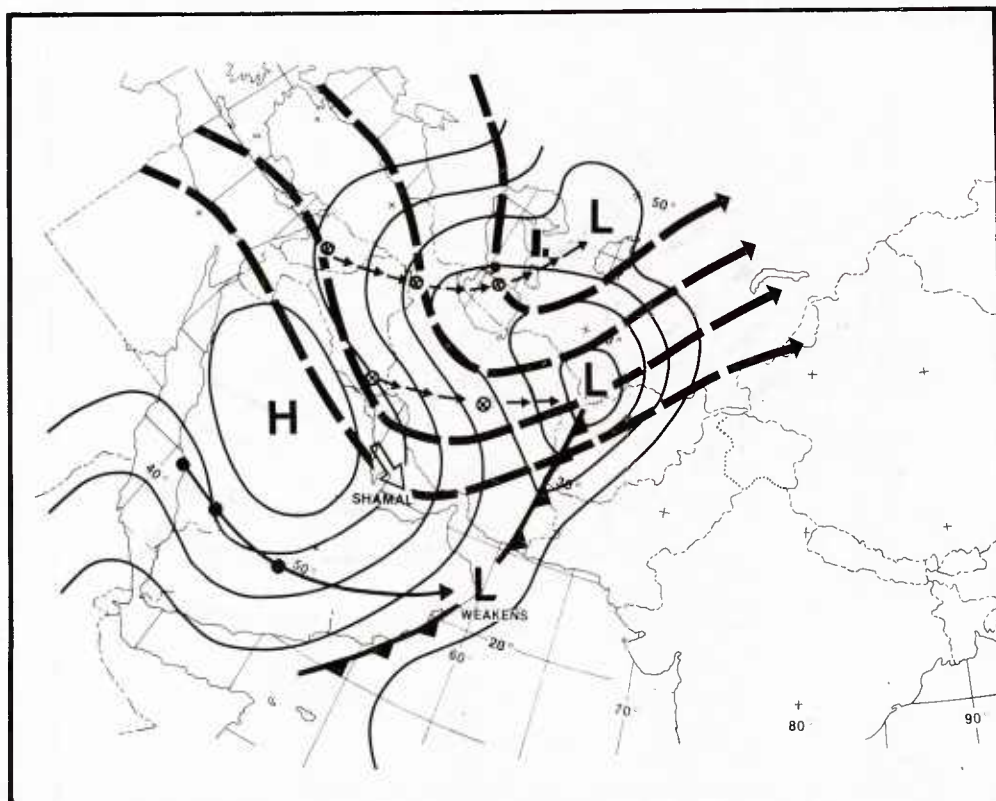


Figure 3-1d. Continued.

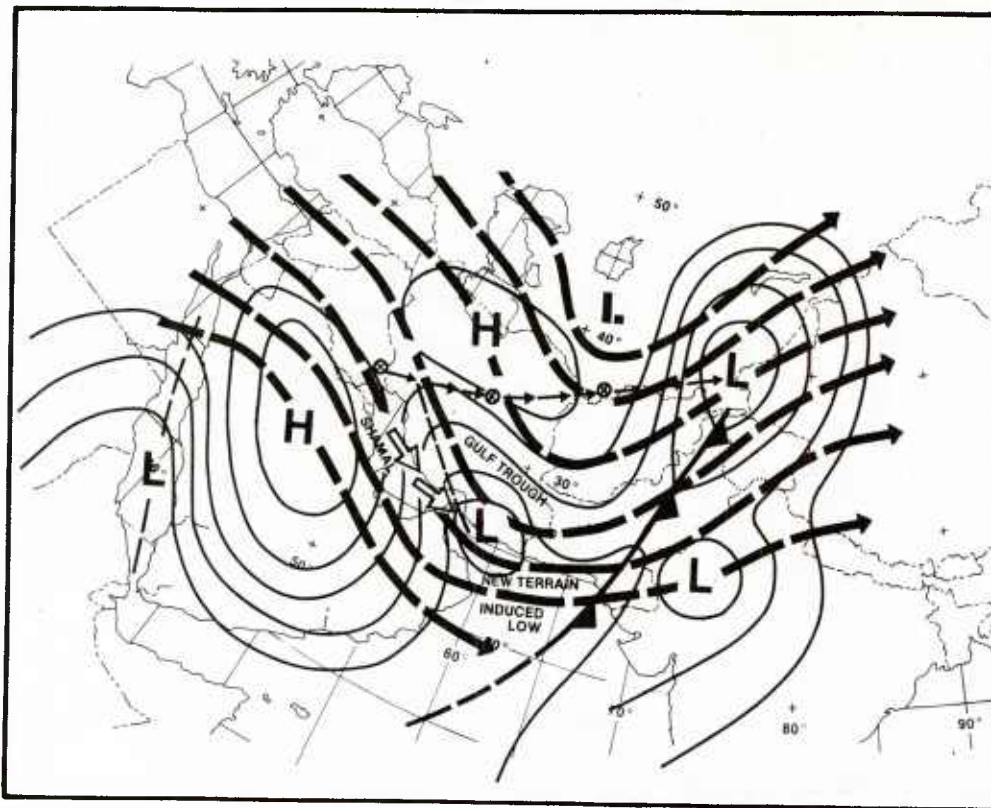


Figure 3-1e. Continued.

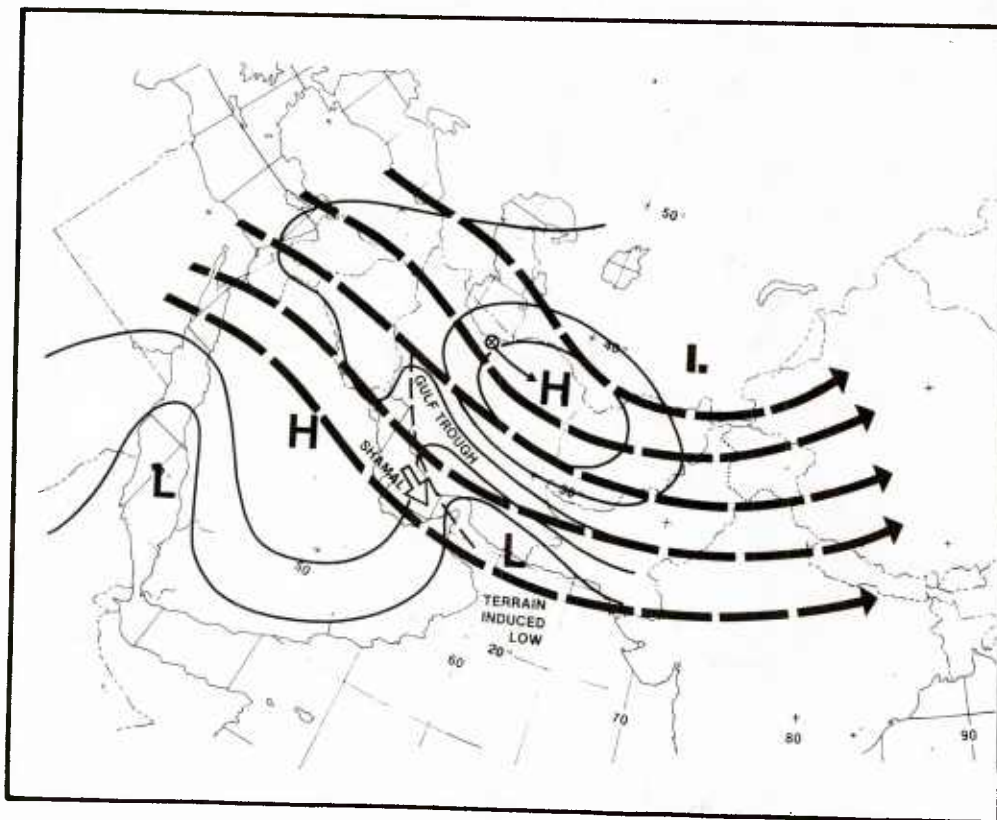


Figure 3-1f. Continued.

over the Gulf of Oman. Subsidence continues in the lower troposphere over Saudi Arabia. A second surface high pressure area forms over the Iranian plateau. The orientation of the Zagros Mountains induces a lee trough which extends from the terrain-induced low over the Gulf of Oman northwestward along the eastern shore of the Gulf. The shamal continues, as do most of the associated weather elements. At this stage, however, wide area subsidence has been established to the west of the trough, so that rain shower and thundershower activity generally is inhibited over the Gulf.

f. Figure 3-1f. The upper air trough eventually moves away to the east. Lower tropospheric subsidence is now stronger over the Iranian plateau than over the Saudi Arabian basin. The high cell over Saudi Arabia weakens and the lee trough begins to move westward across the Gulf.* The shamal weakens and is replaced on the eastern side of the Gulf by local sea breezes, weak southeasterlies, or a vector combination of both. Winds on the western side of the Gulf (lee) trough subside as the shamal "breaks."

Although the 3-5 day shamal is a relatively rare event, typically occurring only once or twice each winter, it brings some of the strongest winds and highest seas of the season to the Persian Gulf region. A case study of this type of shamal is presented in Appendix B.

3.1.2 Shamal Lasting 24-36 Hours

Shamal occurrences measured in hours are experienced more frequently than those measured in days. The synoptic sequence given in Para. 3.1.1 also applies reasonably well for the 24-36 hr event, with one important difference: during the shorter-duration shamal, the upper air trough does not stall in the vicinity of the Strait of Hormuz, but rather moves away quickly and smoothly to the east so that the stage represented by Figure 3-1e is omitted. A case study of this shorter-duration shamal is presented in Appendix A.

3.2 VARIATIONS IN THE TYPICAL SYNOPTIC SEQUENCE

The synoptic sequence depicted by Figures 3-1a through 3-1f is idealized, and it is important to realize that many variations can occur.

If the surface lows and their associated upper air troughs traverse west to east through, or just to the north of, the northern Gulf without sufficient

*The position of the lee trough varies: it responds to local changes in the Gulf region of the atmosphere's dynamic and thermal structure. The trough typically may be found as far west as the western shore of the Gulf and as far east as a position over the Iranian mainland, to the east of the eastern shore of the Gulf (as in Fig. 3-6). In this instance (Fig. 3-1f) the lee trough has begun to move westward in response to dynamic changes associated with differences in the relative strengths of the high pressure areas over the Arabian Peninsula and the Iranian plateau (compare Fig. 3-1e with 3-1f).

intensity to draw cold air southward to the rear of the surface low, only a brief period of gale force northwesterlies, confined to the northern Gulf, may result. This variation typifies the late fall, November to mid-December, as shown in Figure 3-1g.

These conditions can also occur as early as September (as documented by Feteris (1973)), but shamal conditions in the northern Gulf in early fall are rare.

In late winter/early spring (March/early April), the general upper air pattern tends to become less meridional. Before the westerlies retreat northward to be replaced by the easterly upper air regime of summer, the occurrences of brief but frequent periods of gale force northwesterlies seem to coincide better with the progression of shorter wave troughs through the westerlies, than with incursion of the longer wave troughs into the area depicted in the typical sequence.

Another variation involves penetration of cold air into the Persian Gulf where the associated cold front stalls in the middle or southern portions of the Gulf. With sufficient upper air support, a small, intense low may form on or near the stalled front. Gale force northwesterlies may result in the northern Gulf, with gale force northeasterlies, southwesterlies, and southeasterlies locally near the low in the southern Gulf (see Figure 3-1h).

3.3 ONSET

The onset of the shamal may occur at any hour, in association with the passage of cold fronts or the transit of mid-latitude lows through, or just to the north of, the Persian Gulf region.

3.3.1 Conditions Prior to Onset

Before the onset of the shamal, winds in the area ahead of the approaching cold front blow from the south to southeast. These southerly winds (called "Kaus" in Arabic or "Shakki" in Persian) slowly increase in intensity as the front approaches, and may reach gale force before the frontal passage.* The strongest southerly winds tend to occur on the eastern side of the Gulf, due to channeling of the lower level flow by the Zagros Mountains in western Iran (see Figure 3-2). Seas under southerly wind conditions rarely exceed 8-10 ft (2.5-3 m) (significant height - the average of the highest 1/3 of observed waves), due to the relatively short time the winds blow over the Gulf from a southerly direction. These southerly winds bring thick, gloomy weather, often with considerable rain.

*The Kaus may also occur without a cold frontal passage following, as when the surface low passes from west to east far to the north of the Gulf, or when the cold front dissipates before entering the Gulf.

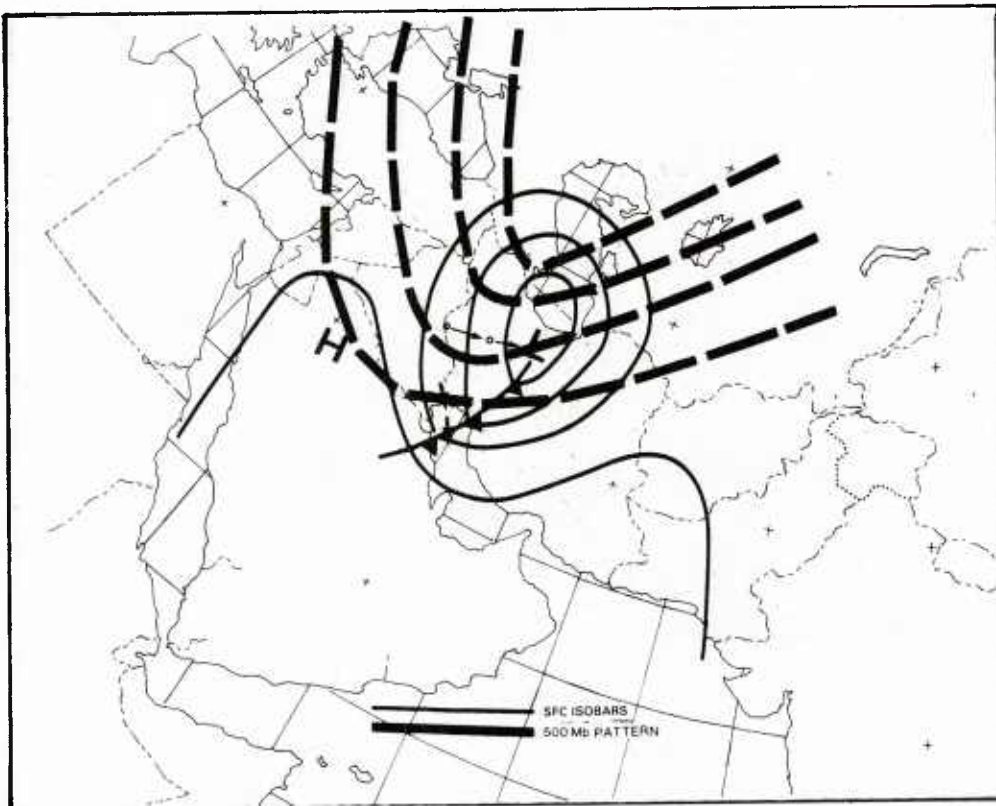


Figure 3-1g. Variations in typical synoptic sequence of the shamal in the northern Gulf.

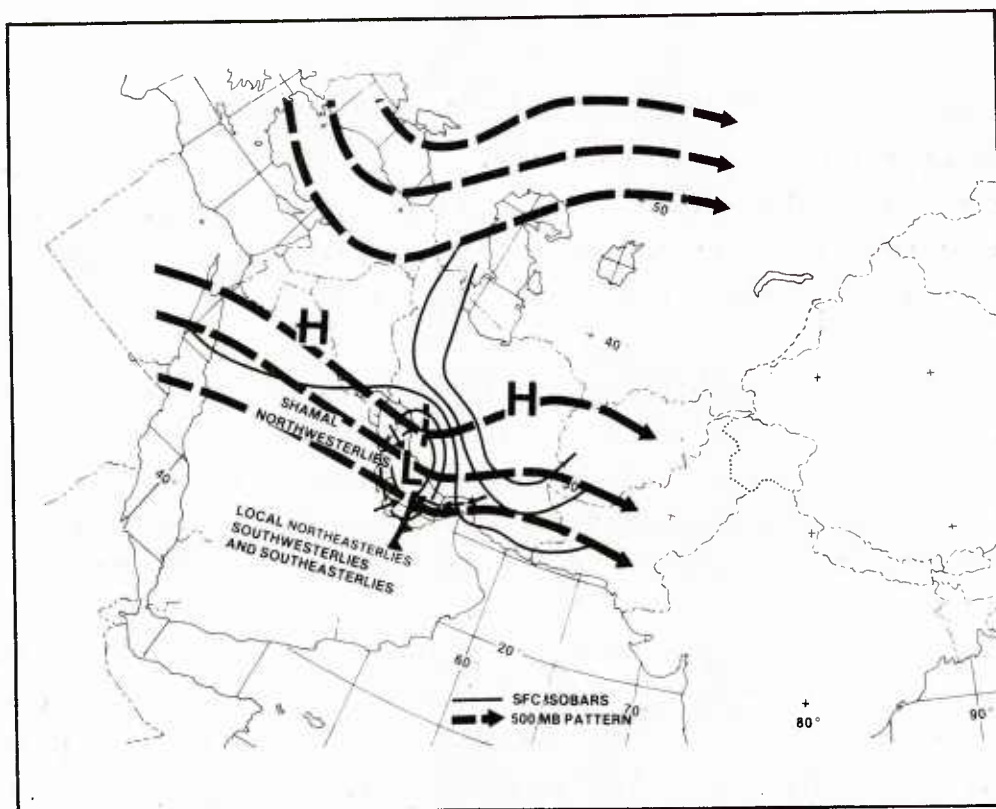


Figure 3-1h. Variations in typical synoptic sequence of the shamal in the northern Gulf, with local northwesterlies, southwesterlies, and southeasterlies in the southern Gulf.

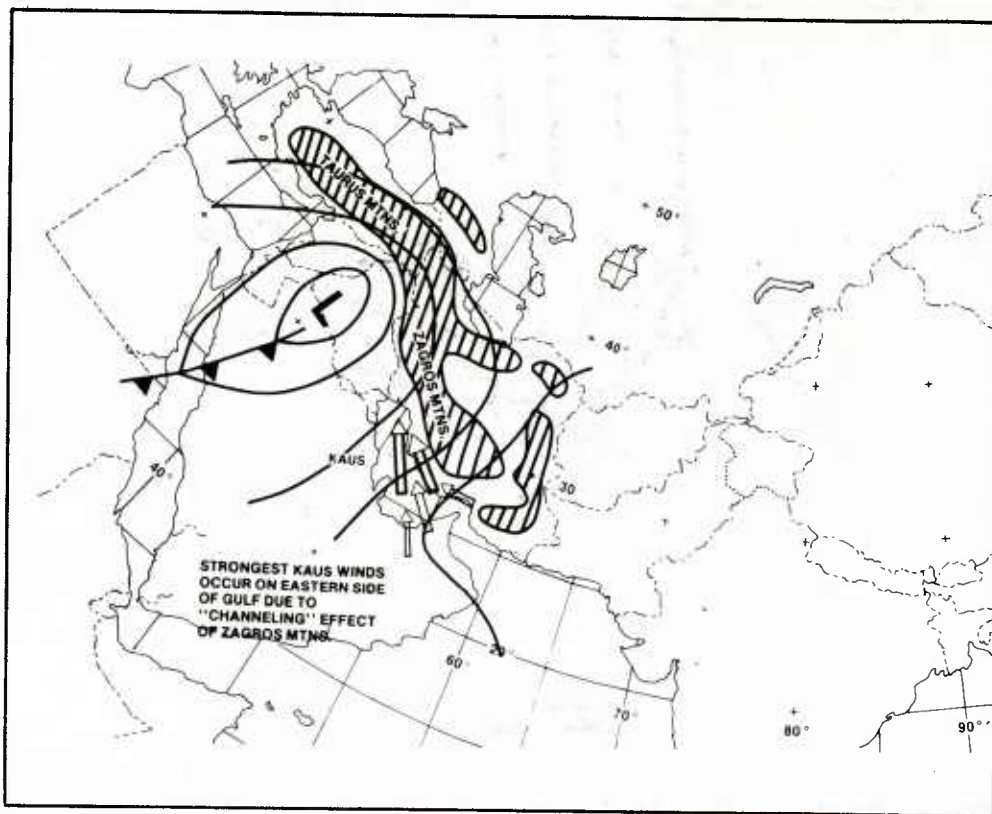


Figure 3-2. Channeling effect of Zagros Mountains on Kaus winds.

3.3.2 Onset in Different Parts of the Gulf

The shamal begins in the northwest corner of the Gulf and spreads south and east behind the advancing cold front. The interval between first onset in the northwest corner of the Gulf and onset in the southern Gulf is typically 12-24 hr. In the first case study, Appendix A, the interval is approximately 12 hr.

A vital key to properly predicting the onset of the shamal is an understanding of the surface/upper air relationships. The onset of the typical mid-winter shamal is associated with the advection of a cold, vigorous upper-air (500 mb) trough (with its associated energy) to the south and east of the Taurus Mountains of Turkey to a position over Syria and Iraq. A surface low typically forms in the area marked in Figure 3-3, just to the east of the upper trough, where positive vorticity advection is strongest. Other factors which favor cyclogenesis in this area include the presence of the relatively warm waters of the Gulf as a sensible heat source, and the vertical motion due to the mechanical lifting by the Zagros Mountains acting on low-level westerly or southwesterly air-flows. Once begun, upward motion is enhanced by the strong southwesterly airflow aloft over the Zagros Mountains, and by the release of latent heat of condensation from the uplifted and condensed warm Gulf surface air (Feteris, 1973).

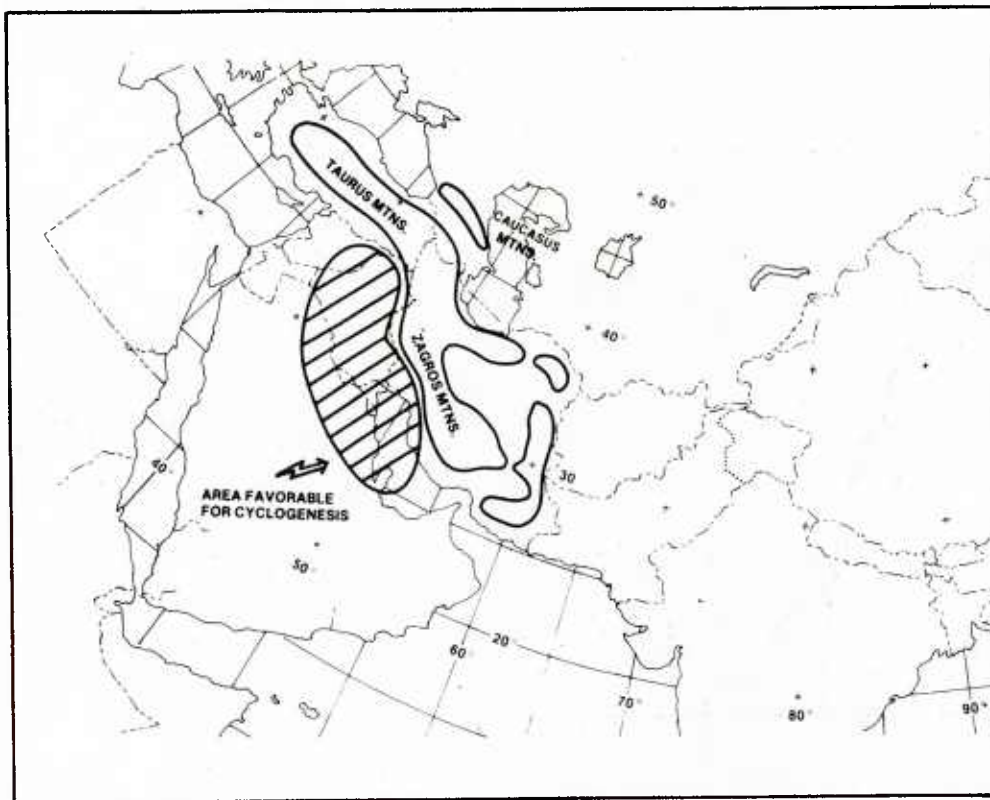


Figure 3-3. Area favorable for shamal-associated cyclogenesis.

Just before the shamal begins, a shallow, narrow tongue of relatively cold air over the upper Tigris-Euphrates valley advances southeastward down the lower part of this valley to underrun and lift the warmer, moist, resident Gulf air. The potential energy in the thermal contrast of the adjacent cold and warm surface air masses is converted to kinetic energy as the cold air lifts the warmer air. The energy conversion relationship forms the basis of a forecast technique -- suggested by Feteris (1973), based on a classic theory of Margules cited in Hess (1959) -- for predicting the initial velocity of the shamal as it enters the Gulf at its northwest corner. (An adaptation of this technique is given in Rule 2, Appendix D, Forecast Guidance.)

Also just before the shamal begins, the vertical structure of the atmosphere in the northern Gulf/lower Tigris-Euphrates valley typically is conditionally unstable (see Figure 3-4).

The DMSP satellite images of 24 January 1974, shown in Figures A-14 and A-15 in Appendix A, indicate a prefrontal line of thunderstorms over the Gulf and western Iran. This line is strikingly similar to ones associated with prefrontal severe weather in the U.S. midwest in spring, where such cloud lines can produce severe thunderstorms and spawn tornadoes. Thunderstorm activity occurs frequently in the northern part of the Persian Gulf region, but tornadic activity has not been observed.

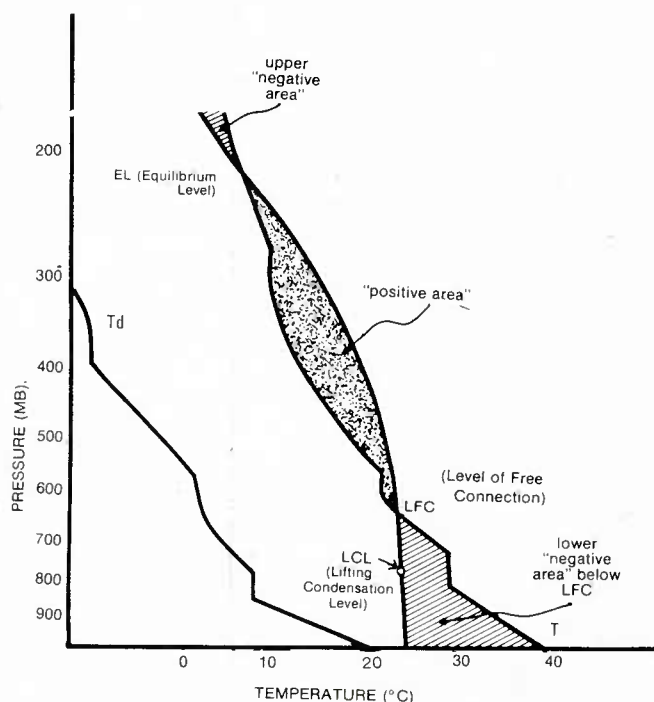


Figure 3-4. Typical pre-shamal atmosphere. (After Feteris, 1973.)

In order to set off thunderstorm activity of the sort indicated by the DMSP images, in a conditionally unstable environment, some sort of "trigger" mechanism is necessary to convert into kinetic energy the available potential energy distributed vertically in the atmosphere when conditional instability is present. While speculation on the precise form of such a trigger mechanism is beyond the scope of this report and the data available, Figure 3-4 presents a typical pre-shamal atmosphere with "positive" and "negative" energy areas analyzed to show qualitatively the amount of available energy capable of being unleashed. Also analyzed are the lifting condensation level (LCL), the level of free convection (LFC), and the equilibrium level (EL).

The energy released by the trigger mechanism has two effects: intense convective activity is produced; and production of convective activity, in turn, may help cyclogenesis to occur more rapidly and with greater intensity than would otherwise be the case (Tracton, 1973).

At the first penetration of cold air into the Gulf region, the lower levels of the troposphere experience strong but shallow northwesterly flow, while at middle and upper tropospheric levels, the flow remains southwesterly. An important forecasting implication is that the onset of the shamal typically precedes the passage of the upper air (500 mb) trough over the Gulf by as much as 12-24 hr.

Iranian shore of the Gulf, induce a lee trough along the Iranian coast, which deforms the surface pressure gradient to a northwest-southeast orientation over the Gulf (see Figure 3-6). As long as the long-wave upper trough remains stationary near the Strait of Hormuz, this pressure gradient produces a strong northwesterly wind over the Gulf. Once the long-wave upper trough moves eastward again, subsidence in the vicinity of northern Saudi Arabia lessens, the pressure gradient relaxes, and the wind subsides. At this point, the shamal has "broken".

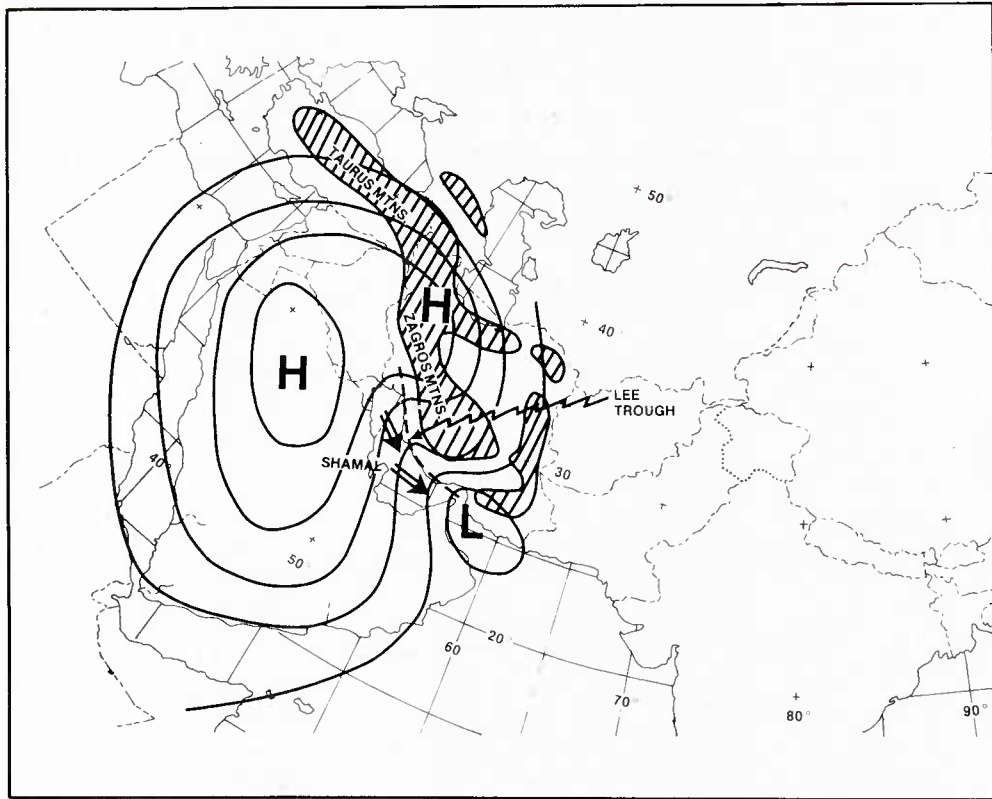


Figure 3-6. Typical surface pressure pattern during 3-5 day shamal with lee trough near Iranian coast of Gulf.

3.5 SIGNIFICANT MESOSCALE WEATHER PHENOMENA

As the shamal cold front sweeps south and eastward down the Gulf, convective cells in the immediate region of the front frequently produce squally, unstable weather with rain showers and thunderstorms. The high resolution DMSP images shown as Figures A-11 and A-12 in Appendix A (Case Study 1) indicate intense convective activity in organized lines occurring ahead of the cold front in the northern Gulf. Convection often is inhibited following cold frontal passage.

The cool air which sweeps southward down the Tigris-Euphrates valley behind the cold front tends to be dry, so that convection is difficult to sustain following cold frontal passage. If a significant amount of subsidence occurs

in the lower troposphere -- directly following surface frontal passage -- over Saudi Arabia, Iraq, and the Persian Gulf, convection over the region will be totally suppressed.

If, on the other hand, the layer of cold air behind the front is unaccompanied by significant subsidence throughout the lower troposphere (this occasionally happens; the onset of subsidence lags passage of the surface cold front by as much as 24 hr), the initially cool, dry air behind the front will be modified from beneath as it streams over the warm moist Gulf and convective activity can recur. The air picks up both sensible heat and moisture from the Gulf and becomes unstable. (Figures A-24 and A-25 in Appendix A show the effects of this process.) If the process proceeds far enough before being capped by the onset of subsidence, showers and thundershowers can develop in the modified cool air over the Gulf behind the cold front.

The northwest wind which sets in after passage of the cold front tends to be strong and gusty. Visibilities are reduced by salt spray haze raised by the winds; this haze is combined with dust and sand advected over the waters of the Gulf from the Tigris-Euphrates valley to the north and from desert regions to the west.

Visibility problems associated with blowing dust can be especially severe in the northern Gulf. If the shamal is the first of the winter season, visibilities due to blowing dust may be exceptionally low. The strong, gusty northwesterlies lift the fine topsoil of the Tigris-Euphrates valley (dried by the over 100°F heat of the previous summer season and untouched by rainfall since the previous winter) and carry it, suspended, out over the northern Gulf. Similar, though less severe, low visibility conditions are produced in winter when long intervals occur between shamals or other rain-producing systems, so that little moisture remains to bind together the fine topsoil of the fertile lower Tigris-Euphrates valley.

3.6 SURFACE WINDS

After onset, the prevailing shamal direction is strongly influenced by coastal contours. In the northern Gulf, the general wind direction is north to west-northwest. At mid-Gulf, shamal winds tend to be west-northwest to northwesterly. On the southeast coast of the Gulf, the prevailing shamal direction is westerly. Near the Strait of Hormuz, shamal winds blow from the southwest. (This pattern is reflected in wind roses for the winter months in the Persian Gulf, given in Appendix C.)

In general terms, average shamal wind speeds range between 20 and 40 kt. A general rule of thumb is to add 10 kt to the onset wind speed given by forecast rule 2a in Appendix D (Forecast Guidance) for average gusts and 15 to 20 kt for peak gusts. This seems to work well for 24-36 hr shamals.

However, when the upper trough becomes stationary over or near the Strait of Hormuz, the surface wind distribution is different. The shamal tends to persist for 3-5 days with gale force northwesterlies prevalent over the entire Gulf. Strongest winds are over the southern and southeastern Gulf, where the surface pressure gradient between the high over Saudi Arabia and the low over the Gulf of Oman is the tightest. Average wind speeds in the southern and southeastern Gulf range from 30 to 40 kt, with peak winds in excess of 50 kt not uncommon in this type of shamal. Winds in the northern Gulf tend to be 5-15 kt less, on average.

3.6.1 Areas of Stronger than Normal Shamal Winds

Two areas of the Gulf seem to experience stronger than average shamal conditions (as suggested by the monthly wind roses and wind exceedance graphs of the wind climatology section, Appendix C^{*}). These areas are depicted in Figure 3-7.

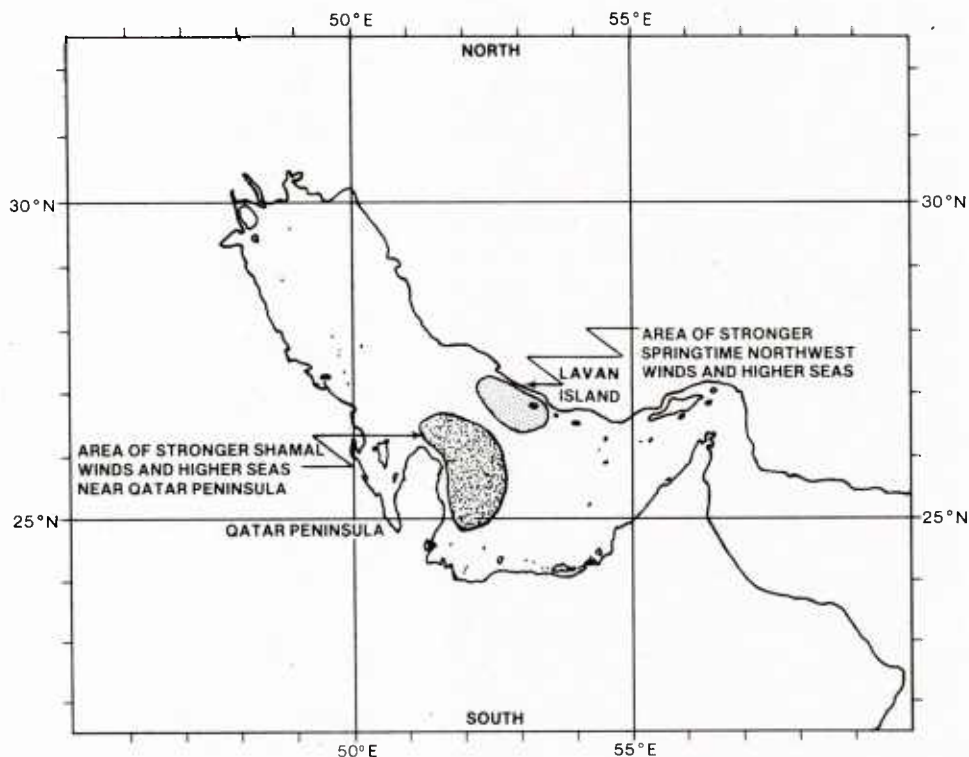


Figure 3-7. Areas of stronger than normal northwesterly winds and higher seas.

*The wind statistics in Appendix C may be biased by considerations such as differences in exposure of the anemometers used to record the data at each location. Other evidence, however, such as wind reports from the oil rig Seashell located between Halul Island and the east shore of the Qatar Peninsula, confirm that higher winds are truly present.

One area is near the Qatar Peninsula, where higher shamal wind values are reflected in the wind roses for both Ras Rakan at the northern end of the Peninsula and Halul Island to the east of the Peninsula. Perhaps this local anomaly is due to small scale influences of the Qatar Peninsula, which juts into the Persian Gulf on local winds. For this region, a good rule of thumb is to add 10-15 kt to the average wind forecast for the rest of the Gulf.

Another area where winds seem to exceed the norm is near Lavan Island; higher than normal values tend to occur here in late winter and early spring. Accordingly, forecast values for the area near Lavan Island should be increased by 10 kt in the late winter-early spring (March) shamals.

Wind speed anomalies probably exist in other areas. The shamal, as an interaction between the synoptic scale and the mesoscale, is highly subject to modification by local conditions. As more data are collected over time in specific areas of the region, the local variations will become clearer.

3.6.2 Diurnal Variations in Surface Winds

Forecasters with experience in the Gulf region report that surface winds intensify over open water by day and diminish somewhat by night. However, the detailed wind information for Ahmadi Sea Island and Das Island (given in Tables A-1 and A-2 of Appendix A, Case Study 1) seems to contradict this "rule of thumb" -- the wind maxima at these islands were recorded at night. This may have occurred because the shamal wind zone extended only a short distance behind the advancing cold front, and subsided within 24 hr after the front passed and the upper air trough moved away to the east. The time of maximum wind intensity in such a situation seems most likely to occur 6-12 hr after frontal passage.

In cases where the upper trough becomes stationary over or near the Strait of Hormuz, however, so that the shamal extends over 3 to 5 days, diurnal effects would appear to have some perceptible influence. The surface pressure gradient and the winds tend to increase by day and slacken to a small extent at night. Typical differences between day and night wind velocities are on the order of 5-10 kt.

3.7 SEAS/SWELL

3.7.1 Seas (Combined Sea Height)*

The Persian Gulf is shallow and highly stratified, and both of these qualities can contribute to the modification of the normal wind speed/sea height relationships applicable to the open sea. The shallowness of the Gulf -- it is only 240 ft (73.3 m) deep at its deepest point -- indicates that deep water

*All heights discussed are significant wave heights ($H_{1/3}$): the average of the highest 1/3 of those observed.

wave approximations for wind speed/wave height relationships are inappropriate. The appropriate approximation, depending upon location in the Gulf, is either that of a shallow water wave or an intermediate depth wave. Both approximations imply steeper waves than expected over the open sea, where deep water approximations apply. Also implied are higher wave heights for a given wind speed than those found over the open sea.

The stratification of the Gulf, due to an excess of evaporation over precipitation, also implies higher sea heights than are found over the open sea. The resulting warmth of the Gulf's surface aids in more efficient coupling through the wind stress on the water surface. This more efficient coupling has been shown to produce a more effective transfer of kinetic energy from air to sea. When the relatively cool, gusty, northwesterly winds of the shamal are advected over these warm, shallow waters, a short-period, steep sea arises quickly. Where gale force winds blow persistently for as little as 12 hr, 10-12 ft seas arise quickly. The wind speeds and sea heights reported by oil rigs and servicing craft in Case Study 1 confirm this. In areas that regularly experience higher than average wind speeds during the shamal (those described in Para. 3.6.1 and shown in Figure 3-7), the seas rise more quickly and are higher. In these areas, a good general rule of thumb is to add 2-4 ft to the typical values given above.

If the upper trough moves through the Gulf region quickly and smoothly (the 24-36 hr shamal), the strong wind zone over the Gulf is advected south-eastward with the surface cold front. This strong wind zone extends from the frontal position back to the northwest. Although the strong winds, blowing for only a short period of time, quickly raise significant seas, combined sea heights may be limited by fetch (particularly in the northern Gulf) and by duration of the strong winds at a given point as the strong wind zone behind the front moves southeastward.

If the 3-5 day shamal occurs (the upper trough stalls over the Strait of Hormuz, or moves very slowly through the Gulf region), the combined sea height will increase further, particularly in the southern Gulf. Three factors combine to produce significant combined sea heights of up to 12-15 ft and more in the southern Gulf:

(1) The increase in wind speed in the southern Gulf; this contributes to higher locally generated seas there.

(2) The longer duration of gale force winds over the whole Gulf; the northern portion of the Gulf becomes a generating area for swell which runs down into the southern Gulf.

(3) The lack of fetch limitation; the entire length of the Gulf experiences at least gale force winds with the strongest winds in the southern Gulf.

Because of (2) and (3), the southern part of the Gulf also experiences a longer period of residual swell decay after the 3-5 day shamal subsides.

3.7.2 Residual Swell

Following the end of 24-36 hr shamals, swells typically decay rapidly to 2-4 ft within 24 hr after the winds subside.

Following the end of the 3-5 day shamals, residual swell may persist for up to three days. If 12-15 ft seas have previously been generated along the whole length of the Gulf, the significant swell heights typically decay in the southern Gulf to 6-8 ft on the second day, 3-5 ft on the third day, and 1-3 ft on the fourth day.

In, and to the southeast of, the areas of higher than normal winds discussed in Section 3.6.1 and shown in Figure 3-7, the swells take longer to decay. Following the end of the 24-36 hr shamal, swells typically decay to 4-6 ft on the first day, and to 2-4 ft on the second day. Following the end of the 3-5 day shamal, swells typically decay to 8-10 ft on the second day, 5-7 ft on the third day, 3-5 ft on the fourth day, and 1-3 ft on the fifth day.

3.8 TURBULENCE

Significant turbulence can be associated with the shamal at lower and upper levels of the troposphere.*

3.8.1 Low Level Turbulence

Low level turbulence (that occurring in the first few thousand feet above the surface) can be associated with the shamal during three distinct time periods: prior to the passage of the cold front which initiates the shamal, in association with the cold front itself, and after the cold front has passed through the Gulf region.

3.8.1.1 Prior to Cold Front Passage

Prior to the passage of the cold front, the southerly wind known as the Kaus frequently occurs. The Kaus winds are "channeled" by the Zagros Mountains (see Section 3.3.1 and Figure 3-2) to cause a zone of higher wind speeds at low levels on the eastern side of the Gulf. Speed shears, therefore, are likely to be found both to the west of the lower level maximum wind zone near the surface, and vertically just above the wind zone maximum. Such speed shears imply light to moderate turbulence, particularly when the low level wind maximum approaches gale force (28-47 kt).

*See Appendix D, Forecast Guidance, rules 11 and 12.

As discussed in Section 3.3.3 and indicated on Figures A-14 and A-15, lines of severe thunderstorm and rainshower activity may occur just ahead of the cold front, particularly in the northern Gulf. Locally severe turbulence is implied in and near these organized convective cells throughout the troposphere.

3.8.1.2 Associated with the Cold Front

Rainshower and occasionally thundershower activity occur in conjunction with the convective clouds that are part of the advancing cold front which marks the onset of the shamal. Near and in these convective cells, moderate to locally severe turbulence is implied.

3.8.1.3 After Cold Front Passage

The shamal wind is strong and gusty (Section 3.5). Gustiness, particularly when associated with wind at or near gale force, implies light to moderate turbulence in the lowest few thousand feet of the atmosphere. Satellite imagery, particularly high resolution DMSP imagery, can aid in pinpointing the more severe occurrences of this sort of low level turbulence.

As indicated in Figures A-24 and A-25 and on Figures B-13, B-18, B-23, and B-30, instability cumulus frequently form over the Gulf after the cold front has passed through, the result of relatively cold air streaming over the warmer Gulf waters.* The lower few thousand feet of the atmosphere can become particularly unstable under these conditions to produce "bumpy" conditions which could adversely affect the performance of low-flying aircraft such as helicopters.

The occurrence of instability cumulus is associated with the advection of cold air at lower levels over the Gulf, during the first 24 hours or so of the shamal. If the shamal persists for 3-5 days, additional occurrences of instability cumulus seem to be associated with short waves in the upper air that move through the stalled long-wave position (see particularly Section B.4 of Appendix B, which discusses the occurrence of this phenomenon in detail, in conjunction with the satellite image depicted in Figure B-23). By closely monitoring available DMSP imagery the forecaster can identify those situations which enhance the likelihood of low level turbulence.

Another part of the Gulf with low level turbulence potential is the area on the eastern side of the Gulf near the Zagros Mountains. Data depicting low level wind trajectories during the shamal are limited; accordingly, direct

*See Appendix A and Appendix B for detailed discussions of this phenomenon, in terms of the interrelationships between the satellite images, and surface and upper air data.

inferences about low level flow are also limited to those which may be drawn from the orientation of the post-frontal instability cumulus. However, it is not unreasonable to assume that while the shamal blows, some air at low levels is drawn from the Iranian plateau southwestward to merge with the prevailing low level northwesterly air flow over the Gulf.

Under these conditions if the speed of the air flowing over the crest of the Zagros Mountains approaches gale force, moderate or greater intensity mechanical turbulence may be encountered in the lee (to the west) of the Zagros Mountains. This condition can be expected particularly during the extended 3-5 day shamal.

3.8.2 Upper Level Turbulence

Significant turbulence also can be associated with the upper air pattern of the shamal. Some turbulence may be associated with the anticyclonic subtropical jet, whose mean position is indicated in Figure 3-8.

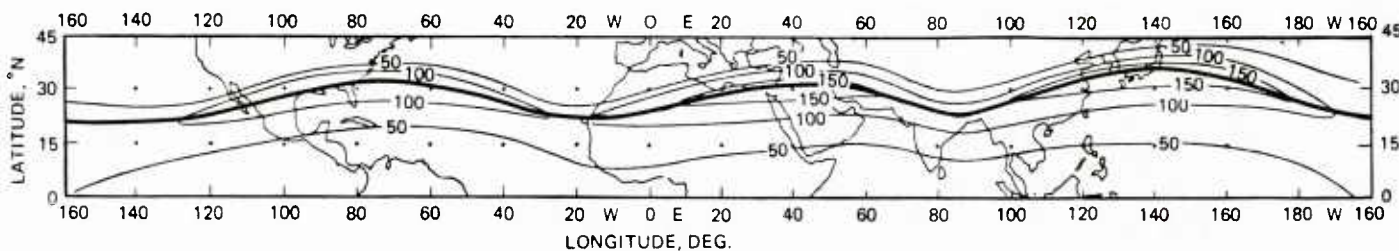


Figure 3-8. Mean subtropical jet stream for winter 1955-1956. Isotach analysis at 200 mb, drawn every 50 kt. Mean latitude of jet axis is 27.5°N. (After Reiter, 1969.)

When the polar jet dips southward over, or just to the north of, the Persian Gulf in association with the onset of the shamal, a complex interaction between the polar and subtropical jets may occur. In some instances, the jets may overlay one another, as suggested by Reiter (1972); in other situations, the two jet regimes may both occur over the Gulf, separate but proximate (see Figures 3-9 and 3-10).

When the polar jet invades the Gulf region, it tends to depress the subtropical jet further southward. In forecasting, this implies that some turbulence may be expected at or near the area of the mean subtropical jet position when the shamal is absent (particularly if the cloud "signature" of the jet can be discerned from a satellite image). (Figure B-6 in Appendix B shows the subtropical jet on DMSP visible imagery near its climatological position.) As the shamal sets in, a broadened and more intense turbulence area is likely, and the area's extent can be moved southward to coincide with the equatorward displacement of the subtropical jet.

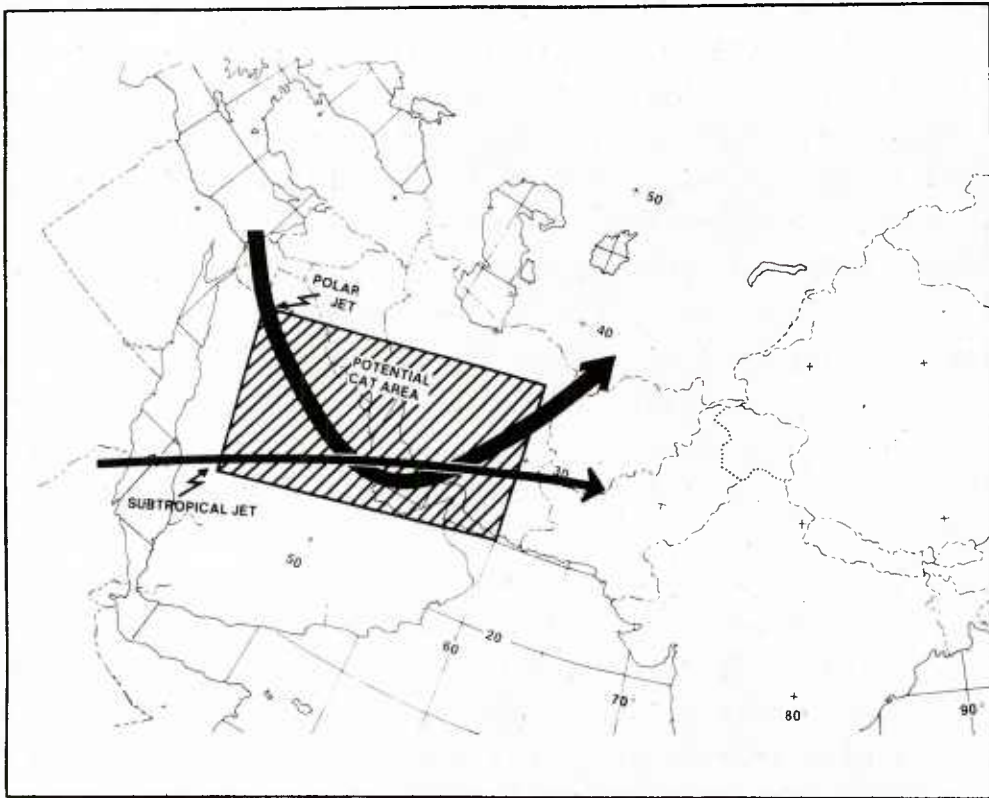


Figure 3-9. Subtropical jet overlays polar jet.

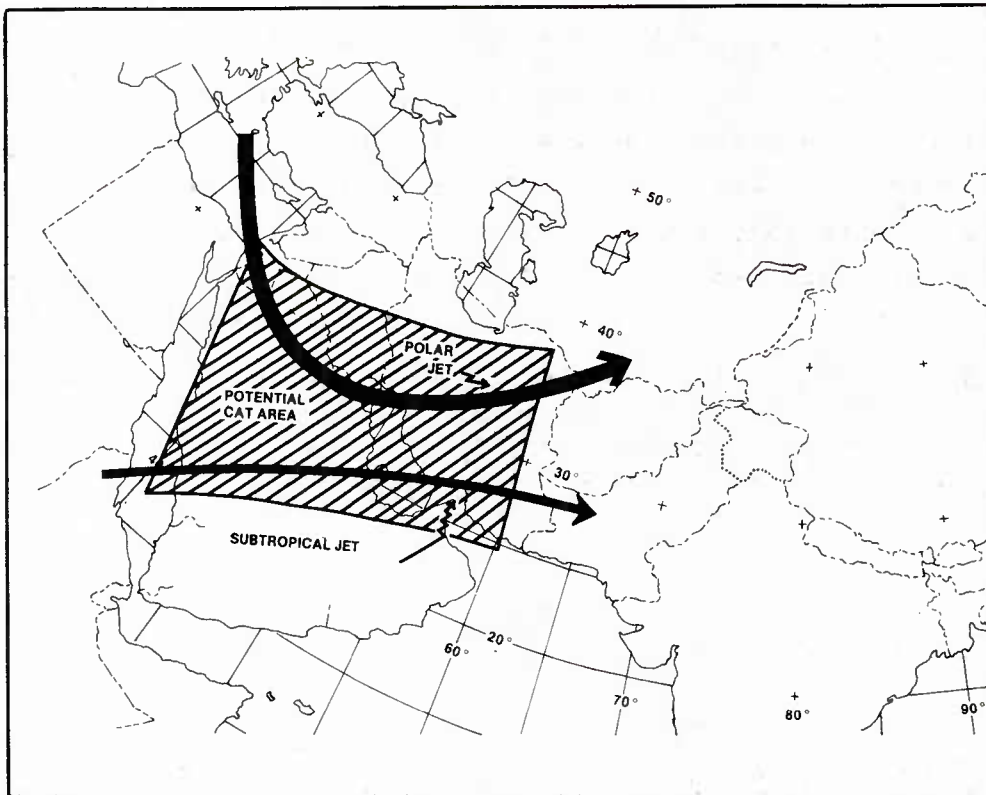


Figure 3-10. Polar and subtropical jets separate but proximate.

Table 3-1 and Figure 3-11 (after Stranz, 1970) constitute a typical space-time cross section from an aircraft report of winds and turbulence at 20,000 ft (6096 m), near but below the location of the jet axis during a winter shamal situation. The aircraft appears to be flying beneath the jet core in a region of strong vertical shear. Strongest turbulence effects are generally encountered when the flight path is normal to the jet stream axis; the angle the aircraft makes with the jet stream axis (in Stranz's example) is close to 90°. Stranz's data is plotted in Figure 3-11 with positions of the polar and subtropical jet, as suggested by Reiter's (1972) model.

Turbulence at all levels of the troposphere may also be induced by mountains in the Persian Gulf region. Examples of mountain waves in the area surrounding the Persian Gulf are observed in the DMSP imagery presented in Appendices A and B.

Figure A-14 shows mountain waves induced by the subtropical jet as it passes over the Hejaz Mountains (which are located along the western edge of the Arabian peninsula) and as it passes over the southern portion of the Zagros Mountains (to the east of Baudar Abbas and to the north of the Gulf of Oman). A particularly striking example of mountain wave clouds is shown at Area I in Figure B-23. The polar jet, depressed southward to a position of the southern Persian Gulf in association with the extended 3-5 day shamal, induces the wave clouds over the northern portion of the Gulf of Oman (just to the south of the Strait of Hormuz) as the air streams over the northern part of the Hajar Mountains. The orientation of the northern part of the mountain chain, in this instance, is nearly at right angles to the wind flow.

Moderate to severe turbulence can be expected downstream of the mountains in the region where the waves form, from an altitude well below the height of the mountain peaks -- in some instances, all the way down to the surface of the downstream terrain -- extending upward to as high as jet stream altitudes. The altitude range of the occurrence is a function of local atmospheric stability, and other factors, such as wind speed and direction, specific terrain configuration, and vertical wind profile.

Table 3-1. Debrief Aircraft, 14 Dec 1970, Bahrain.

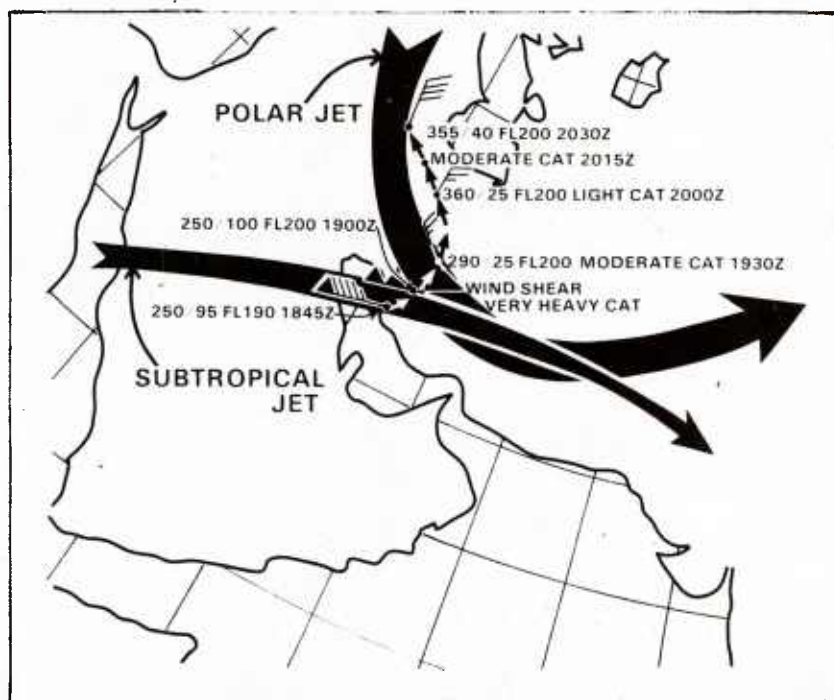
| GMT | Position | Altitude (ft)* | Wind | Temperature (°C) |
|------|------------------|----------------|------------------------------------|------------------|
| 1845 | 28°30'N, 51°40'E | 19,000 | 250° 95 kt | -15 |
| 1900 | 29°32 N, 52°38 E | 20,000 | 250° 100 kt | -19 |
| 1920 | 31° to 32°N | | wind shear, very heavy CAT** | |
| 1930 | 32°N, 52°E | 20,000 | 295° 25 kt, moderate CAT | -35 |
| 2000 | 35°N, 50°22'E | 20,000 | 360° 25 kt, light CAT | -35 |
| 2015 | 36°N, 49°E | 20,000 | moderate CAT | |
| 2030 | 37°N, 47°E | 20,000 | 355° 40 kt | -32 |
| 2100 | 37°33'N, 45°04'E | 20,000 | 340° 45 kt | -28 |
| 2130 | 38°30'N, 42°16'E | 20,000 | 335° 40 kt | -28 |
| 2200 | 38°36'N, 39°18 E | 20,000 | 335° 40 kt | -28 |
| 2230 | 38°N, 38°40 E | 20,000 | 340° 20 kt | -24 |

SIGMET (morning of 15 Dec 1970): "VERY HEAVY CLEAR AIR TURBULENCE REPORTED AND FORECAST FOR LOW LEVELS OVER THE PERSIAN GULF."

*19,000 ft = 5791 m
20,000 ft = 6096 m

**CAT - Clear Air Turbulence

Figure 3-11. Pilot report after Stranz (1970). The subtropical jet overrides the polar jet, as suggested by Reiter's model. (See Figure 3-9.)



REFERENCES

- Anderson, R.K., et al., 1974: Application of meteorological satellite data in analysis and forecasting. NOAA, Washington, D.C. Reprint of ESSA Tech. Rept. NES-51, incl. Supplements 1, Nov 1971, and 2, Mar 1973. (Also available as Air Weather Service Tech. Rept. 212.)
- Defense Mapping Agency Hydrographic Center: Standard Time Zone Chart of the World, Washington, D.C.
- Feteris, P.J., 1973: The role of deep convection and strong winds aloft in triggering gales over the Persian Gulf: Comparative case studies. Mon. Wea. Rev., 101, No. 3, 455-460.
- Godev, H., 1970: On the cyclogenetic nature of the Earth's orographic form. Arch. Meteor. Geophys. Bioklim, Ser A, 19, 299-310.
- Godev, H., 1971: The cyclogenetic properties of the Pacific Coast: Possible source of errors in numerical weather prediction. J. Atmos. Sci., 28, 968-972.
- Hess, H.L., 1959: Introduction to theoretical meteorology. New York: Holt, Rinehart and Winston, pp 297-302.
- Hibbert, D.L., 1966: Weather forecast services for offshore oil operations. Weather, 21, No. 4, 114-119.
- Oil Companies' Weather Co-Ordination Scheme, 1974: Handbook of weather in the Gulf, surface wind data. London: IMCOS Marine Ltd., 101 pp.
- Reiter, E.R., 1969: Atmospheric transport processes, part 1: energy transfers and transformations, AEC Critical Review Series, USAEC Report TID-24868.
- Reiter, E.R., 1972: Atmospheric transport processes, part 3: hydrodynamic tracers, AEC Critical Review Series, USAEC Report TID-25731.
- Stranz, D., 1970: Strong shamal in the Arabian Gulf. Rivista Di Geofisica, 22, No. 5/6, 296-298.
- Stranz, D., 1973: Ein ausgeprägter schamal im Arabischen Golf. Der Seewart, 34, No. 4, 138-146.
- Tracton, M.S., 1973: The role of cumulus convection in the development of extratropical cyclones. Mon. Wea. Rev., 101, 537-592.
- U.S. Air Force, 1969: Use of the Skew T, Log P diagram in analysis and forecasting. Air Weather Service, AWSM 105-124, pp. 4-13 - 4-15. (Also available as NAVAIR 50-1P-5.)
- U.S. Naval Oceanographic Office, 1960: Sailing directions for the Persian Gulf. Fifth ed., Washington, D.C., 50-52.
- U.S. Navy, 1968: Clear-air turbulence. Part II: a survey of contemporary prediction techniques and recommended operational procedure. NWRP 15-0568-137(II), 13-15.

U.S. Navy, 1974: Aerographer's Mate 1 and C Rate Training Manual. NAVEDTRA
10362-B, 52-55.

U.S. Navy, 1976: Aerographer's Mate 3 and 2 Rate Training Manual. NAVEDTRA
10363-E, 236-238.

APPENDIX A - CASE STUDY 1

TYPICAL SYNOPTIC SEQUENCE OF THE 24-36 HOUR SHAMAL

This case study describes a January 1974 synoptic sequence which is typical of the 24-36 hr shamal (see discussion in Para. 3.1.2). Where appropriate to the case study, surface charts drawn at 3-hr intervals are included to depict the movement down the Persian Gulf of the cold front that precedes the onset of the shamal. These detailed surface charts will acquaint the user with the meso-scale wind and wave structures that accompany shamal occurrences.

Some of the observations used to develop the analyses are not available on standard weather collectives. They were recorded by professional meteorologists and by trained oil company observers (Hibbert, 1966) in support of commercial oil-drilling operations.

Combined sea heights expressed as ranges of heights in feet (e.g., 2-4 ft) are also included on surface charts. It has been the experience of local observers that the first number tends to indicate the significant combined sea height ($H_{1/3}$) (the average of the highest one-third of waves observed). The second number seems to be an imperfect approximation to another commonly encountered measure of wave height, $H_{1/10}$, the average of the highest one-tenth of the waves observed. In the wave heights presented on these surface charts, the second figure seems to be an underestimate of the $H_{1/10}$ that might be expected from wind-wave theory. If only one height is given, it indicates an $H_{1/3}$ (i.e., significant combined) observation.

This case study is presented in five steps of synoptic development (Paras. A.1-A.5) and a summary of important points (Para. A.6). The texts for steps 3, 4, and 5 are subdivided into two parts: synoptic discussions, and satellite data interpretation. The quoted statements of conditions that introduce each step are taken from the discussions presented in the main body of the report, Para. 3.1.

Constant pressure 500 mb analyses are provided to illustrate general surface/upper air relationships discussed in the main body of this report; some analyses at 700 mb and 200 mb are also included. DMSP satellite images are provided to enrich the surface and upper air analyses. In a data-sparse region like the Persian Gulf, such satellite data may help to fill the gaps left by inadequate surface and upper air data.

A.1 STEP ONE

"An upper trough is reflected in a surface low advected over Syria from the eastern Mediterranean area" (ref. Figure 3-1a).

On 20 Jan 1974, a sharp upper trough located over the eastern Mediterranean Sea moved slowly eastward. An associated surface low moved with the upper trough from the vicinity of 37°N , 32°E at 20/00Z into Syria (near 35°N , 38°E at 21/12Z). Both features then remained quasi-stationary over Syria until early on 24 Jan (Figures A-1 through A-8, 500 mb upper air analyses). The surface low was positioned to the east of the upper air trough and moved eastward ahead of the trough as the trough moved from the Mediterranean into Syria. Surface low positions are indicated by dots, and long wave trough positions by shaded bars, on these figures.

The sequence in Figures A-1 through A-8 also illustrates the tendency of the upper air long wave trough to favor a position near the eastern Mediterranean shore (as described in Para. 3.3.4 and illustrated in Figures 3-5a through 3-5e). A series of short waves moved through the long wave position (over the eastern coast of the Mediterranean Sea) before the long wave trough position moved eastward at 00Z on 24 January. Movements of the short waves A, B, C, and D are indicated in Figures A-3 through A-8 by circled letters.

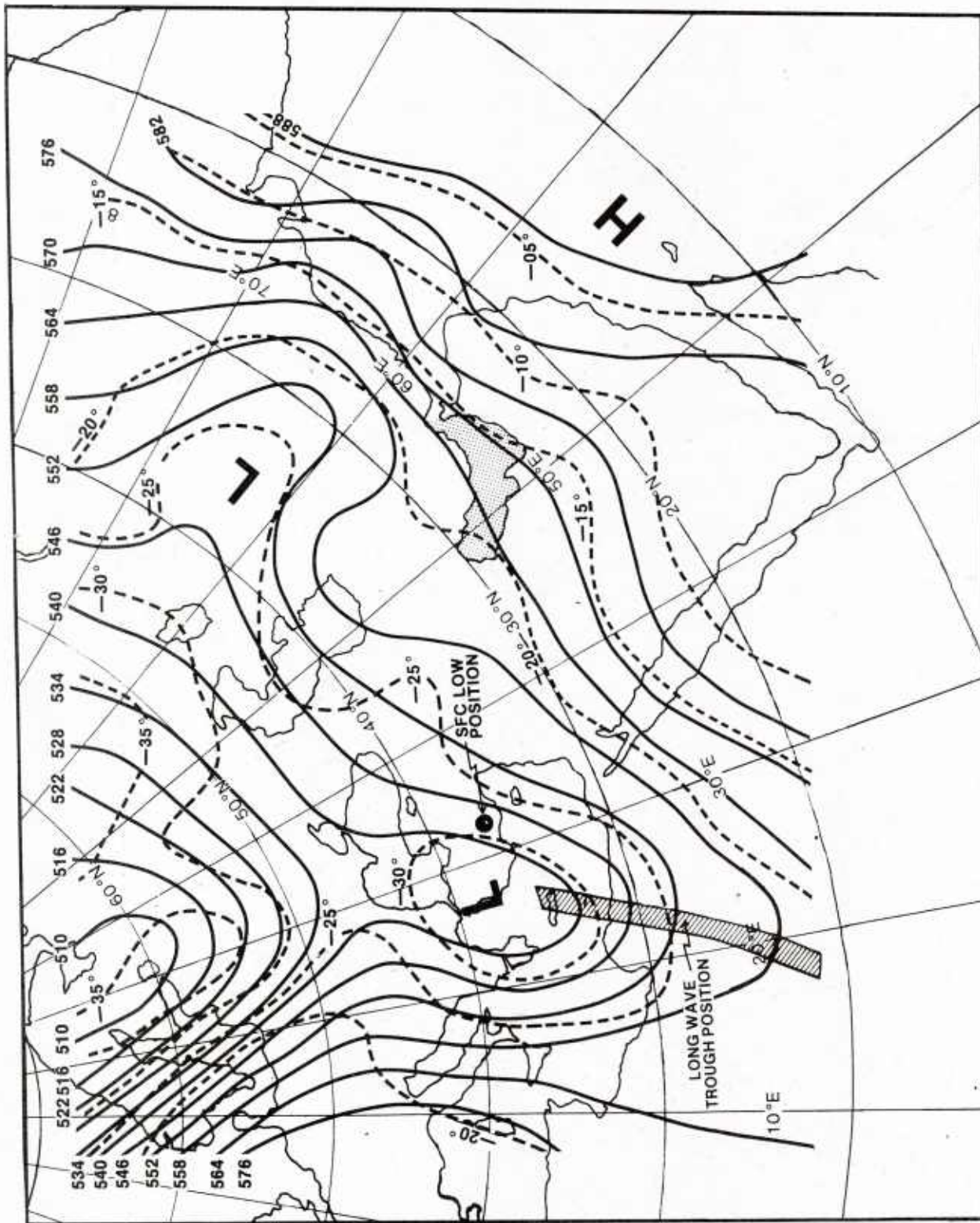


Figure A-1. 500 mb analysis, 20 Jan 1974 0000Z.

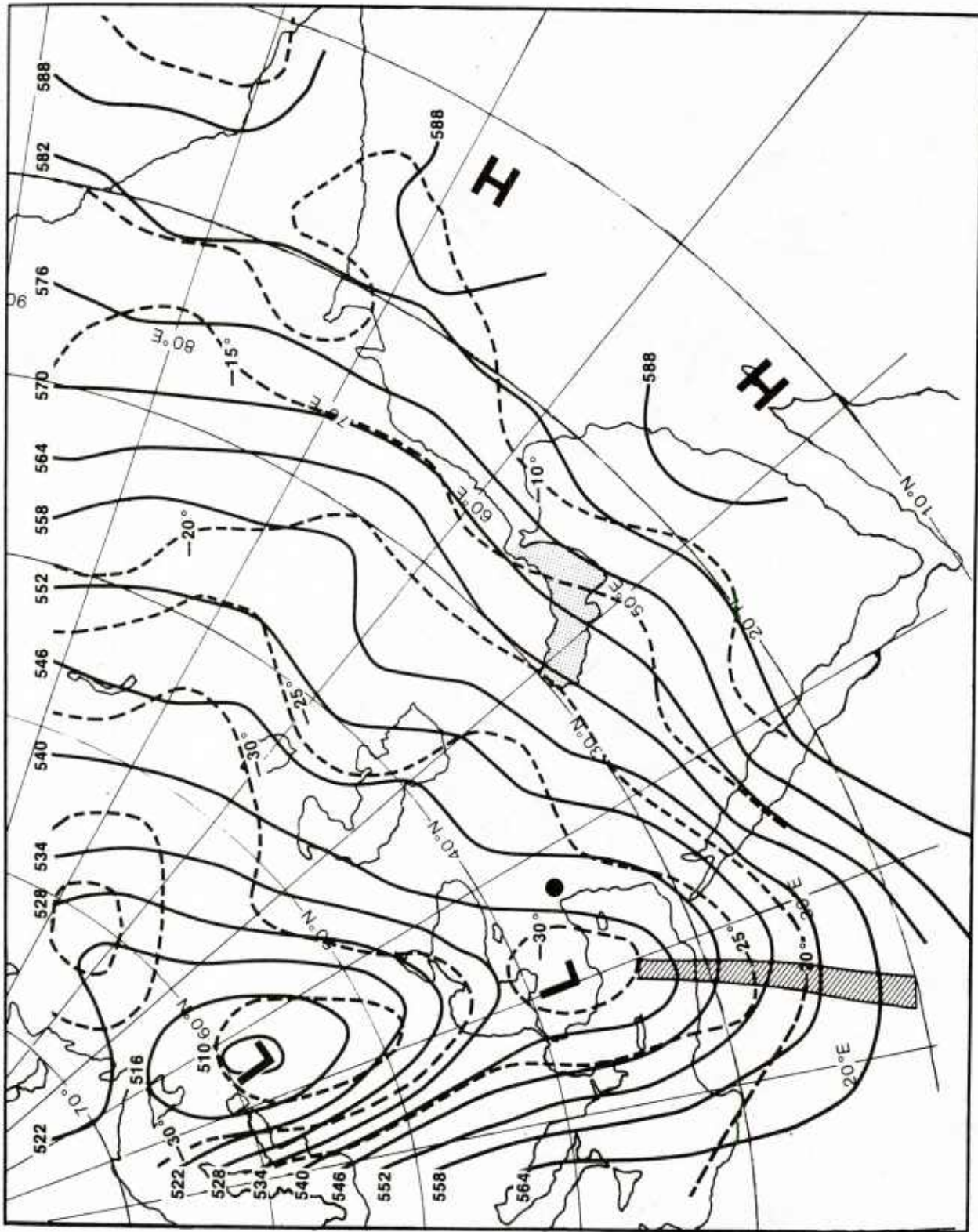


Figure A-2. 500 mb analysis, 20 Jan 1974 1200Z.

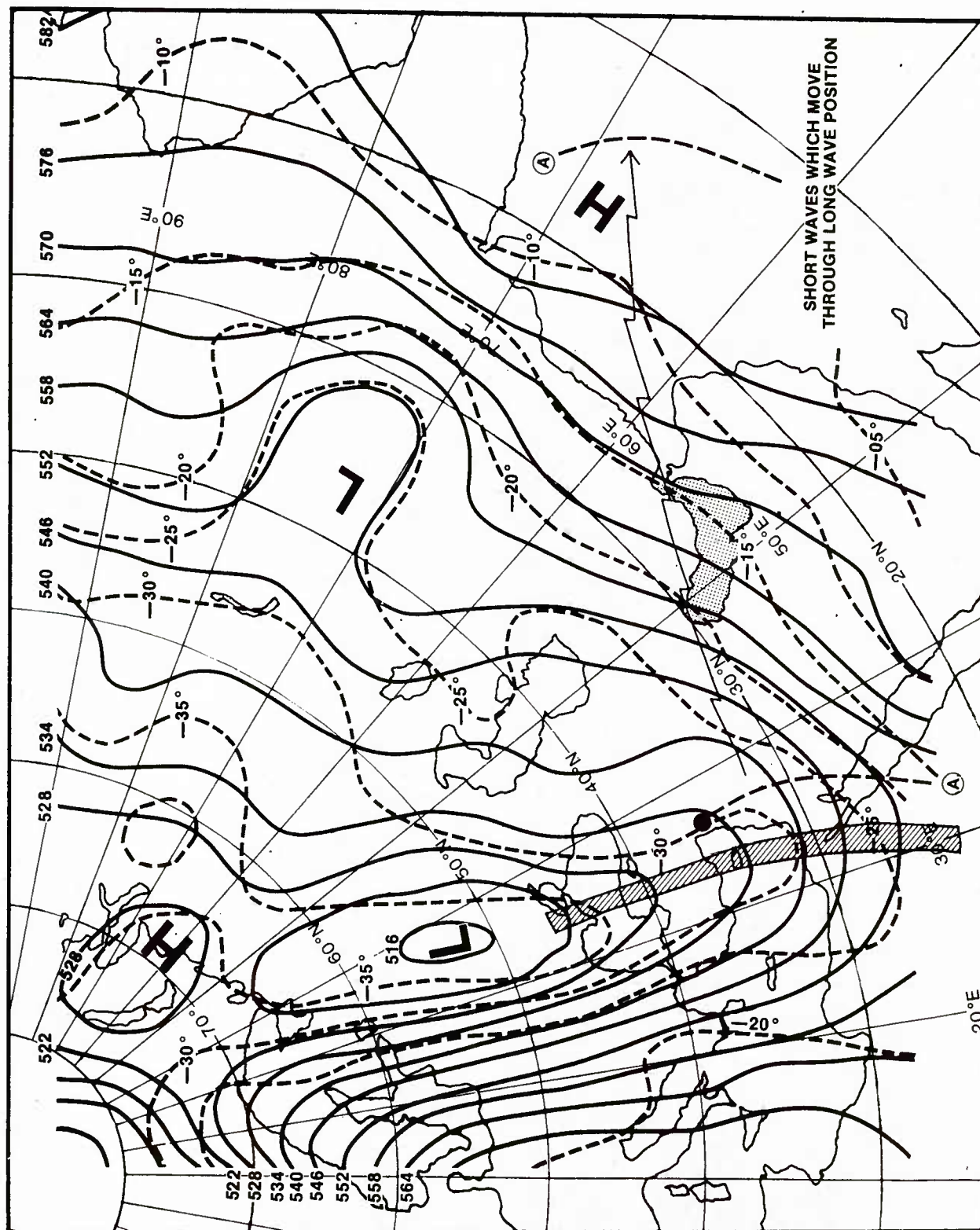


Figure A-3. 500 mb analysis, 21 Jan 1974 0000Z.

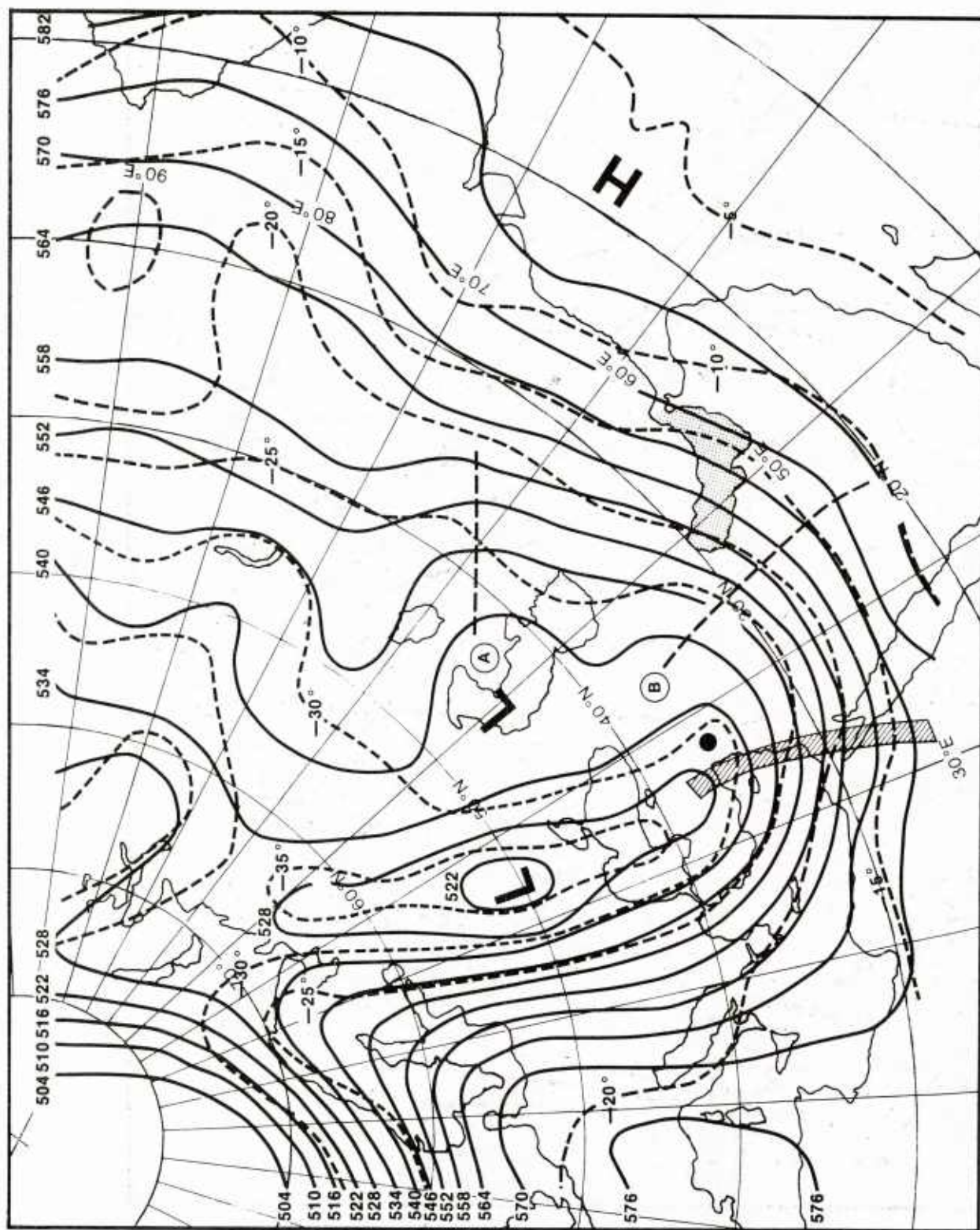


Figure A-4. 500 mb analysis, 21 Jan 1974 1200Z.

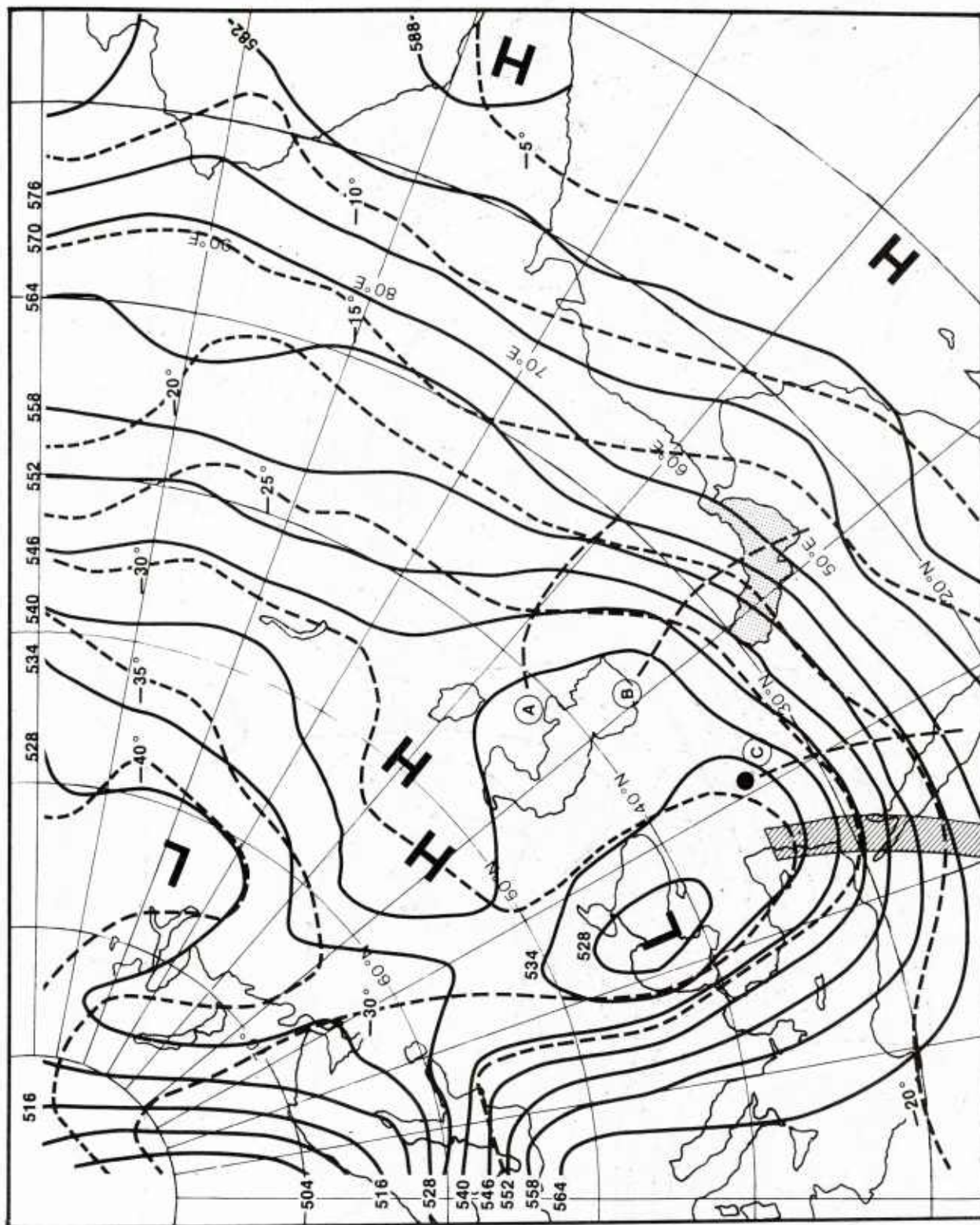


Figure A-5. 500 mb analysis, 22 Jan 1974 0000Z.

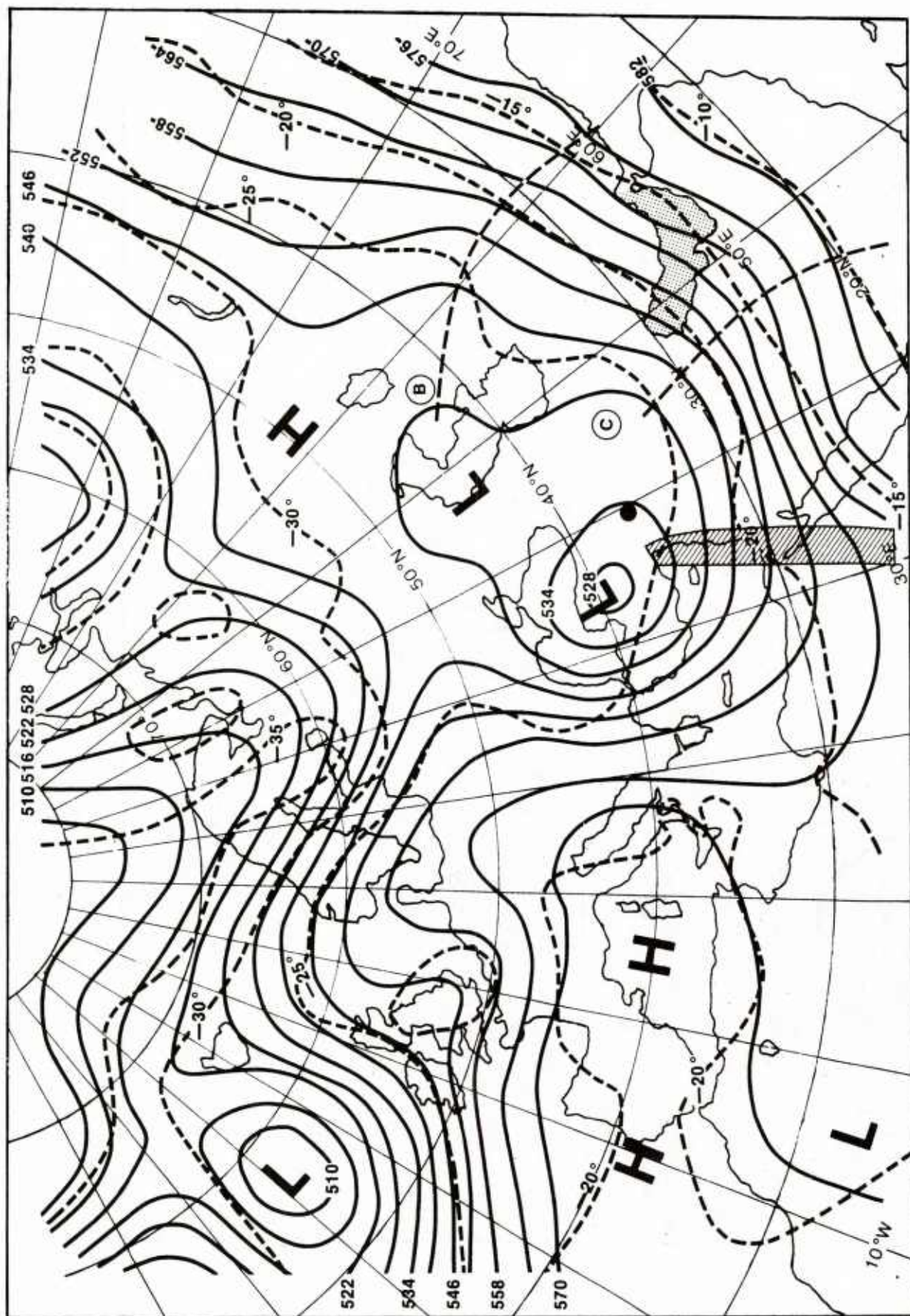


Figure A-6. 500 mb analysis, 22 Jan 1974 1200Z.

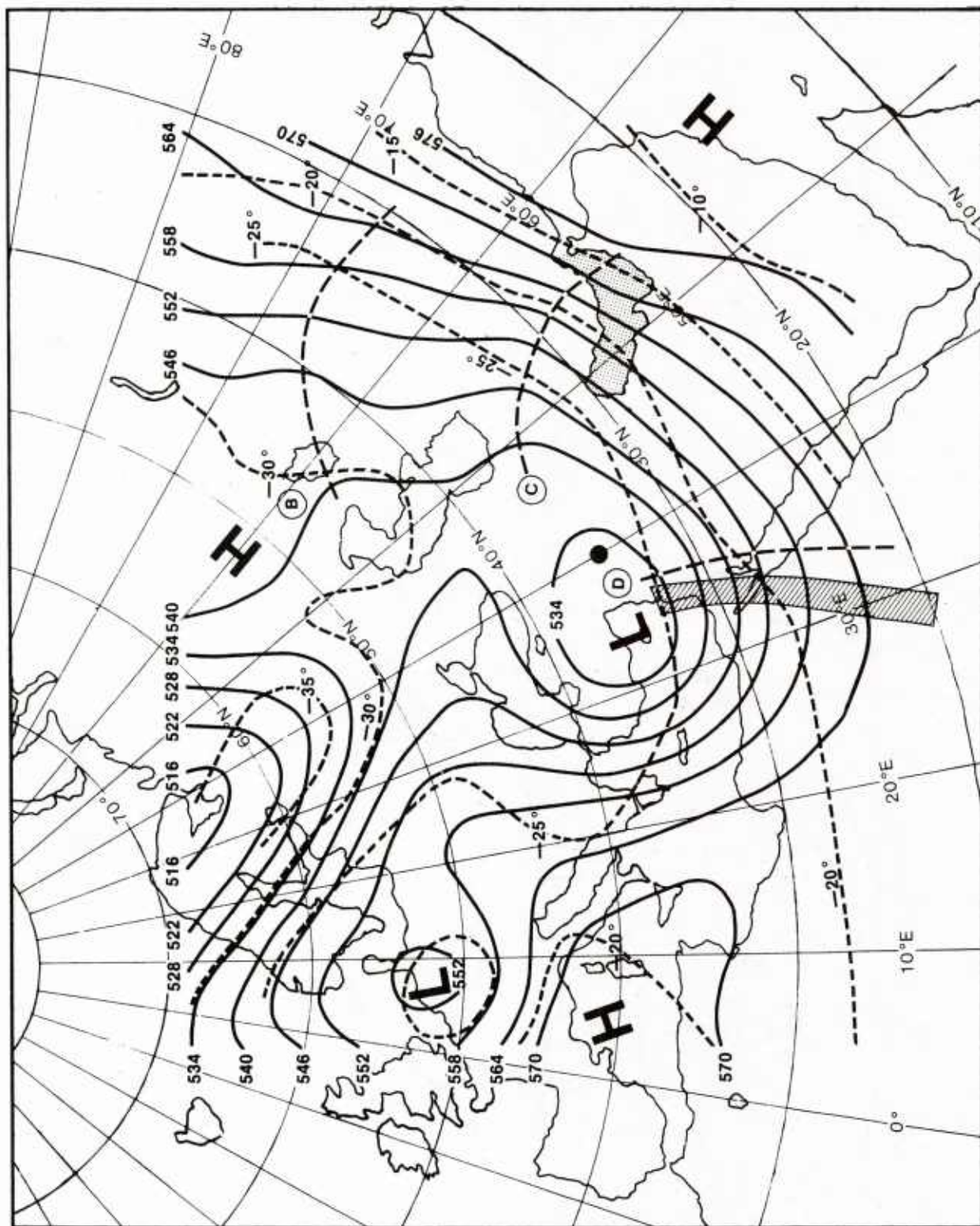


Figure A-7. 500 mb analysis, 23 Jan 1974 0000Z.

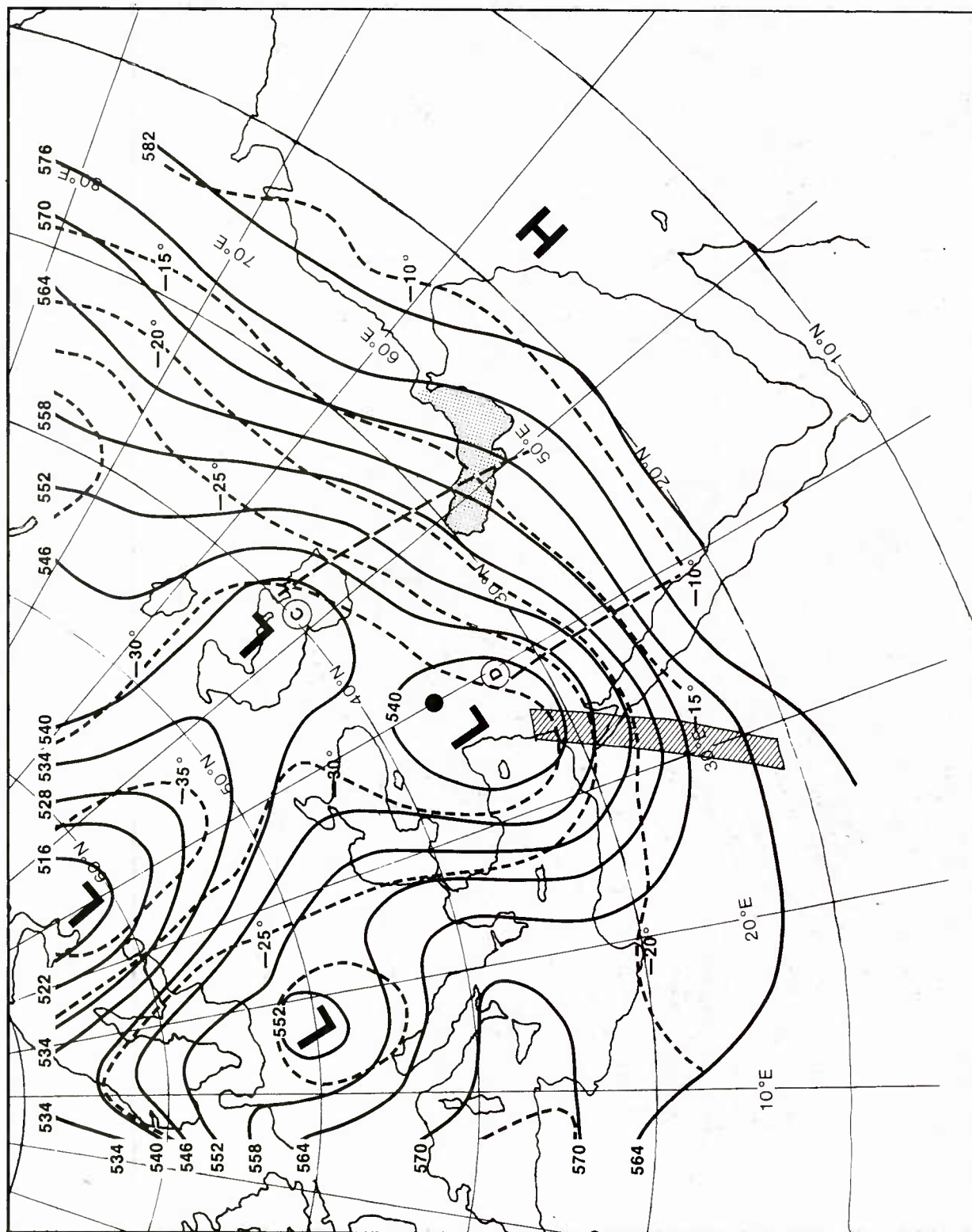


Figure A-8. 500 mb analysis, 23 Jan 1974 1200Z.

A.2 STEP TWO

"The upper trough and associated surface low move eastward. A surface cold front extends south, then west, from the low. A second low moves eastward across Saudi Arabia from the Red Sea. The Kaus, a southeasterly wind, occurs in the Gulf" (ref. Figure 3-1b).

The 500 mb upper air trough began to move eastward again at 00Z on 24 Jan (Figure A-9). Two surface lows appeared, one near the 500 mb center and another to the east of the 500 mb upper trough axis. A surface low pressure trough was also located over Saudi Arabia at 00Z, centered near 22°N, 50°E (Figure A-10).

A moderate southerly wind (the Kaus) set in over the Gulf ahead of the approaching cold front, as indicated in the 06Z surface analyses (Figures A-11 and A-12b).

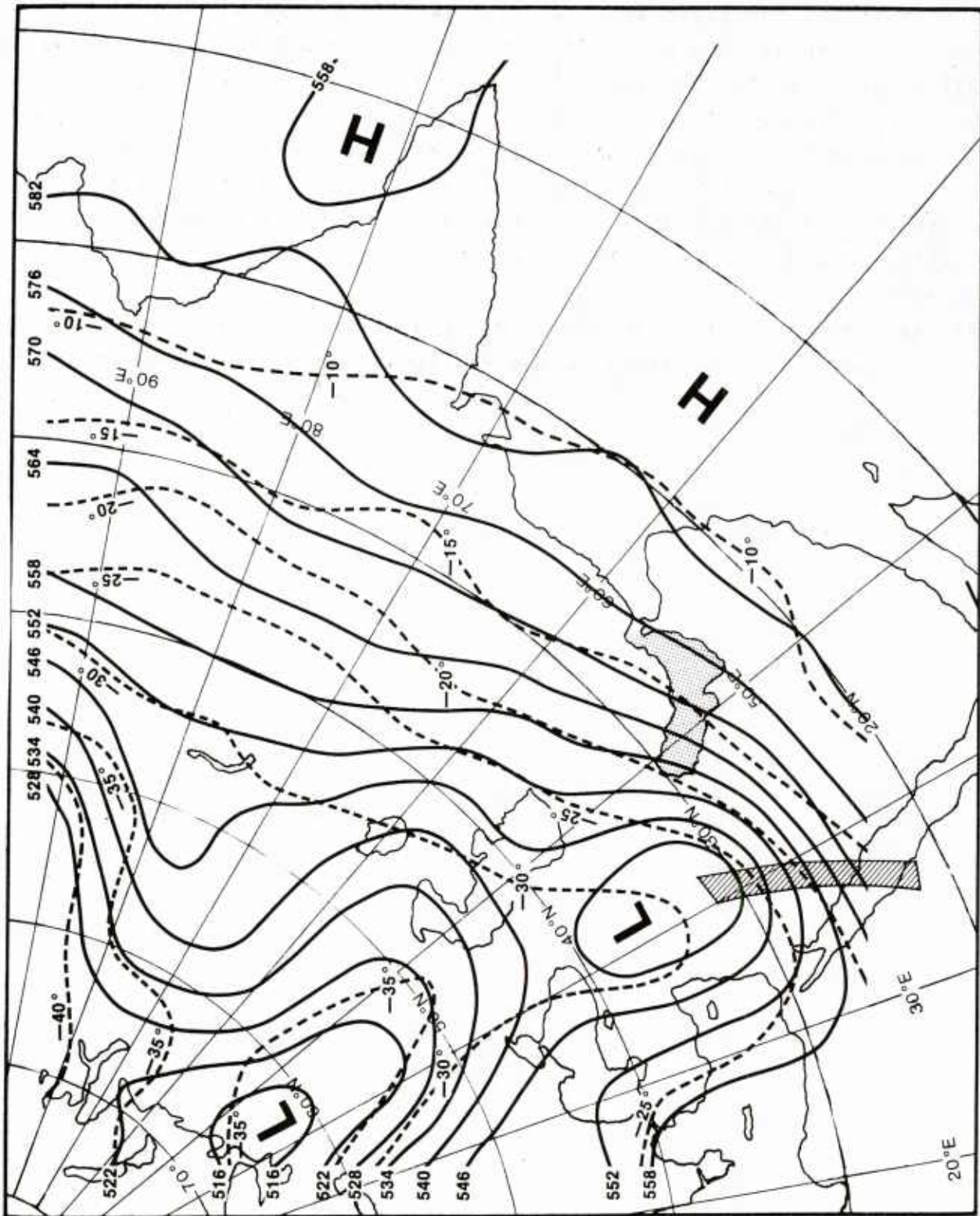


Figure A-9. 500 mb analysis, 24 Jan 1974 0000Z.

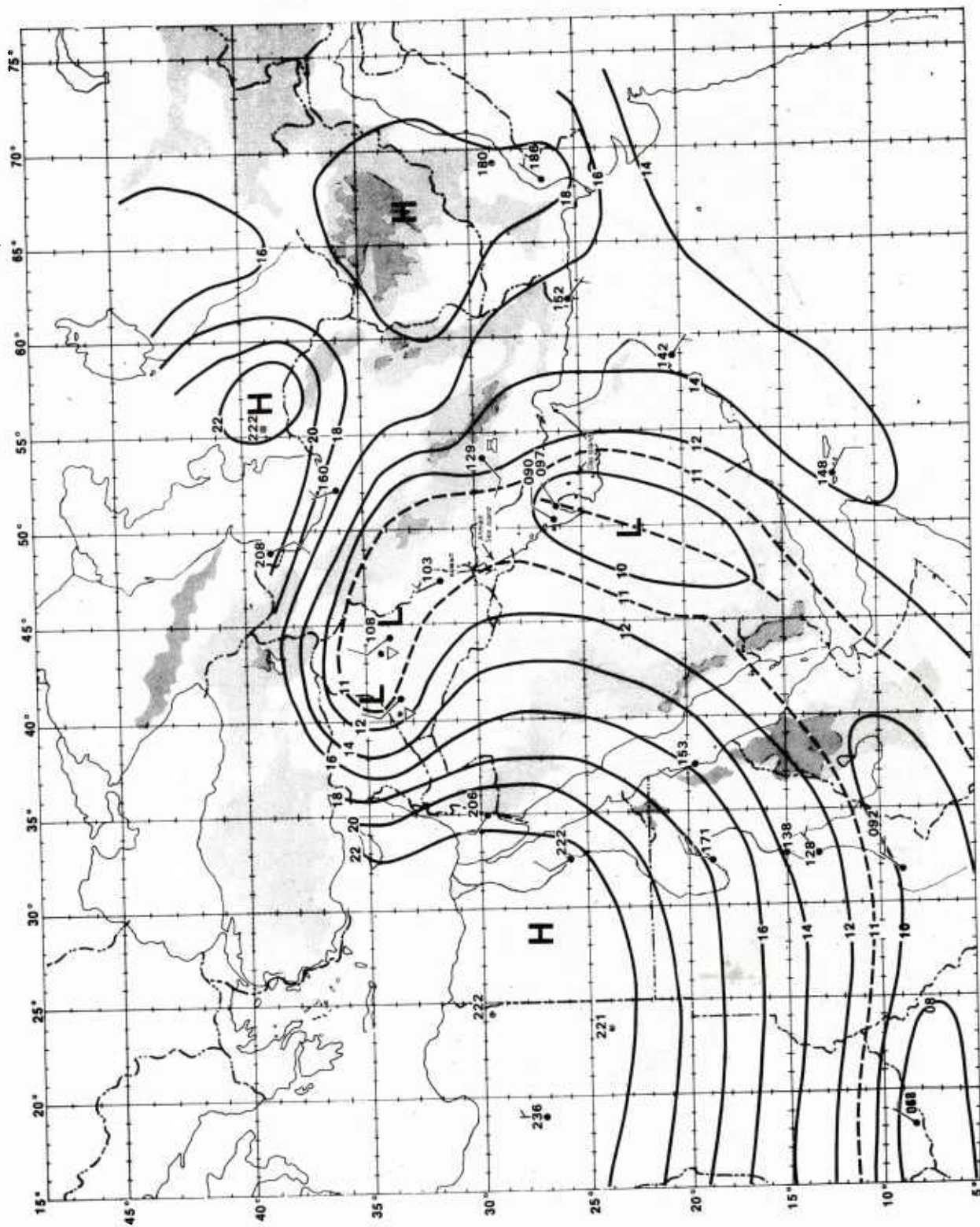


Figure A-10. Surface analysis, 24 Jan 1974 0000Z.

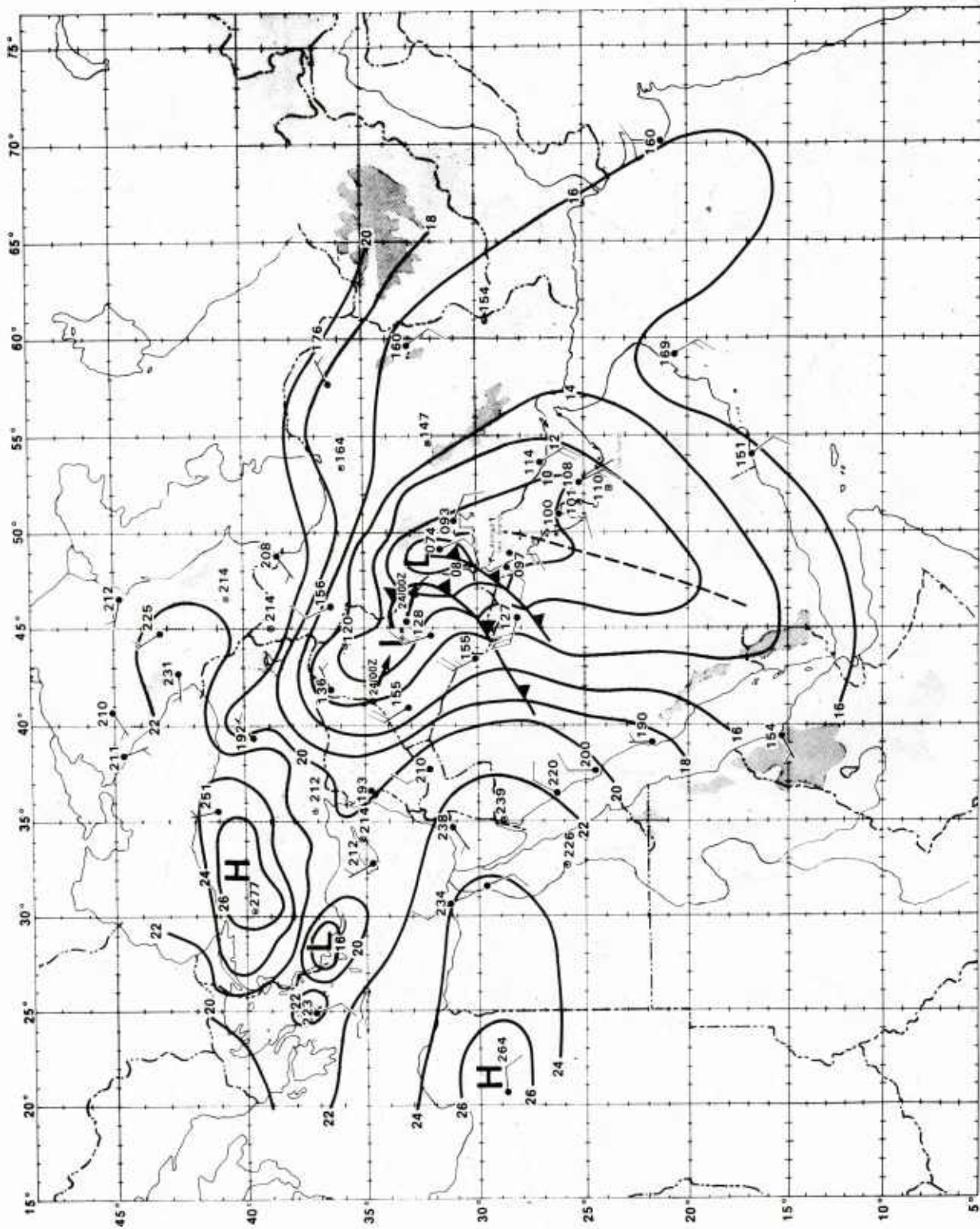


Figure A-11. Surface analysis, 24 Jan 1974 0600Z.

A.3 STEP THREE

A.3.1 Synoptic Discussion

"The upper trough moves eastward; a new low forms on the front in the general area as far north as the southern Tigris-Euphrates valley and as far south as the central Persian Gulf. The original low fills over northern Iraq or retains some surface identity as it is advected with the upper trough to the northeast toward the Caspian Sea. Subsidence in the lower troposphere induces a surface high pressure area over northern Saudi Arabia.

"A strong but shallow northwesterly airstream sets in, west of the new surface low. This the winter shamal, which produces gale force winds, raises a short-period, steep sea, sets off thunderstorms, and advects dust and sand over the Persian Gulf to sharply reduce visibilities" (ref. Figure 3-1C).

Cyclogenesis occurred over the lower Tigris-Euphrates valley near 33.5°N, 45.5°E (Figure A-11). At 06Z on 24 Jan, the new low, over western Iran near 32.5°N, 49°E, was deeper than the original surface low over central Iraq near 34°N, 44°E. Based on additional information provided by DMSP satellite images at 24/0838Z, a decaying surface cold front was linked to the original surface low over central Iraq; and a second, developing cold front was linked to the newly formed low over western Iran. The developing cold front pushed out over the northwestern portion of the Gulf at 06Z and swept down the Gulf, as shown on the detailed surface analyses for 09Z, 12Z, and 15Z (Figs. A-12c-e). The gale force northwesterlies which set in behind the cold front formed the winter shamal.

By 12Z on 24 Jan (Figure A-12), the original surface low, then over western Iran near 34°N, 47.5°E, filled to the extent that it became little more than a surface reflection of the 24/12Z 500 mb upper trough (Figure A-13). The newly developed surface low continued to deepen and moved eastward over central Iran. At 24/12Z, it was located near 32.5°N, 53.5°E. The cold front from this low extended southward over the central Persian Gulf, and thence southwestward across central Saudi Arabia. By 24/12Z, surface pressures had begun to rise over northern Saudi Arabia to the rear of the cold front.

A detailed examination of the 24 Jan sequence is suggested (Figures A-12a-e). Note the contrast between the light to moderate southeasterly wind conditions (Kaus) which precede the penetration of the cold front into the Gulf, and the suddenness and intensity with which gale force shamal northwesterlies occur at and behind the cold front. These gale force northwesterlies are rare events; they occur less than 5% of the time in winter at most Gulf locations. These twin characteristics of rarity and suddenness in onset dramatically highlight the operational significance of the shamal gale force northwesterlies when compared to the normally light to moderate winter wind conditions in the Persian Gulf.

Also of interest is the velocity with which the front propagates down the Gulf: in excess of 40 kt. This velocity is not at all inconsistent with the gale force winds near the surface which propelled the front southeastward. These gale force northwesterly winds appear in this case to blow through a relatively shallow layer. A comparison of the 24/12Z surface analysis with the 24/12Z 500 mb analysis (Figure A-13) shows surface winds to be northwesterly behind the cold front but southwesterly at 500 mb, because the upper trough has not yet moved eastward over the Gulf.

Hour-by-hour wind averages taken from anemographs on Ahmadi Sea Island near Kuwait in the northern Gulf (Table A-1) and Das Island near 25°N, 53°E in the southern Gulf (Table A-2) indicate the onset of the shamal. In the north, onset of the shamal was comparatively abrupt and occurred between 24/06Z and 24/08Z. In the south, the wind veered more gradually than in the north. A northwesterly direction was established at Das Island by 24/14Z.

Seas rose rapidly in response to the action of the gale force winds over the shallow, warm waters of the Gulf. Combined sea heights of 5-6 ft were reported at AOC Gathering Station (southeast of Kuwait and near 28.5°N, 49°E) shortly after the shamal began at 24/09Z (Figure A-12c); they rose to 8-12 ft only three hours later at 24/12Z (Figure A-12d). Rigs in the vicinity of Ras Tanura, near 26.5°N, 50°E in the central Gulf, reported 7-10 ft combined sea heights within hours of the cold frontal passage and the onset of the shamal (Figure A-12d). By 24/15Z, observers at oil rig Seashell -- located east of the Qatar Peninsula at approximately 25.5°N, 52°E in a region subject to particularly strong wind conditions -- reported 12-15 ft combined sea heights under 40-50 kt northwest winds (Figure A-12e). Although these observations may have reflected some overestimation, they nonetheless illustrate graphically the rapid response of Gulf waters to the sudden surface stress applied by the gale force northwesterly winds of the shamal.

Thunderstorms occurred ahead of the cold front; they are apparent from surface observations near 30°N, 50°E at 24/06Z and 24/09Z (Figures A-12b and A-12c). Some past thundershower activity is also indicated in the same area at 24/12Z (Figure A-12d).

Reductions in surface visibility due to dust, haze, and blowing sand raised by the gale force winds behind the cold front are indicated in several areas: on the 24/09Z surface analysis, Figure A-12c, at Ras al Khafji near 28.5°N, 48.5°E on the northwestern shore of the Gulf, just south of Kuwait; on the 24/12Z surface analysis, Figure A-12d, at Ras al Khafji and AOC Gathering Station in the Gulf just to the east of Ras al Khafji; and on the 24/15Z surface analysis, Figure A-12e, in the southern Gulf at Doha near 25.5°N, 51.5°E and Umm Said near 24.5°N, 51.5°E (both on the eastern shore of the Qatar Peninsula), and further east at Das Island near 25°N, 53°E.

Table A-1. Hourly winds reported at Ahmadi Sea Island for 24 June 1974.

| <u>LT</u> <u>(LT=GMT+3)*</u> | <u>GMT</u> | <u>Direction</u> <u>(°)</u> | <u>Mean Speed</u> <u>(kt)</u> | <u>Max Gusts</u> <u>(kt)</u> |
|---------------------------------|------------|--------------------------------|----------------------------------|---------------------------------|
| 0100 | 23/2200Z | 060 | 8 | 11 |
| 0200 | 23/2300Z | 070 | 7 | 9 |
| 0300 | 24/0000Z | 100 | 7 | 9 |
| 0400 | 24/0100Z | 130 | 11 | 19 |
| 0500 | 24/0200Z | 140 | 13 | 24 |
| 0600 | 24/0300Z | 140 | 11 | 16 |
| 0700 | 24/0400Z | 120 | 6 | 12 |
| 0800 | 24/0500Z | 210 | 7 | 14 |
| 0900 | 24/0600Z | 220 | 13 | 26 |
| 1000 | 24/0700Z | 290 | 20 | 28 |
| 1100 | 24/0800Z | 300 | 20 | 31 |
| 1200 | 24/0900Z | 300 | 20 | 35 |
| 1300 | 24/1000Z | 290 | 36 | 49 |
| 1400 | 24/1100Z | 290 | 33 | 48 |
| 1500 | 24/1200Z | 280 | 26 | 39 |
| 1600 | 24/1300Z | 280 | 30 | 42 |
| 1700 | 24/1400Z | 280 | 31 | 42 |
| 1800 | 24/1500Z | 280 | 26 | 38 |
| 1900 | 24/1600Z | 300 | 22 | 34 |
| 2000 | 24/1700Z | 270 | 31 | 46 |
| 2100 | 24/1800Z | 260 | 28 | 42 |
| 2200 | 24/1900Z | 270 | 33 | 48 |
| 2300 | 24/2000Z | 280 | 32 | 42 |

Table A-2. Hourly winds reported at Das Island for 24 June 1974.

| <u>LT</u> <u>(LT=GMT+4)*</u> | <u>GMT</u> | <u>Direction</u> <u>(°)</u> | <u>Mean Speed</u> <u>(kt)</u> | <u>Max Gusts</u> <u>(kt)</u> |
|---------------------------------|------------|--------------------------------|----------------------------------|---------------------------------|
| 0100 | 23/2100Z | 080 | 16 | 20 |
| 0200 | 23/2200Z | 080 | 16 | 20 |
| 0300 | 23/2300Z | 080 | 14 | 19 |
| 0400 | 24/0000Z | 090 | 15 | 18 |
| 0500 | 24/0100Z | 090 | 15 | 19 |
| 0600 | 24/0200Z | 120 | 15 | 18 |
| 0700 | 24/0300Z | 140 | 15 | 19 |
| 0800 | 24/0400Z | 150 | 16 | 20 |
| 0900 | 24/0500Z | 160 | 15 | 19 |
| 1000 | 24/0600Z | 160 | 14 | 19 |
| 1100 | 24/0700Z | 180 | 14 | 18 |
| 1200 | 24/0800Z | 190 | 10 | 16 |
| 1300 | 24/0900Z | 230 | 9 | 12 |
| 1400 | 24/1000Z | 230 | 10 | 13 |
| 1500 | 24/1100Z | 230 | 10 | 14 |
| 1600 | 24/1200Z | 240 | 13 | 19 |
| 1700 | 24/1300Z | 290 | 13 | 34 |
| 1800 | 24/1400Z | 310 | 22 | 33 |
| 1900 | 24/1500Z | 310 | 24 | 37 |
| 2000 | 24/1600Z | 320 | 24 | 36 |
| 2100 | 24/1700Z | 310 | 24 | 38 |
| 2200 | 24/1800Z | 300 | 26 | 40 |
| 2300 | 24/1900Z | 300 | 28 | 41 |

*Local time/GMT differences vary in the Persian Gulf region. For detailed information consult the Standard Time Zone Chart of the World, published by the Defense Mapping Agency Hydrographic Center, Washington, D.C. 20390.

A.3.2 Satellite Data Interpretation

Satellite data, particularly from high resolution sensors such as those aboard the DMSP system, can provide valuable supplementary information to analysts and forecasters in the Persian Gulf region. In the following discussion, the figures referenced are the surface analyses discussed above (Figures A-10, A-11, A-12a,b,c,d); the 700 mb analysis at 24/00Z (Figure A-16); the 500 mb analyses at 24/00Z and 24/12Z (Figures A-9 and A-13); and the 200 mb analyses at 24/00Z and 24/12Z (Figures A-17 and A-18).

Vortex A in the left central portion of the visible and infrared satellite images (Figures A-14 and A-15, made at 24/0838Z) is the original, decaying surface low. Comparison of the satellite images with selected analyses -- surface at 24/06Z and 24/09Z, 700 mb at 24/00Z, and 500 mb at 24/00Z and 24/12Z -- indicates that the low was of considerable vertical extent and nearly vertically "stacked" at 24/00Z. This surface low, the one associated with the satellite image vortex, is depicted on the 24/12Z surface analysis (near 34°N, 47.5°E on Figure A-12) and subsequent analyses as a slowly filling surface trough, generally aligned with the 500 mb trough position, but surpassed in intensity by the newly developed low over Iran (near 32.5°N, 53°E). The position of vortex A shows a reasonably good match with both the 24/00Z and 24/12Z 500 mb centers and the 700 mb low center at 24/00Z.

The bright area, B, in the central position of Figures A-14 and A-15, corresponds well to the newly developing surface low on the 24/06Z, 24/09Z, and 24/12Z surface analyses (near 32°N, 49°E; 32°N, 50°E; and 32.5°N, 53°E, respectively). This is the low which underwent rapid development on 24 Jan and was favorably located to the east of the 500 mb trough line and near the polar jet axis (discussed below). The brightness of infrared returns of this developing feature suggests constituent cloud elements of considerable vertical extent. It should be noted that area B and the bright band, E, are decidedly convective in character. This lends support to the observation of Tracton (1973) that the occurrence of mesoscale convective activity can help trigger and enhance cyclogenesis. //

The northernmost spiral band, C, appears to be a cold front extending from the decaying vortex over Iraq. This agrees reasonably well with the surface analysis at 24/06Z (Figures A-11 and A-12b). The middle band, D, appears to be a newly developing cold front that extends from the developing surface low under area B. This agrees well with the 24/06Z and 24/09Z surface analyses (Figures A-12b,c). This front is the leading edge of the shamal, whose initial onset occurred in the northwestern part of the Gulf.

Perhaps the most striking band is that labeled E on Figures A-14 and A-15, a line of vigorous thunderstorm cells that extend from the center of the Gulf northward into central Iran and the developing surface low in area B. Band E looks strikingly similar to a prefrontal severe weather line in the U.S. Midwest in spring. Such lines are capable of producing severe thunderstorms and spawning tornadoes. Evidence of thunderstorm activity in this case study is pointed out in Section A.3.1 above. From the information available, however, there is no confirmation of tornado activity. The vertical extent of the thunderstorm line, E, is indicated by the bright returns in the infrared spectrum, Figure A-15. The parallel billows, G, extending east-northeastward from the line represent cirrus blowoff from the thunderstorm cells which is generally aligned in the direction of the average shear from the lower to upper levels of the troposphere.* Shearing-off of higher clouds with the upper winds is apparent at area H, corresponding to cirrus outflow from the developing low over western Iran. Surface reports for 24/06Z and 24/09Z near 30°N, 50°E (Figures A-12b,c) confirm the presence of cumulonimbus and thunderstorm activity over Iran near cloud band E.

The 200 mb analyses for 24 Jan suggest that the polar jet had intruded well south of the Taurus Mountains of Turkey. The cirrus blowoff from band E at lines G, from the developing low at B, and from cloud mass H, indicates the direction of the upper flow.

Notice that the cyclogenesis under area B occurs to the north of the polar jet position. Notice also that the thunderstorm activity in band E is most intense north of the northernmost edge of the subtropical jet. Anderson et al. (1974) have indicated that thunderstorm line development frequently is most intense north of the intersection of the subtropical jet with the squall line.

*Some indication of the shear can be obtained through examination of the available 700 mb, 500 mb, and 200 mb analysis for 24/00Z (Figs. A-16, A-9, and A-17, respectively). The general orientation of the vertical shear is southwesterly.

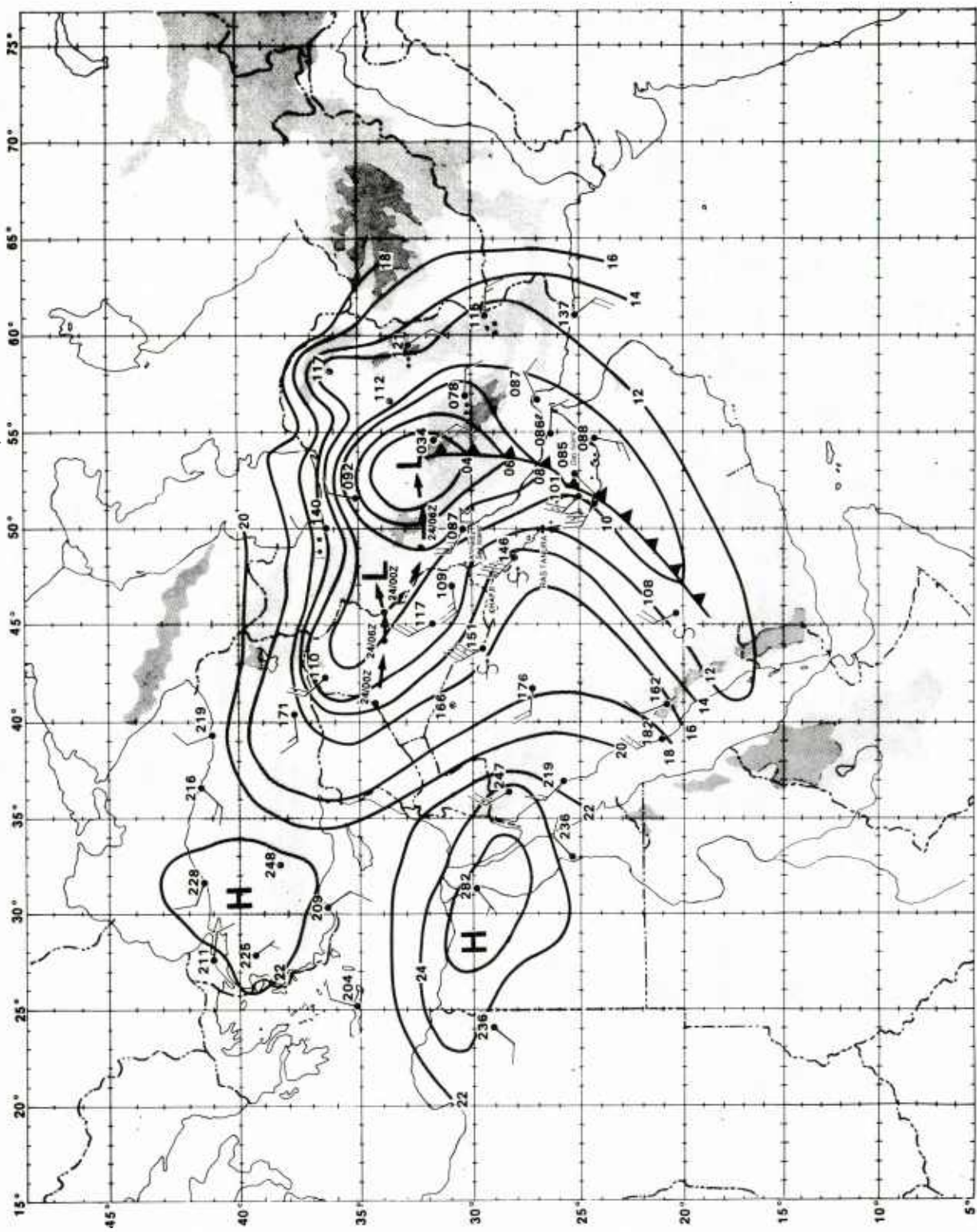


Figure A-12. Surface analysis, 24 Jan 1974 1200Z.

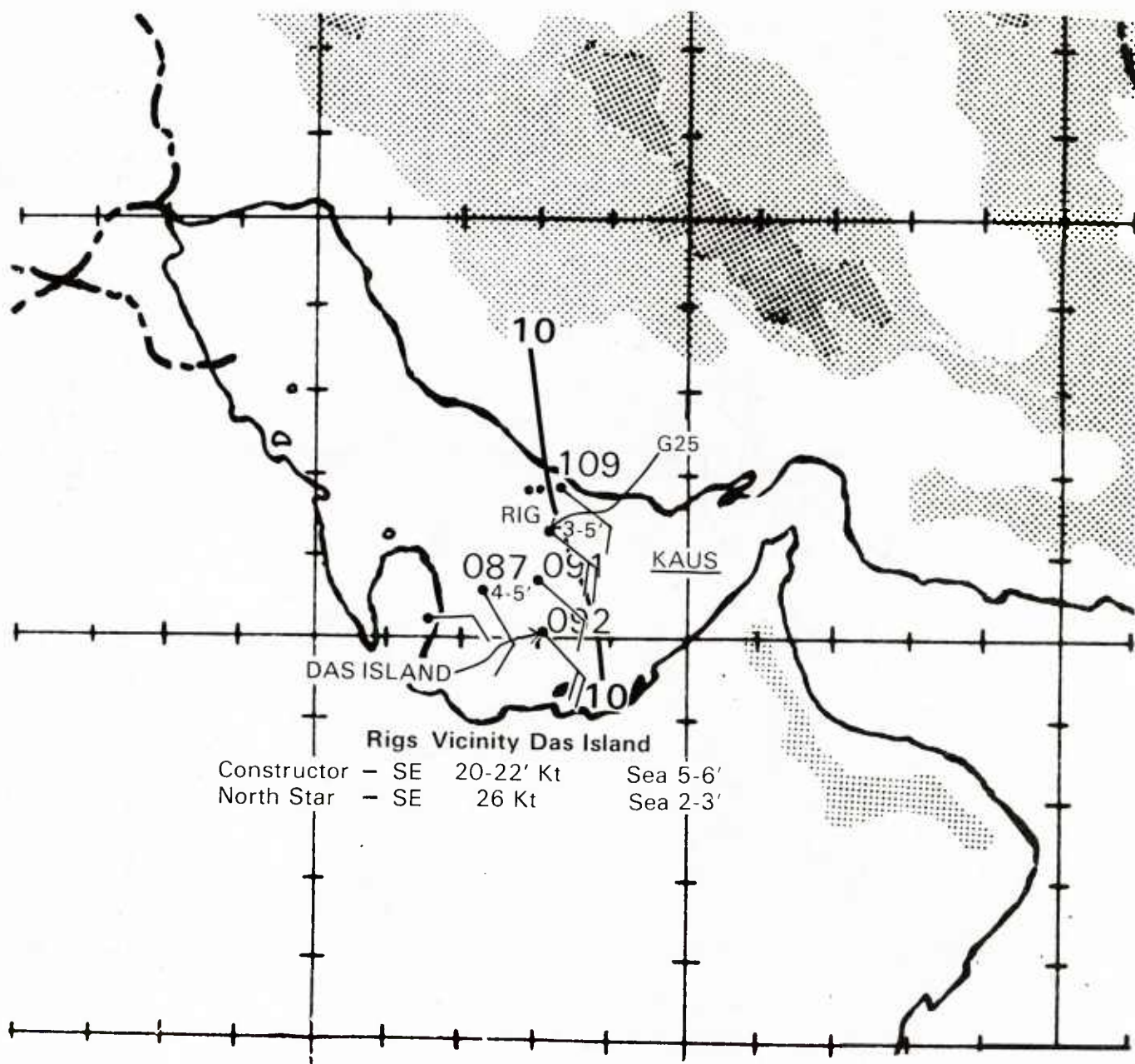
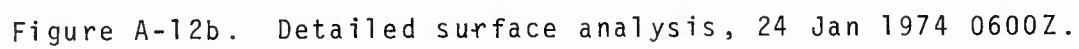


Figure A-12a. Detailed surface analysis, 24 Jan 1974 0300Z.



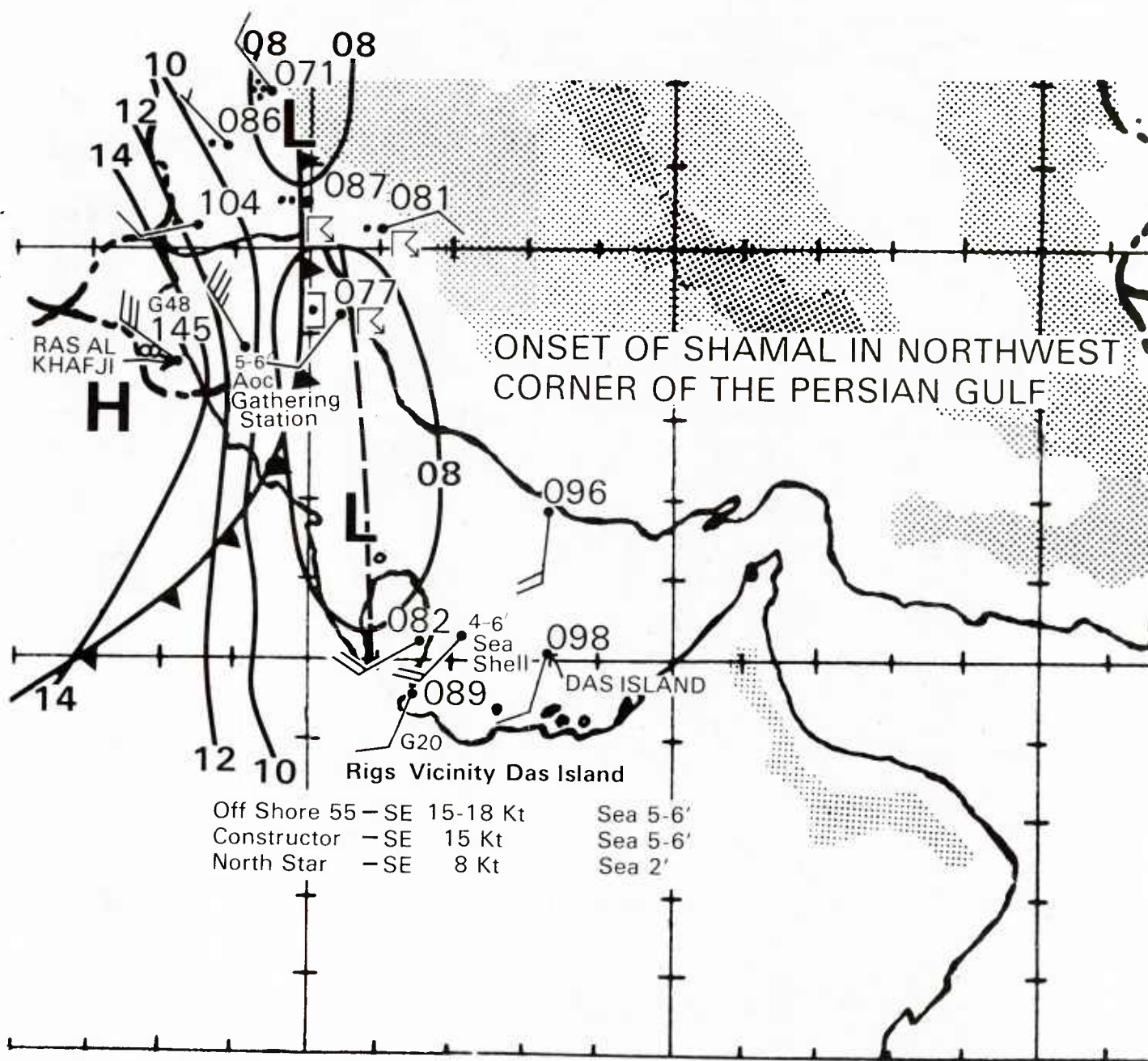


Figure A-12c. Detailed surface analysis, 24 Jan 1974 0900Z.

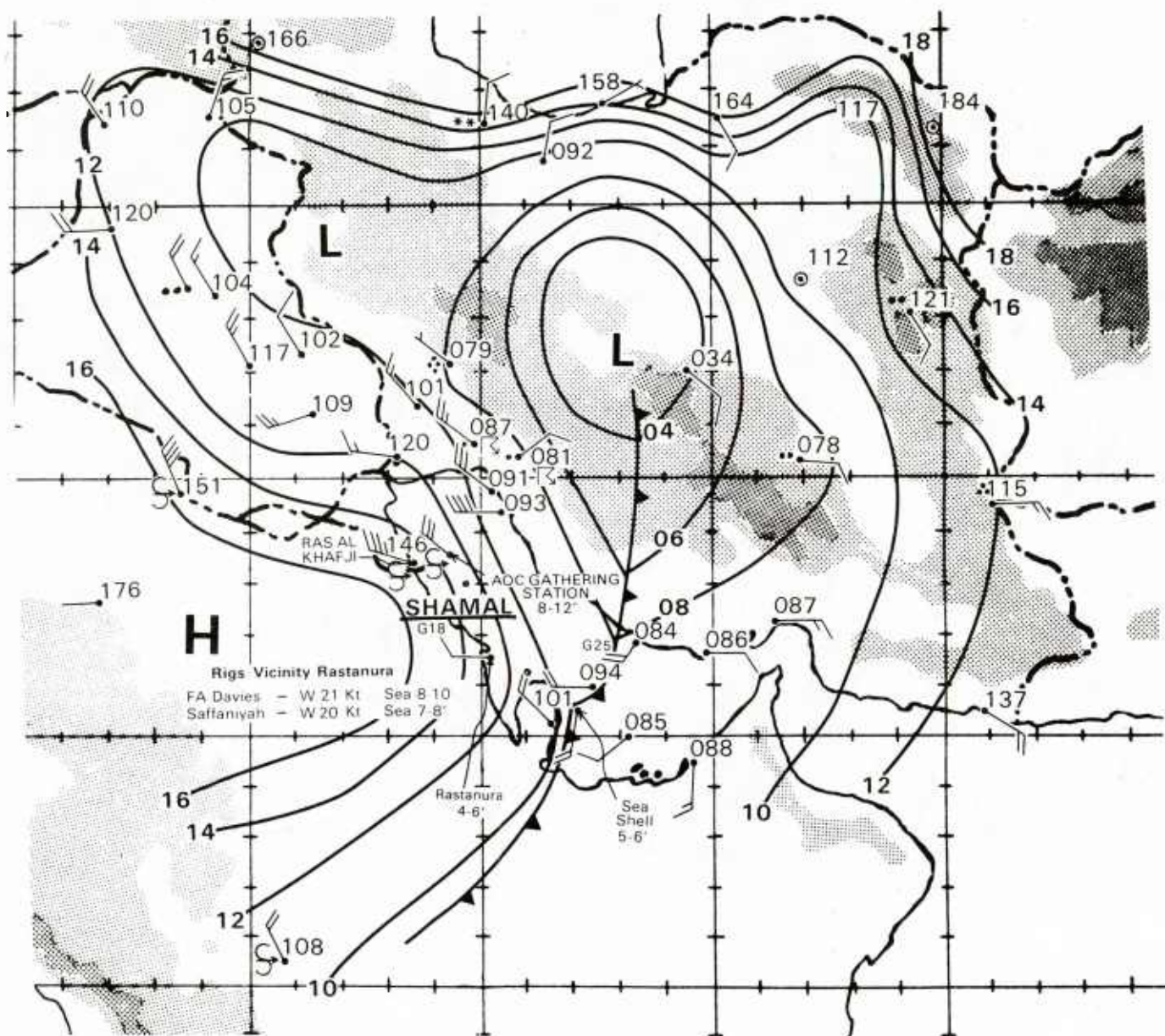


Figure A-12d. Detailed surface analysis, 24 Jan 1974 1200Z.

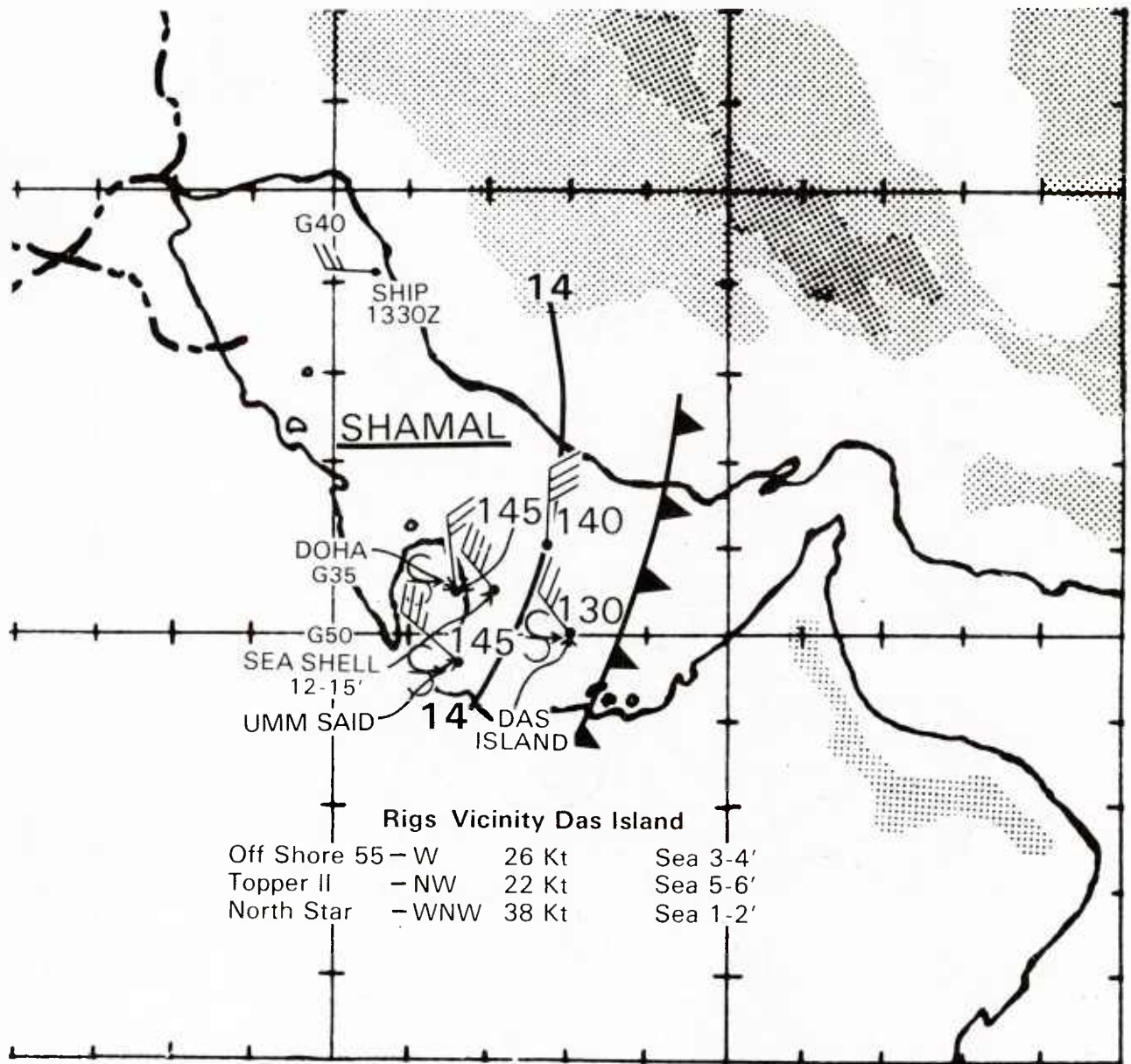


Figure A-12e. Detailed surface analysis, 24 Jan 1974 1500Z.

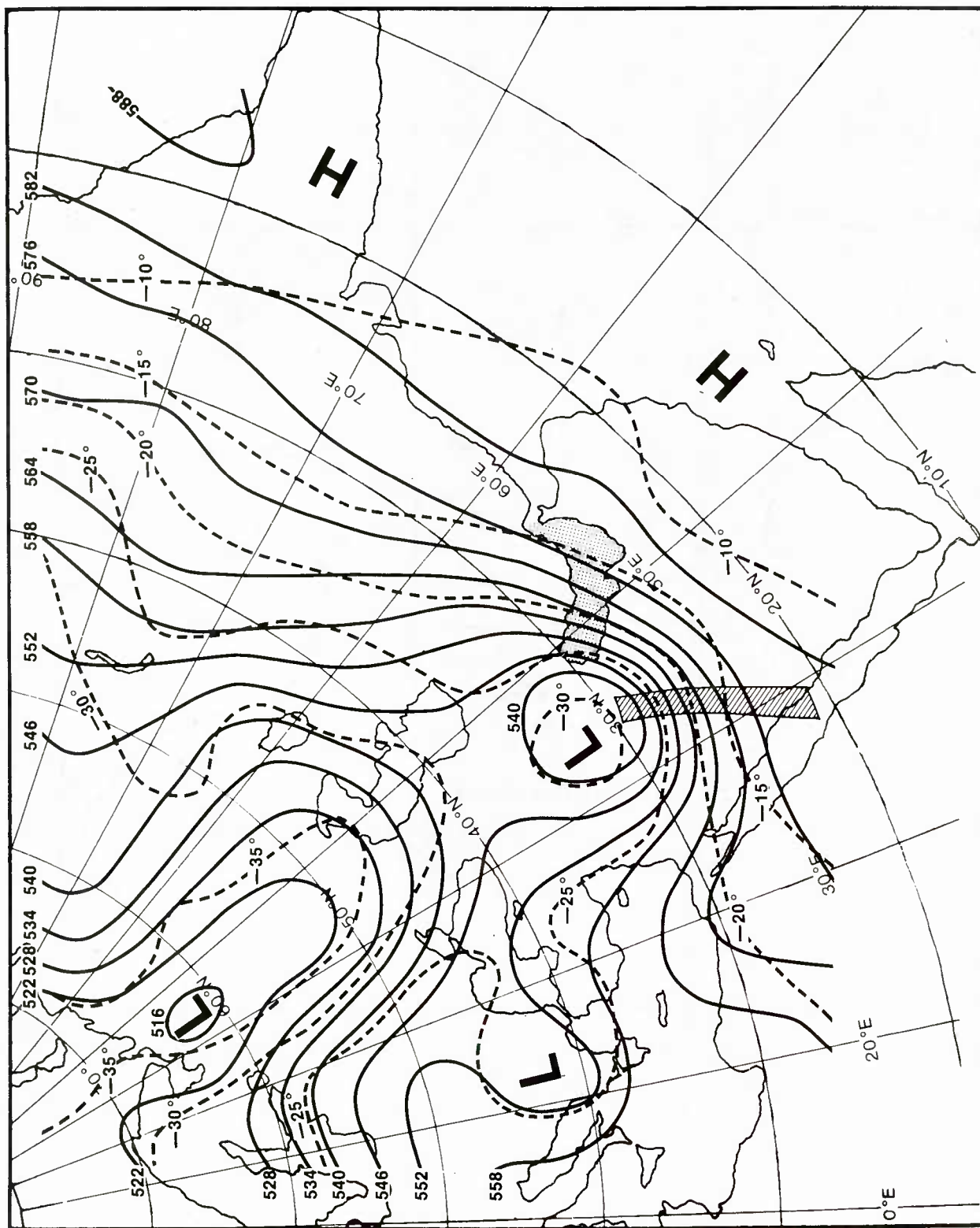


Figure A-13. 500 mb analysis, 24 Jan 1974 1200Z.

-- SATELLITE IMAGERY SHOWN ON NEXT FACING PAGES --



Figure A-14. DMSP visible image, 24 Jan 1974 0838Z.

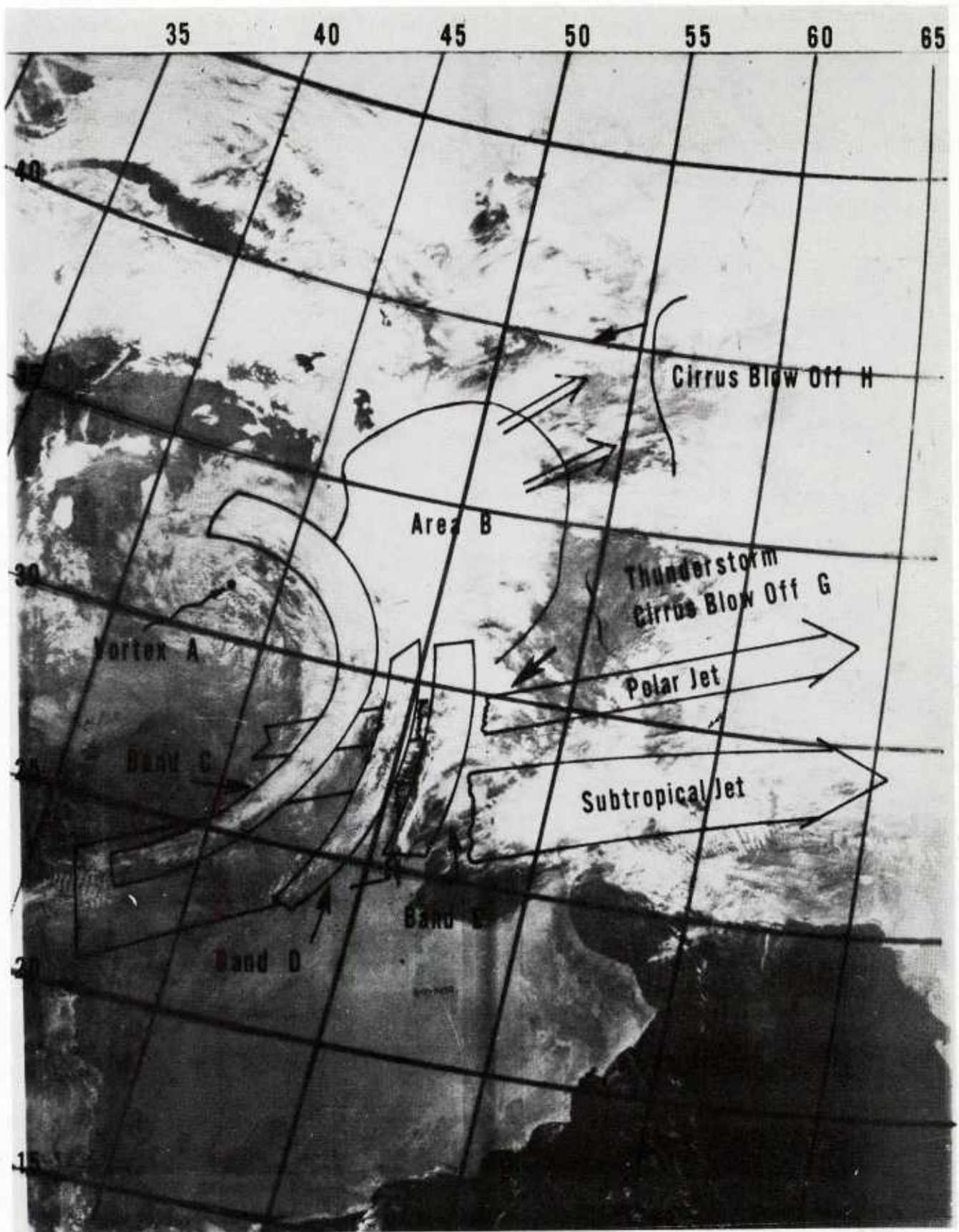


Figure A-14. Continued.

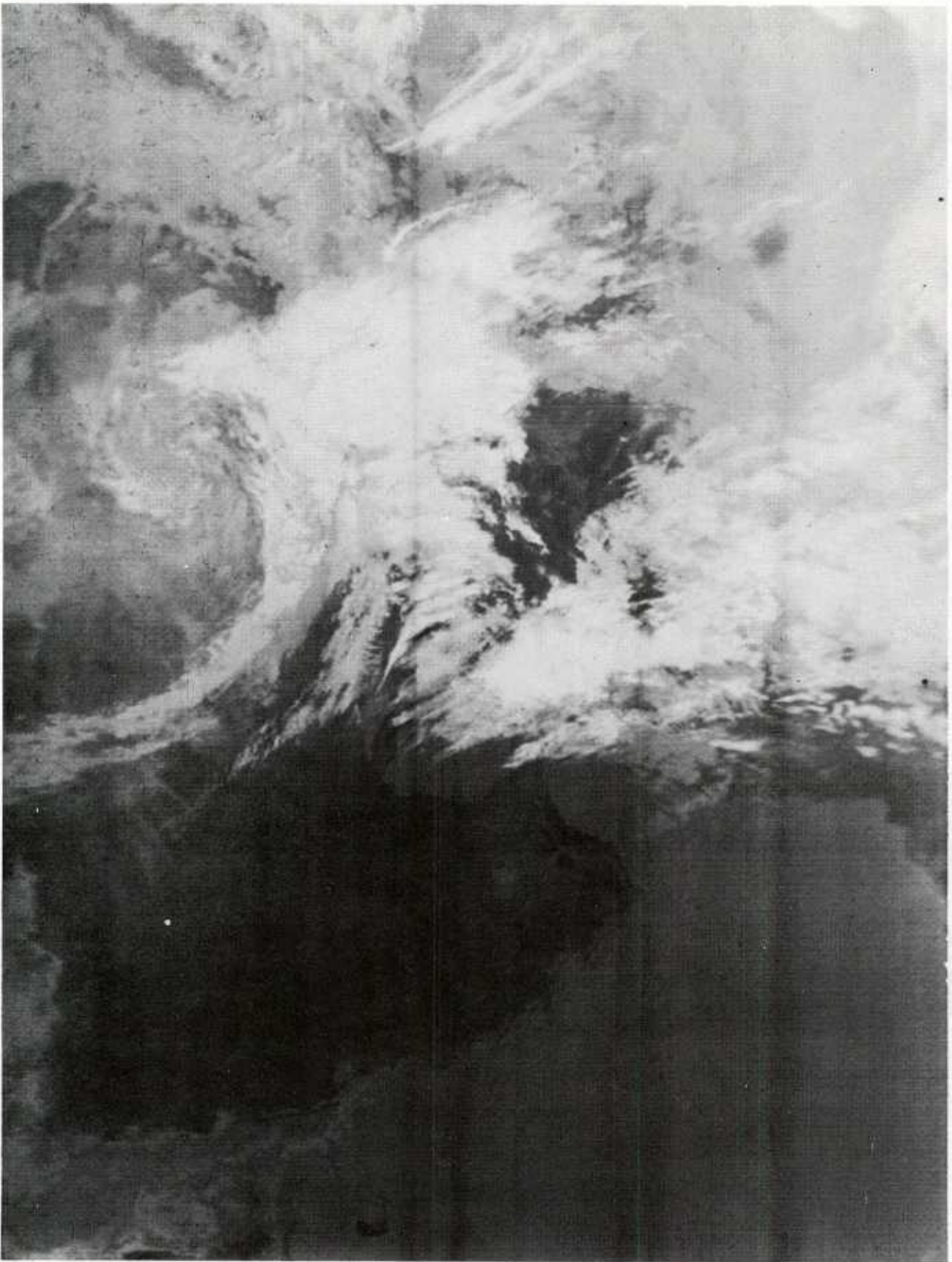


Figure A-15. DMSP IR image, 24 Jan 1974 0838Z.

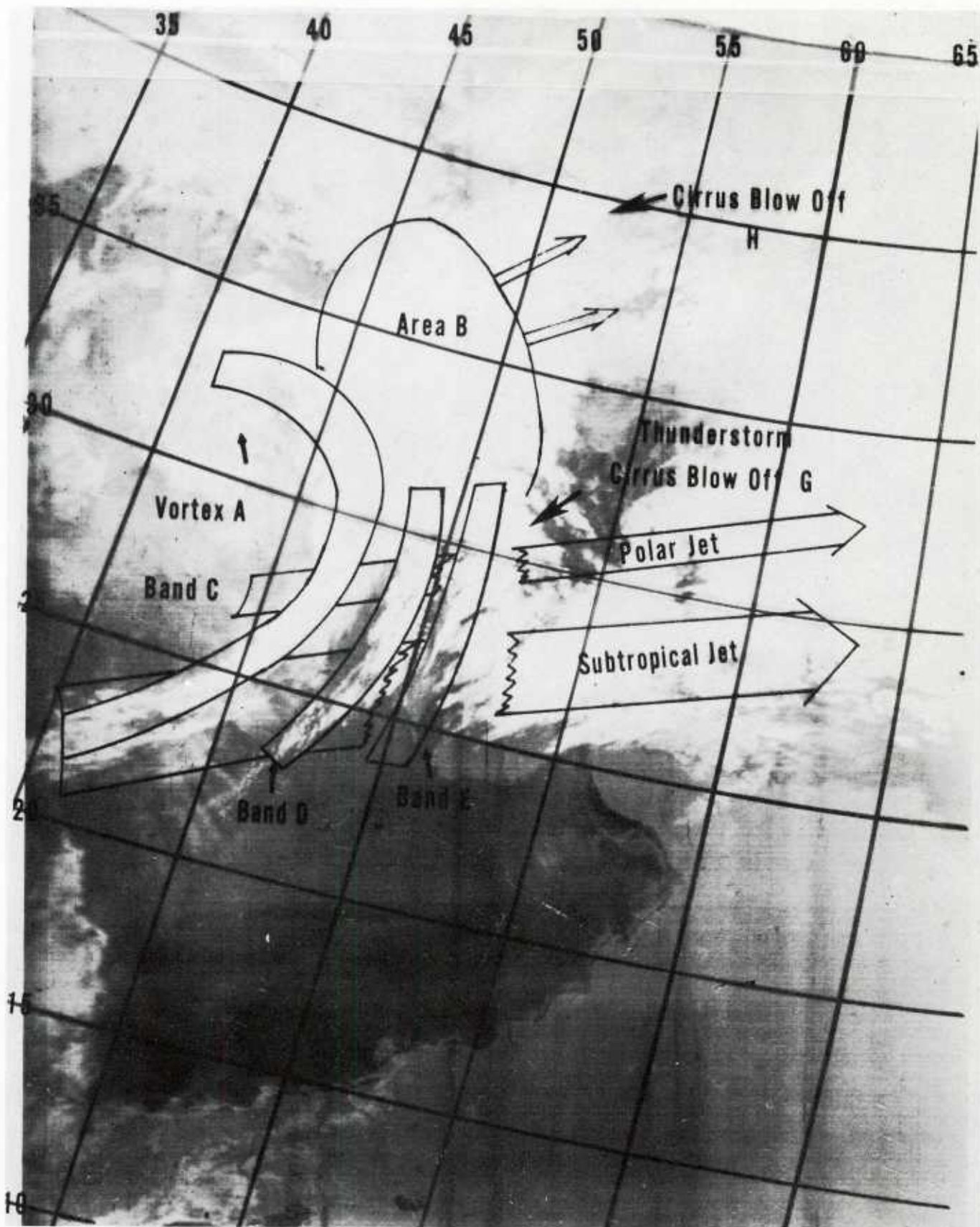


Figure A-15. Continued.

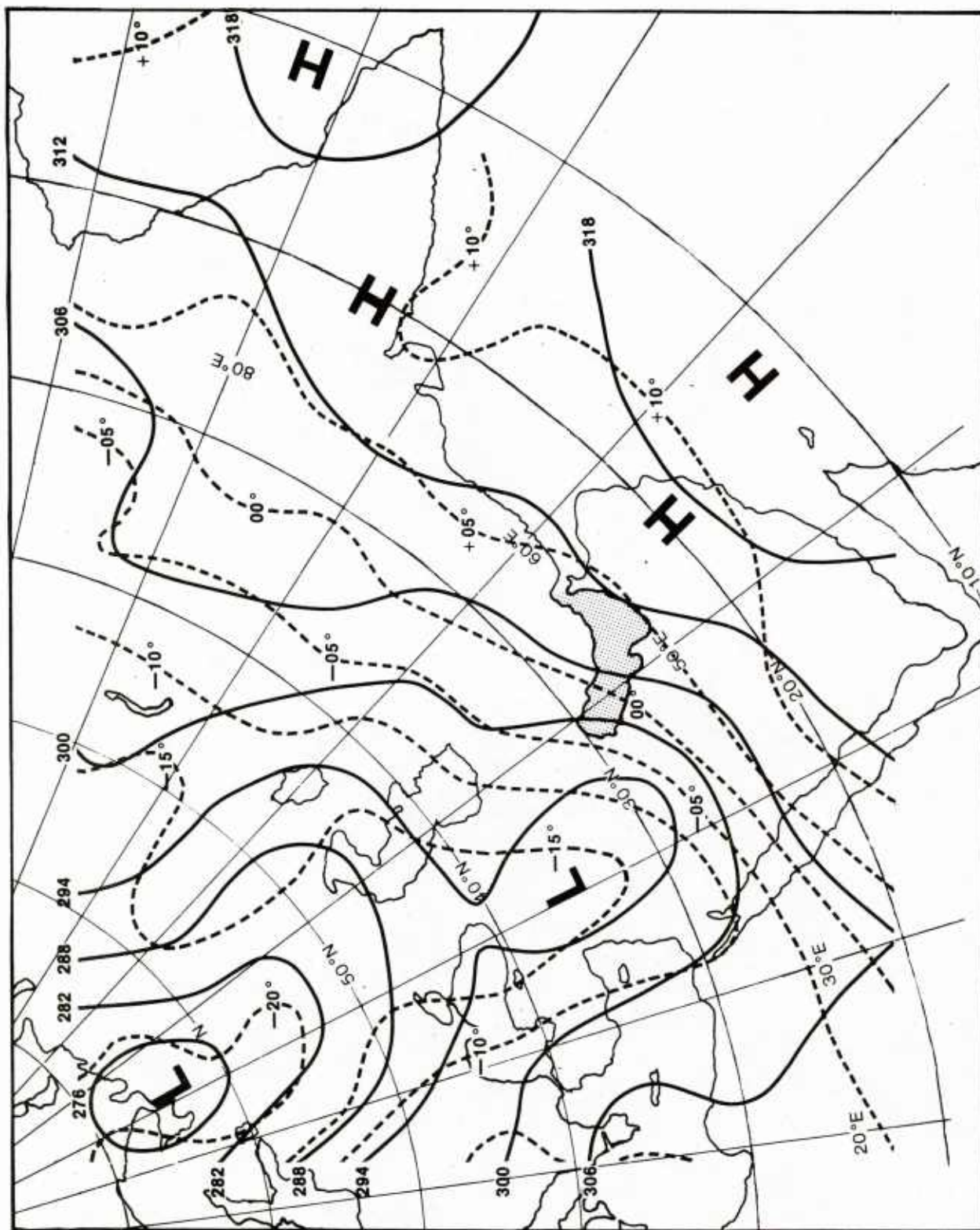


Figure A-16. 700 mb analysis, 24 Jan 1974 0000Z.

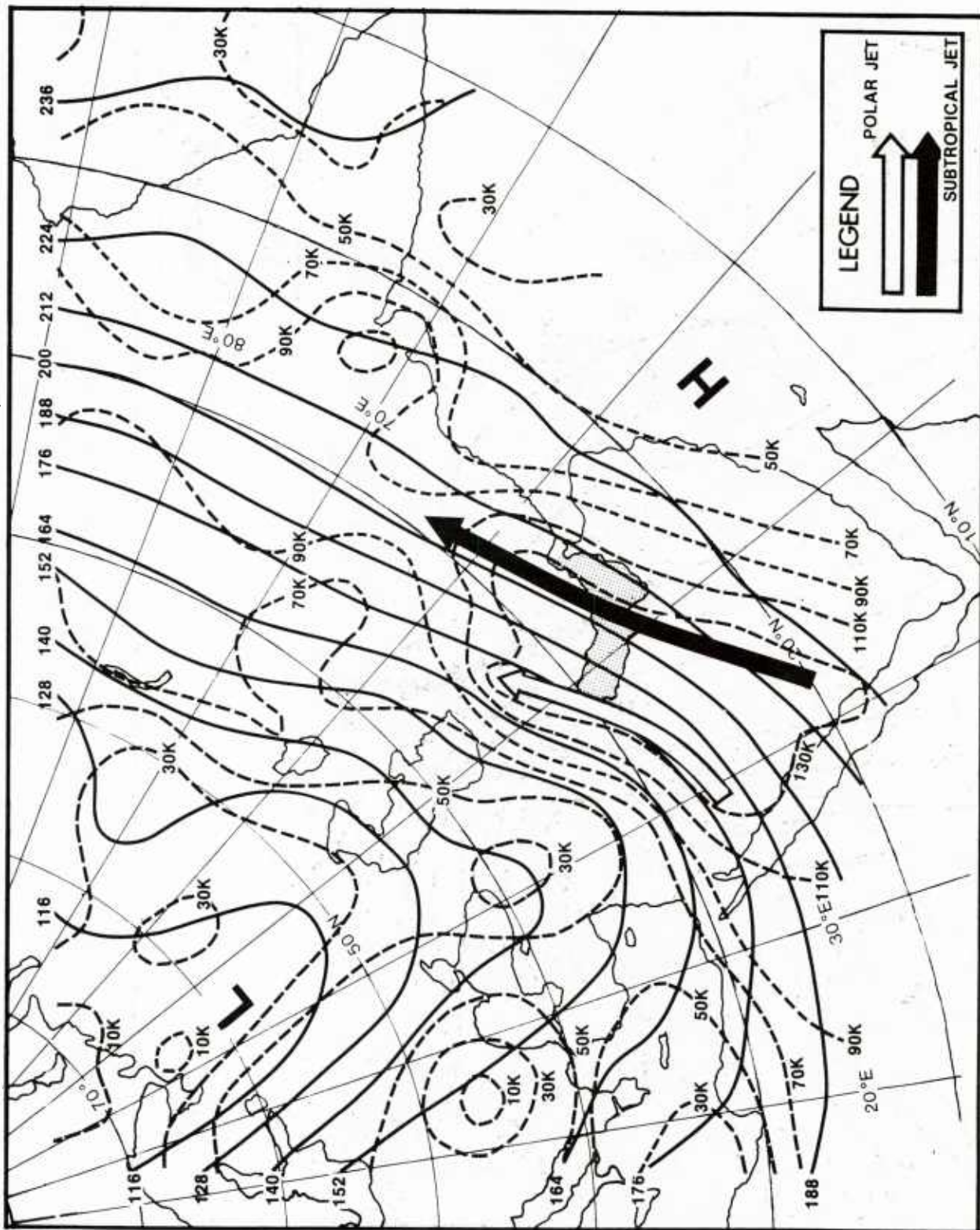


Figure A-17. 200 mb analysis, 24 Jan 1974 0000Z.

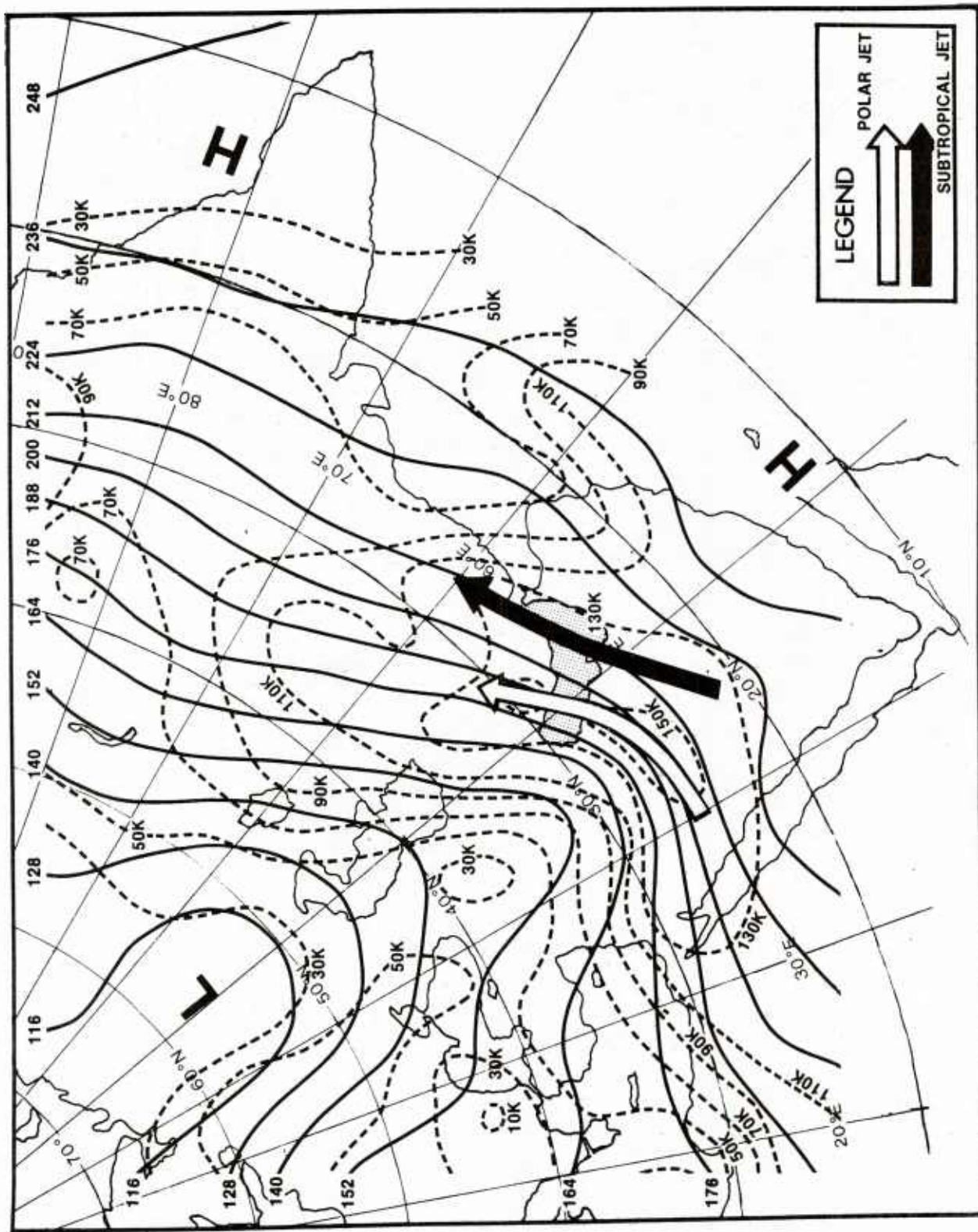


Figure A-18. 200 mb analysis, 24 Jan 1974 1200Z.

A.4 STEP FOUR

A.4.1 Synoptic Discussion

"The surface low ... [which formed at the previous step] ... becomes fully developed. It is advected by, and ahead of, the upper trough to eastern Iran. The associated cold front has swept down the Gulf into the Arabian Sea. Subsidence continues in the lower troposphere over northern Saudi Arabia to the west of the upper trough. The surface pressure over Saudi Arabia increases. The pressure gradient between the Saudi Arabian high and the lower pressure in the Gulf of Oman sustains the gale force shamal" (ref. Figure 3-1d).

The 500 mb analyses for 25/00Z and 25/12Z (Figures A-19 and A-20) show continued eastward progression of the upper trough. The 25/00Z, 25/06Z, and 25/12Z surface analyses (Figures A-21, A-22, A-23) show the movement of the surface cold front eastward well ahead of the upper trough axis. The detailed surface analyses for 25/03Z, 25/06Z, 25/09Z, 25/12Z, and 25/15Z (Figures A-23a, b,c,d,e) illustrate the continued strength and persistence of the surface winds in the region behind the cold front. At 25/03Z, for example, wind speeds with gusts to 40 kt were commonplace, as indicated by surface observations at the oil rigs and islands in the Gulf. Rig Seashell (near the Qatar Peninsula at approximately 25.5°N, 52°E) reported 15-20 ft combined sea heights; rig Wodeco III (near Lavan Island at 26.5°N, 53°E) reported 12-14 ft combined sea heights; and oil rigs near Das Island (25°N, 53°E) reported 7-12 ft combined sea heights. At 25/06Z, 25/09Z, 25/12Z, and 25/15Z, rig Seashell reported combined sea heights in the range 12-16 ft. Rig Wodeco III reported 6-8 ft at 25/12Z, and a rig near Das Island reported 8-10 ft at 25/15Z.

Tables A-3 and A-4 are hour-by-hour wind averages taken from anemographs on Ahmadi Sea Island off Kuwait and Das Island (25°N, 53°E), respectively. These tables show that the strongest winds during the period of this case study occurred after the cold frontal passage and for a time thereafter, then decreased slowly. At Ahmadi Sea Island in the northern Gulf, where the front passed near noon local time on 24 Jan, winds on 25 Jan were about 25 kt with gusts to 38 kt at 25/00L (24/21Z); these winds then decreased slowly during the morning hours to 10-15 kt by 25/12L (25/09Z). At Das Island in the southern Gulf, where the front passed later on 24 Jan, winds on 25 Jan reached a maximum near 25/00L (24/20Z), with winds of 25 kt and gust to 48 kt; these winds then decreased slowly through the day to 16 kt with gusts to 23 kt at 25/23L (25/19Z). Lavan Island, near 27°N, 53°E on the eastern side of the southern Gulf, reported a peak wind of 58 kt at 25/0145L (24/2215Z).

Reduced visibilities due to blowing sand and dust were reported at stations throughout the southern Gulf from 25/03Z-25/15Z. Recently concluded thunderstorm activity occurred again over the Iranian highlands and at Bushire

Table A-3. Hourly winds reported at Ahmadi Sea Island for 25 Jan 1974.

| <u>LT</u> <u>(LT=GMT+3)*</u> | <u>GMT</u> | <u>Direction</u> <u>(°)</u> | <u>Mean Speed</u> <u>(kt)</u> | <u>Max Gusts</u> <u>(kt)</u> |
|---------------------------------|------------|--------------------------------|----------------------------------|---------------------------------|
| 0000 | 24/2100Z | 290 | 25 | 38 |
| 0100 | 24/2200Z | 290 | 25 | 35 |
| 0200 | 24/2300Z | 290 | 27 | 36 |
| 0300 | 25/0000Z | 290 | 26 | 34 |
| 0400 | 25/0100Z | 300 | 25 | 34 |
| 0500 | 25/0200Z | 300 | 25 | 33 |
| 0600 | 25/0300Z | 300 | 23 | 31 |
| 0700 | 25/0400Z | 320 | 24 | 31 |
| 0800 | 25/0500Z | 320 | 24 | 32 |
| 0900 | 25/0600Z | 320 | 22 | 28 |
| 1000 | 25/0700Z | 330 | 17 | 24 |
| 1100 | 25/0800Z | 330 | 13 | 17 |
| 1200 | 25/0900Z | 310 | 10 | 15 |

Table A-4. Hourly winds reported at Das Island for 25 Jan 1974

| <u>LT</u> <u>(LT=GMT+4)*</u> | <u>GMT</u> | <u>Direction</u> <u>(°)</u> | <u>Mean Speed</u> <u>(kt)</u> | <u>Max Gusts</u> <u>(kt)</u> |
|---------------------------------|------------|--------------------------------|----------------------------------|---------------------------------|
| 0000 | 24/2000Z | 300 | 25 | 48 |
| 0100 | 24/2100Z | 300 | 25 | 38 |
| 0200 | 24/2200Z | 290 | 27 | 41 |
| 0300 | 24/2300Z | 290 | 27 | 40 |
| 0400 | 25/0000Z | 300 | 25 | 40 |
| 0500 | 25/0100Z | 300 | 27 | 40 |
| 0600 | 25/0200Z | 300 | 25 | 40 |
| 0700 | 25/0300Z | 300 | 21 | 38 |
| 0800 | 25/0400Z | 310 | 21 | 37 |
| 0900 | 25/0500Z | 300 | 20 | 32 |
| 1000 | 25/0600Z | 290 | 19 | 28 |
| 1100 | 25/0700Z | 290 | 18 | 26 |
| 1200 | 25/0800Z | 290 | 18 | 28 |
| 1300 | 25/0900Z | 290 | 18 | 26 |
| 1400 | 25/1000Z | 280 | 19 | 27 |
| 1500 | 25/1100Z | 290 | 18 | 26 |
| 1600 | 25/1200Z | 290 | 18 | 27 |
| 1700 | 25/1300Z | 290 | 18 | 28 |
| 1800 | 25/1400Z | 290 | 19 | 30 |
| 1900 | 25/1500Z | 300 | 19 | 30 |
| 2000 | 25/1600Z | 300 | 18 | 26 |
| 2100 | 25/1700Z | 300 | 17 | 26 |
| 2200 | 25/1800Z | 310 | 16 | 26 |
| 2300 | 25/1900Z | 300 | 16 | 23 |

*See footnote to Tables A-1 and A-2.

(vicinity of 30°N, 50°E) at about 25/06Z (see Figure A-23b). The surface pressure over northern Saudi Arabia and Iraq increased on the order of 10-15 mb between 24/06Z and 25/06Z and between 24/12Z and 25/12Z. (Compare Figures A-11 with A-22 and A-12 with A-23.) The intensification of surface high pressure over northern Saudi Arabia is associated with the subsidence that occurred in the lower troposphere in the region to the northwest of the surface cold front to the rear of the upper trough axis. The 25/06Z and 25/12Z surface analyses show the surface pressure gradient between the Gulf of Oman and the high pressure over northern Saudi Arabia: this is the gradient that drives the shamal.

A.4.2 Satellite Data Interpretation

The DMSP visible and IR images for 25 Jan, Figures A-24 and A-25, show a "frontal rope," line A, positioned just southeast of the Arabian Peninsula. The frontal rope, a manifestation of a cold front, is a thin cloud line associated with the leading edge of an advancing cold air mass. When the cold air pushes out from a land mass over the open sea, as is the case here, the frontal rope typically takes the shape of the coastline. An average southeastward speed of movement of near 40 kt would have been required for the cold front to have moved in 24 hr from the northern portion of the Persian Gulf to the position in the Arabian Sea depicted on the satellite images. Such movement is unsupported by the 500 mb upper air pattern, which was west to southwesterly at this time over the Arabian Peninsula. However, the frontal movement was related to the wind flow in a shallow layer near the surface, characterized by the 30-40 kt surface winds reported at or near the cold front as it moved southeastward down the Gulf on 24 Jan.

The somewhat characteristic "signature" of relatively colder air streaming over warmer waters appeared over the Gulf on 25 Jan. Heated from below, the air soon became unstable and cumulus convection developed. Some indication of at least moderate vertical extent can be seen by the relative brightness of these clouds on the IR image (Figure A-25). Convective activity is further indicated by past thundershower activity reported at Kharg Island (near 29°N, 50.5°E) (see 25/06Z surface analysis, Figure A-23b).

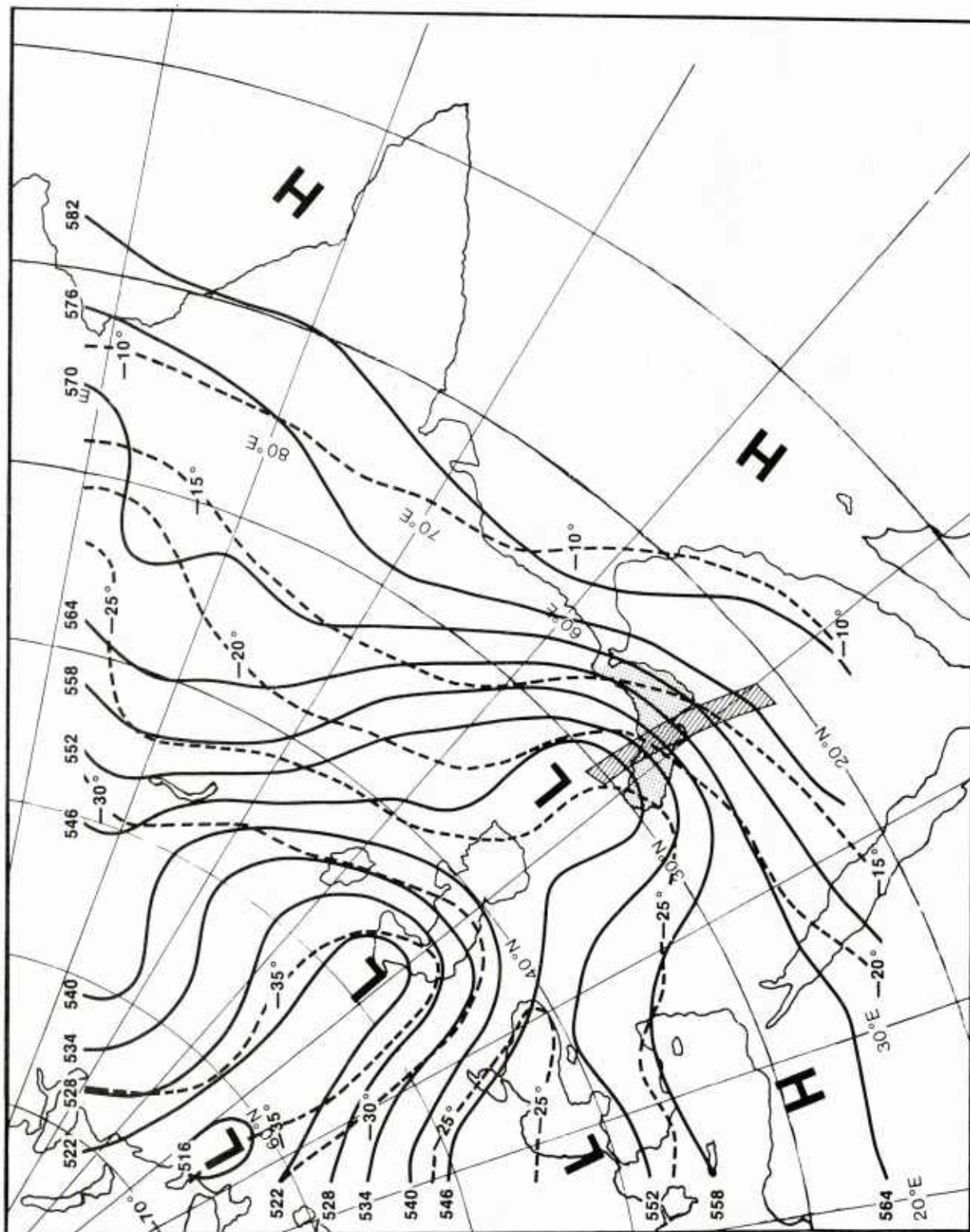


Figure A-19. 500 mb analysis, 25 Jan 1974 0000Z.

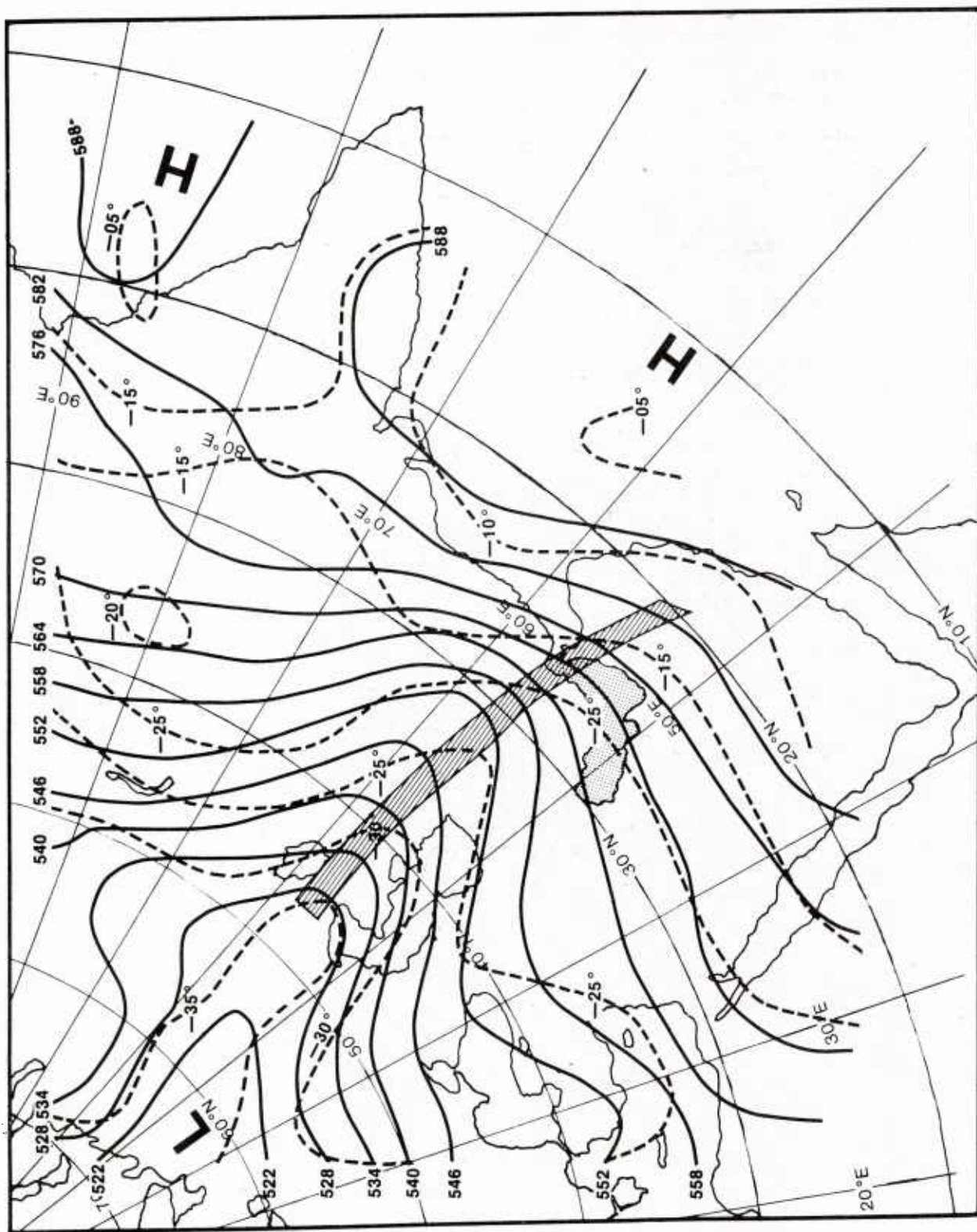


Figure A-20. 500 mb analysis, 25 Jan 1974 1200Z.

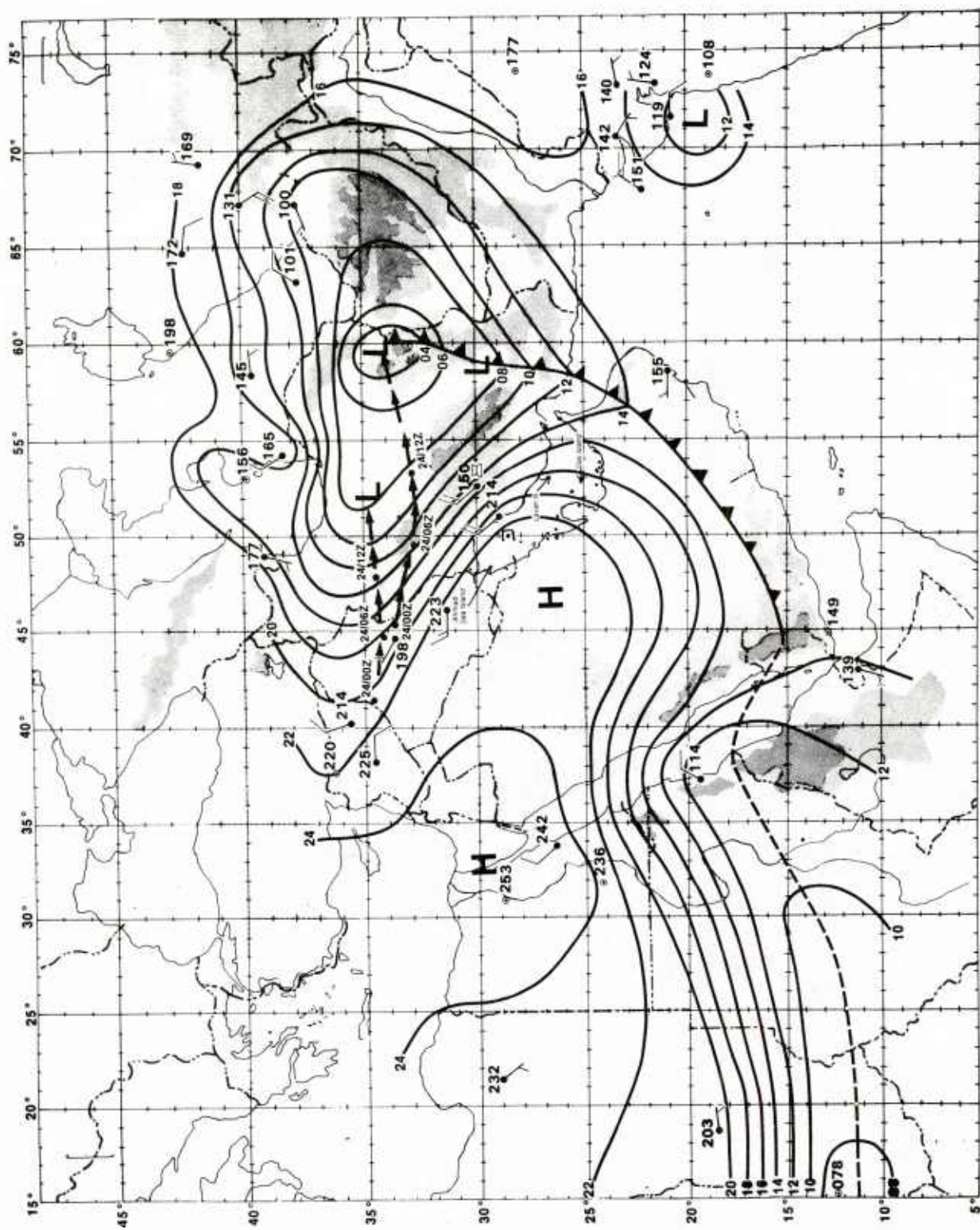


Figure A-21. Surface analysis, 25 Jan 1974 0000Z.

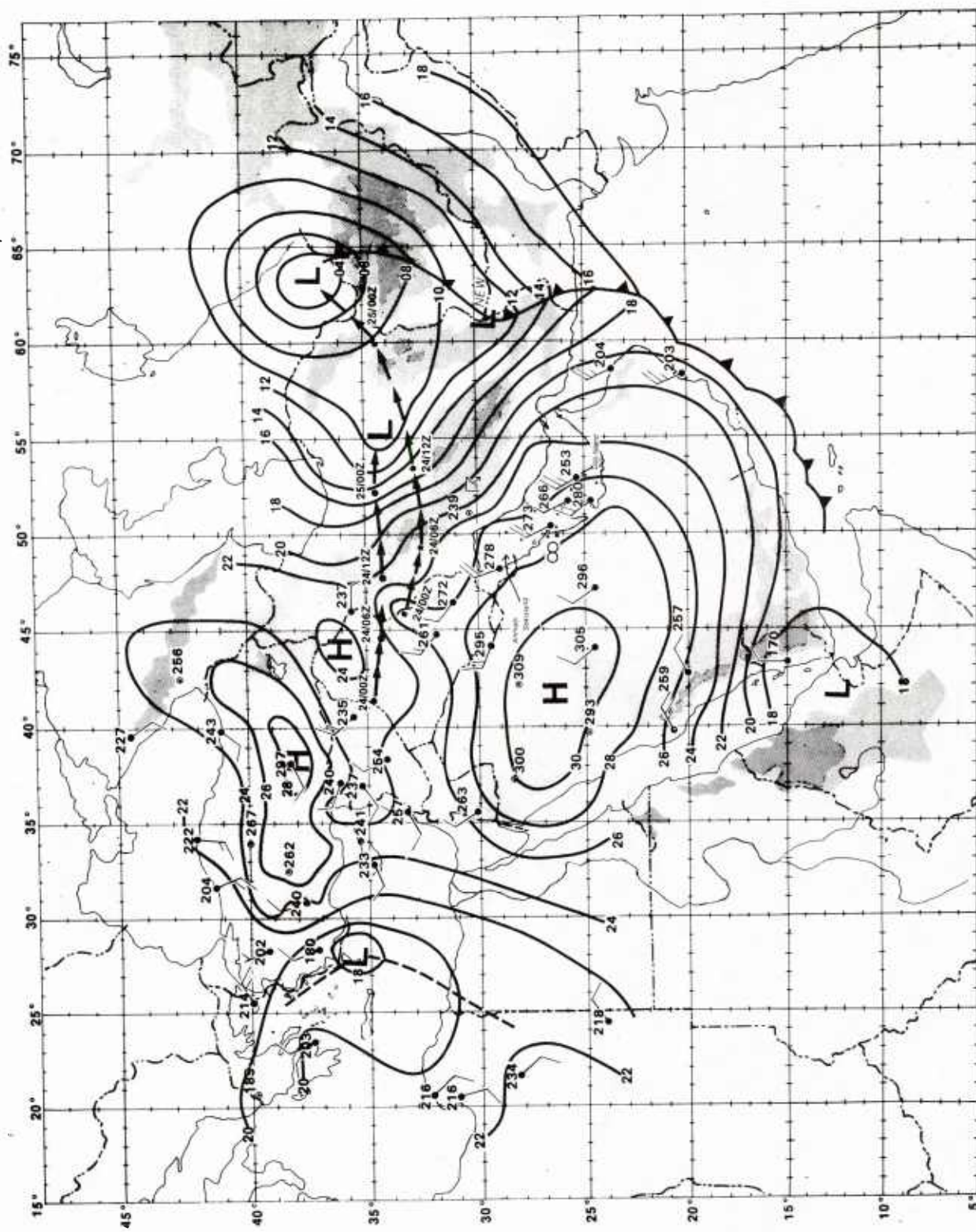


Figure A-22. Surface analysis, 25 Jan 1974 0600Z.

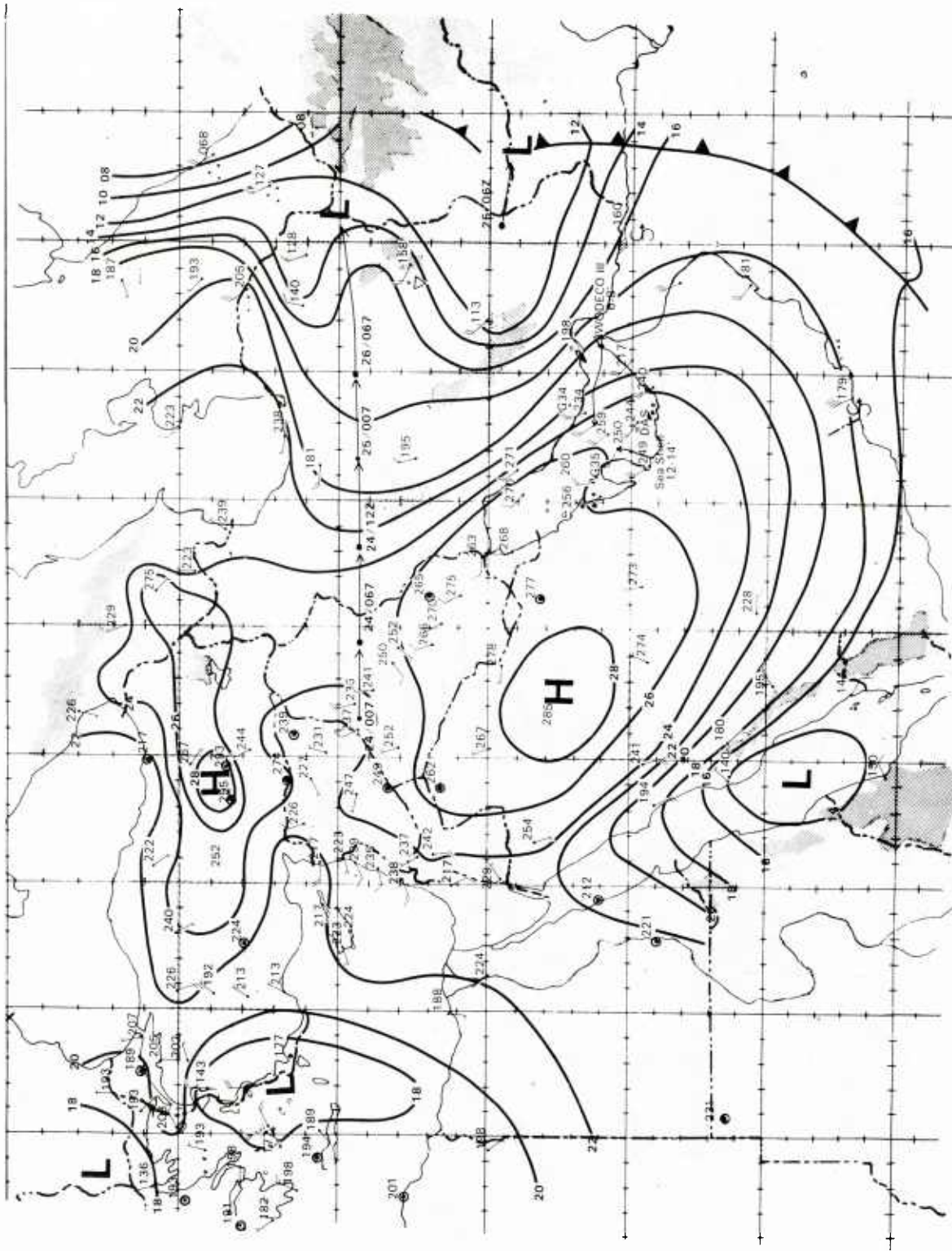


Figure 23. Surface analysis, 25 Jan 1974, 1200Z.

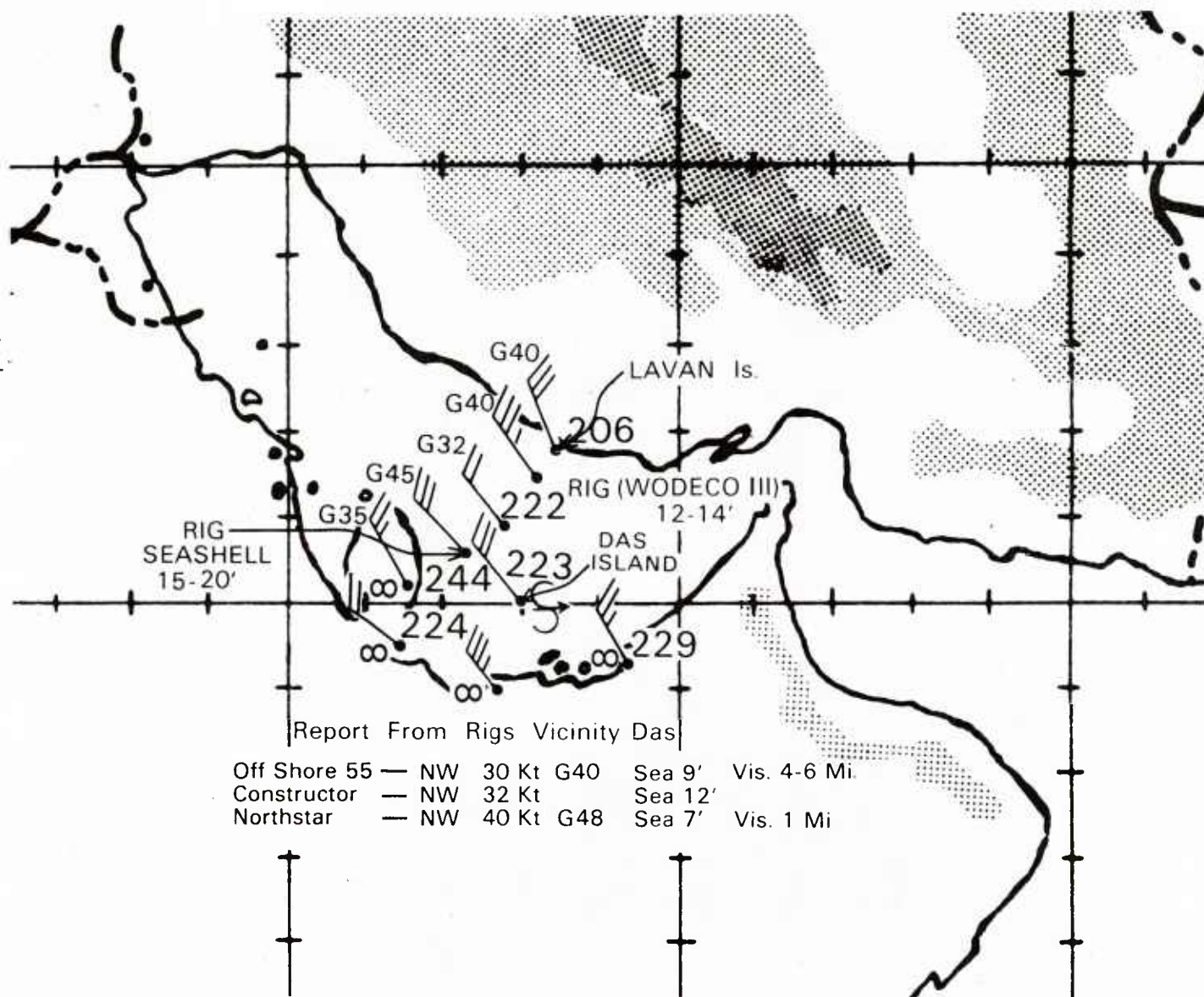


Figure A-23a. Detailed surface analysis, 25 Jan 1974 0300Z.

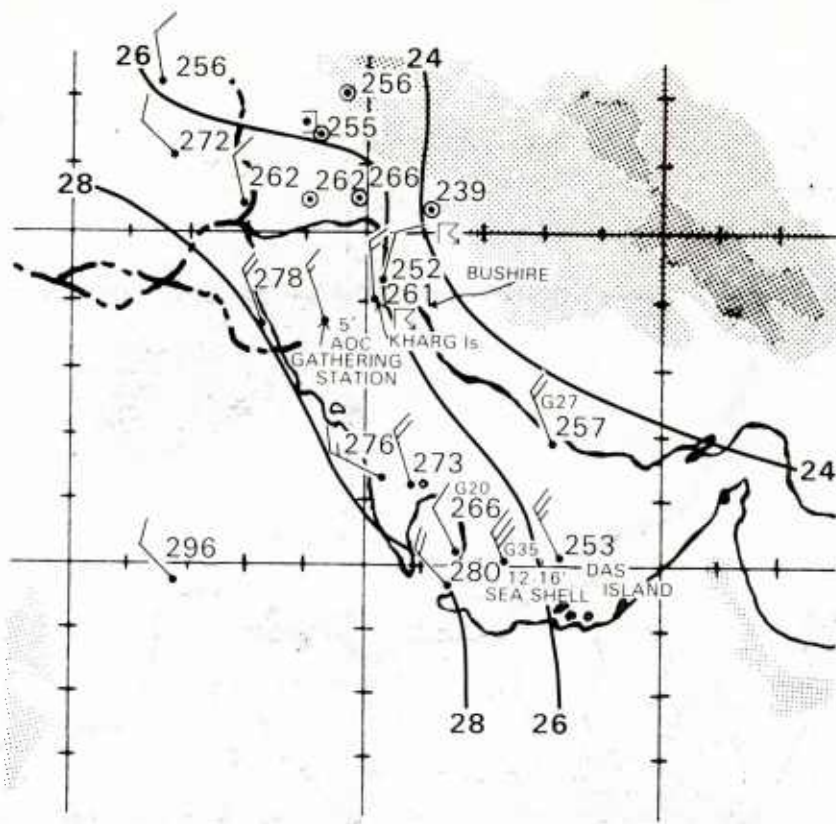


Figure A-23b. Detailed surface analysis, 25 Jan 1974 0600Z.

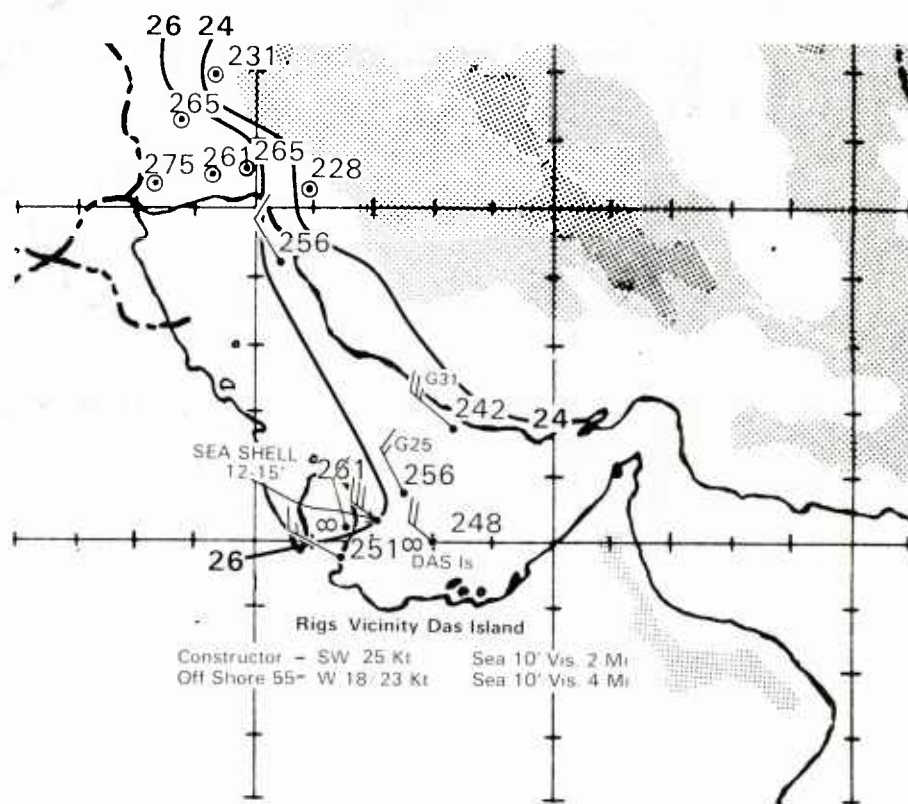


Figure A-23c. Detailed surface analysis, 25 Jan 1974 0900Z.

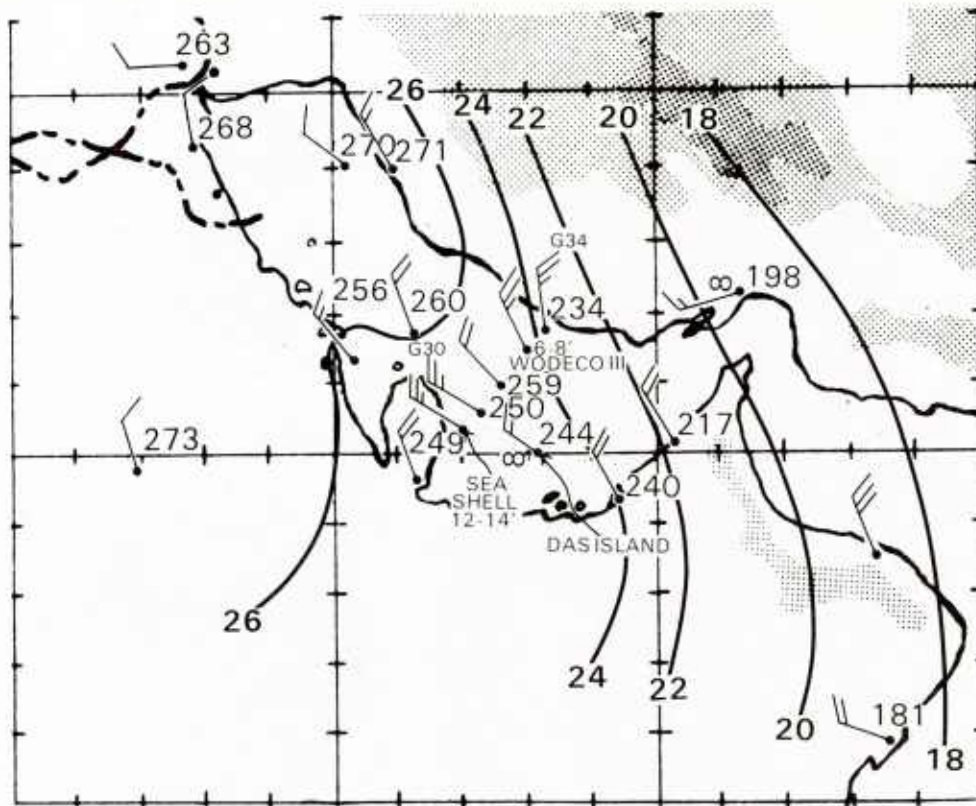


Figure A-23d. Detailed surface analysis, 25 Jan 1974 1200Z.

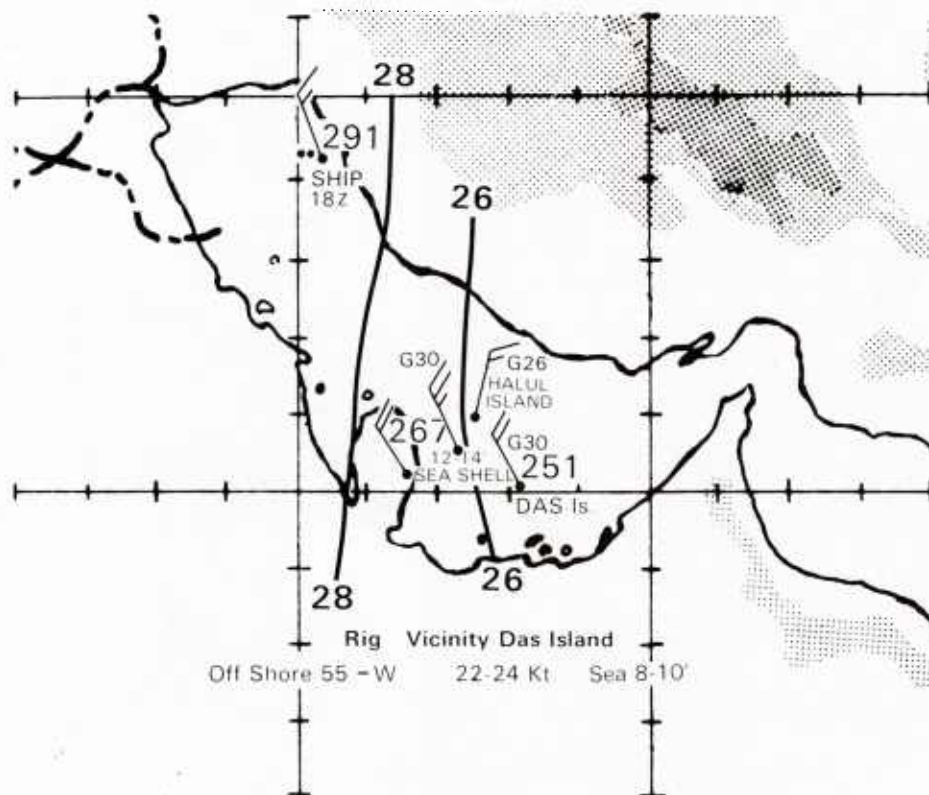


Figure A-23e. Detailed surface analysis, 25 Jan 1974 1500Z.

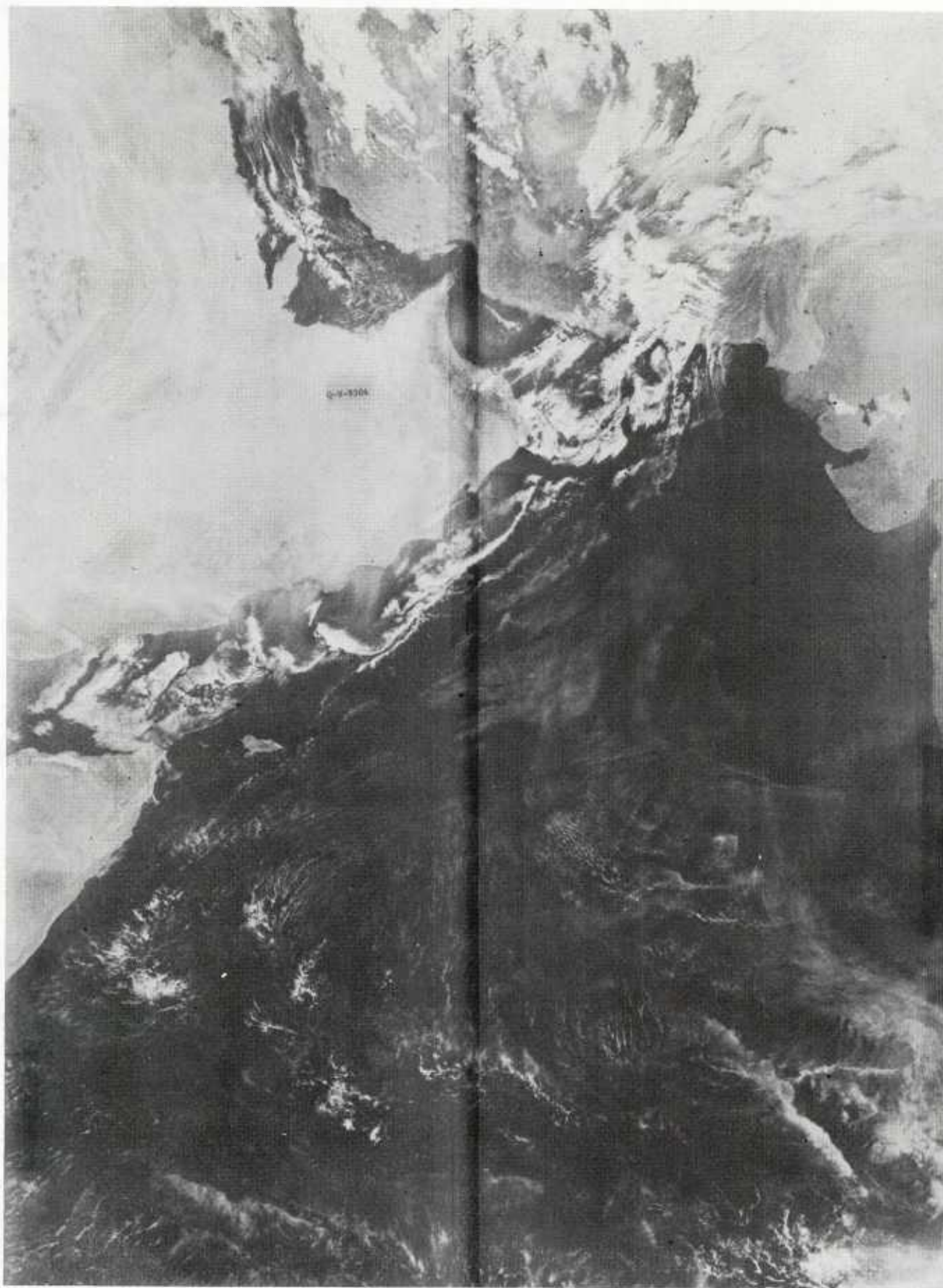


Figure A-24. DMSP visible image, 25 Jan 1974 0838Z.

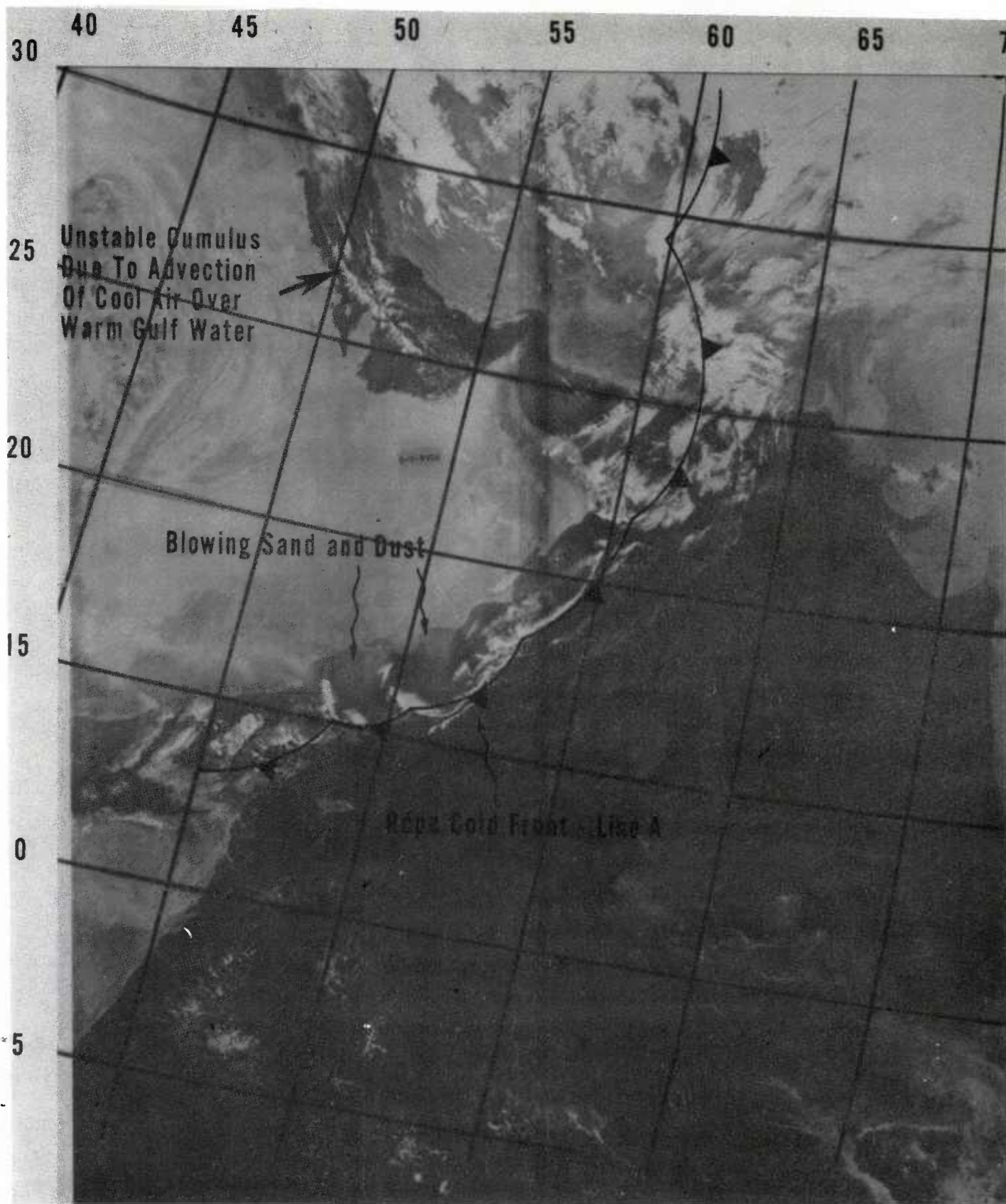


Figure A-24. Continued.

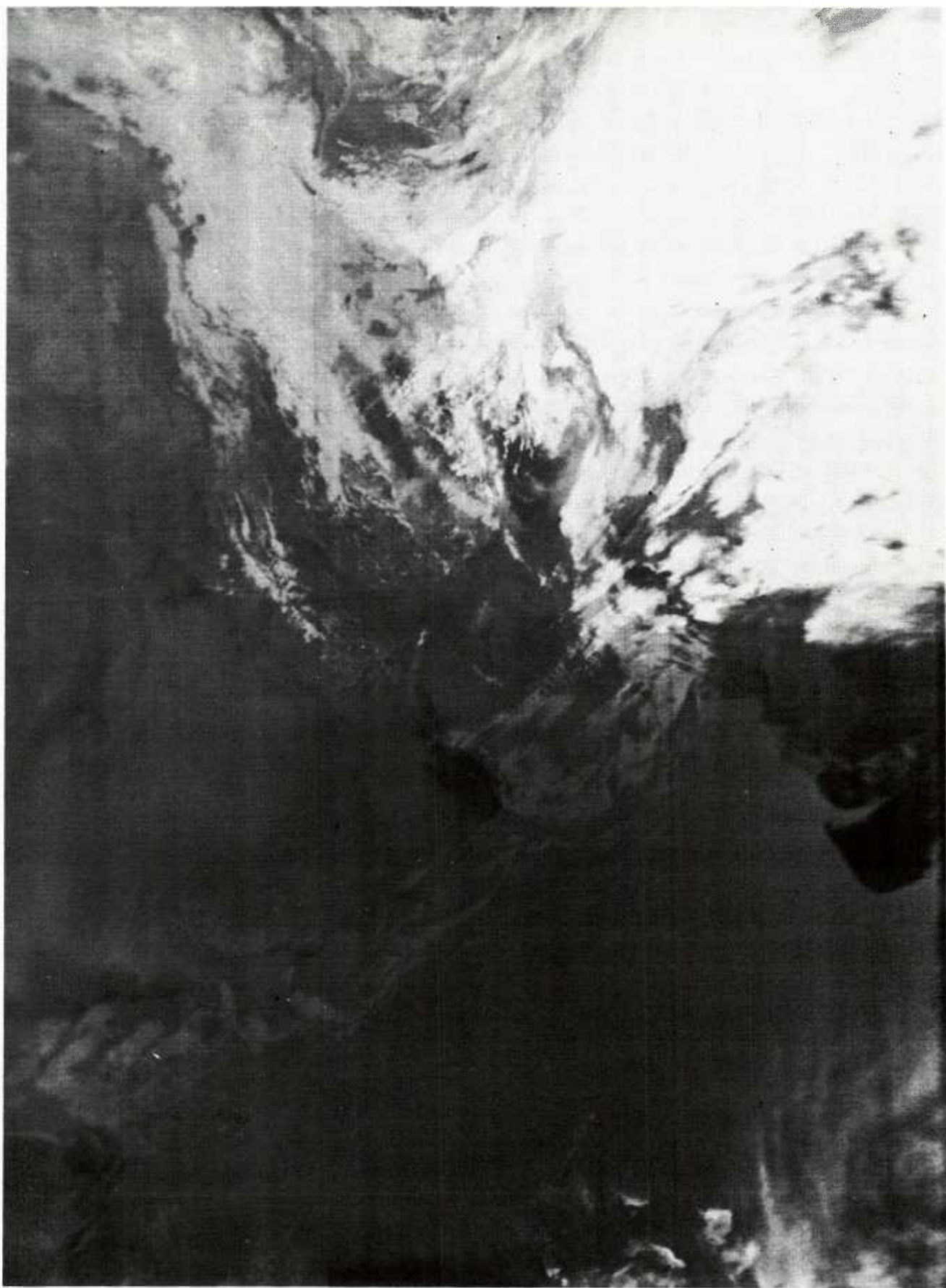


Figure A-25. DMSP IR image, 25 Jan 1974 0838Z.

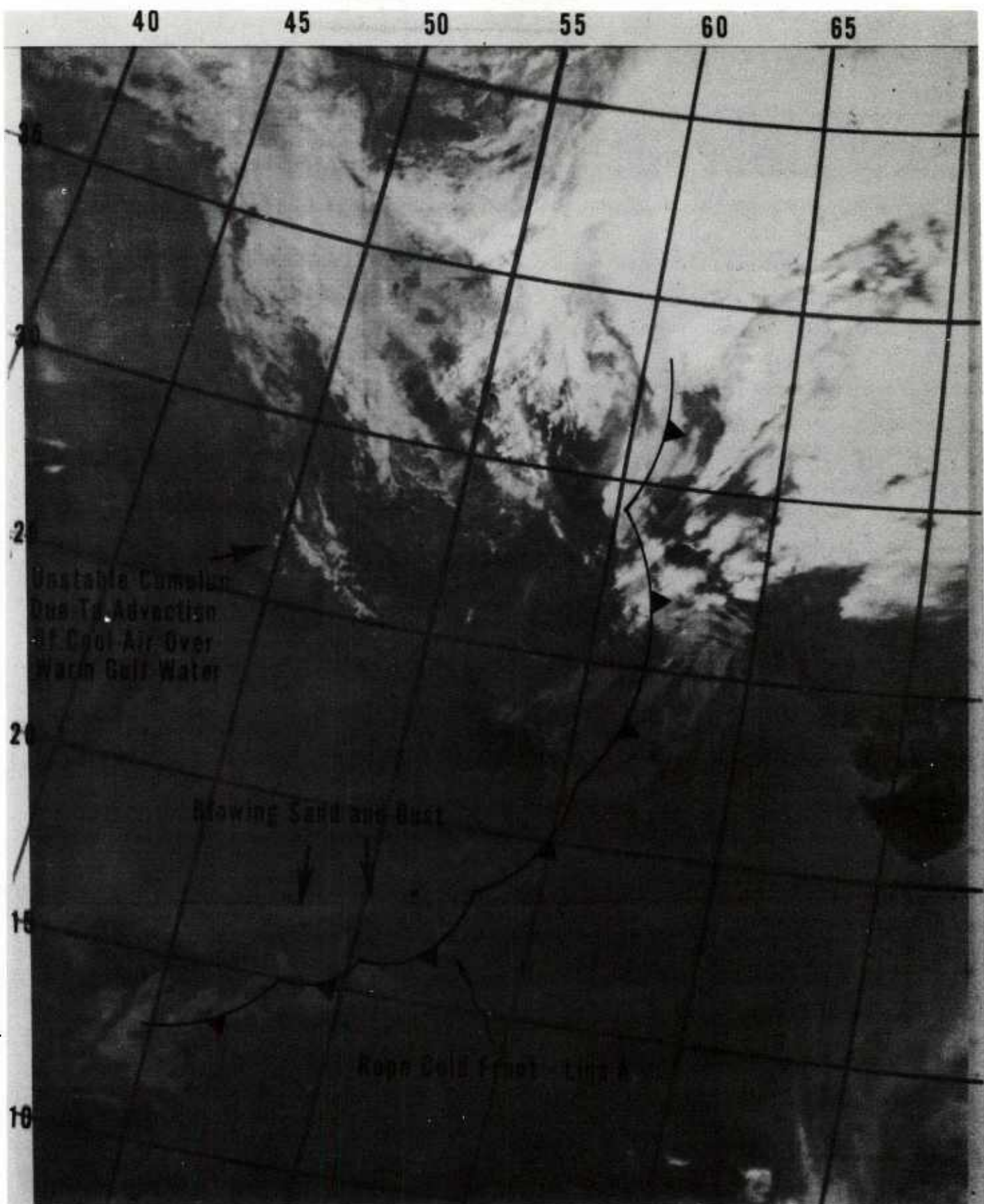


Figure A-25. Continued.

A.5 STEP FIVE

A.5.1 Synoptic Discussion

"Subsidence continues in the lower troposphere over Saudi Arabia. A second surface high pressure area forms over the Iranian plateau. The orientation of the Zagros Mountains induces a lee trough which extends from the ... Gulf of Oman northwestward along the eastern shore of the Gulf. The shamal continues The upper air trough eventually moves away to the east. Lower tropospheric subsidence is now stronger over the Iranian plateau than over the Saudi Arabian basin. The high cell over Saudi Arabia weakens and the lee trough begins to move westward across the Gulf. The shamal weakens and is replaced on the eastern side of the Gulf by local sea breezes, weak southeasterlies, or a vector combination of both. Winds on the western side of the Gulf (lee) trough subside as the shamal "breaks". (Ref. Figures 3-1e,f.)

The 500 mb trough in this instance did not "stall" over Iran, but continued to move away to the east (see Figures A-26 and A-27). Consequently, subsidence to the west of the upper trough axis was short-lived. The surface high over Saudi Arabia began to weaken, the pressure gradient lessened over the Gulf, and the shamal wind slowly subsided. The chief factor which distinguishes the 3-5 day shamal from the 24-36 hour shamal is the upper air trough's movement: in the 3-5 day shamal, it either "stalls" over or near the Strait of Hormuz (near 26.5°N, 56.5°E), or moves very slowly through the region; in the 24-36 hr shamal, it moves through rapidly.

The surface analyses for 26/00Z, 26/06Z, and 26/12Z (Figures A-28 through A-30) show how the high pressure over Saudi Arabia at 26/00Z (03L) strengthened at 26/06Z (09L) and weakened again by 26/12Z (15L), a reflection in part of semi-diurnal variation.

Another high pressure area, a ridge oriented east-west along 35°N at 26/00Z, split into two cells at 26/06Z. One cell was centered over northwestern Iran on 26/06Z and remained there at 26/12Z.

Determination of the precise movement of the center of the other, easternmost, cell is difficult, because data is sparse at 26/06Z. The general movement of this easternmost cell, from 26/00Z (just before it split off from the ridge) to 26/12Z, seems to be to the northeast, in conjunction with the eastward moving cold front depicted on the extreme right-hand portion of the 26/00Z and 26/12Z surface analyses.

Also indicated on the 26/00Z, 26/06Z, and 26/12Z surface analyses is a lee trough induced by the Zagros Mountains and located on the eastern side of the Gulf, between the high pressure cells. The strongest of the northwesterly winds over the Gulf persisted on the western side of the Gulf, away from the lee trough. By 26/12Z, easterly and southeasterly winds occurred on the eastern

side of the Gulf (Figures A-30 and A-30a). Combined sea heights reported by rig Seashell in the southern Gulf was generally 6-8 ft at 26/06Z, 26/09Z, and 26/12Z.

The hourly wind speed averages derived from the anemograph at Das Island indicate a gradual decrease in the northwesterly winds as the day progressed (Table A-5). Das Island peak wind speeds are well below gale force intensity on 25 Jan. By 26/15Z, the shamal had virtually subsided in the southern Gulf. Combined sea heights of 5-8 ft were reported by oil rigs near Das Island at 26/15Z; these gradually diminished through the night. (A surface chart for 26/15Z is not depicted.) By 27/03Z (Figure A-30b) the shamal had definitely ended; winds were light and combined sea heights were 3 ft or less.

Table A-5. Hourly winds reported at Das Island for 26 Jan 1974.

| <u>LT</u> <u>(LT=GMT+3)*</u> | <u>GMT</u> | <u>Direction</u> <u>(°)</u> | <u>Mean Speed</u> <u>(kt)</u> | <u>Max Gusts</u> <u>(kt)</u> |
|---------------------------------|------------|--------------------------------|----------------------------------|---------------------------------|
| 0000 | 25/2000Z | 310 | 16 | 23 |
| 0100 | 25/2100Z | 310 | 17 | 25 |
| 0200 | 25/2200Z | 310 | 17 | 26 |
| 0300 | 25/2300Z | 300 | 16 | 25 |
| 0400 | 26/0000Z | 300 | 16 | 26 |
| 0500 | 26/0100Z | 300 | 15 | 28 |
| 0600 | 26/0200Z | 310 | 16 | 23 |
| 0700 | 26/0300Z | 310 | 15 | 24 |
| 0800 | 26/0400Z | 310 | 14 | 22 |
| 0900 | 26/0500Z | 310 | 13 | 18 |
| 1000 | 26/0600Z | 300 | 14 | 18 |
| 1100 | 26/0700Z | 300 | 13 | 21 |
| 1200 | 26/0800Z | 300 | 13 | 20 |
| 1300 | 26/0900Z | 300 | 14 | 22 |
| 1400 | 26/1000Z | 300 | 14 | 22 |
| 1500 | 26/1100Z | 300 | 14 | 22 |
| 1600 | 26/1200Z | 300 | 13 | 20 |
| 1700 | 26/1300Z | 300 | 12 | 18 |
| 1800 | 26/1400Z | 310 | 11 | 17 |
| 1900 | 26/1500Z | 320 | 9 | 16 |

A.5.2 Satellite Data Interpretation

The DMSP images for 26 Jan (Figures A-31 and A-32) indicate subsidence over the northern Gulf at clear area A. The remnants of the cumulus which formed over the southern Gulf on 25 Jan are shown clearly -- area B on the high resolution visible image, Figure A-31 -- as "capped off" closed-cell strato-cumulus. The "capping off" of the cumuliform cloudiness and the general anticyclonic turning of the low level flow are further indications of pronounced sinking motion in the lower part of the troposphere.

*See footnote to Tables A-1 and A-2.

The rapid modifying remnants of the 25 Jan frontal rope over the Arabian Sea appears to be Area D. Although a cold front has been positioned in the center of the diffuse cloud Area D, the precise location of the front is difficult to determine because of the lack of detailed surface data, and because the air in the diffuse frontal zone appears to be undergoing rapid modification over the warm Arabian Sea. A reasonable alternative to the position of the cold front indicated in Figure A-31 would be a position approximately 2-3° further south, at, or just south of, the leading edge of the diffuse cloud band. A convergence band, C, appears in the Gulf of Oman. The appearance of band C seems to coincide with the dying phase of the shamal; a similar pattern is discerned near the end of the 3-5 day shamal described in Appendix B, a case study from January 1973. If this convergence band, C, occurs on a 1200 LT satellite image, it appears to indicate, based on the information contained in the case studies described here, that the shamal has ceased in eastern side of the Gulf, has diminished to the 15-20 kt range on the western side of the Gulf (see Figures A-29 and A-30 and Table A-5), and will probably die off completely that evening. This phenomenon is discussed in more detail in Appendix B.

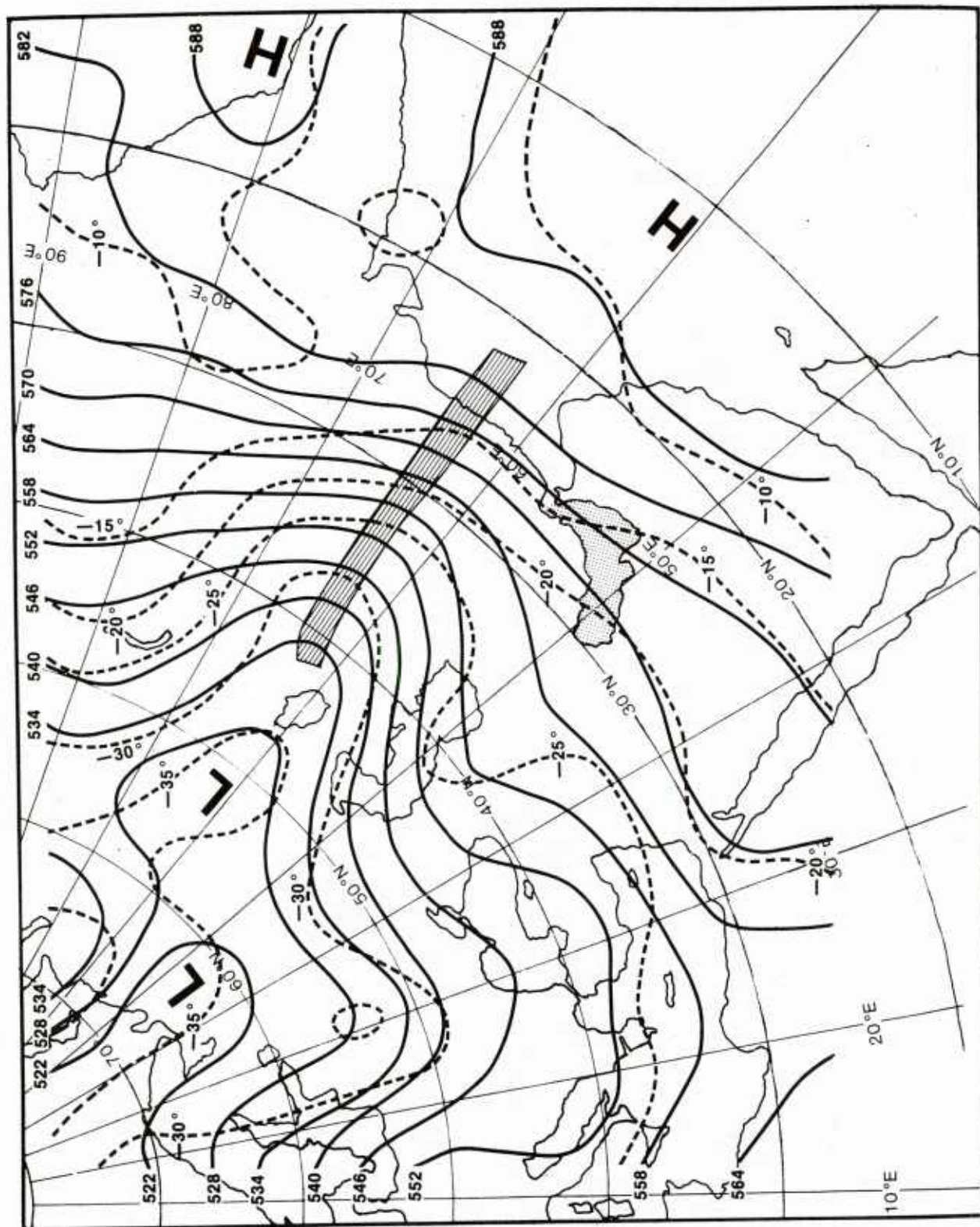


Figure A-26. 500 mb analysis, 26 Jan 1974 0000Z.

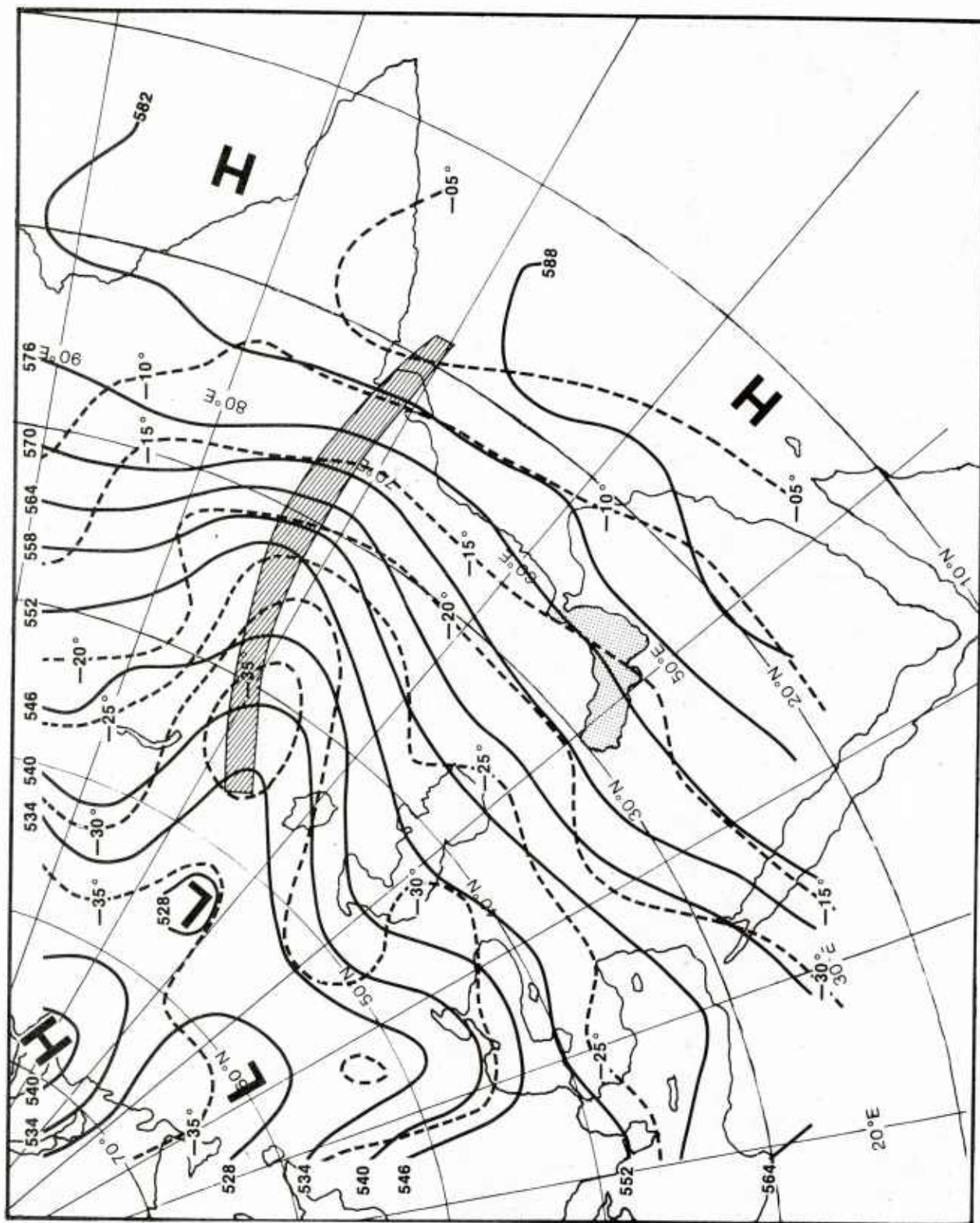


Figure A-27. 500 mb analysis, 26 Jan 1974 1200Z.

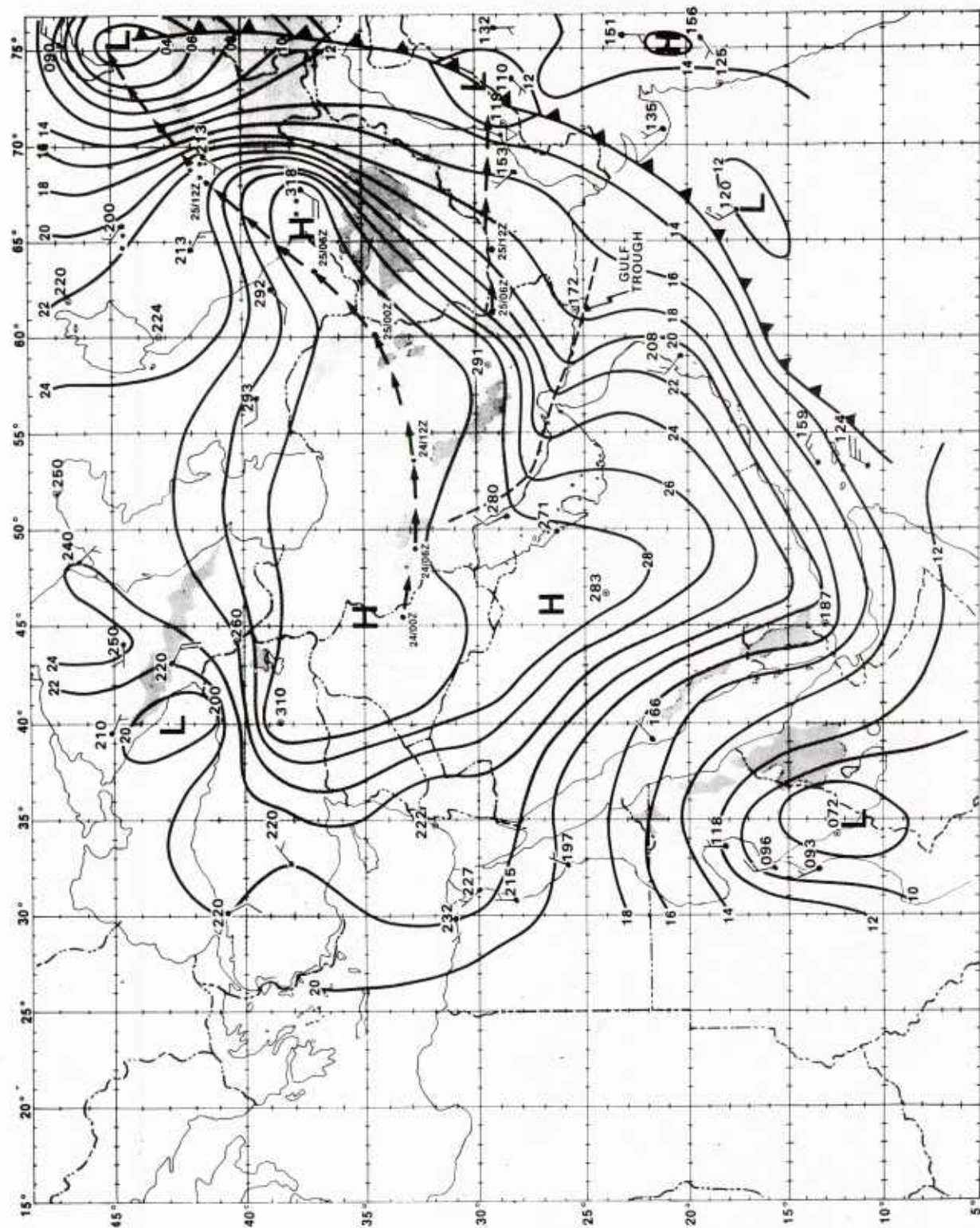


Figure A-28. Surface analysis, 26 Jan 1974 0000Z.

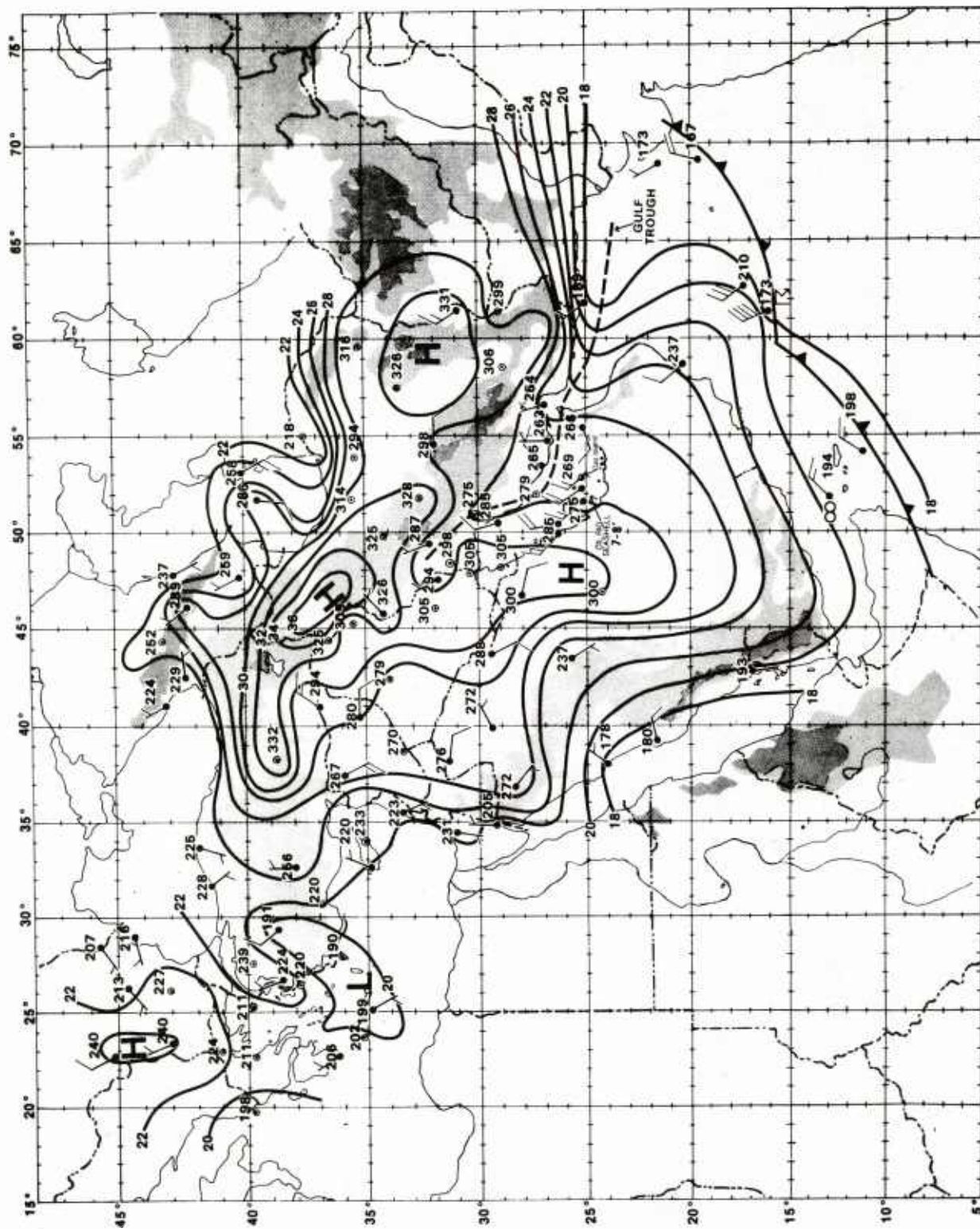


Figure A-29. Surface analysis, 26 Jan 1974 0600Z.

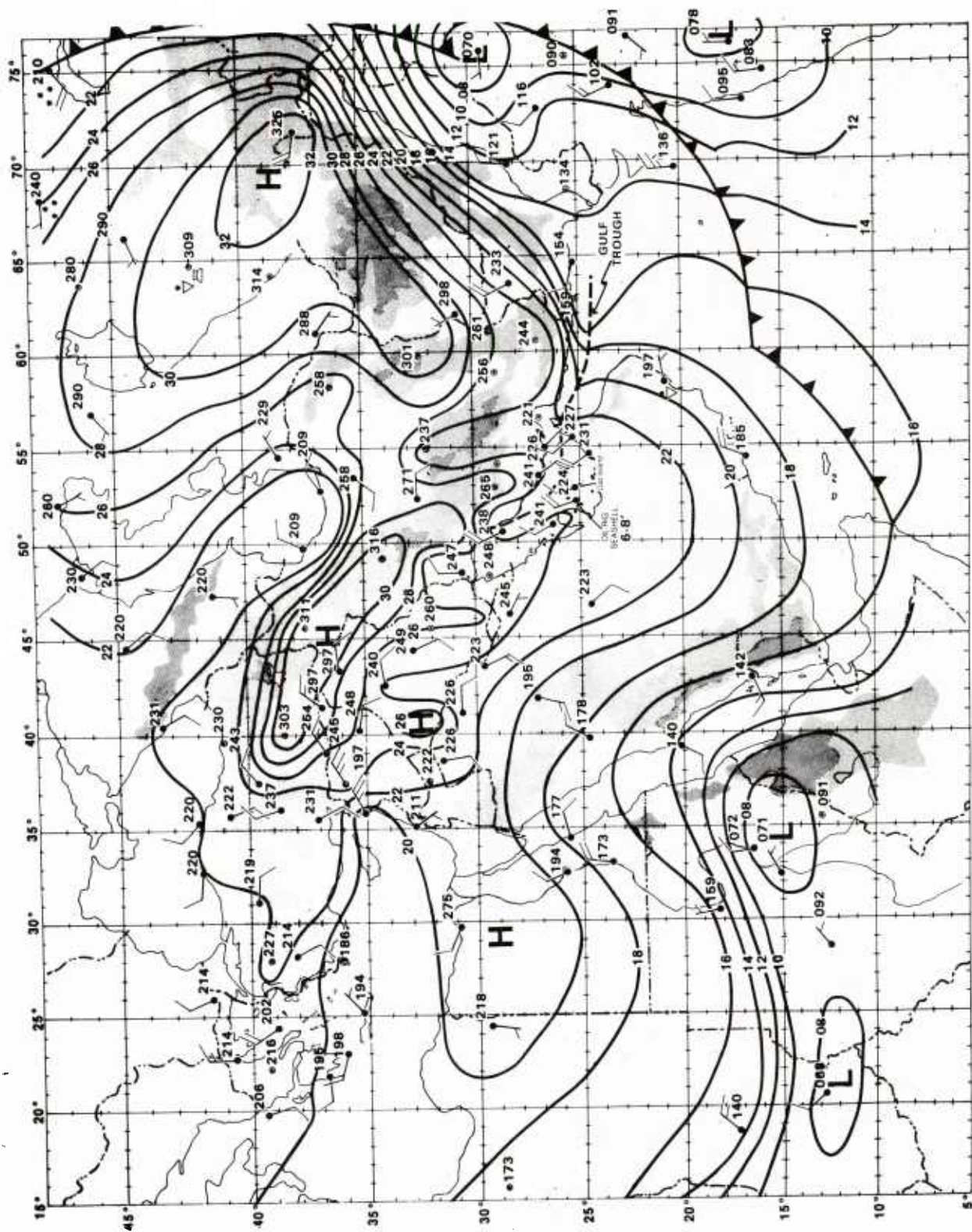


Figure A-30. Surface analysis, 26 Jan 1974 1200Z.

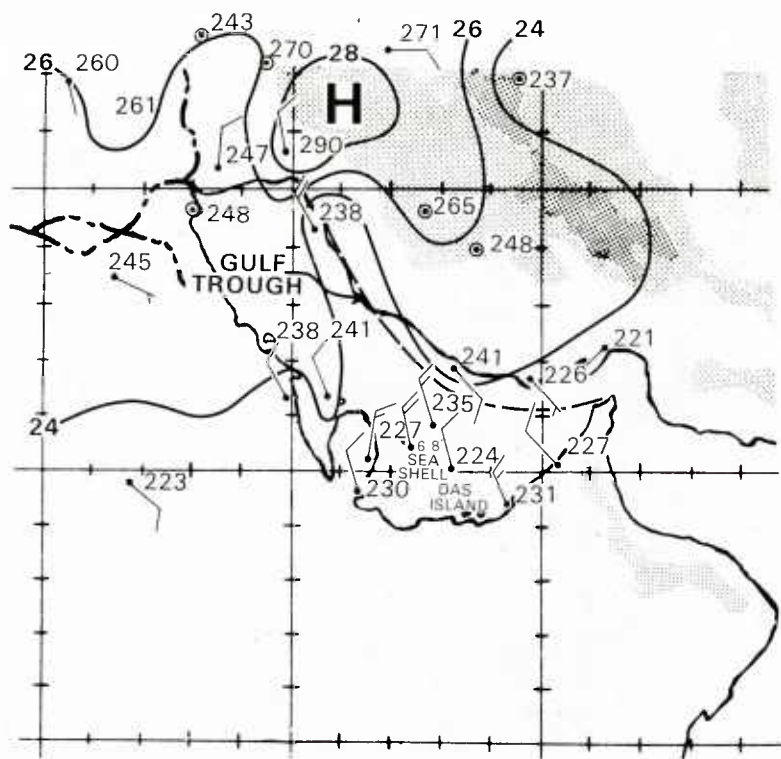


Figure A-30a. Detailed surface analysis, 26 Jan 1974 1200Z.

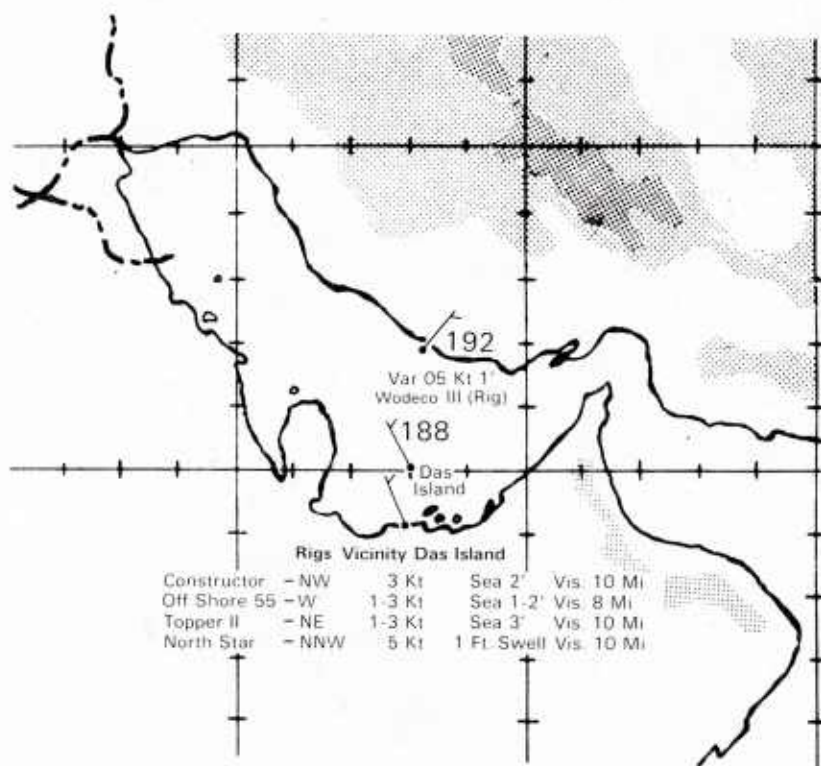


Figure A-30b. Surface analysis, 27 Jan 1974 0300Z.

-- SATELLITE IMAGERY SHOWN ON NEXT FACING PAGES --

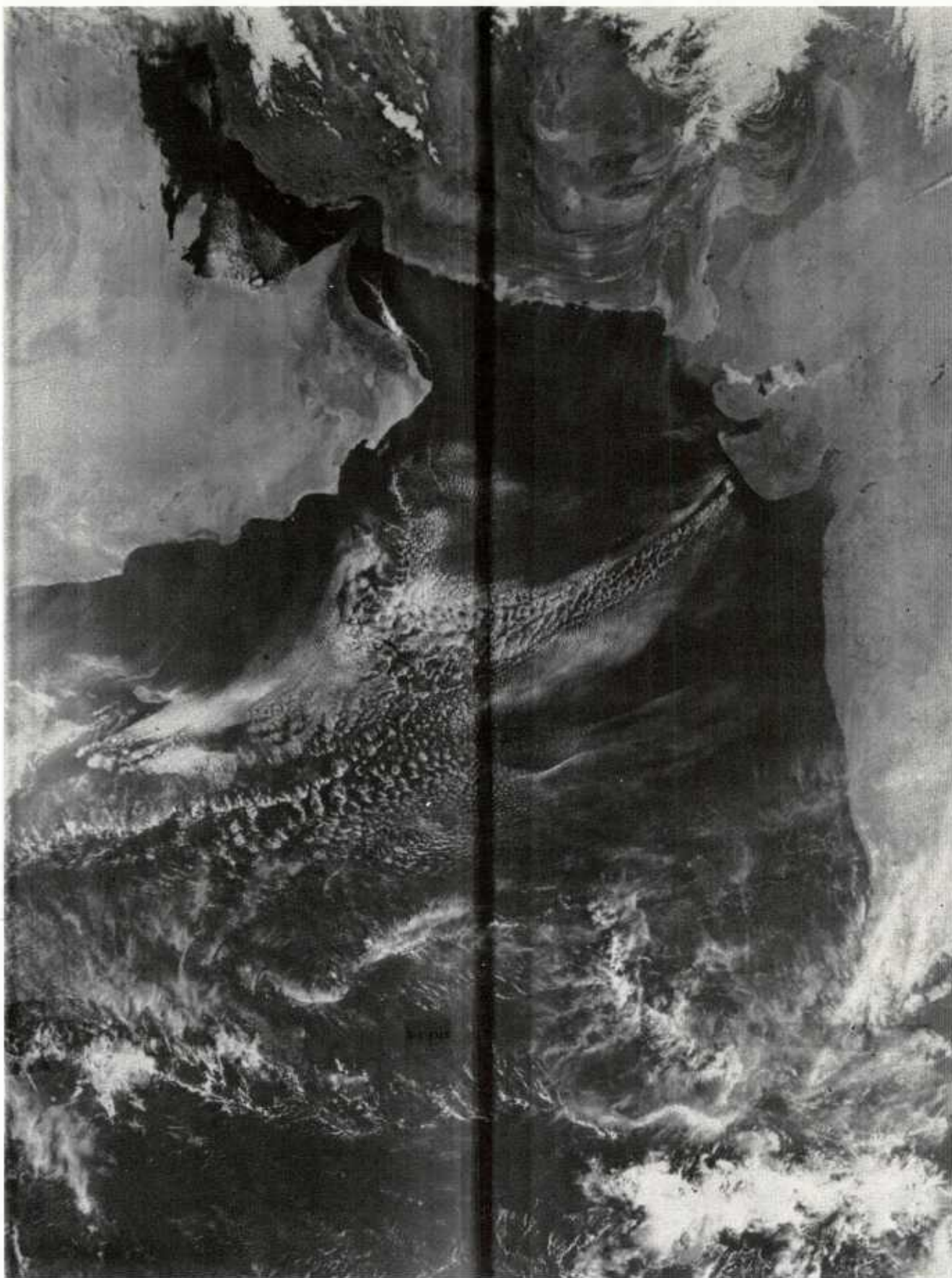


Figure A-31. DMSP visible image, 26 Jan 1974 0838Z.

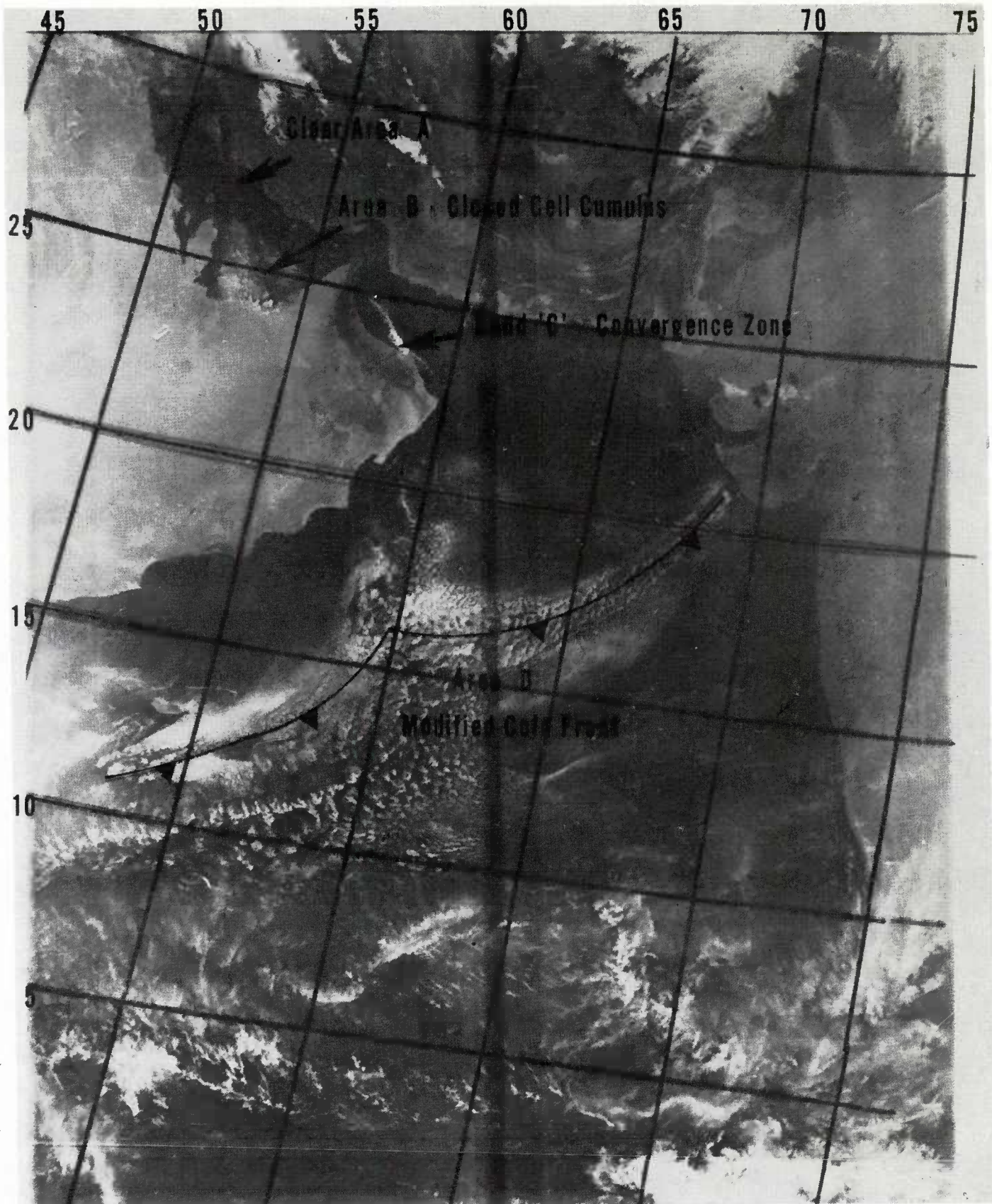


Figure A-31. Continued.

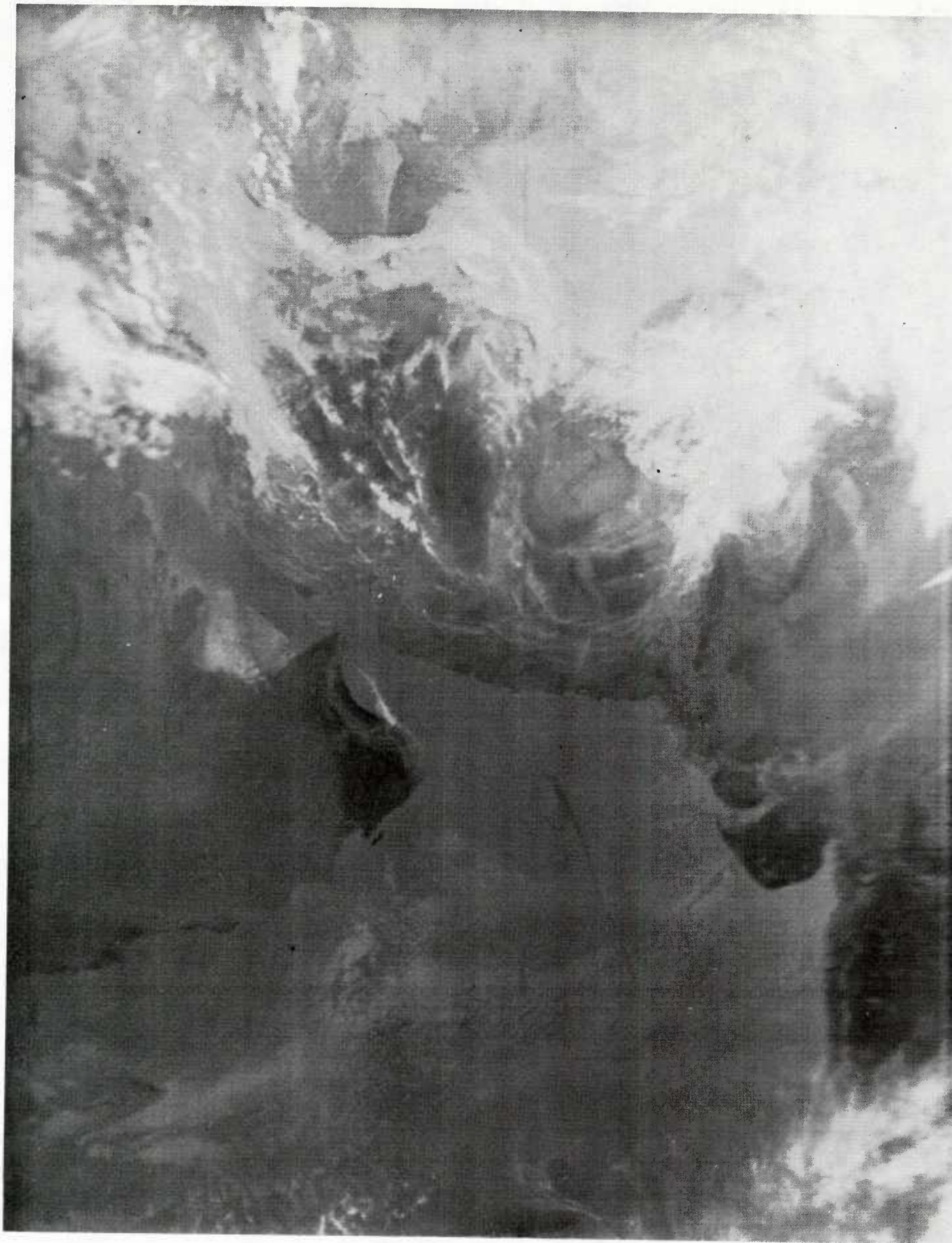


Figure A-32. DMSP IR image, 26 Jan 1974 0838Z.

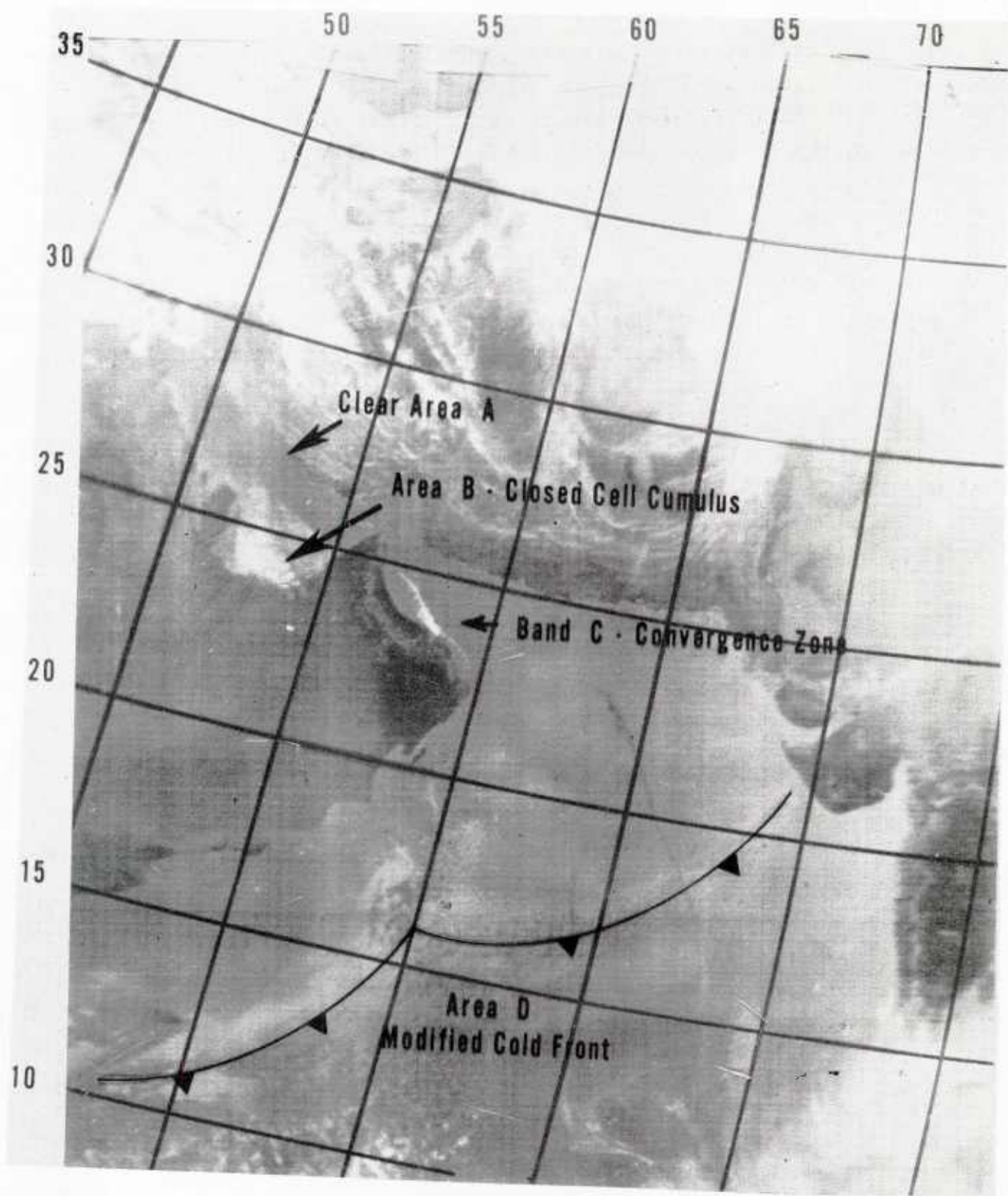


Figure A-32. Continued.

A.6 SUMMARY

(1) This case study has described the typical 24-36 hr shamal pattern discussed in Section 3.1.

(2) The shamal typically begins as an abrupt transition from gradually increasing southerly or southeasterly winds (the Kaus) to gale force north-westerly winds.

(3) The cold front which precedes the onset of the shamal typically propagates rapidly southeastward down the Persian Gulf and over the Arabian Peninsula. Frontal velocities of 35-40 kt are not uncommon. The shamal begins while the upper wind flow (500 mb) pattern is still southwesterly over the Gulf.

(4) The warm, shallow waters of the Persian Gulf rise quickly into a short, steep sea under the stress of gale force winds. The sea heights rise more rapidly in the Gulf than in the open sea.

(5) Cyclogenesis in the area depicted in Figure 3-3 of Section 3 typically accompanies the onset of the shamal. Cyclogenesis tends to occur north of the polar jet position, while severe thunderstorm activity can occur at the same time in the area north of the subtropical jet. The DMSP images which accompany this case study support these generalizations.

(6) The shamal subsides within 24-36 hr after onset, if the upper air trough moves smoothly and rapidly eastward through the Persian Gulf/Strait of Hormuz/Gulf of Oman areas.

(7) A distinctive convergence cloud band signals the demise of the shamal. It first appears in the Gulf of Oman on the 1200 LT DMSP satellite image on the day the shamal "breaks." The shamal ends that evening.

APPENDIX B - CASE STUDY 2

TYPICAL SYNOPTIC SEQUENCE OF THE 3-5 DAY SHAMAL

B.1 INTRODUCTION

The onset of the 3-5 day winter shamal* is triggered by the passage of a cold front down the Persian Gulf, an event that typically occurs ahead of the passage of the upper trough over the Gulf. If the upper trough moves away quickly to the east, as in Case Study 1 given in Appendix A, the shamal soon subsides. If, however, the upper trough becomes quasi-stationary over, or just to the east of, the southern Gulf, then the shamal appears to be sustained by three factors:

(1) Negative vorticity advection to the rear (west) of the upper trough axis produces convergence aloft, and subsidence through the lower troposphere. The pressure at the surface rises over the Arabian Peninsula in association with the subsidence.

(2) The bowl-like shape of the Arabian Peninsula -- which is ringed by the Taurus Mountains of Turkey to the north, the Zagros Mountains of Iran to the east, and the Hejaz and Hajar Mountains on the western, southwestern, and southeastern parts of the Arabian Peninsula, as shown by Figure B-1 -- inhibits the horizontal outflow of the subsiding air in the lower layers of the atmosphere over the Peninsula. The air in the lower layers is virtually "trapped," except for outlets through the Strait of Hormuz and the southeastern portion of the Peninsula between Masirah Island and Salalah. This virtual trapping also contributes to the building of the surface pressure over the Peninsula.

(3) Orographic curvature effects, combined with vertical motion over the Gulf of Oman ahead of (to the east of) the upper trough axis, lower the surface pressure over the Gulf of Oman.

The combination of increased surface pressure over the Arabian Peninsula and lower surface pressure over the Gulf of Oman produces a surface pressure gradient oriented northwest-southeast along the Persian Gulf (especially in the southern portion) to sustain northwesterly the gale force shamal wind.

A long wave upper trough position consistent in day-to-day continuity is marked on each of the 500 mb analyses in this case study. During the middle period of the sequence, the long wave trough becomes rather shallow and difficult to locate because a number of short waves move through the long wave position. Consequently, the location of the long-wave trough cannot be precisely determined during this period.

*The shamal used as an example in this case study occurred in mid-January 1973; subsequent discussions trace its occurrence day by day from 15 through 20-21 Jan.

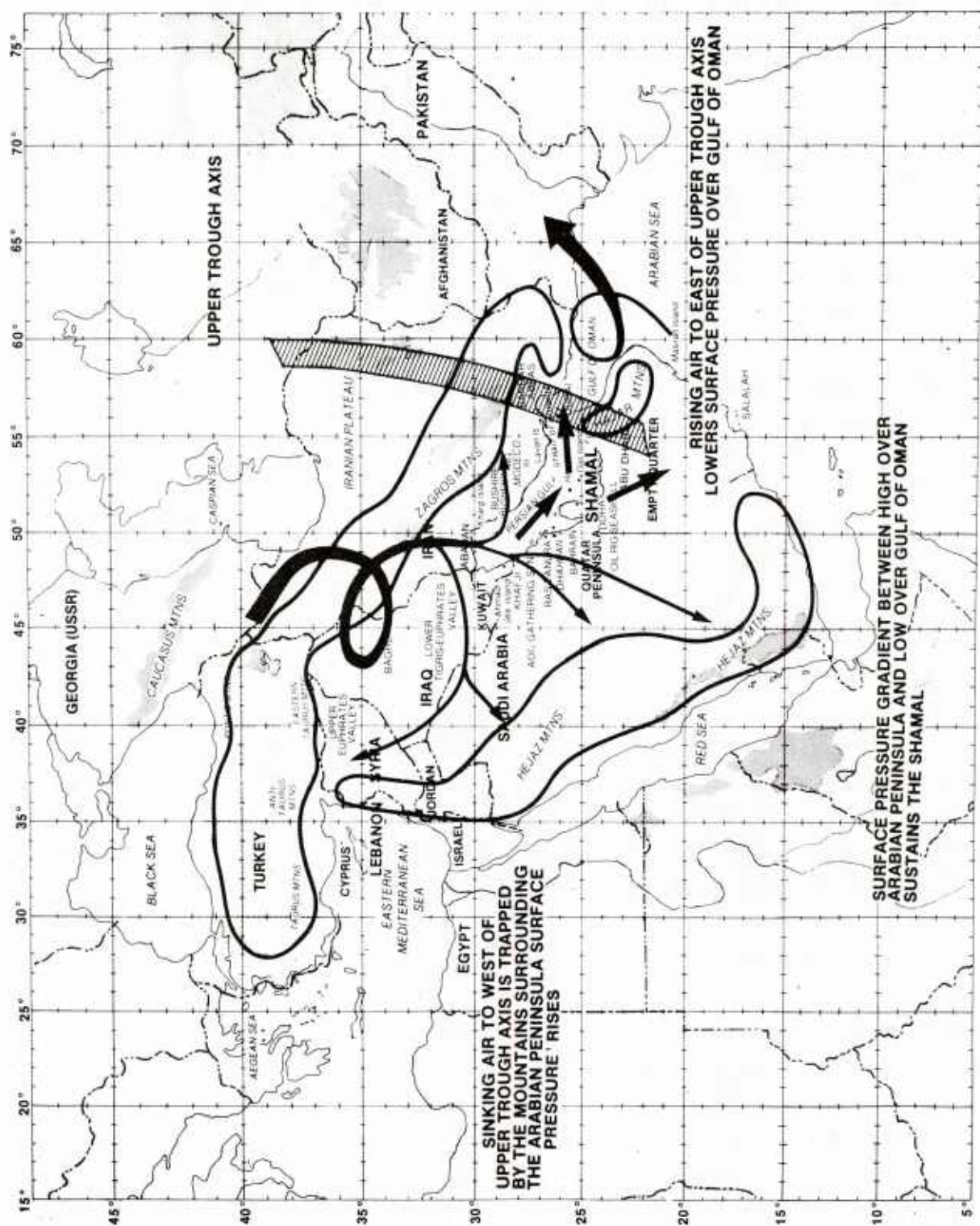


Figure B-1. Relationship among upper trough axis, surface high pressure to west of trough axis, and surface low pressure to east of trough axis during 3-5 day shamal.

B.2 15 JANUARY 1973

A deep, upper air trough over the eastern Mediterranean Sea, coupled with a blocking high over central Europe, forced cold air southward to the rear/west of the upper trough axis through a deep layer. (The direction of the geostrophic wind at 500 mb is typical, in this instance, of the wind direction through the surface-500 mb layer.) The cold air in the lower layers of the atmosphere was advected first southward over the western portion of the Taurus Mountains and through the Aegean Sea; then eastward over and around the mountains of the narrow, coastal mountain range of Syria and Lebanon on the eastern Mediterranean shore, into the upper Euphrates Valley. This less direct route of cold air penetration is traced on Figure B-2. A tongue of -25°C to -30°C air was also advected eastward at 500 mb (see Figures B-3 and B-5) with the upper trough.

Figure B-6 comprises a surface chart (a) and satellite images (b) for 15 Jan. The DMSP visible image near noon local time (approximately 15/08Z), Figure B-6b, shows the "signature" of the cumulus that formed as the colder air in the lower layers of the atmosphere streamed over the warmer waters of the eastern Mediterranean following passage over the eastern portion of the Taurus Mountains and through the Aegean Sea. As the lower layers of the deep, cold, northerly airstream were warmed from below by contact with the comparatively warm Mediterranean Sea, the airstream as a whole became unstable and cumulus developed downstream (area A on Figure B-6b).

The satellite image also shows the surface low, area B, and the associated cold front, band C. Band D shows the subtropical jet slightly to the north of its climatological position, curved anticyclonically to the northeast of the Gulf (see also 200 mb analyses at 15/00Z and 15/12Z, Figures B-7 and B-8).

The cold front advanced rapidly southeastward down the Tigris-Euphrates valley at nearly 40 kt. This movement is shown by comparison of frontal positions on the surface analyses for 15/00Z and 15/12Z, Figures B-4 and B-6a, respectively. The 15/12Z surface analysis shows such movement to be supported by 30-40 kt surface winds in northern Saudi Arabia (Figure B-6a). The speed of movement of the cold front is comparable to that described in Case Study 1, Appendix A.

B.3 16 JANUARY 1973

Under the influence of the eastward-moving 500 mb upper trough shown on Figures B-9 and B-11 (see also Figure B-10, 16/00Z surface analysis), cyclogenesis occurred in and near the area to the east of the northern end of the Persian Gulf (an area generally favorable for cyclogenesis). This area was under the region of strong, positive-vorticity advection to the east of the upper trough axis (marked R for rising vertical motion on Figures B-9 and B-11). Two surface lows formed between 15/12Z and 16/00Z, one over the lower

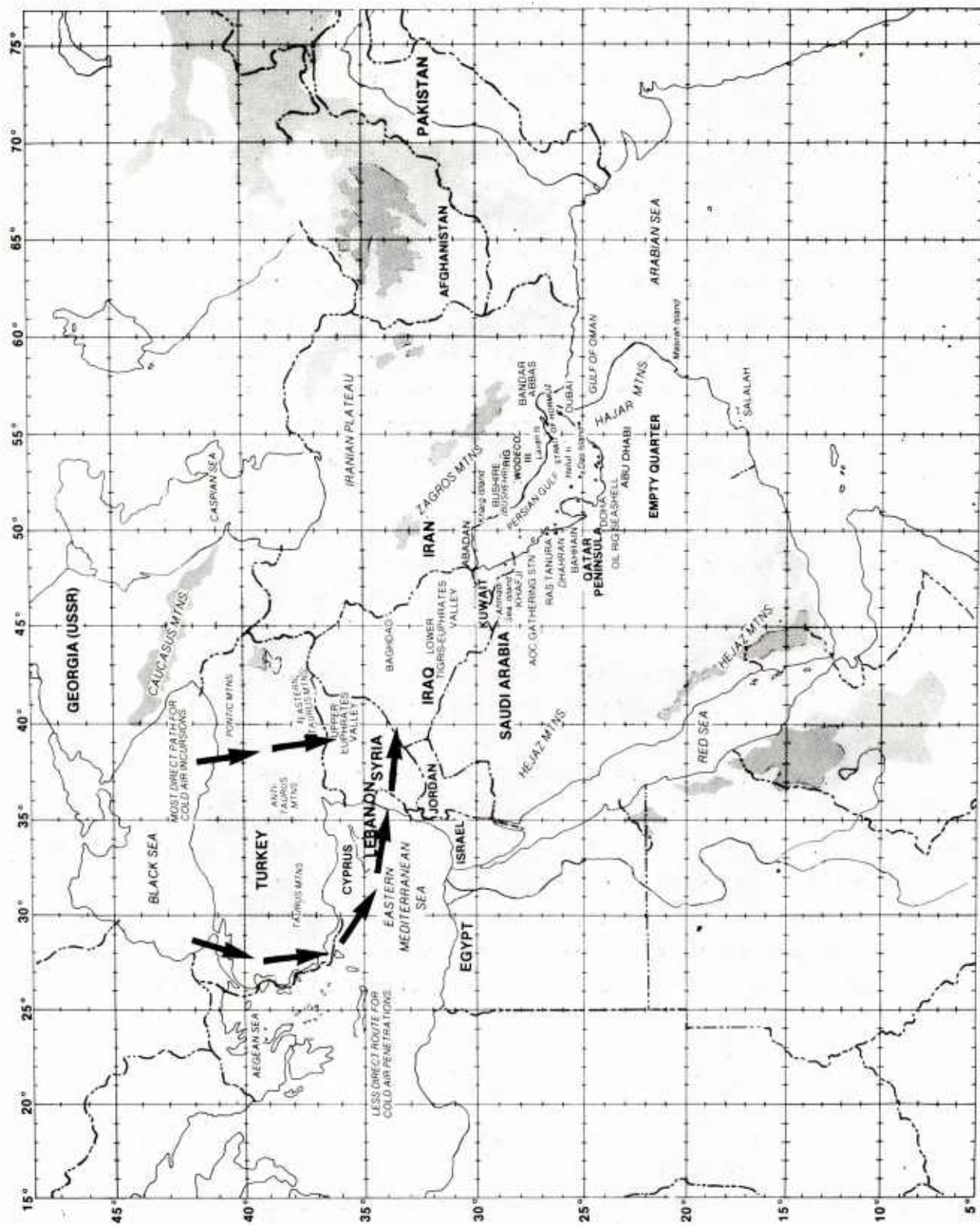


Figure B-2. Paths of cold air incursions into upper Euphrates valley prior to onset of shamal.

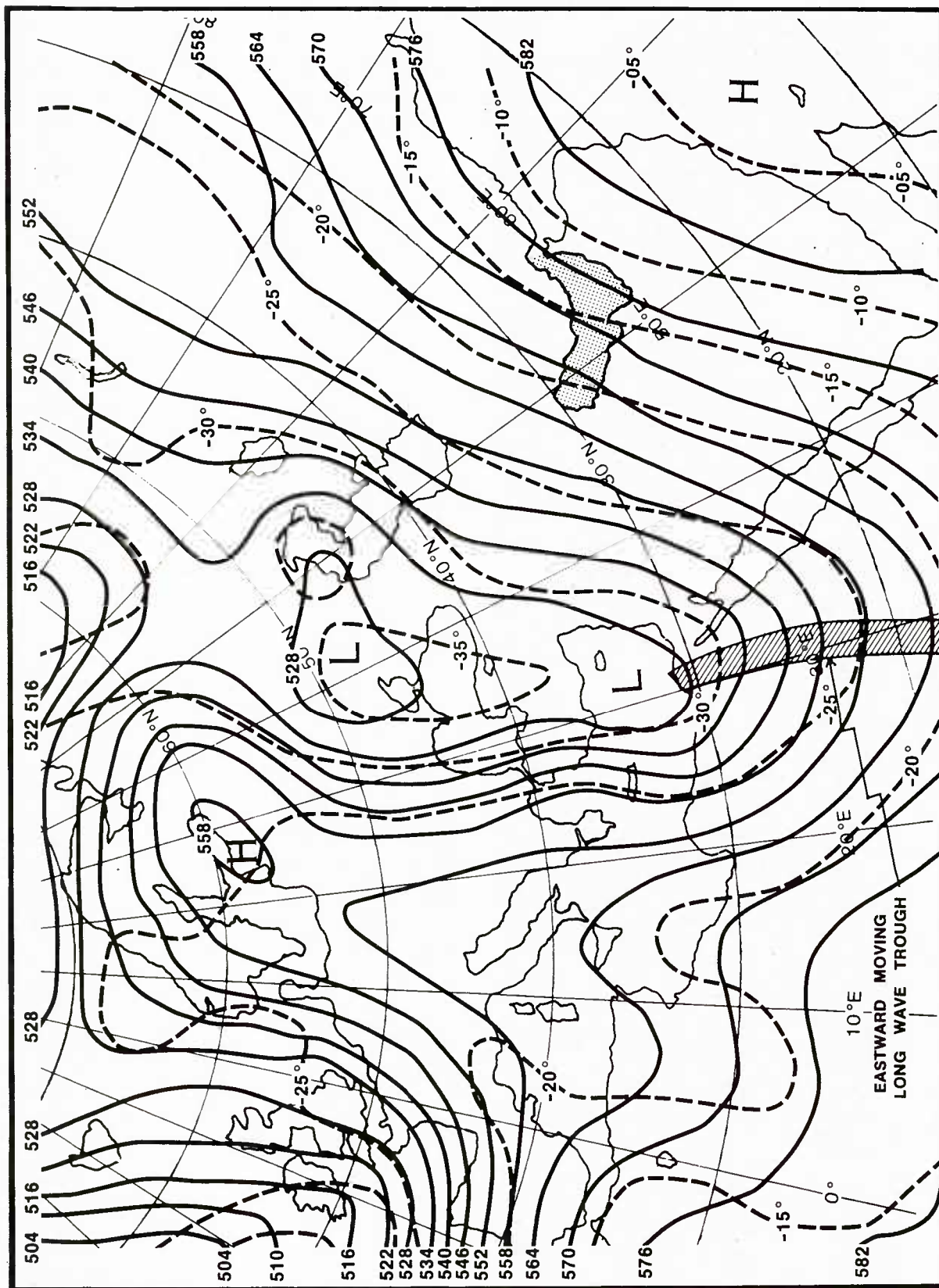


Figure B-3. 500 mb analysis, 15 Jan 1973 0000Z.

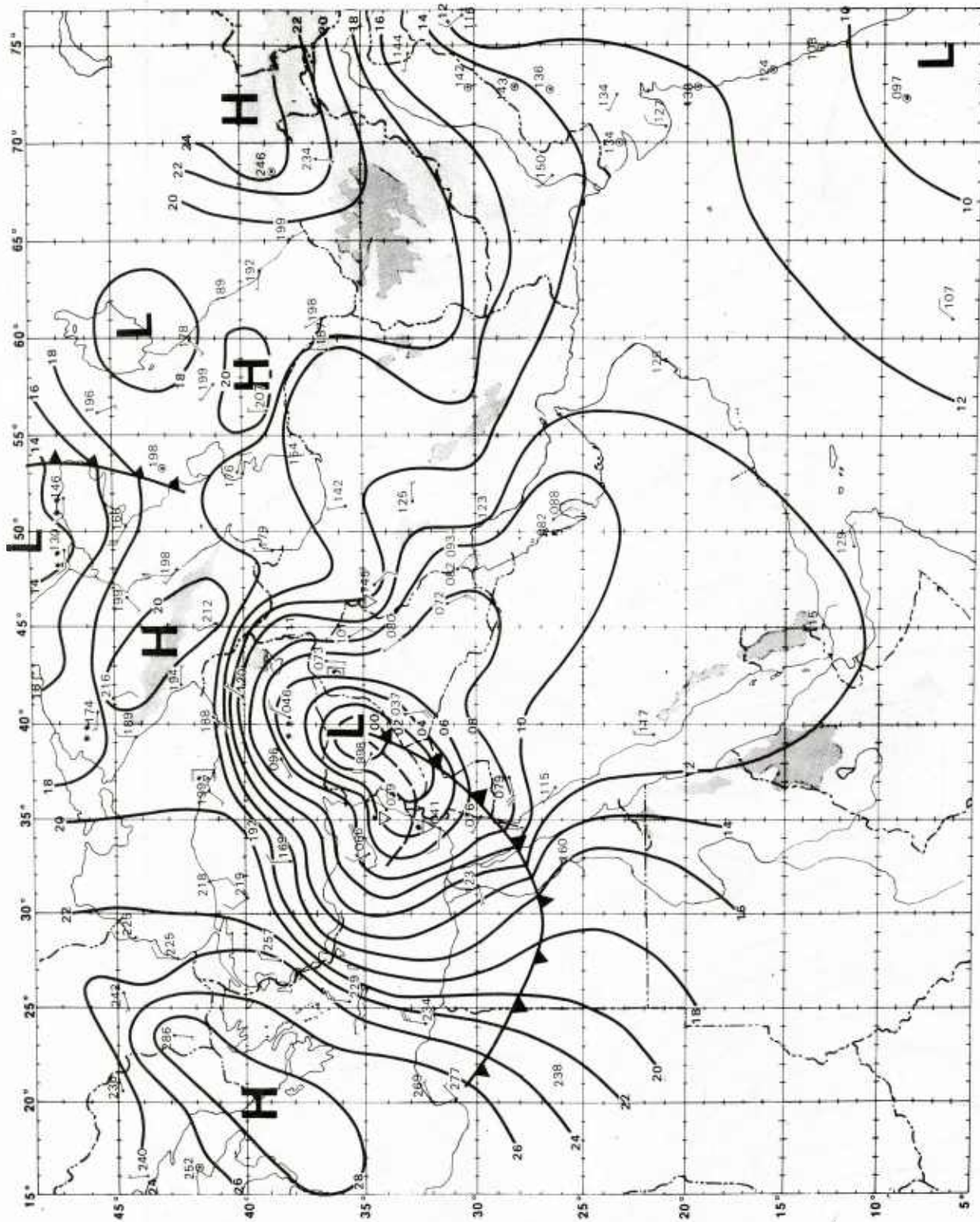


Figure B-4. Surface analysis, 15 Jan 1973 0000Z.

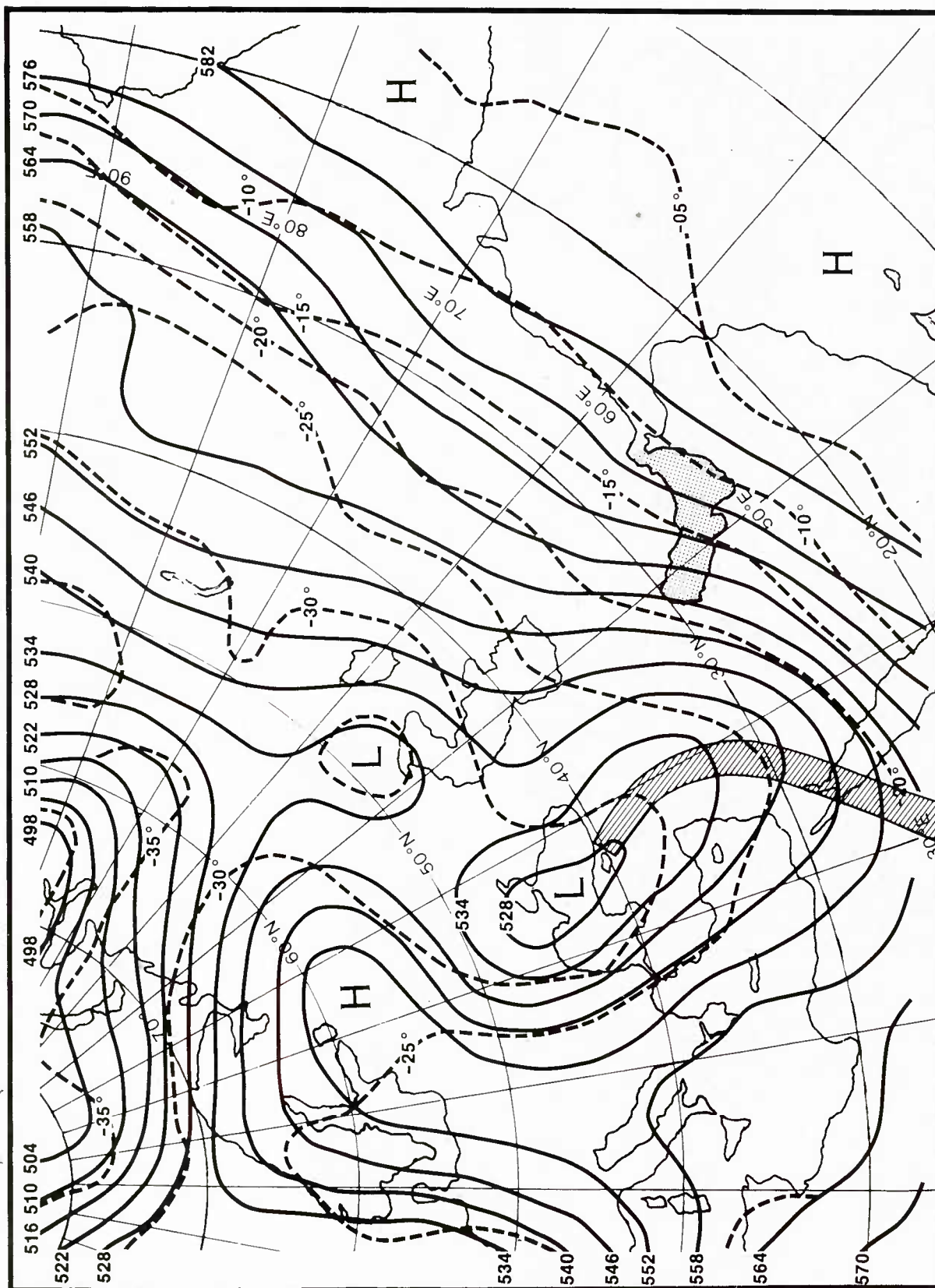


Figure B-5. 500 mb analysis, 15 Jan 1973 1200Z.

-- SATELLITE IMAGERY SHOWN ON NEXT FACING PAGES --



Figure B-6b, left. DMSP visible image, 15 Jan 1973 local noon.



Figure B-6b, left. Continued.

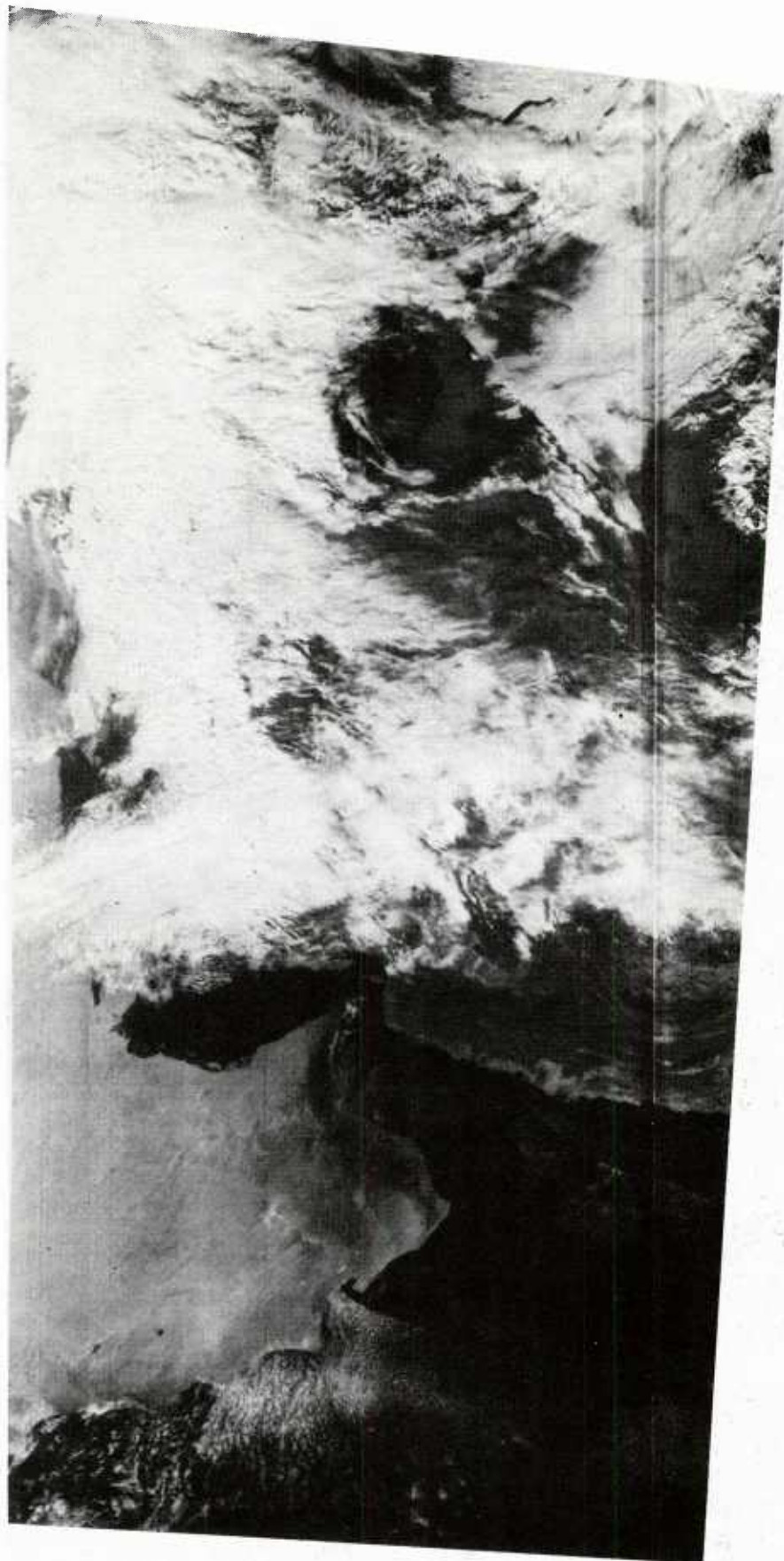


Figure B-6b, right. Continued.

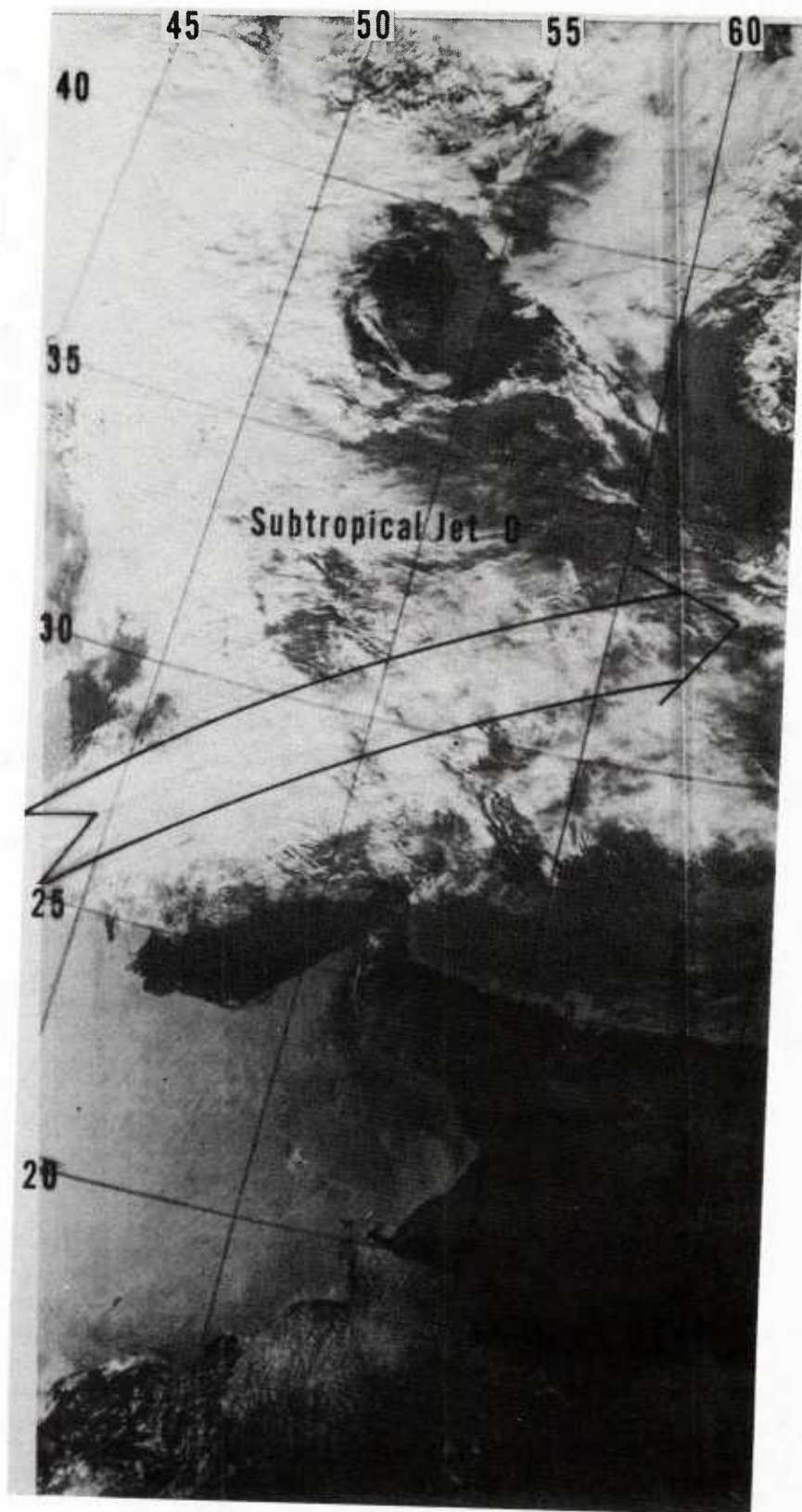


Figure B-6b, right. Continued.

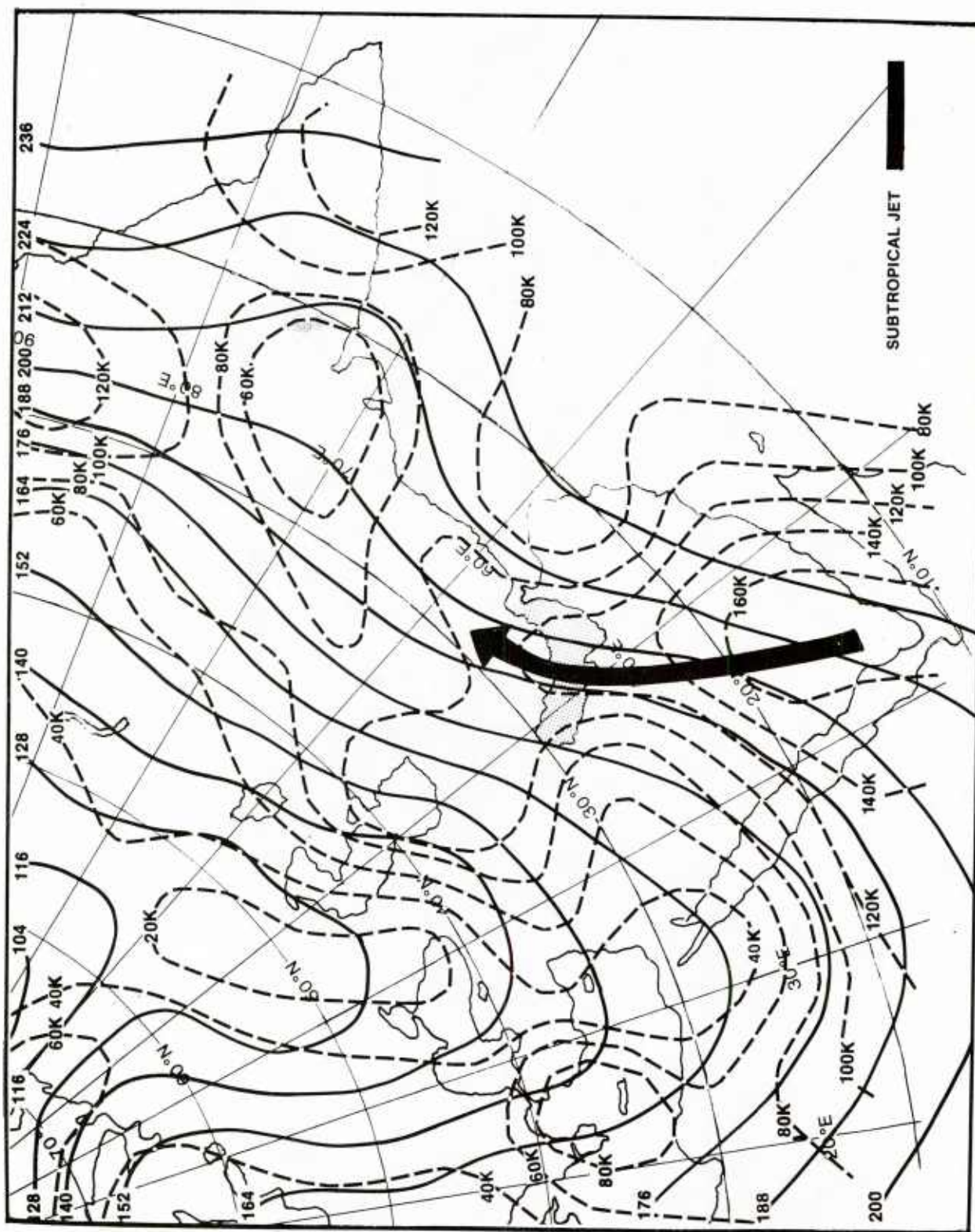


Figure B-7. 200 mb analysis, 15 Jan 1973 0000Z.

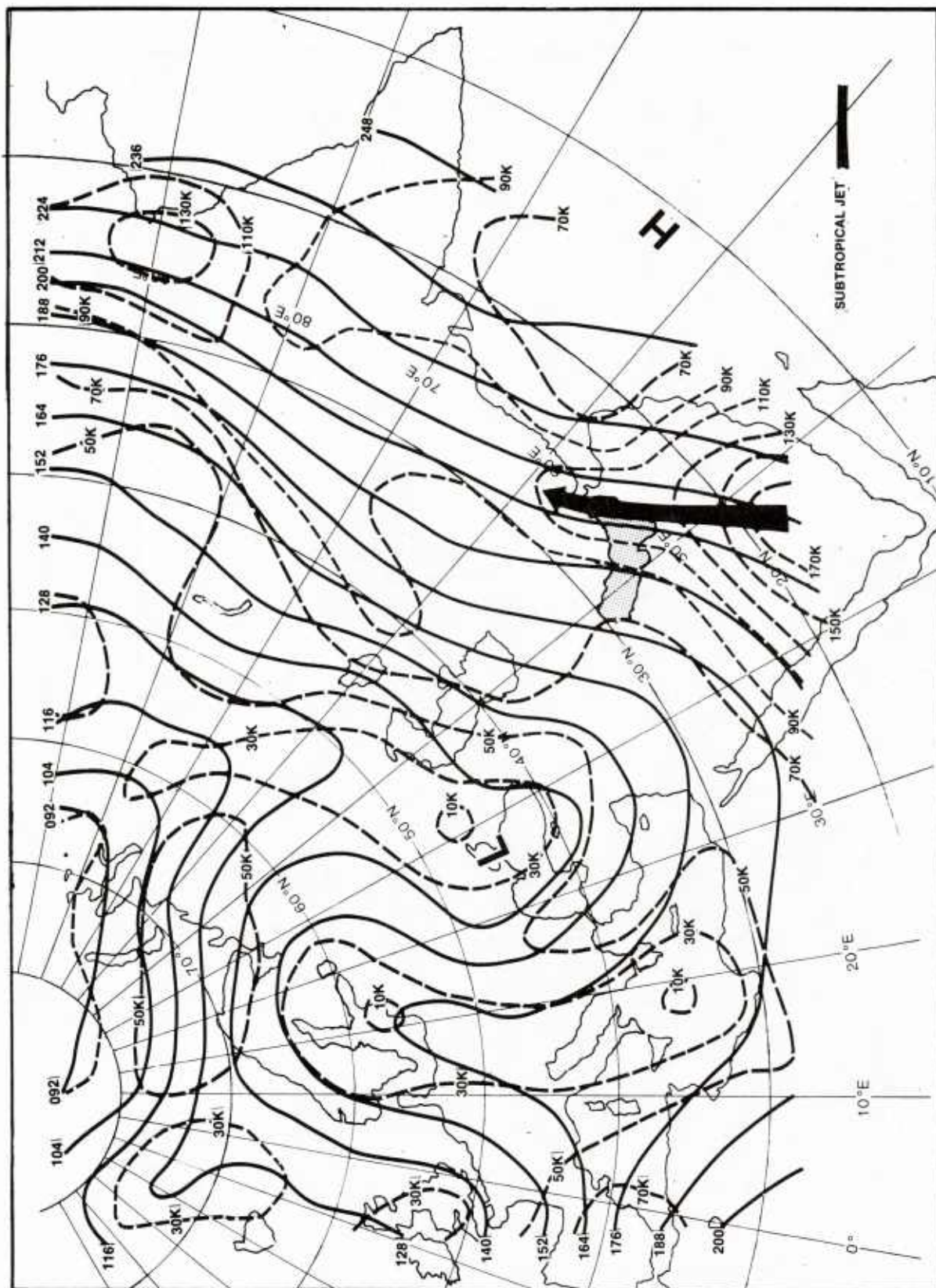


Figure B-8. 200 mb analysis, 15 Jan 1973 1200Z.

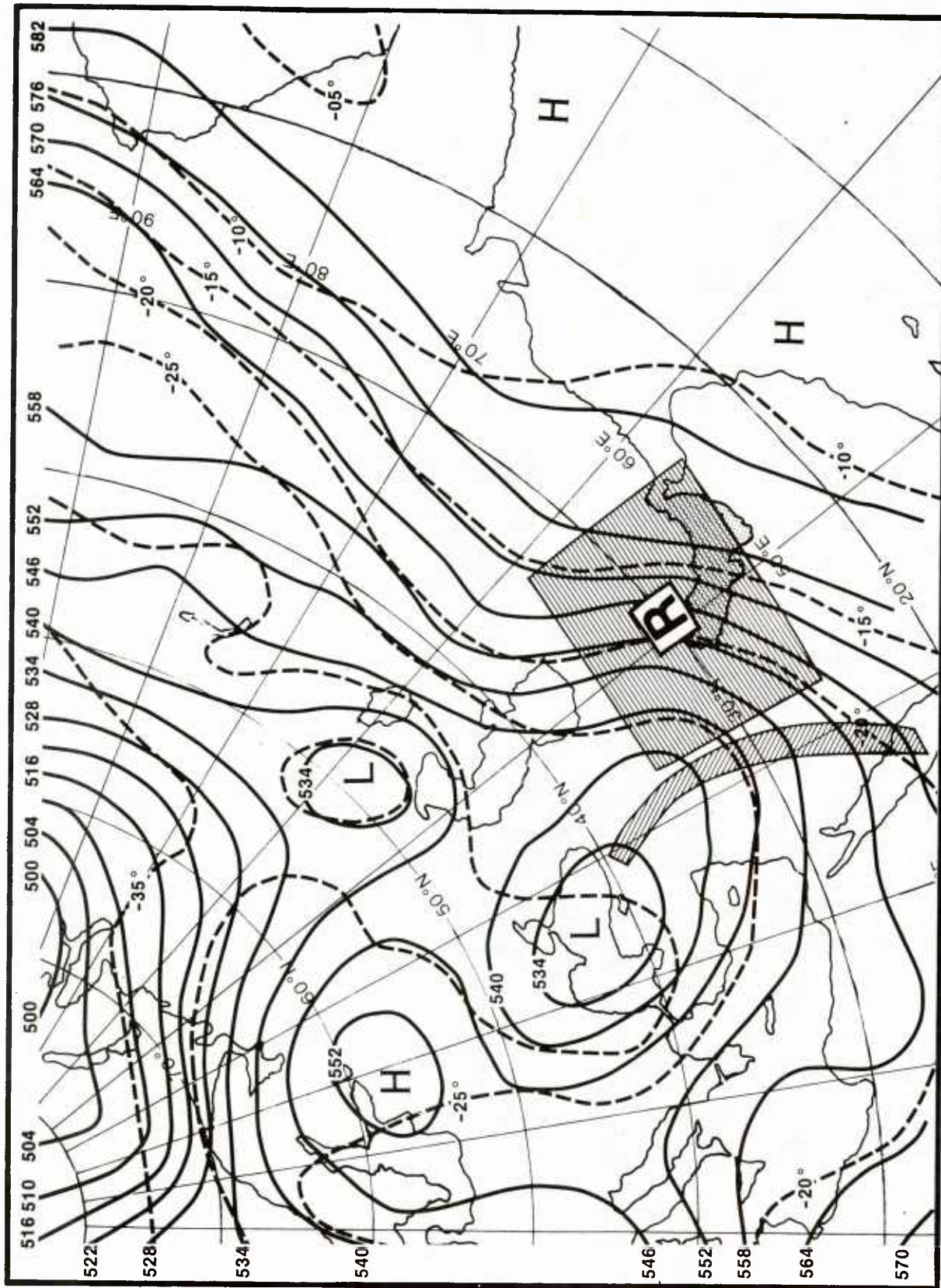


Figure B-9. 500 mb analysis, 16 Jan 1973 0000Z.

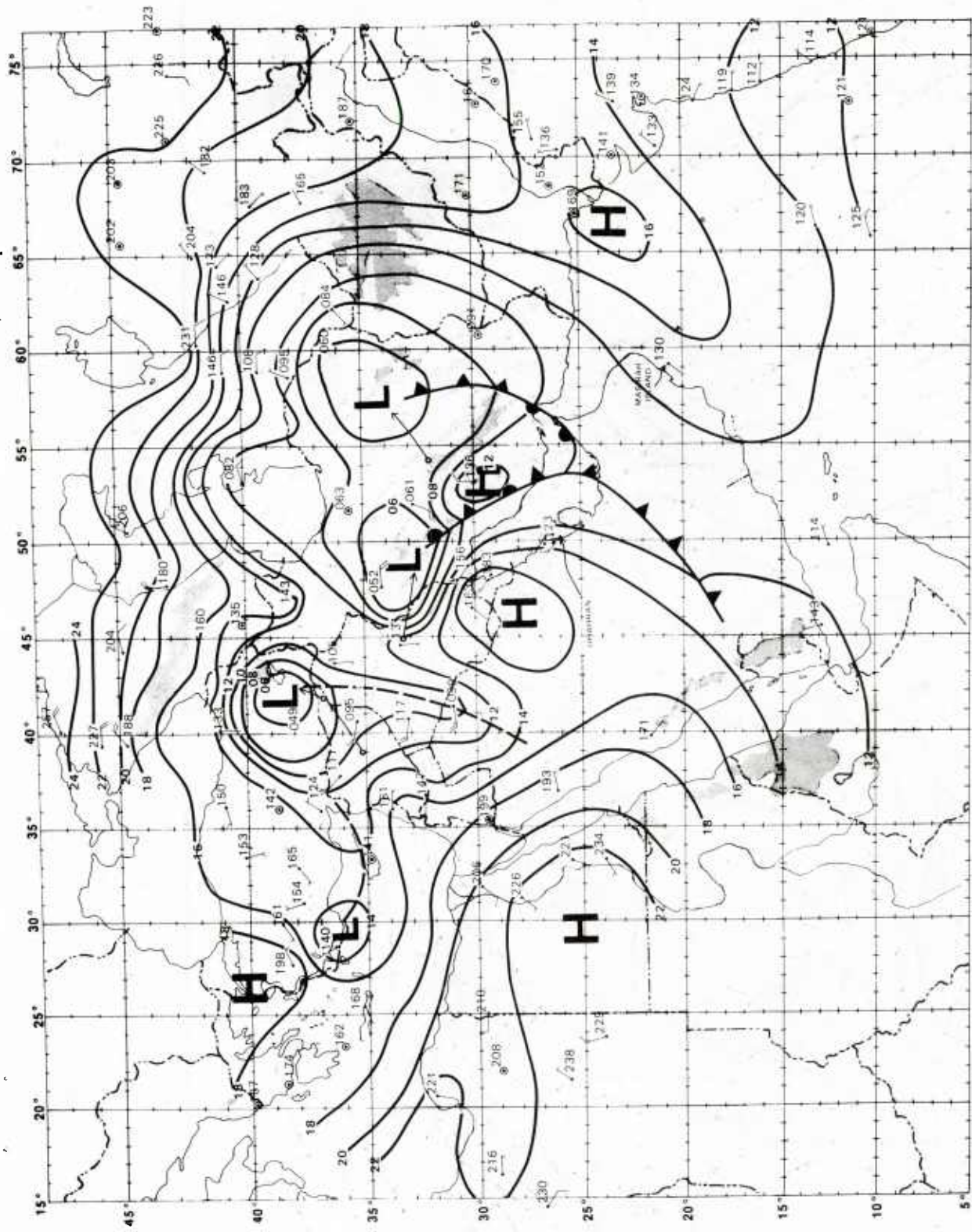


Figure B-10. Surface analysis, 16 Jan 1973 0000Z.

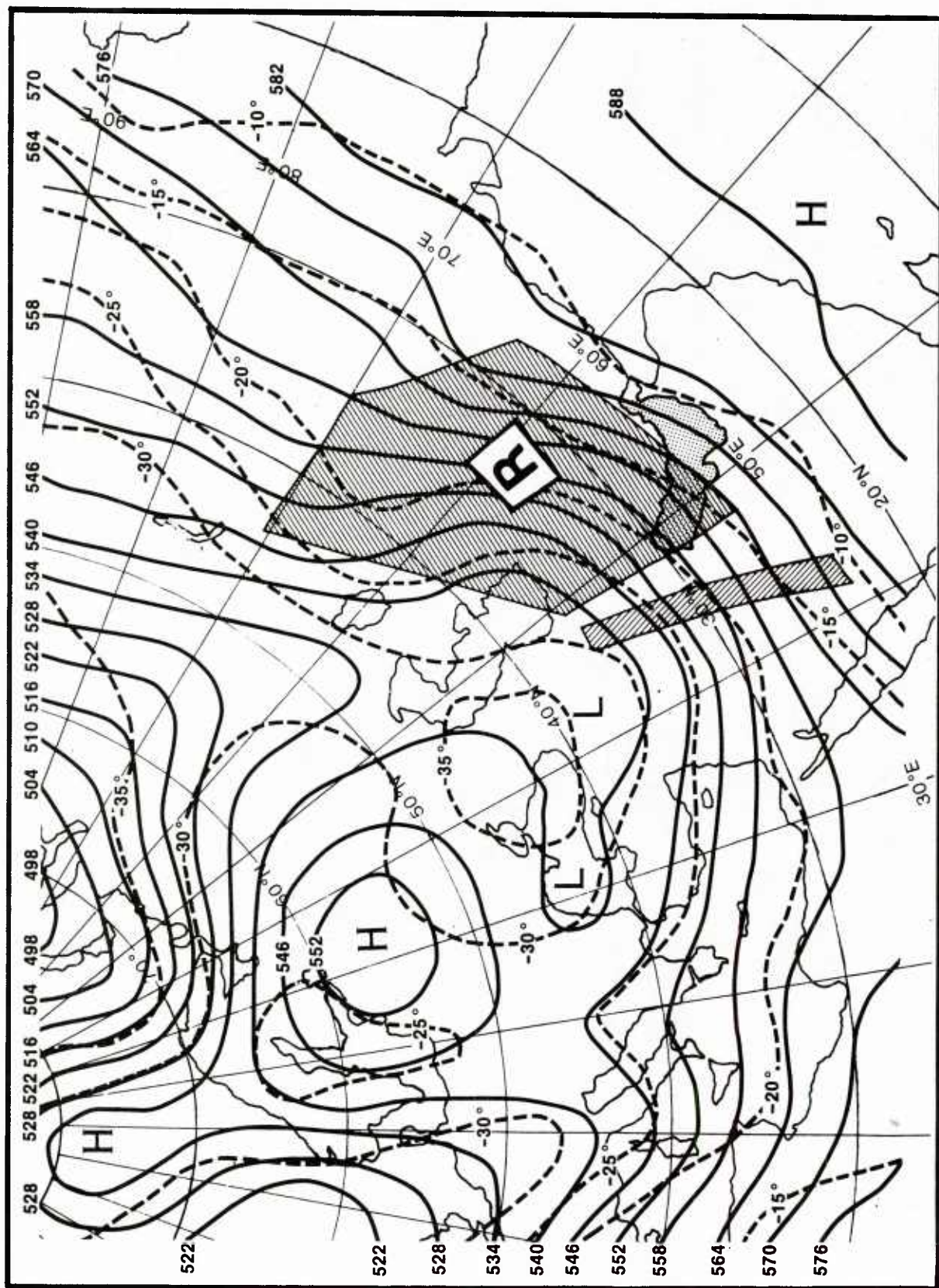


Figure B-11. 500 mb analysis, 16 Jan 1973 1200Z.

Tigris-Euphrates valley near 33°N, 45°E, and the other over central Iran near 32°N, 54°E. They appear on the 16/00Z surface analysis, Figure B-10, as 1005 mb lows over western and eastern Iran.

These surface lows then tracked further northeastward under the northeasterly airstream at 500 mb to new positions at 16/12Z near 33°N, 55°E, and 37°N, 63°E, respectively (Figure B-12). The parent surface low, which was located near 35°N, 39°E at 15/00Z, moved to the northeast to near 38°N, 42°E (see 16/00Z surface analysis, Figure B-10), where it remained quasi-stationary and subsequently weakened, under the 500 mb low center position (see 16/12Z 500 mb analysis, Figure B-11).

Without detailed surface data (such as that available in Appendix A), it is difficult to fix the time of the frontal intrusion into the Gulf that marked the onset of the shamal in this case study. Wind reports available from the west coast of the central Gulf indicate that the onset had not yet occurred at 15/12Z (the wind at Dhahran, near 26°N, 50°E was east-southeasterly, as shown in Figure B-6a). The shamal may have just begun at 16/00Z -- at Dhahran the wind shifted northwesterly to 15 kt, as shown in Figure B-10 -- and seems to have become established by 16/12Z when the wind at Bahrain, near Dhahran, was northwesterly at 20 kt with blowing sand.

It is also difficult to do more than speculate about the strength of the winds over the open waters of the Persian Gulf. Wind speeds over these waters are frequently higher than at shore stations. It is not unreasonable, therefore, to expect that wind speeds in the zone near the cold front are at or near gale force.

The DMSP visible satellite image for noon local time on 16 Jan, Figure B-13, shows cloudiness labeled area E near the Strait of Hormuz in the vicinity of 26.5°N, 56.5°E, and a band of cloudiness labeled band F along and near the southeastern coast of the Arabian Peninsula. It is difficult to locate the cold front which forms the leading edge of the shamal, but the analyses shown in Figures B-10 and B-12 seem a reasonable fit to the available data.

The cold front advanced rapidly southeastward down the Gulf over the Arabian Peninsula early on 16 Jan, but apparently slowed its forward movement later in the day. Area E could have been the result of a small area of warm air overrunning the frontal surface near the triple point in the vicinity of the Strait of Hormuz. Band F is too indistinct to be definitely related to a cold front. A portion of band F could be the result of local sea breeze effects along the coast of the Arabian Sea.

Typical cold frontal cloudiness cannot be detected in this instance, although an air mass contrast may exist near the coastal area. The cloud pattern in and near Band F indicates an onshore component to the wind west of 55°E, so the front probably had not yet reached the shoreline. Further

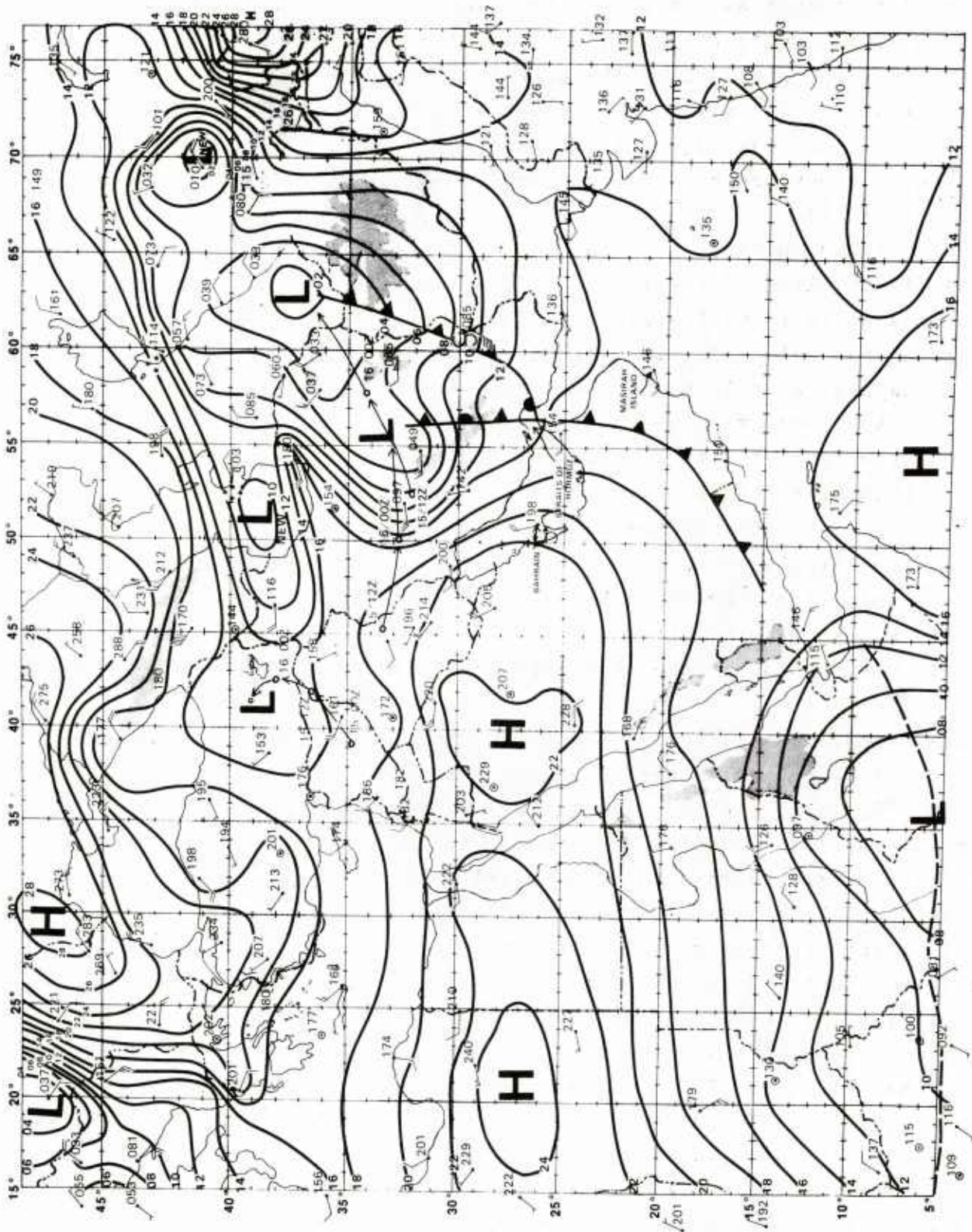


Figure B-12. Surface analysis, 16 Jan 1973 1200Z.

-- SATELLITE IMAGERY SHOWN ON NEXT FACING PAGES --

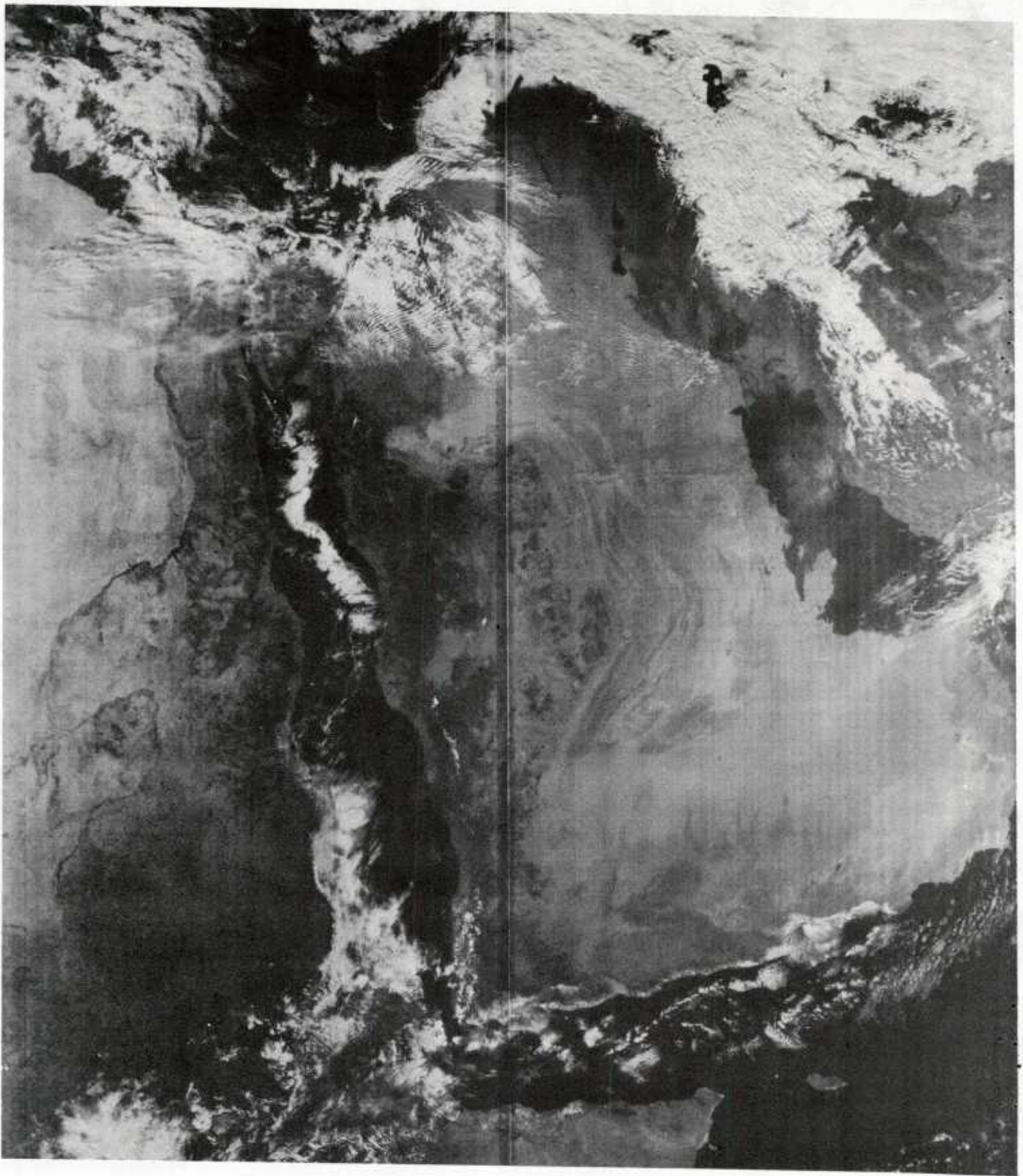


Figure B-13. DMSP visible image, 16 Jan 1973 local noon.



Figure B-13. Continued.

confirmation lies in the fact that following a cold frontal passage, the winds at Masirah Island (near 20.5°N, 59°E) typically blow northwesterly 20-25 kt with blowing dust and sand. These conditions, however, did not occur on 16 Jan.

It should be noted that the cold air behind the cold front is subject to rapid modification by warming from below as it advances southeastward over the Arabian Peninsula, much of which is desert. This includes the so-called "Empty Quarter" in the southeastern part of the Peninsula, which is one of the world's most arid regions. The amount of solar insolation incident upon the Peninsula in mid-winter is considerably less than during the mid-summer maximum. Nonetheless, during mid-winter the solar insolation may be enough to warm the earth's surface to the point that it can significantly modify some of the cool air masses which pass over the empty quarter behind the fronts associated with the shamal.

Except in the immediate region of the Persian Gulf, there is little low level moisture available over the Arabian Peninsula to produce frontal cloudiness. By the time these fronts reach the Arabian Sea coastline, they often have lost much of their cold frontal characteristics because of modification of the cold air mass as it passes over the warmer land mass and lack of low level moisture. The "front" therefore may well be little more than a wind shear line or shear zone.

Area G in the northern Gulf indicates the modification of colder air as it streams over warmer Gulf waters. Here, low level moisture is abundant, so that cumulus forms as the lower layers of the troposphere become unstable. The size of the white cloud elements involved seem to be at or near the resolution threshold of the DMSP high resolution sensor, suggesting that the cloud formation process has just begun. The general grayishness of the image in the northern Gulf may also represent low level dust and sand being advected by the shamal winds out over the region from the lower Tigris-Euphrates valley. Reduced visibilities near the surface in this region are implied.

B.4 17 JANUARY 1973

On 17 Jan, the upper level flow formed a shallow trough over the Arabian Peninsula, as shown by the 500 mb analyses in Figures B-14 and B-16). Shamal conditions persisted in the southern Gulf, as indicated by the 30 kt northwesterly wind reported by a ship at 17/00Z (Figure B-15).

The two surface lows over Iran on 16 Jan moved eastward the next day -- one to the northeast to become centered at 42°N, 65°E at 17/00Z, and the other to the east to become centered near 33°N, 63°E at 17/00Z (Figure B-15). By 17/12Z, Figure B-17, the surface lows were positioned near 48°N, 70°E and 32°N, 68°E, respectively.

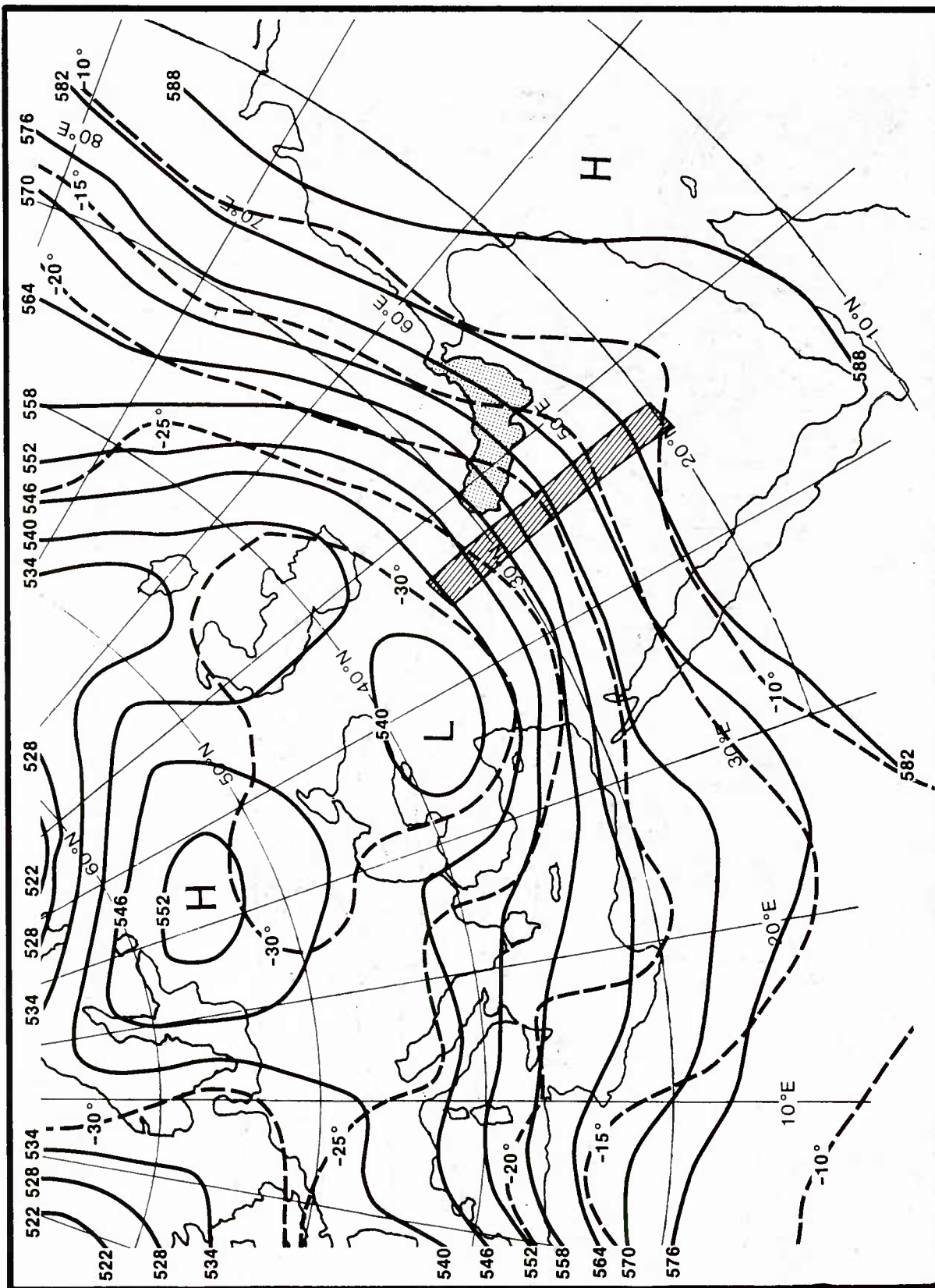


Figure B-14. 500 mb analysis, 17 Jan 1973 0000Z.

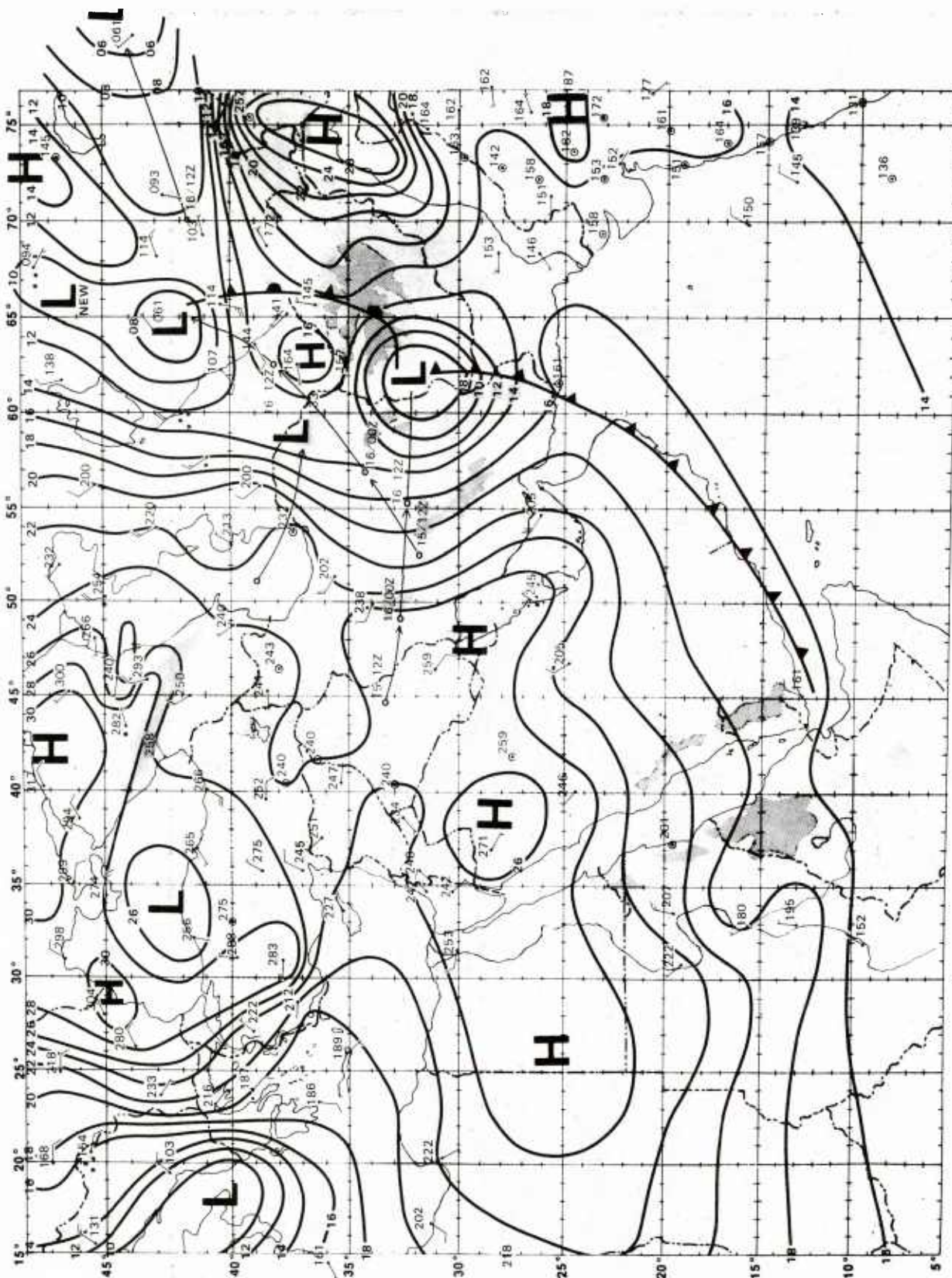


Figure B-15. Surface analysis, 17 Jan 1973 0000Z.

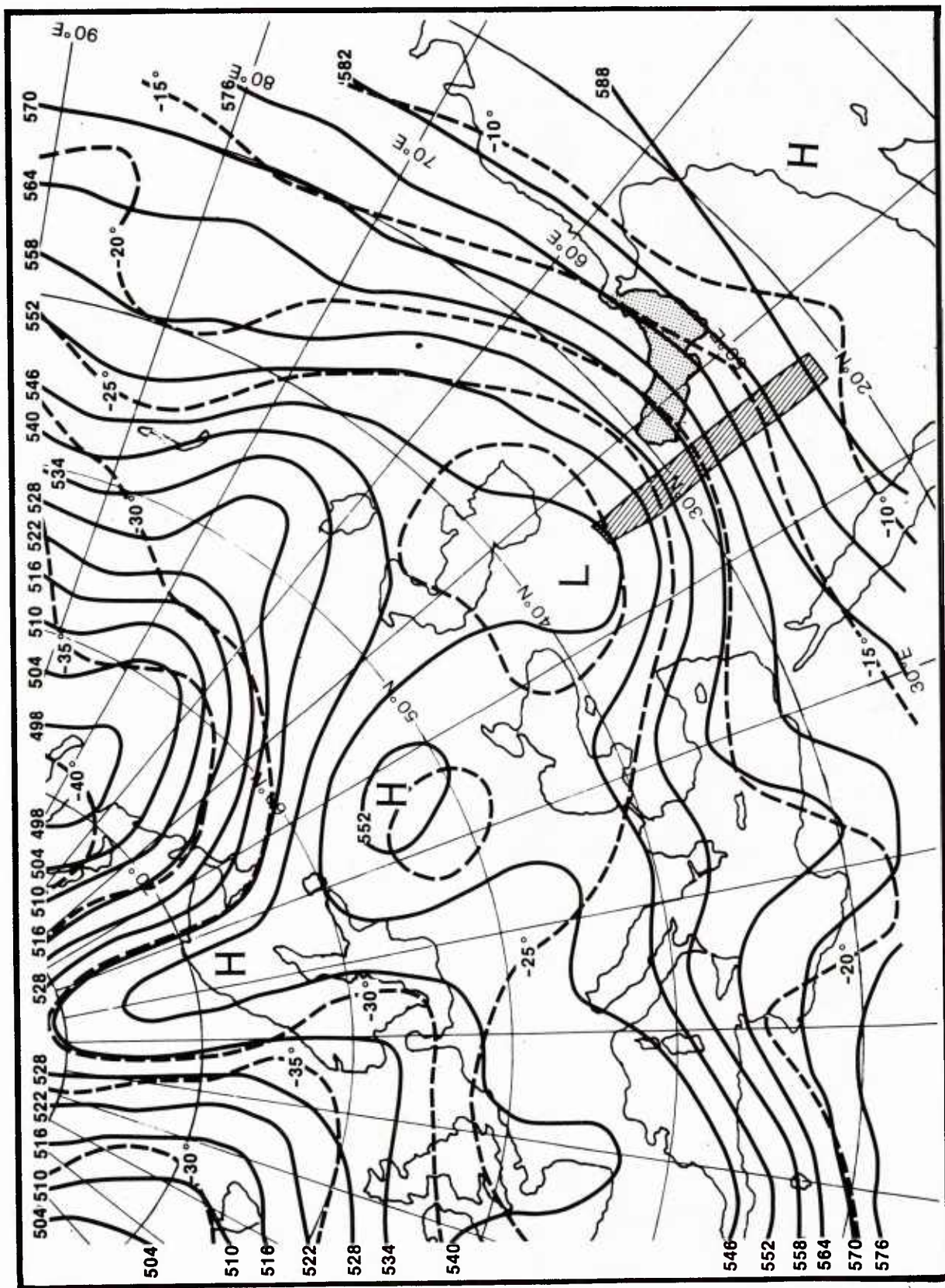


Figure B-16. 500 mb analysis, 17 Jan 1973 1200Z.

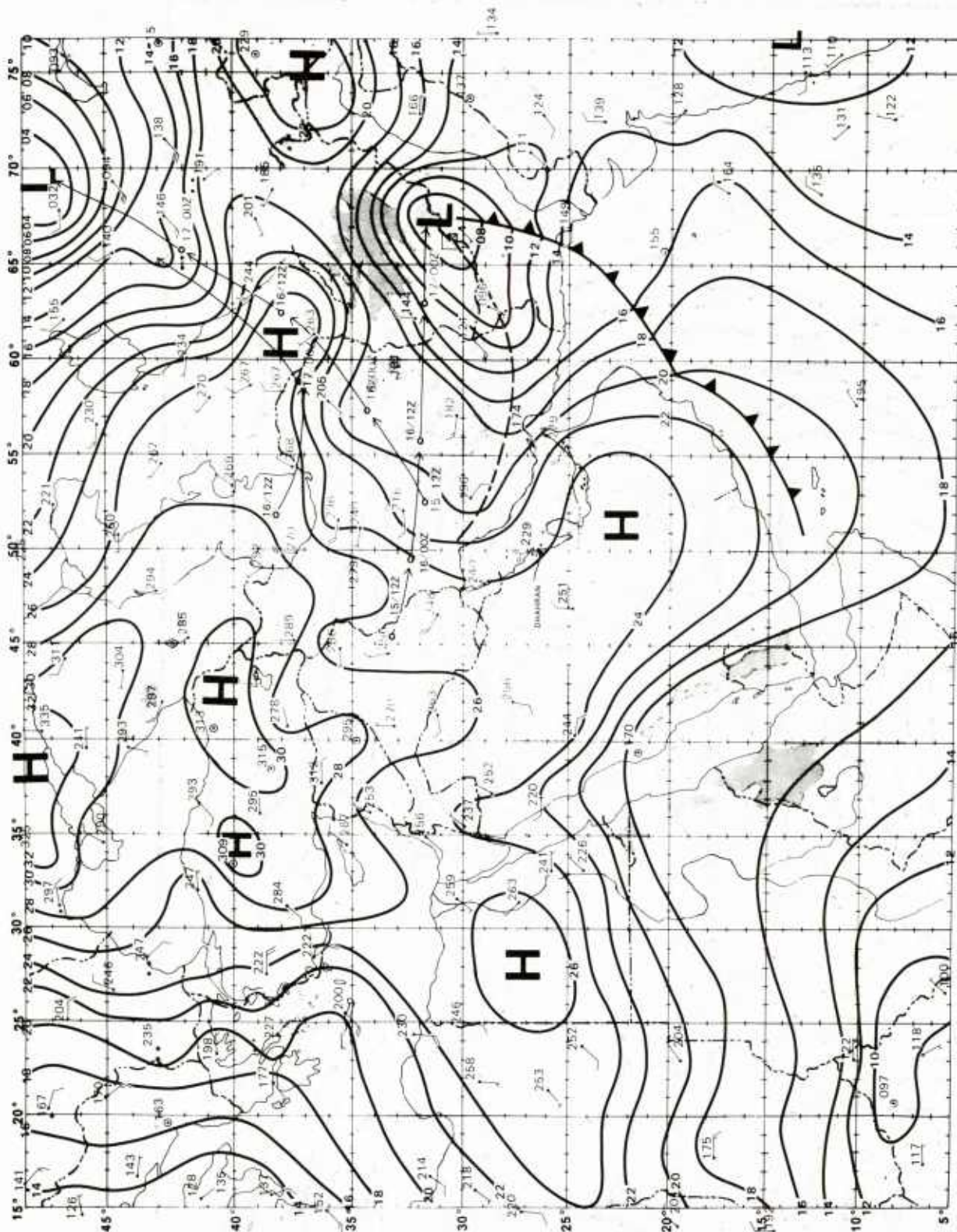


Figure B-17. Surface analysis, 17 Jan 1973 1200Z.

-- SATELLITE IMAGERY SHOWN ON NEXT FACING PAGES --

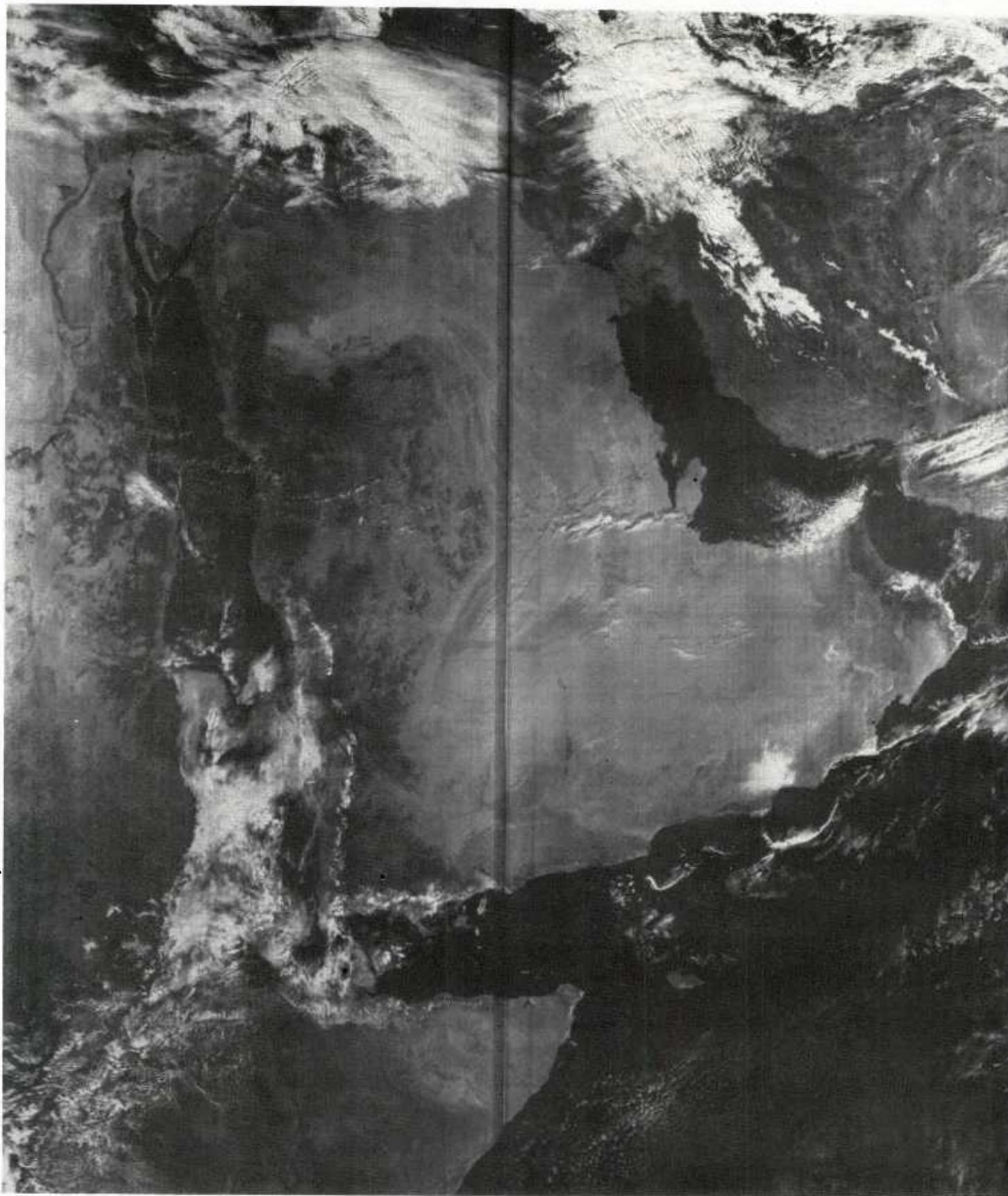


Figure B-18. DMSP visible image, 17 Jan 1973 local noon.

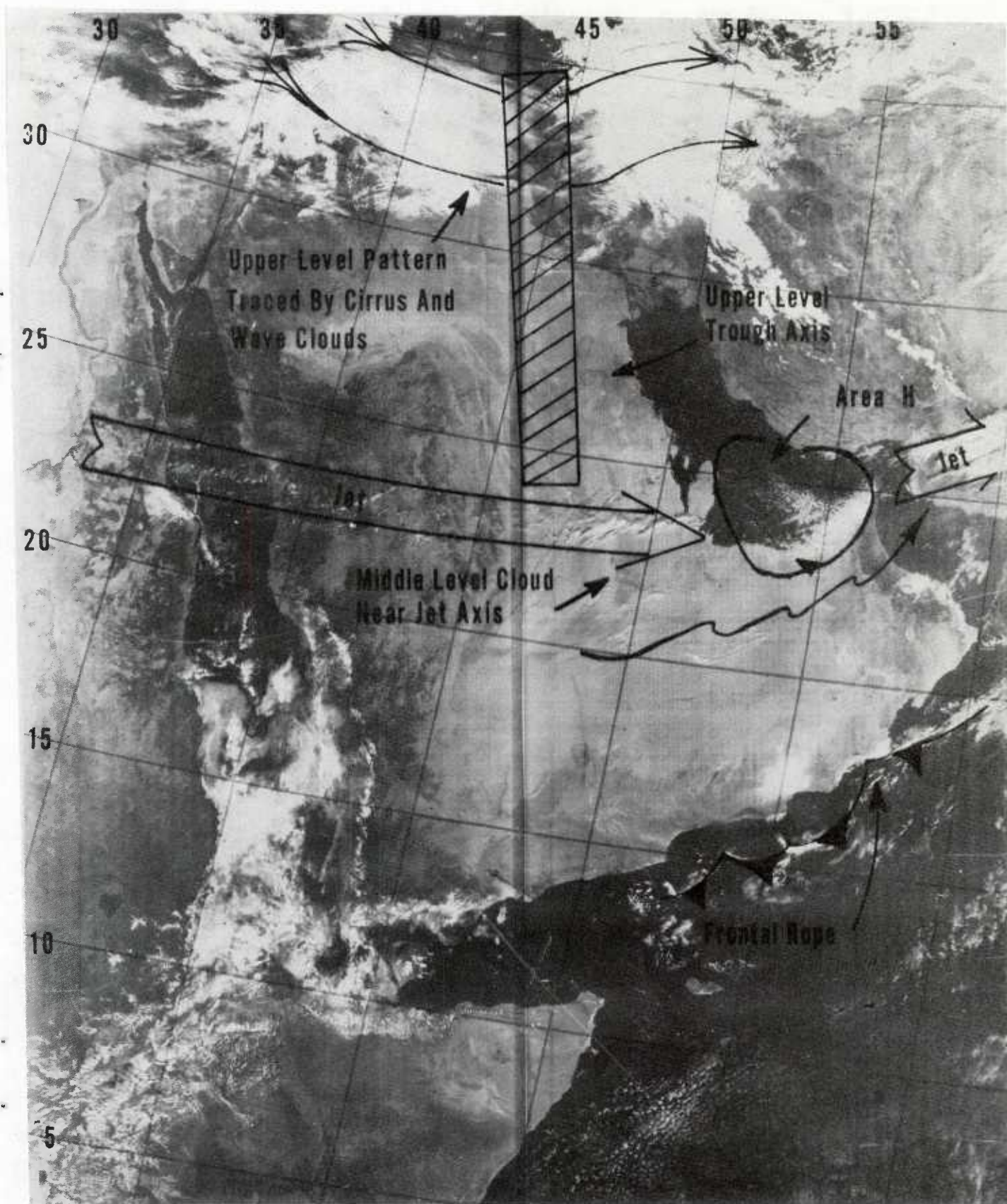


Figure B-18. Continued.

The DMSP satellite visible image for 17 Jan, Figure B-18, offers further evidence of the continuance of the shamal. The cloud pattern labeled H and aligned northwest-southeast is the typical satellite-image "signature" of a relatively cold northwesterly air stream (behind a cold front) which has been advected over relatively warmer water. The lower right portion of area H confirms the northwesterly direction of the wind. The clouds formed over the waters of the southern Gulf and were advected onto the southeastern shore.

The broad upper trough is also traced out on Figure B-18: by the cirrus pattern at the top of the image; and by the middle-level cloudiness near the jet axis across the central portion of the Arabian Peninsula.

The visible image also reveals that the elements of a frontal rope were present as the modified cold air mass over the Arabian Peninsula began to move off in the Arabian Sea. It can not be stated with certainty that this was a "cold" frontal rope, particularly in view of the probable modification of the air mass discussed in connection with the events of 16 Jan. The organized cloud line shown in Figure B-18 seems to mark a shear line boundary between the modified air advancing southeastward off the Arabian Peninsula and the resident air over the Arabian Sea. The cloud elements were to become more fully organized into a line on 18 Jan.

B.5 18 JANUARY 1973

The axis of the relatively flat upper long wave trough moved southeastward to a position over the southern Gulf on 18 Jan. Accordingly, the associated upper westerlies were displaced far enough southward to flow over southern Iran and the Strait of Hormuz. This is confirmed by the 500 mb analyses at 18/00Z and 18/12Z (Figures B-19 and B-21) and the DMSP visible satellite image near noon local time on 18 Jan (Figure B-23). Wave clouds downstream of the Hajar Mountains of the Oman Peninsula appear at right angles to this moderately strong upper flow at area I on Figure B-23.

The 18/00Z surface chart, Figure B-20, indicates a recently-formed surface trough with central pressure of 1011 mb over the Arabian Sea; the trough extends back into the Gulf of Oman and along the eastern shore of the Persian Gulf. It appears that the trough over the Gulf of Oman was induced by a combination of concave terrain effects* (Figure B-24) and upward motion associated with positive vorticity advection (vertical motion) to the east of the 500 mb long wave upper trough axis (Figures B-19 and B-21). Evidence of a weak vortex appears in cloud pattern J on the local noon DMSP visible image, Figure B-23. The vortex is also reflected in the surface analysis, Figure B-20, near 21°N, 63°E.

*See Godev, 1970 1971.

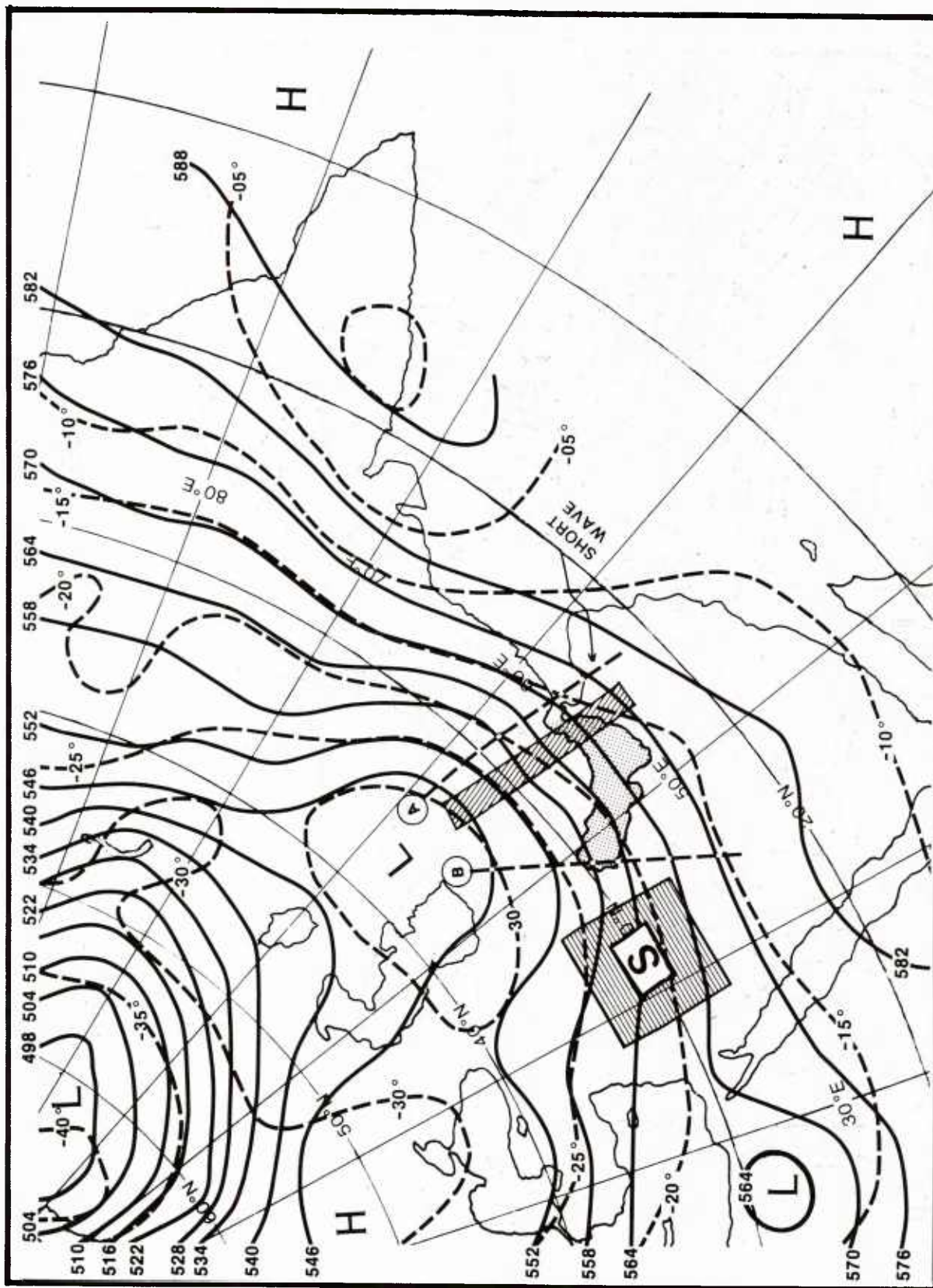


Figure B-19. 500 mb analysis, 18 Jan 1973 0000Z.

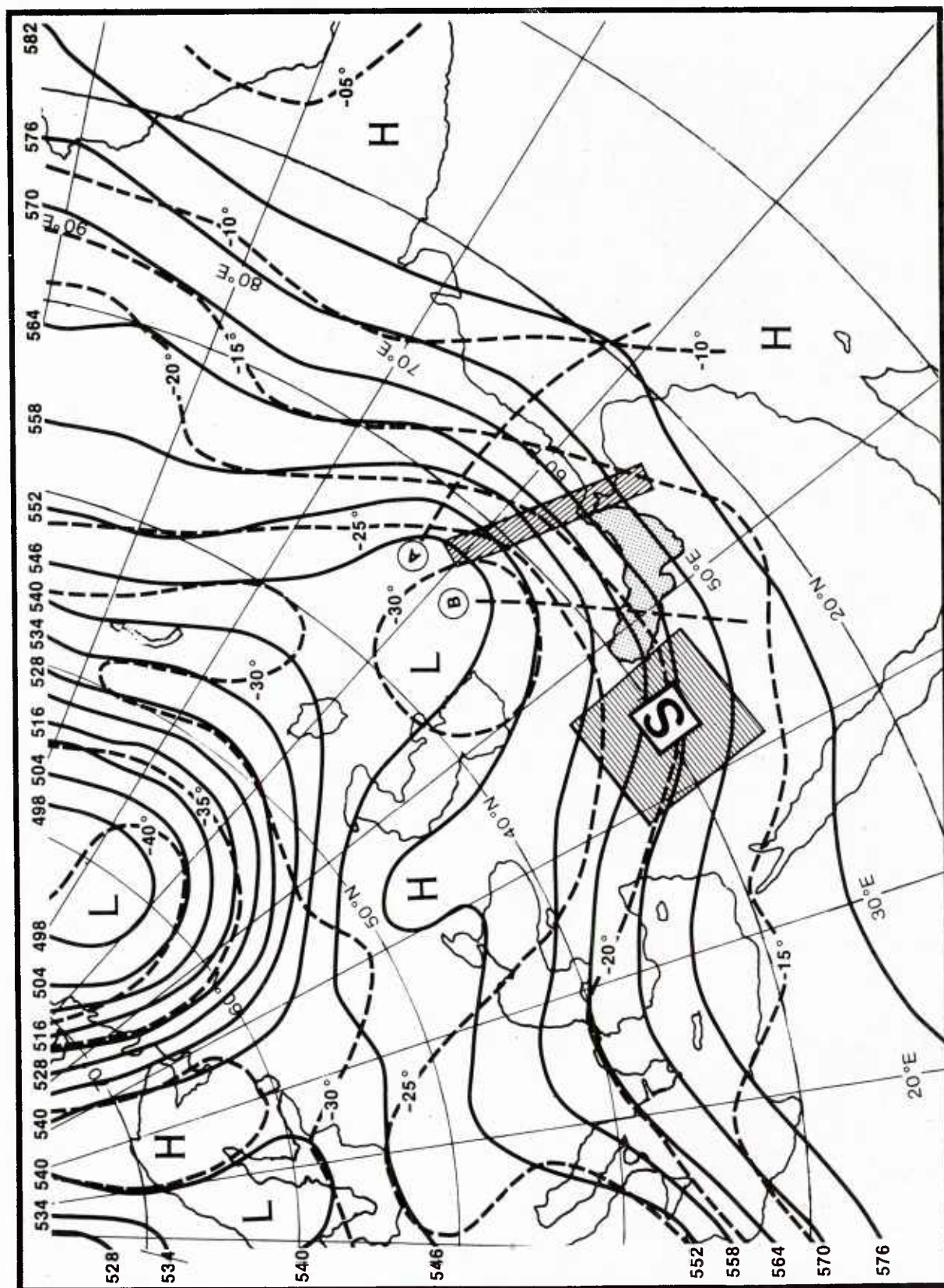


Figure B-21. 500 mb analysis, 18 Jan 1973 1200Z.

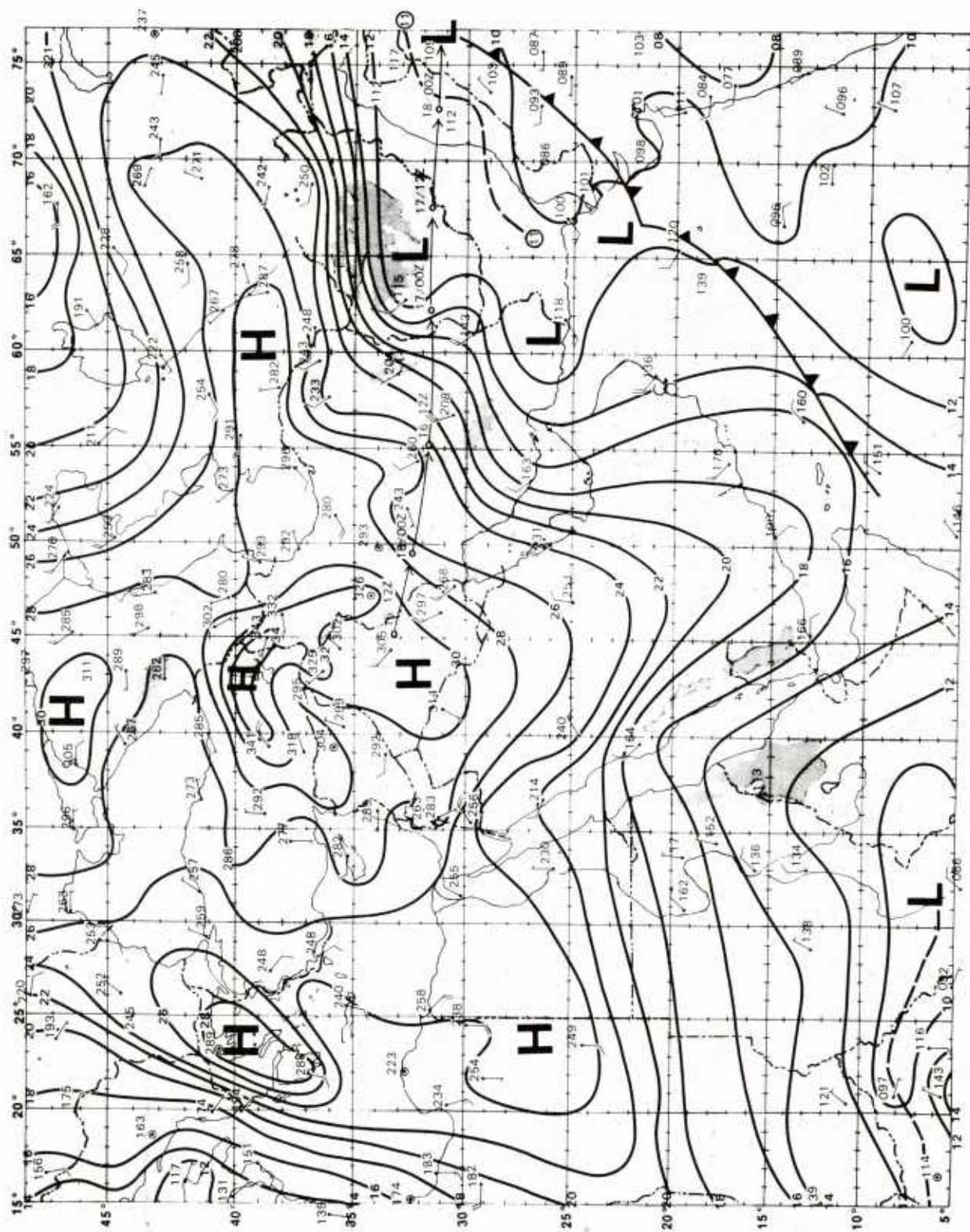


Figure B-22. Surface analysis, 18 Jan 1973 1200Z..

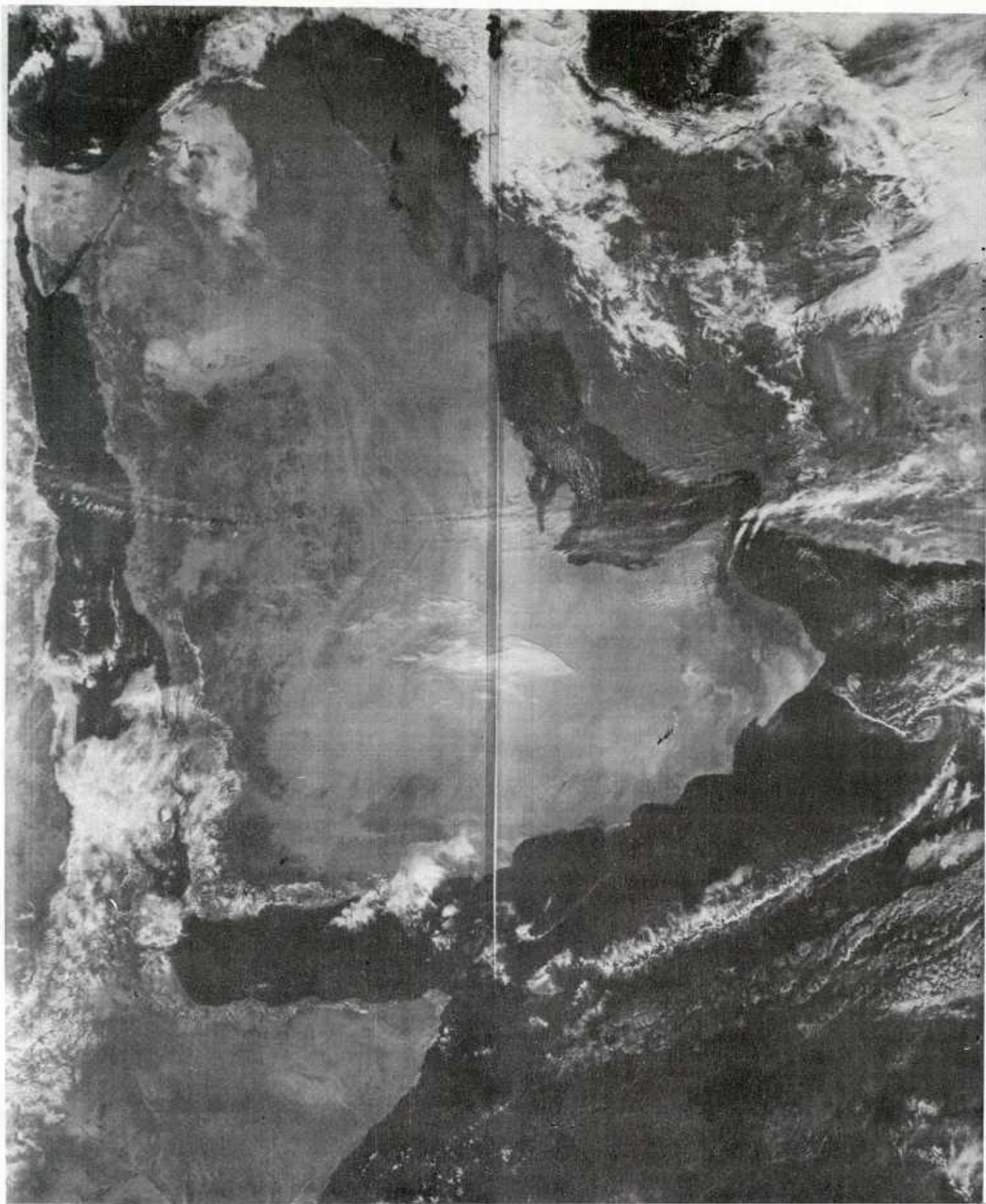


Figure B-23. DMSP visible image, 18 Jan 1973 local noon.

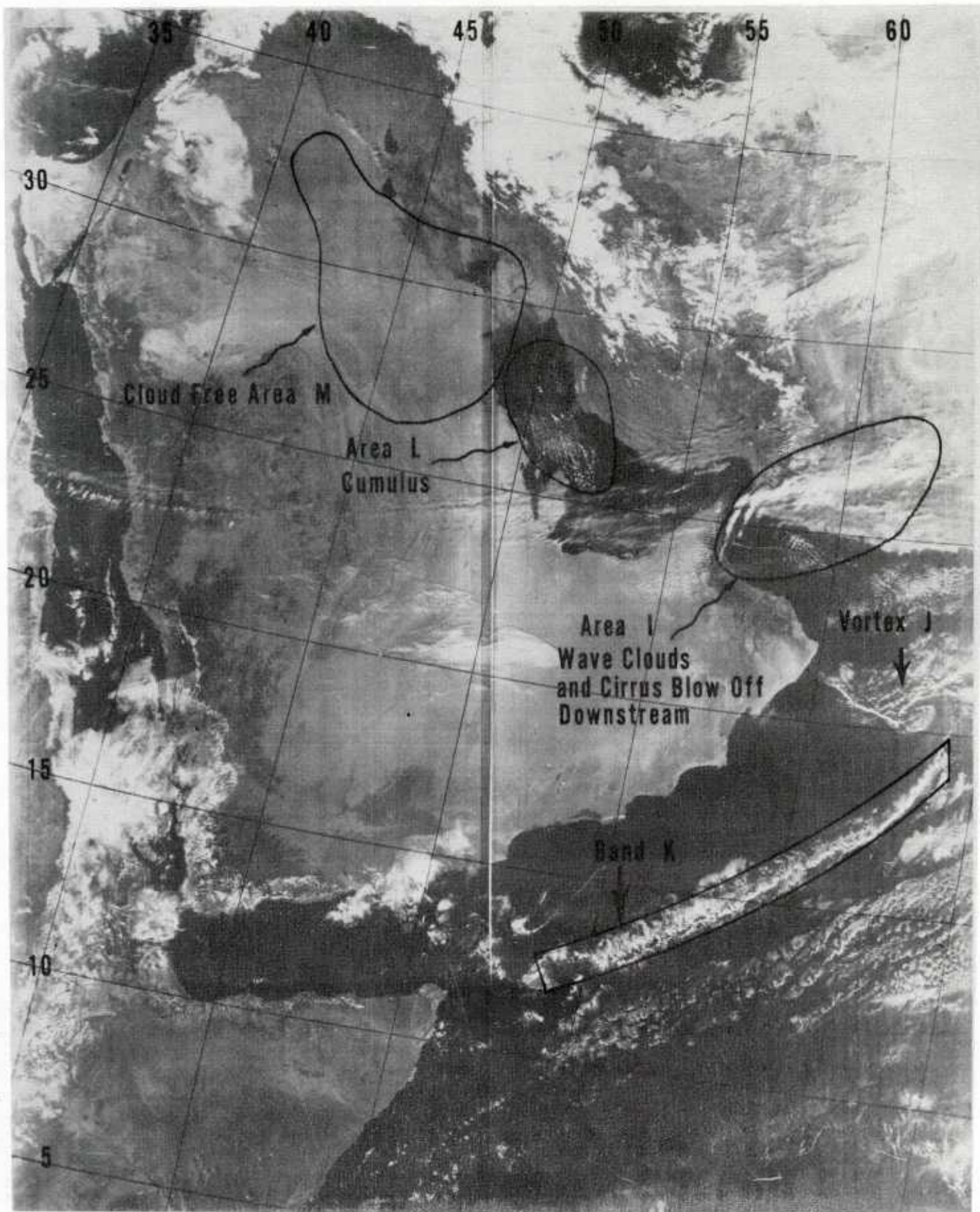


Figure B-23. Continued.

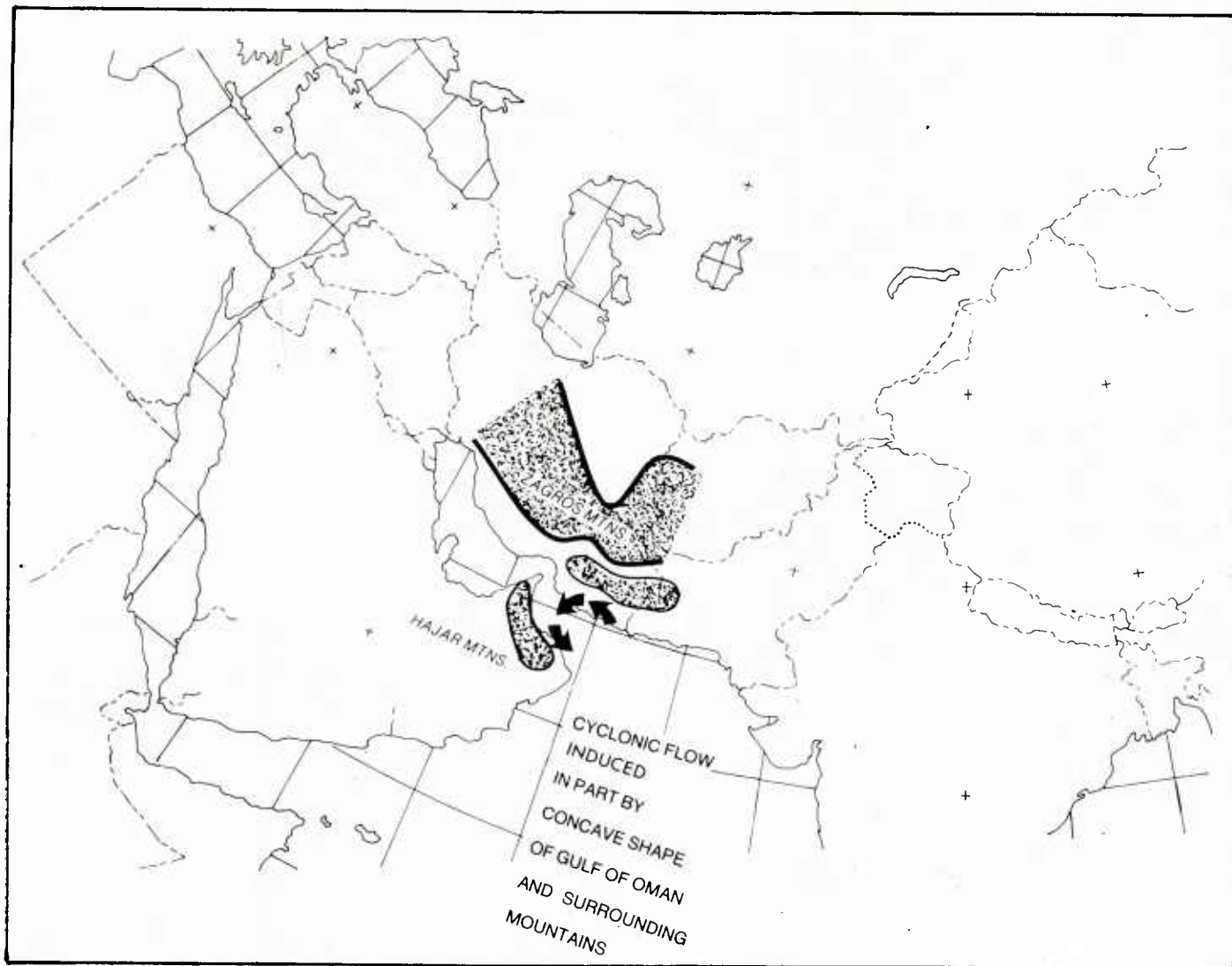


Figure B-24. Cyclonic surface circulation in Gulf of Oman induced by Gulf's concave shape and surrounding mountains.

Of the many short waves that moved through the long wave trough position, two are of particular interest (see 500 mb analyses, Figures B-19 and B-21). Short wave A on Figure B-21, to the east of the long wave position, is associated with vortex J over the Arabian Sea. Also associated with the vortex is band K on Figure B-23, the frontal rope structure. This cloud structure lay just off the Arabian coast on 17 Jan and then became more fully organized and lay further east in the Arabian Sea on 18 Jan. This structure is indicated as a weak cold front on the 18/00Z and 18/12Z surface analyses, Figures B-20 and B-22.

Short wave B on Figure B-21, to the west of the long wave position, is associated with freshly-formed cumulus convection over the northern and central Persian Gulf (area L in Figure B-23). The northwest-southeast orientation of the cumulus lines confirms the continued northwesterly flow in the lower levels over the Gulf.

A 6-8 mb surface pressure gradient oriented northwest-southeast was maintained between the Gulf of Oman and the northern Persian Gulf. Forecasting experience in the region indicates that such a pressure gradient is more than sufficient to sustain a gale force shamal, particularly in the southern Persian Gulf.

Well to the rear of the upper air trough axis, sinking motion occurred in the lower troposphere over northern Saudi Arabia, Iraq and Syria. This motion is indicated by the clear area labeled M on the visible image, Figure B-23; and by an S, for sinking motion, on the 500 mb analyses, Figures B-19 and B-21).

The central surface pressures near the surface high centered over Iraq rose at least 4 mb in 24 hr (computing 24 hour surface pressure changes takes diurnal surface pressure variations into account). This increase occurred at both 00Z and 12Z on 18 Jan (Figures B-20 and B-22), compared with the same time charts on 17 Jan (Figures B-15 and B-17).

B.6 19 JANUARY 1973

At 19/00Z, Figure B-25, the long wave upper trough remained virtually stalled near the Strait of Hormuz, where it had been since 18/00Z. By 19/12Z, it had begun to move eastward again, and was centered near the Afghanistan-Iran border at about 60°E by 12Z (Figure B-27). The surface analyses suggest that the shamal continued at 00Z (Figure B-26) with northwesterly 20 kt winds at Dhahran near 26°N, 50°E. The wind remained at 20 kt at Dhahran at 20/12Z (Figure B-28). There are signs, however, that the shamal is about to weaken. The surface pressure gradient began to slacken in the southern Persian Gulf. The 19/12Z surface analysis, Figure B-28, suggests a phenomenon that tends to foretell the end of the shamal. Easterly winds, local sea breeze effects, or a combination of the two, began to appear in the extreme eastern part of the Gulf

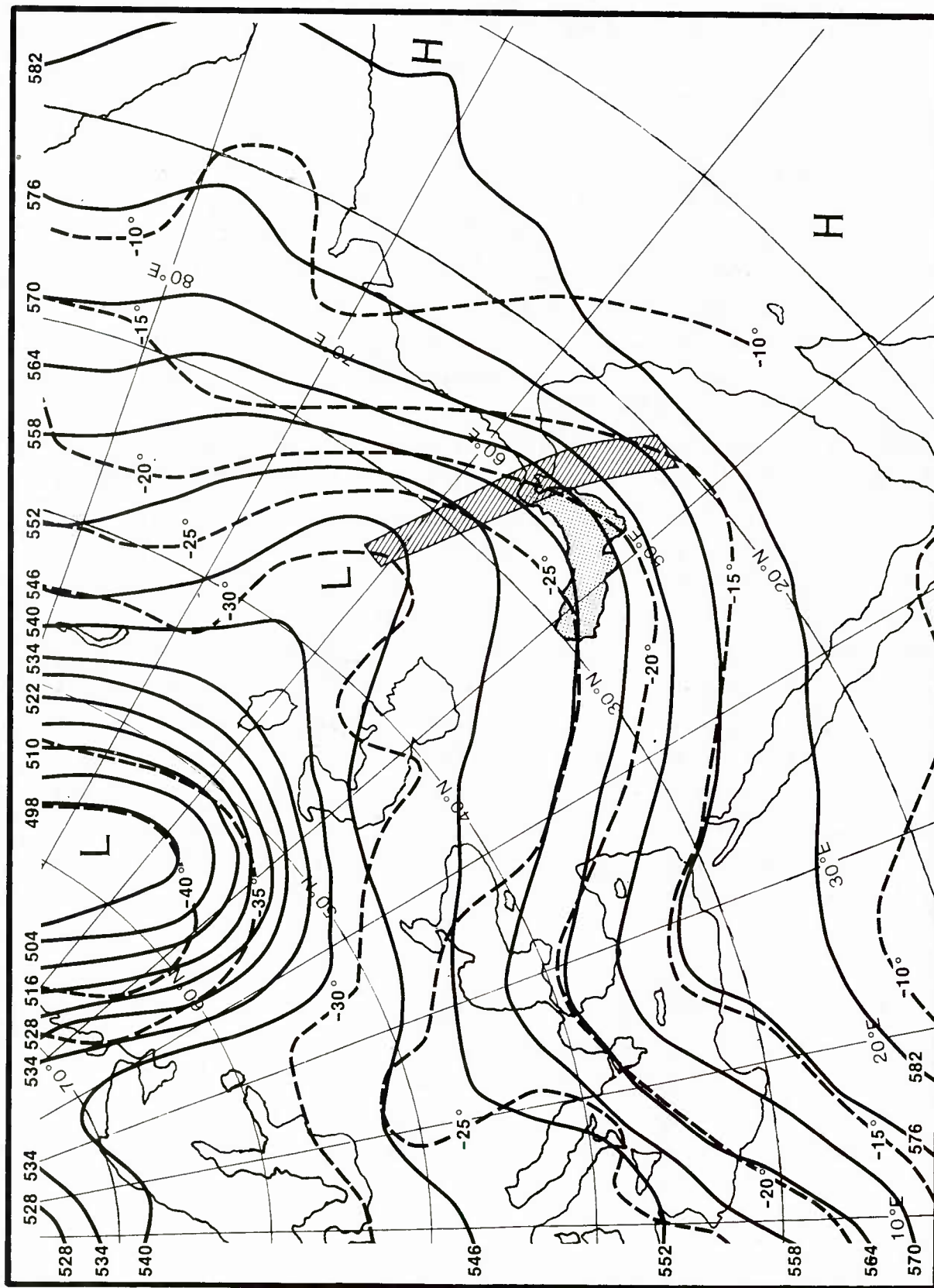


Figure B-25. 500 mb analysis, 19 Jan 1973 0000Z.

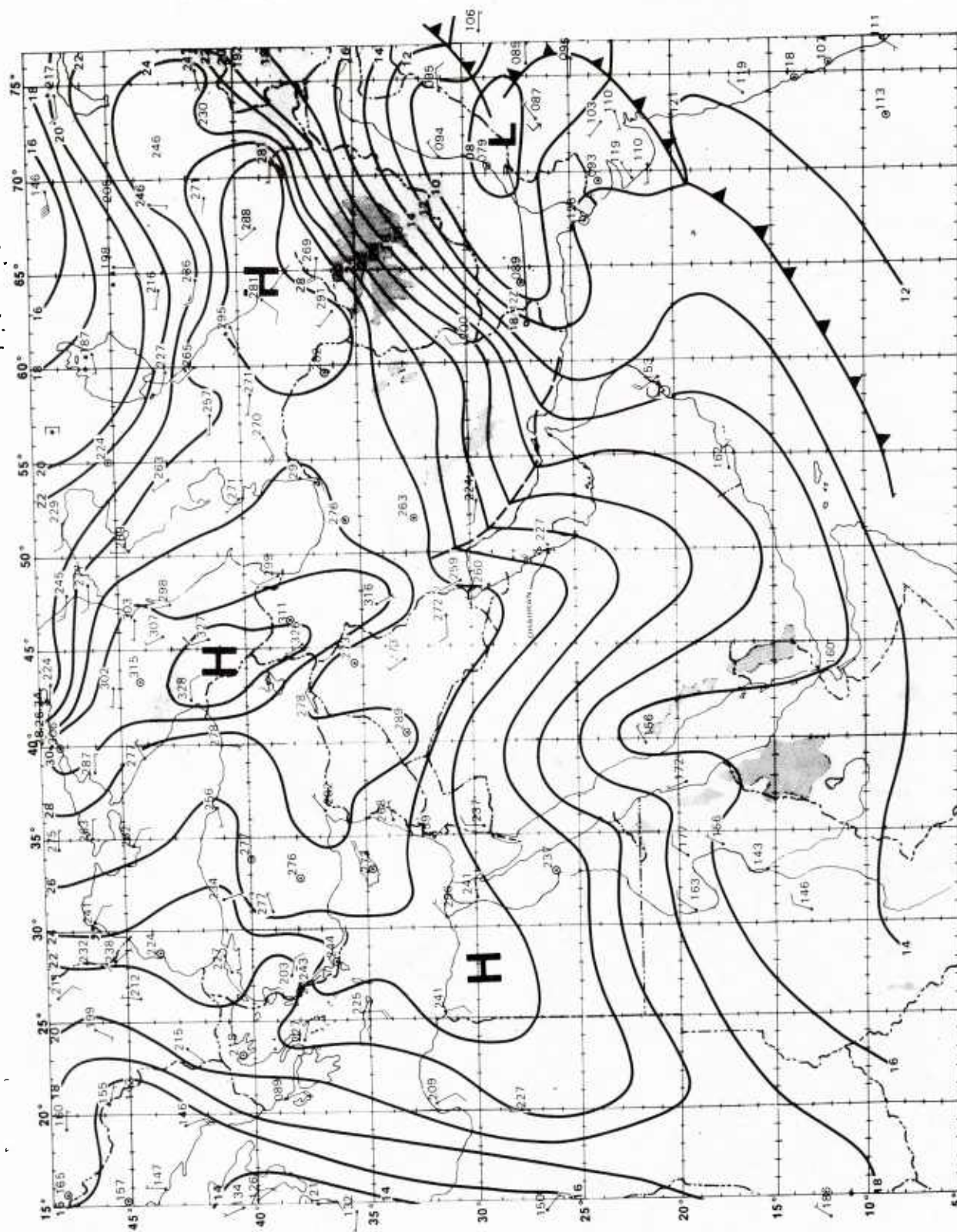


Figure B-26. Surface analysis, 19 Jan 1973 0000Z.

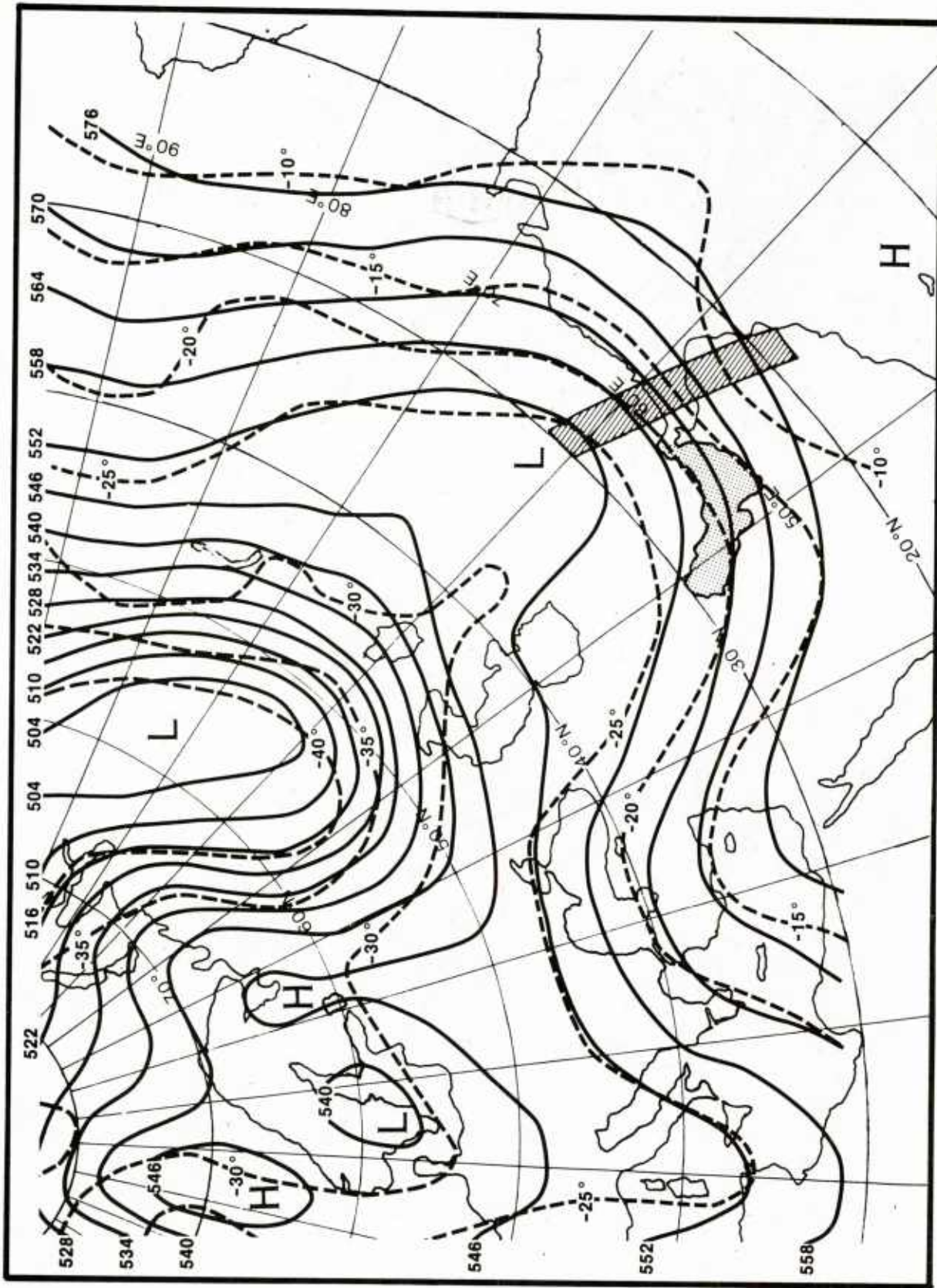


Figure B-27. 500 mb analysis, 19 Jan 1973 1200Z.

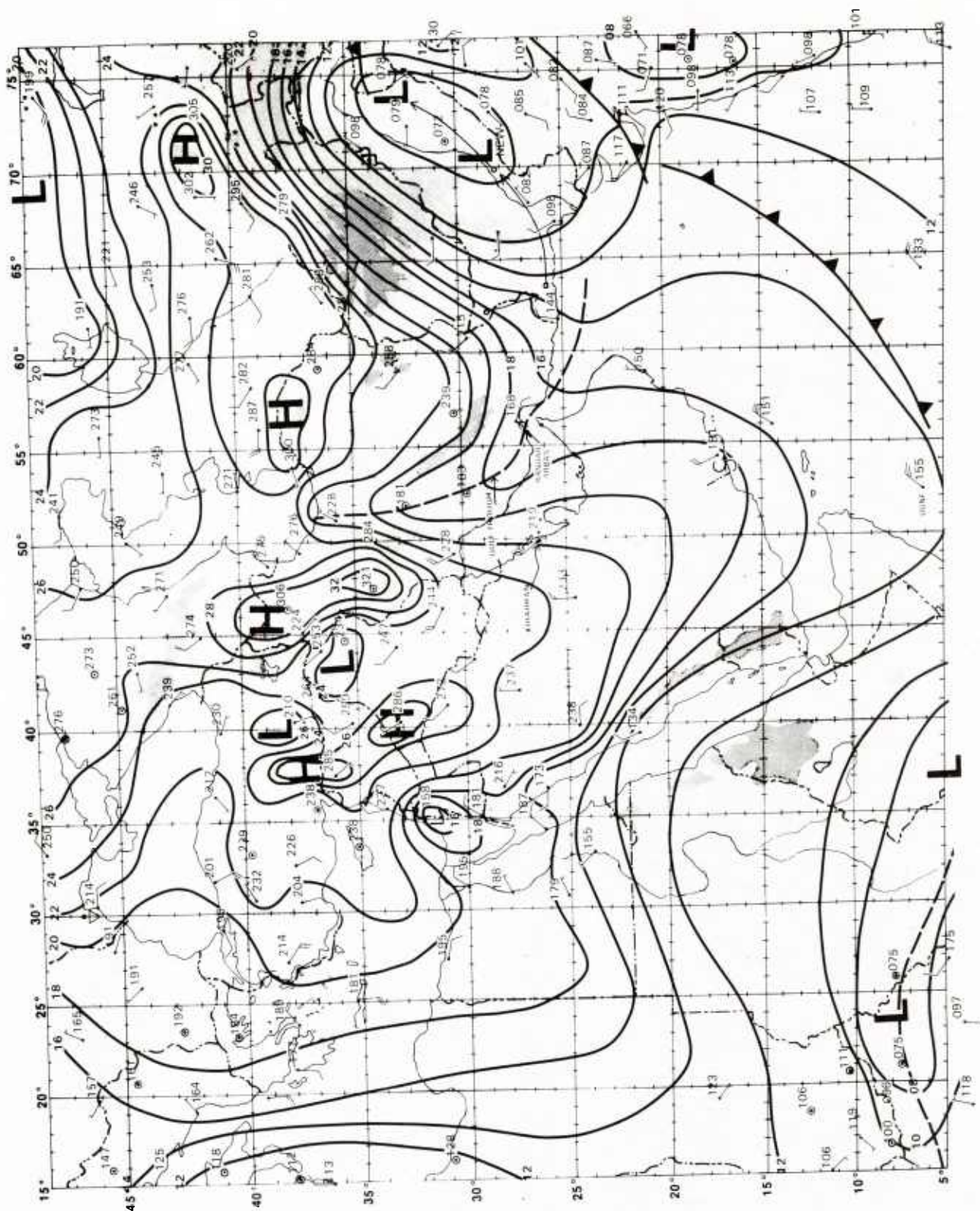


Figure B-28. Surface analysis, 19 Jan 1973 1200Z.

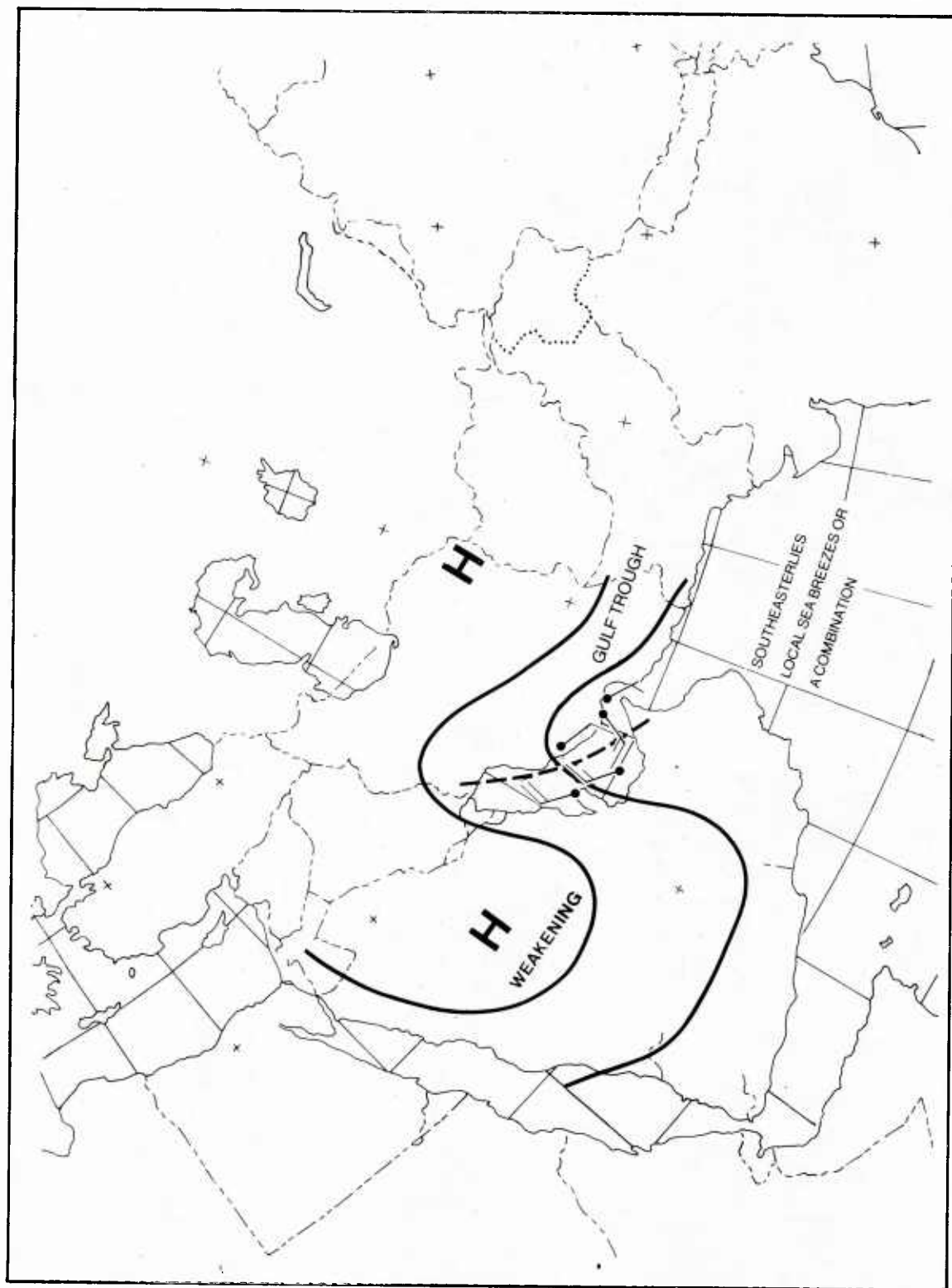


Figure B-29. Typical end-of-shamal surface wind pattern.

-- SATELLITE IMAGERY SHOWN ON NEXT FACING PAGES --

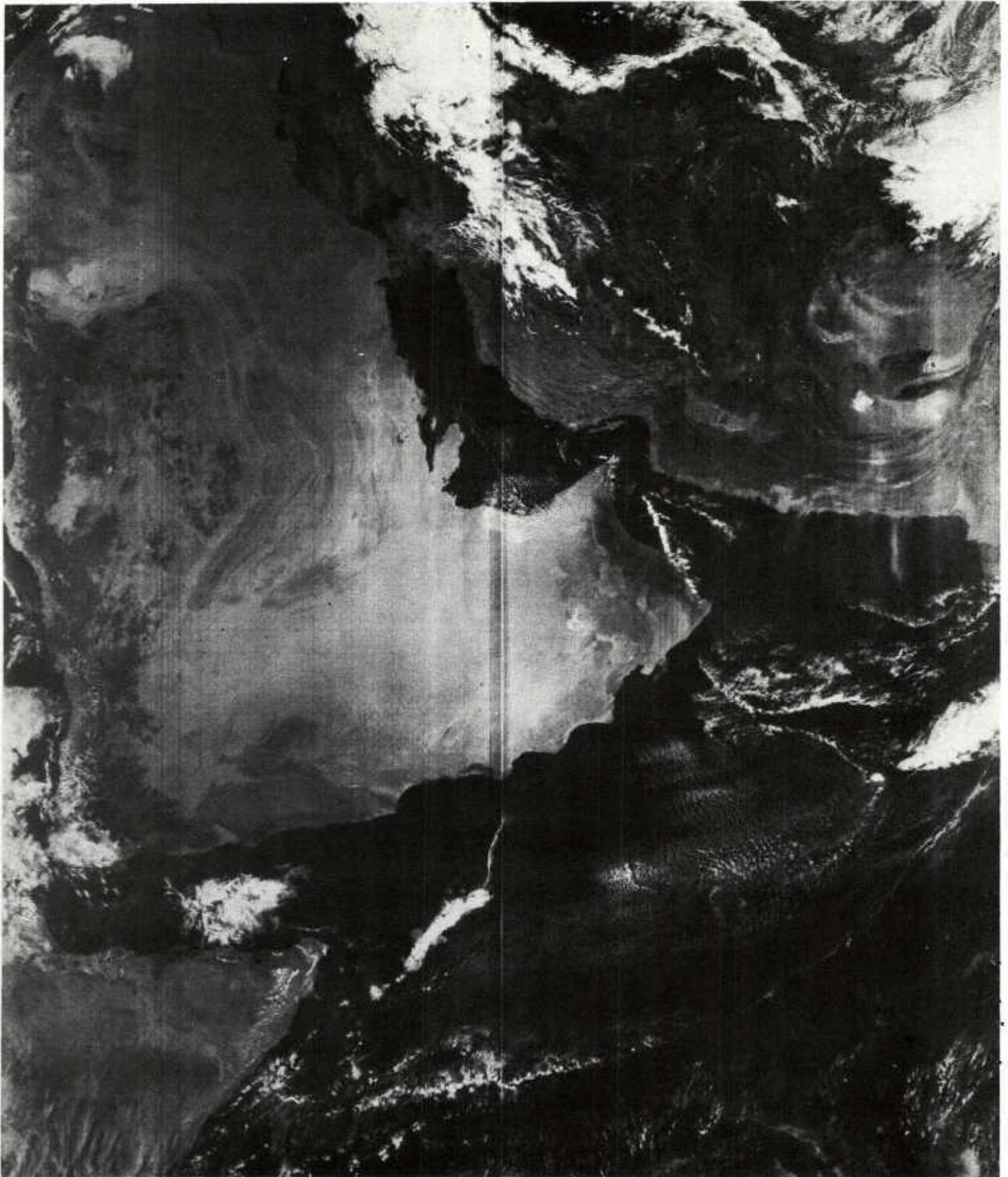


Figure B-30. DMSP visible image, 19 Jan 1973 local noon.

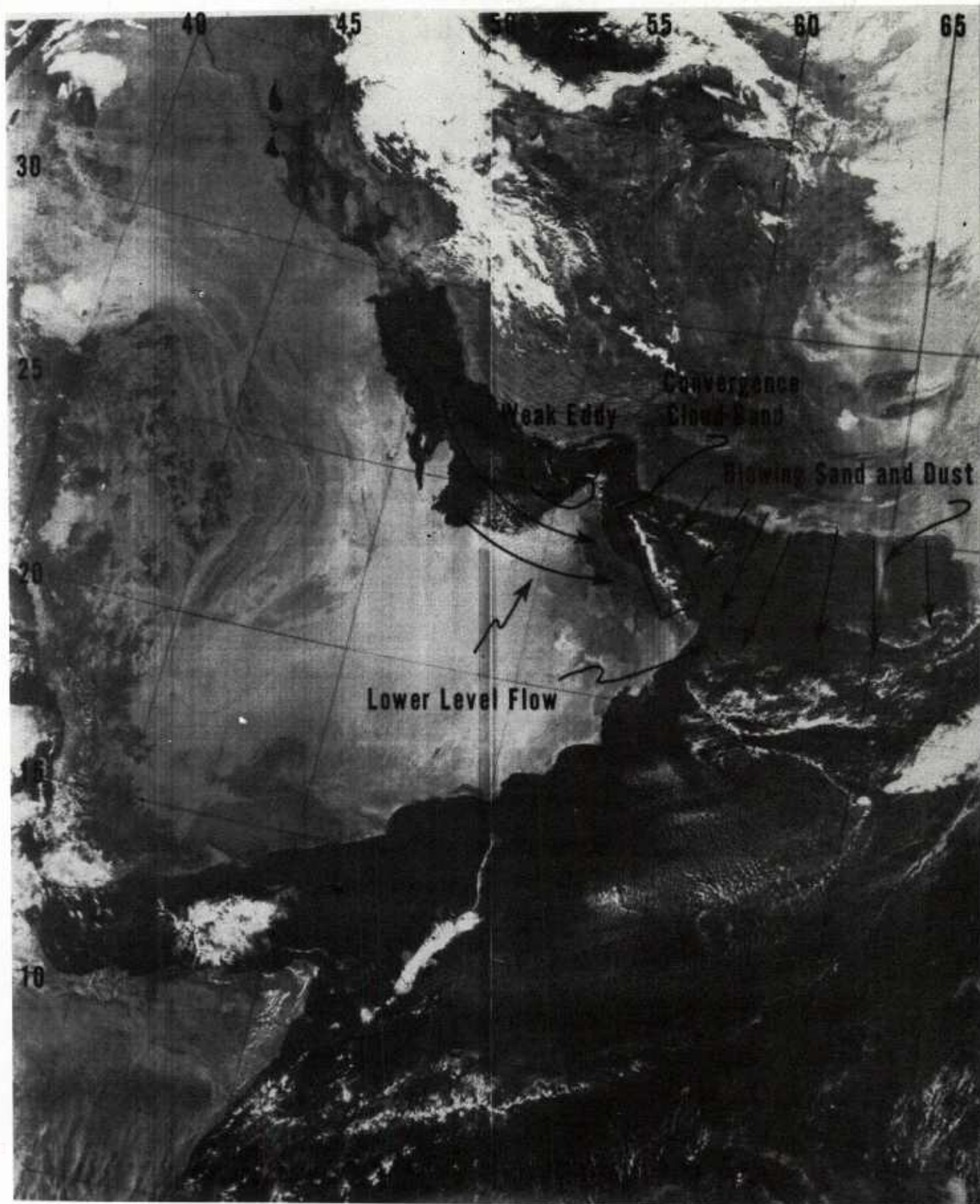


Figure B-30. Continued.

(note southeasterly winds at Bandar Abbas near 27°N, 56°E), while 15-20 kt northwesterlies persisted on the western side (see Figure B-29).

The DMSP visible image near local noon on 19 Jan, Figure B-30, also foretells the breaking of the shamal. Note a convergence band oriented northwest-southeast, on the visible image. No complete explanation can be offered for the presence of this feature without more supporting data; however, its shape suggests a convergence zone for offshore low level flow.*

Analysis of the DMSP visible image for 19 Jan (Figure B-30) suggests that the convergence band was formed by the meeting of a westerly flow off the Hajar Mountains with a north-to-northeasterly flow off the Iran-Pakistan mainland. The westerly flow is suggested by the alignment of the lower-level cloud elements over the southern Persian Gulf (including a weak eddy in the southern Gulf just to the east of the Strait of Hormuz). The northerly flow is traced by blowing sand and dust advected out over the Arabian Sea between 60°E to 67°E near 25°N.

B.7 20 AND 21 JANUARY 1973

On 20 Jan the upper air trough was just east of 60°E at 00Z, Figure B-31; it moved to near 65°E by 12Z, Figure B-33. The shamal had broken on the western side of the Gulf by 20/00Z. The surface wind at Dhahran, near 26°N, 50°E, was 05 kt at 20/00Z (Figure B-32) and 15 kt at 20/12Z (Figure B-34). The convergence band in the Gulf of Oman also occurs on the local noon DMSP visible satellite image of 20 Jan (Figure B-35); however, is located closer to the Arabian Peninsula coast of the Gulf of Oman than on the visible image of 19 Jan (Figure B-30). This suggests that the strength of the air flow on the western side of the cloud band had become weaker than on its eastern side. This, in turn, is consistent with the abatement of the shamal in the Persian Gulf.

By 21/00Z, the upper air trough had moved well eastward to western India (upper trough axis near 70°E, Figure B-36).

*Compare this with the DMSP images of 26 Jan 1974 (Figures A-31 and A-32, Case Study 1, Appendix A) at the end of that shamal -- they appear to be similar cloud structures.

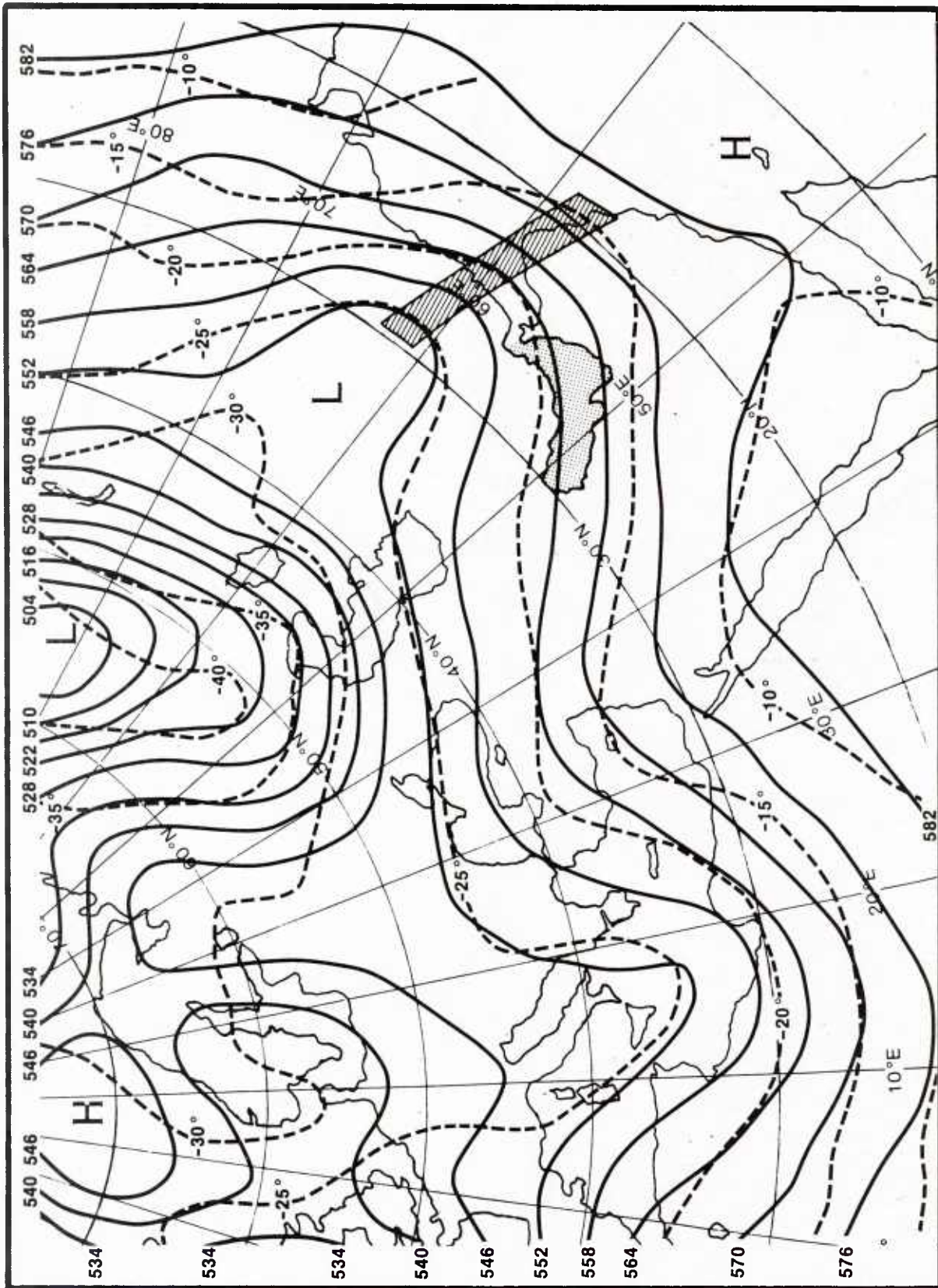


Figure B-31. 500 mb analysis, 20 Jan 1973 0000Z.

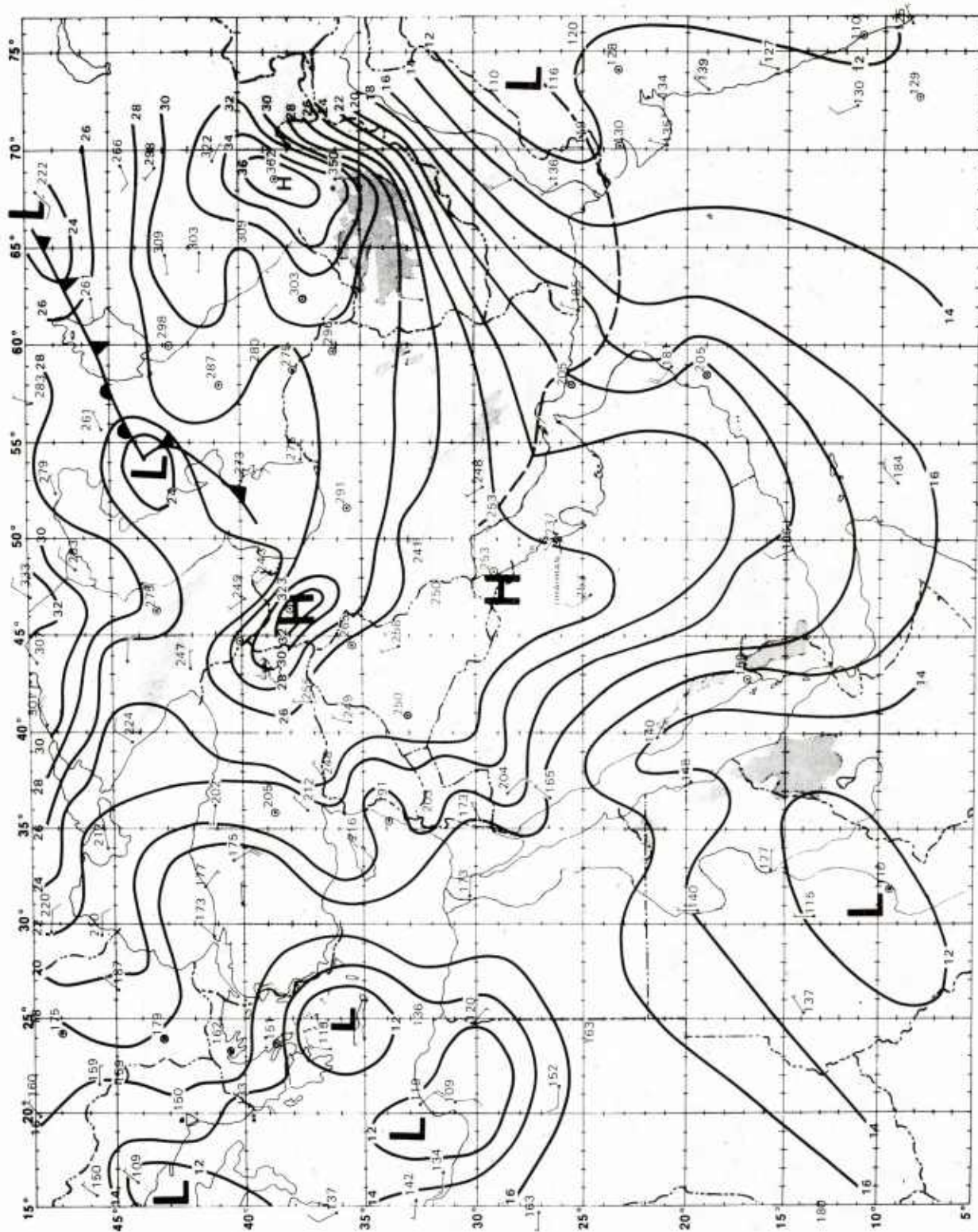


Figure B-32. Surface analysis, 20 Jan 1973 0000Z...

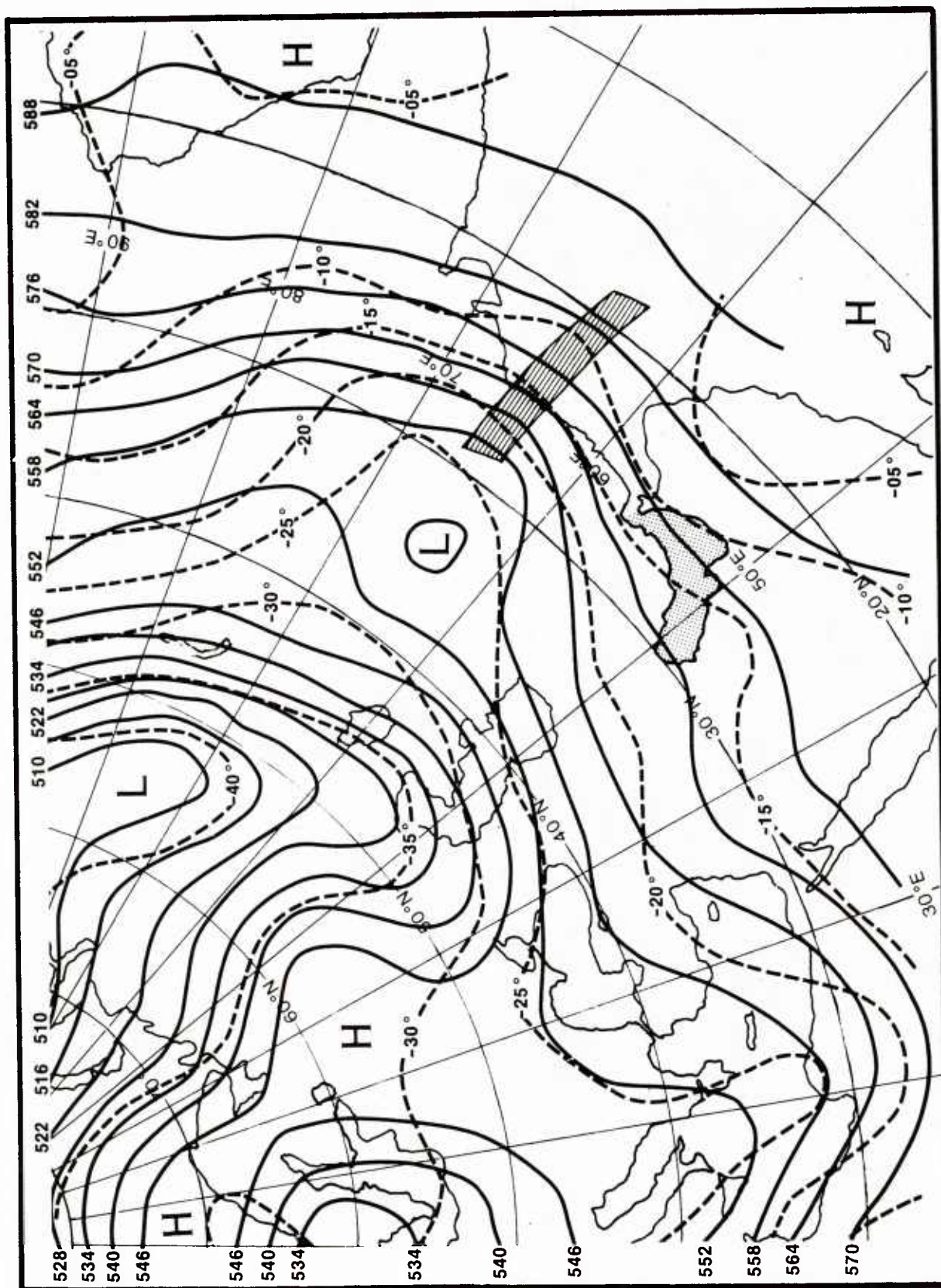


Figure B-33. 500 mb analysis, 20 Jan 1973 1200Z.

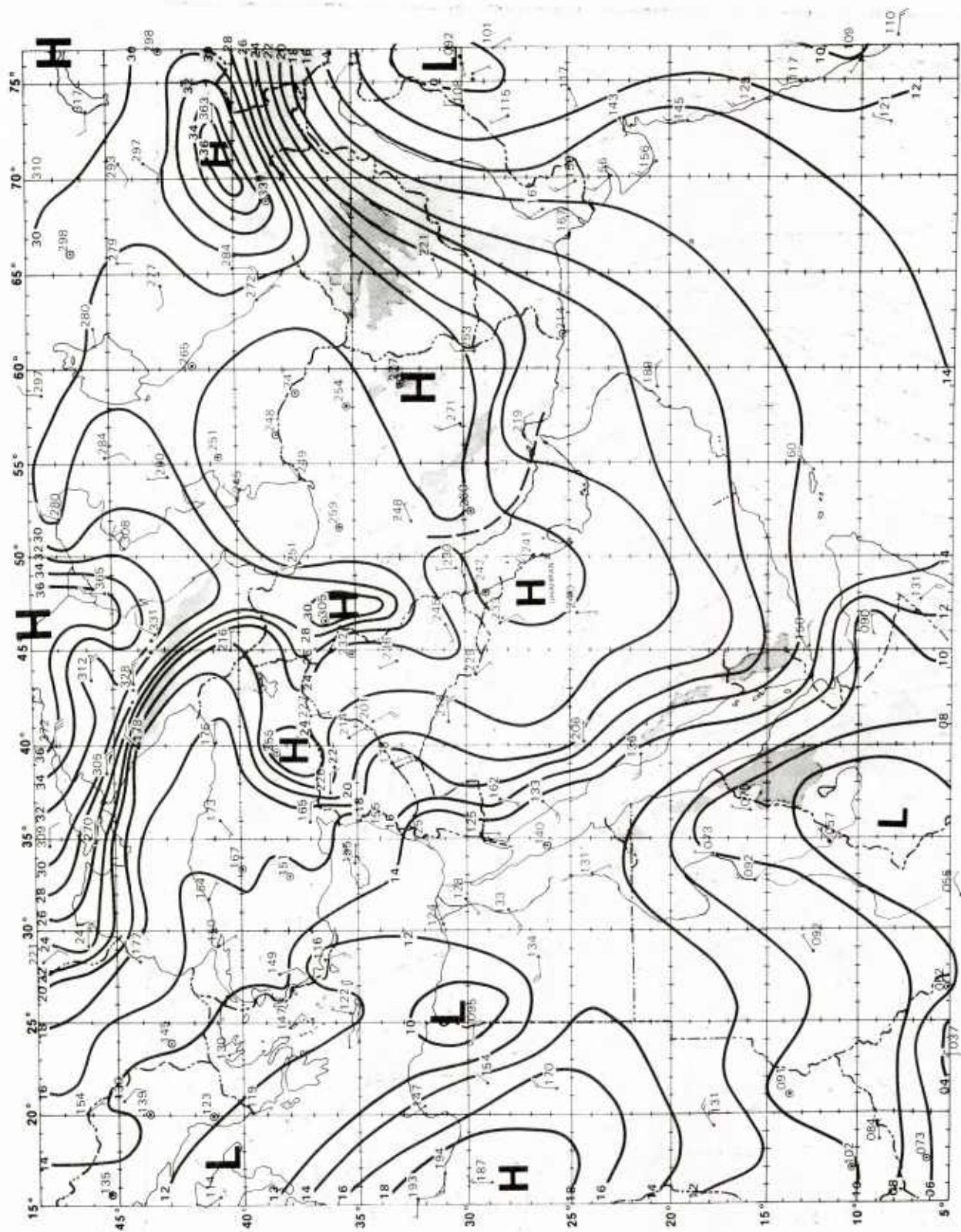


Figure B-34. Surface analysis, 20 Jan 1973 1200Z.

-- SATELLITE IMAGERY SHOWN ON NEXT FACING PAGES --



Figure B-35. DMSP visible image, 20 Jan 1973 local noon.

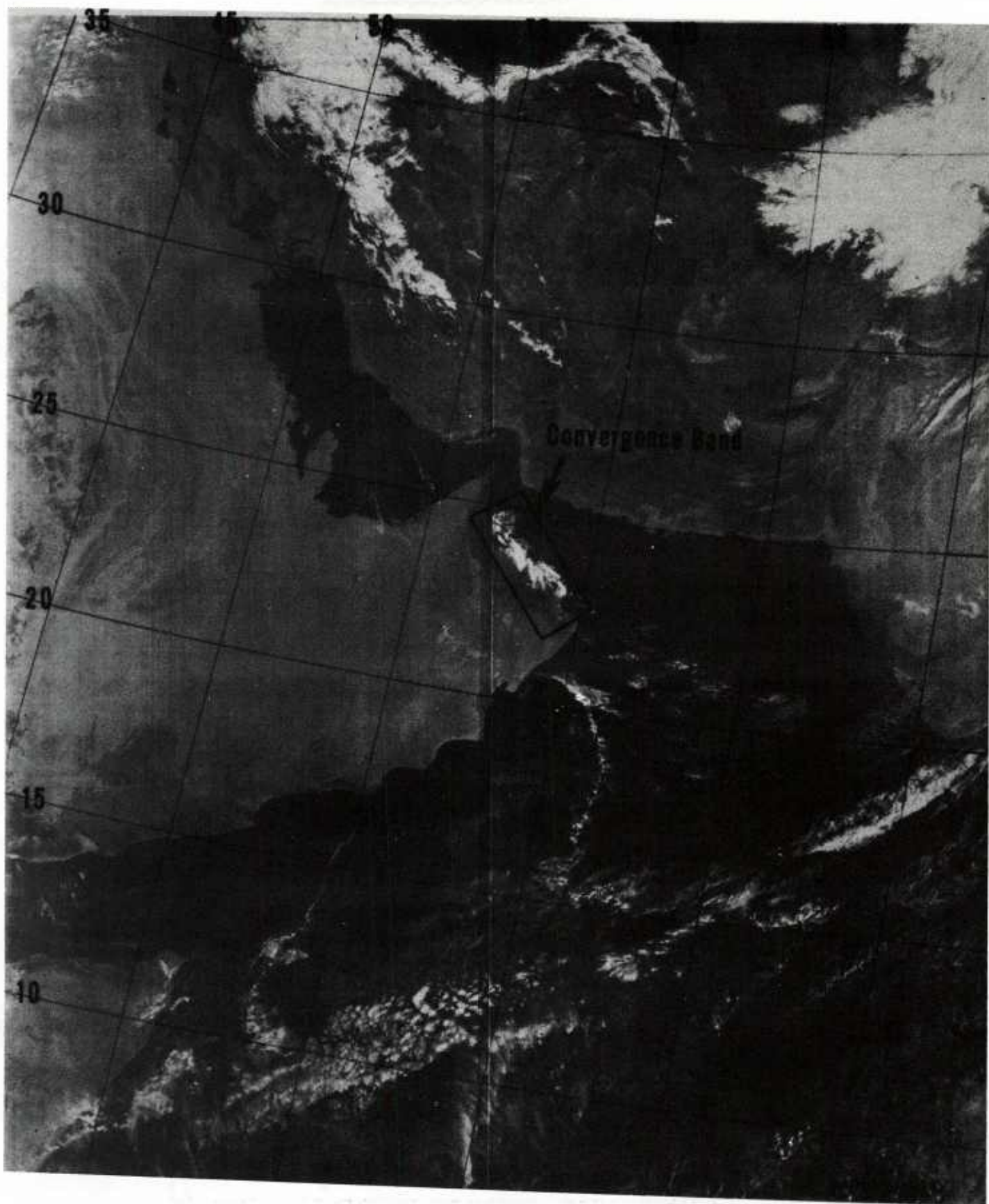


Figure B-35. Continued.

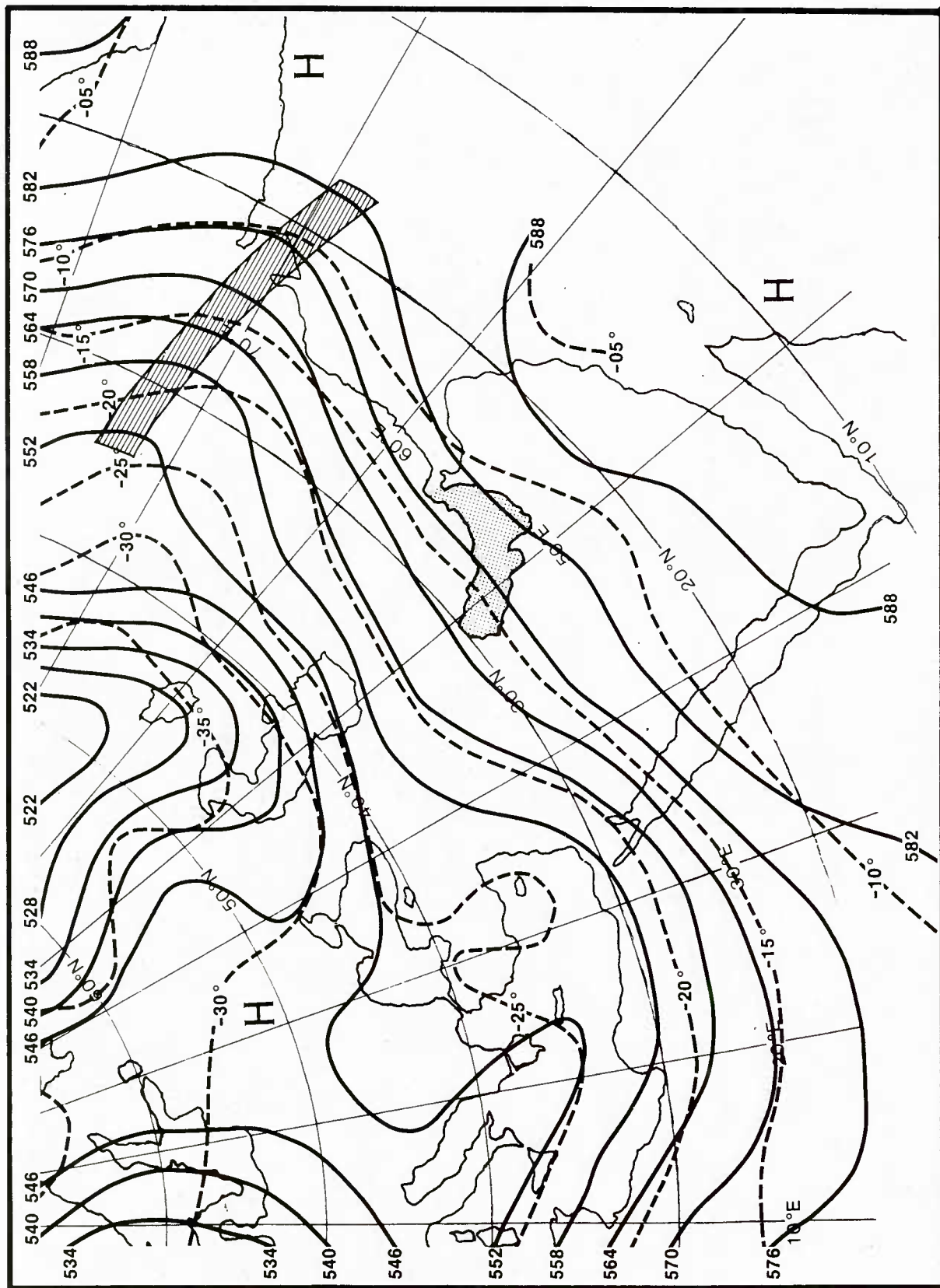


Figure B-36. 500 mb analysis, 21 Jan 1973 0000Z.

B.8 SUMMARY

(1) This case study has described the typical 3-5 day shamal pattern discussed in Section 3.1.

(2) The DMSP satellite visible images help to illustrate the indirect path of cold air into the upper Tigris-Euphrates valley. The presence of cold air in this valley area seems important for the triggering of shamals occurring from mid-December through February.

(3) The upper air long wave trough position scalls near the Strait of Hormuz, after the surface cold front which initiates the shamal has been advected away to east. The combination of two factors maintains the pressure gradient over the Persian Gulf and sustains the shamal: (a) lower surface pressure induced to the east of the trough over the Gulf of Oman; (b) the increase of surface pressure over the Arabian Peninsula associated with subsidence in the lower troposphere to the west of the trough.

(4) A convergence cloud band appears over the Gulf of Oman near the end of the shamal. This appearance seems to be associated with converging low level wind flows from the Arabian Peninsula and the Iran-Pakistan mainland.

APPENDIX C

WIND CLIMATOLOGY OF THE WINTER SHAMAL

The winter shamal is a relatively rare event, with winds at most Persian Gulf locations exceeding 20 kt less than 5% of the time during the season. The exceptions to this fact are the areas near Lavan Island, Halul Island, and Ras Rakan at the tip of the Qatar Peninsula, where winter winds in excess of 20 kt occur from 5% to 10% of the time. The operational significance of the relatively rare and irregularly occurring gale force winds of the stronger shamals stands out in marked contrast to the more common conditions of lighter winds.

Figures C-1 through C-5^{*} are wind roses for selected Gulf locations for November through March. The winds are predominantly northwesterly over most of the Gulf, but blow westerly or southwesterly in the southeast part of the Gulf.

Figure C-6 presents annual wind exceedance graphs for the same locations. They show the percentage frequency with which wind velocities exceed a given value at a certain location for a particular month. Values for each month are then connected together to yield an annual pattern.

No other statistics are readily available to assess the frequency of shamal occurrence. Forecasting experience indicates, however, that shamals with gale force winds lasting 24-36 hr following cold frontal passages (the type described in Case Study 1, Appendix A) may occur as frequently as two to three times per month from December through February. Briefer, but more frequent, periods of gale force winds follow the weaker cold frontal passages in March. The persistent 3-to-5 day shamal (the type described in Case Study 2, Appendix B) usually occurs only once or twice in a winter season; it is accompanied by exceptionally high winds and seas.

*Figures in this Appendix developed by IMCOS Marine, Ltd., London, from data collected at oil company locations around the Persian Gulf -- Oil Companies Weather Coordination Scheme, 1974.

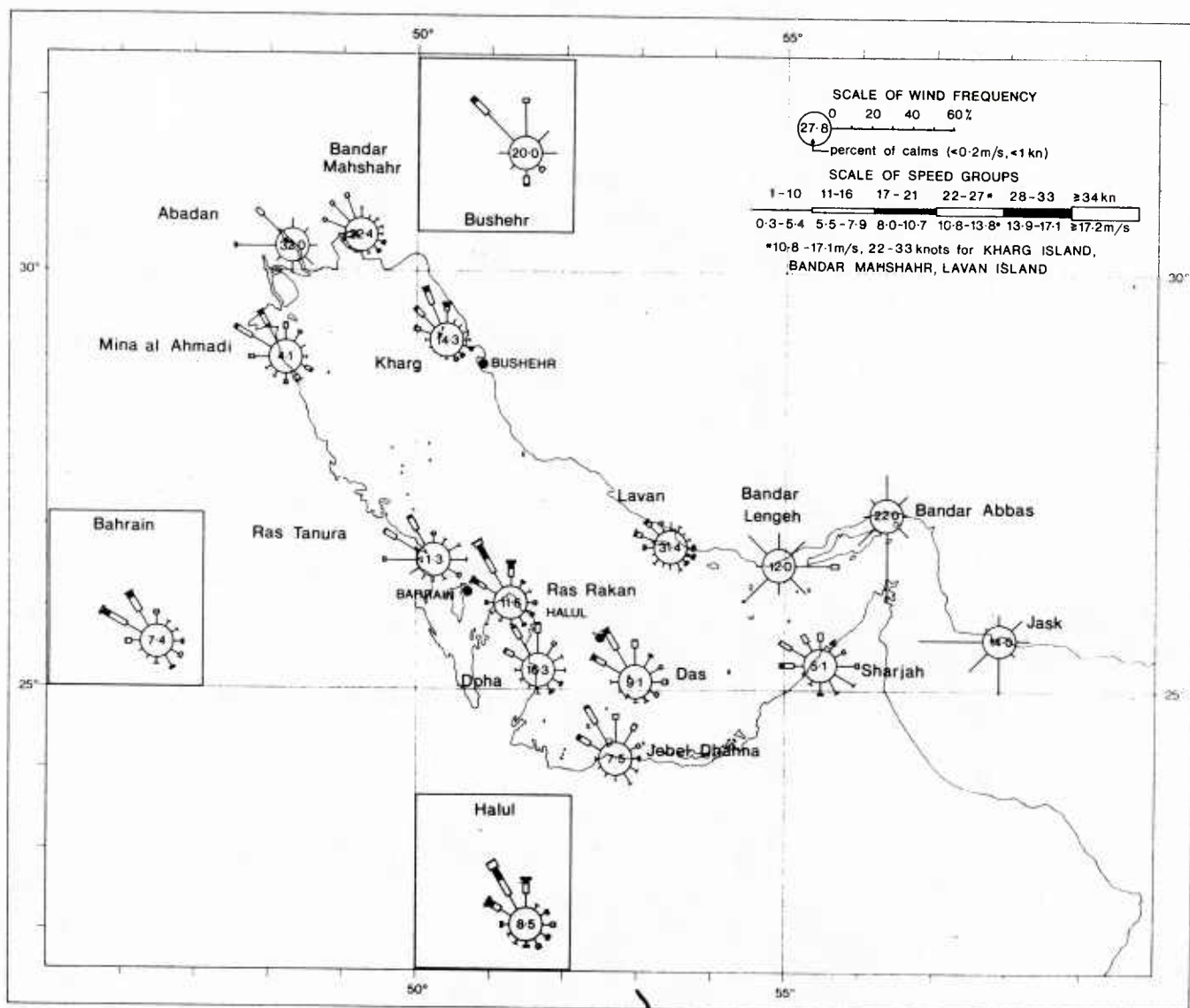


Figure C-1. Distribution of surface winds for November.

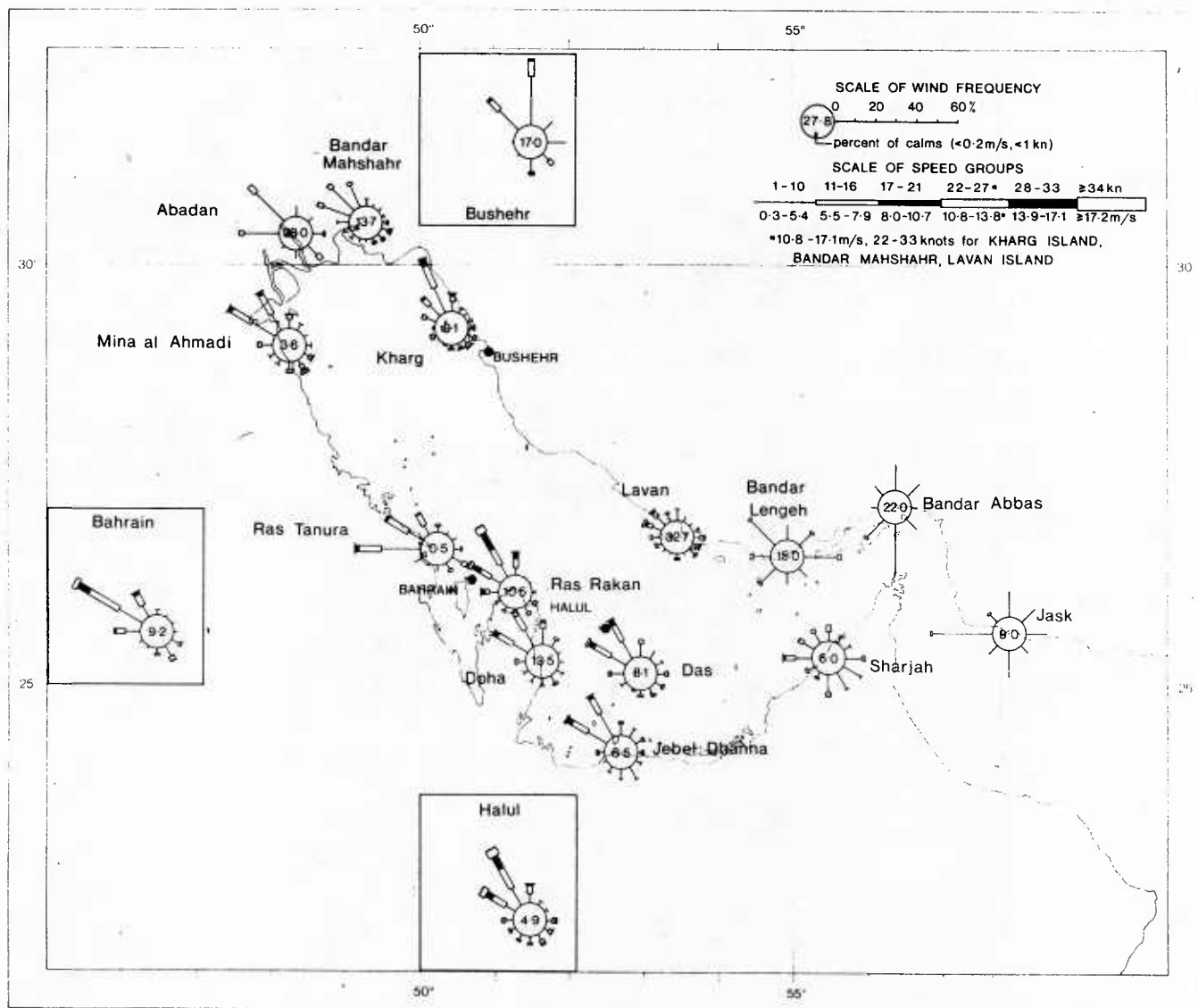


Figure C-2. Distribution of surface winds for December.

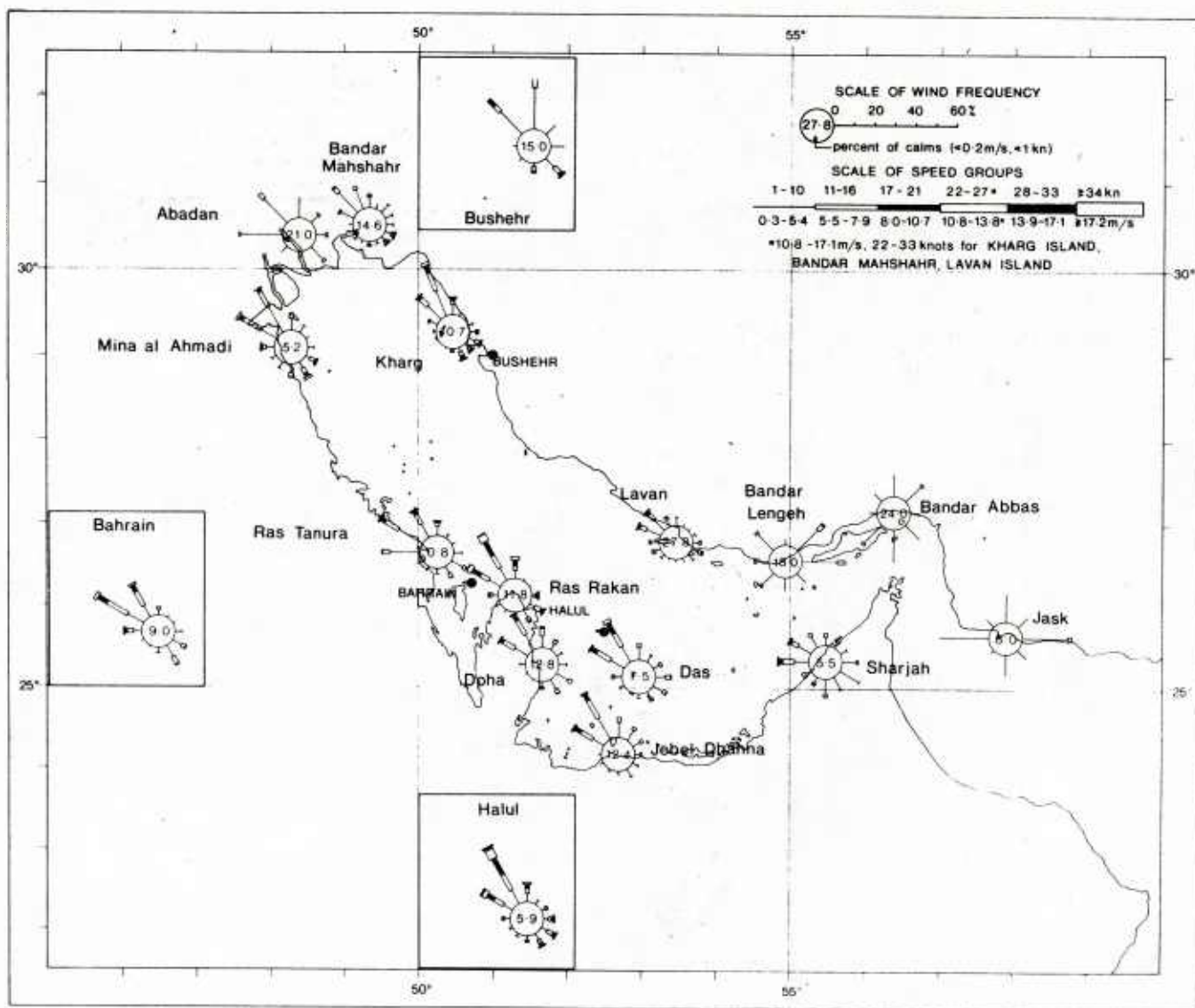


Figure C-3. Distribution of surface winds for January.

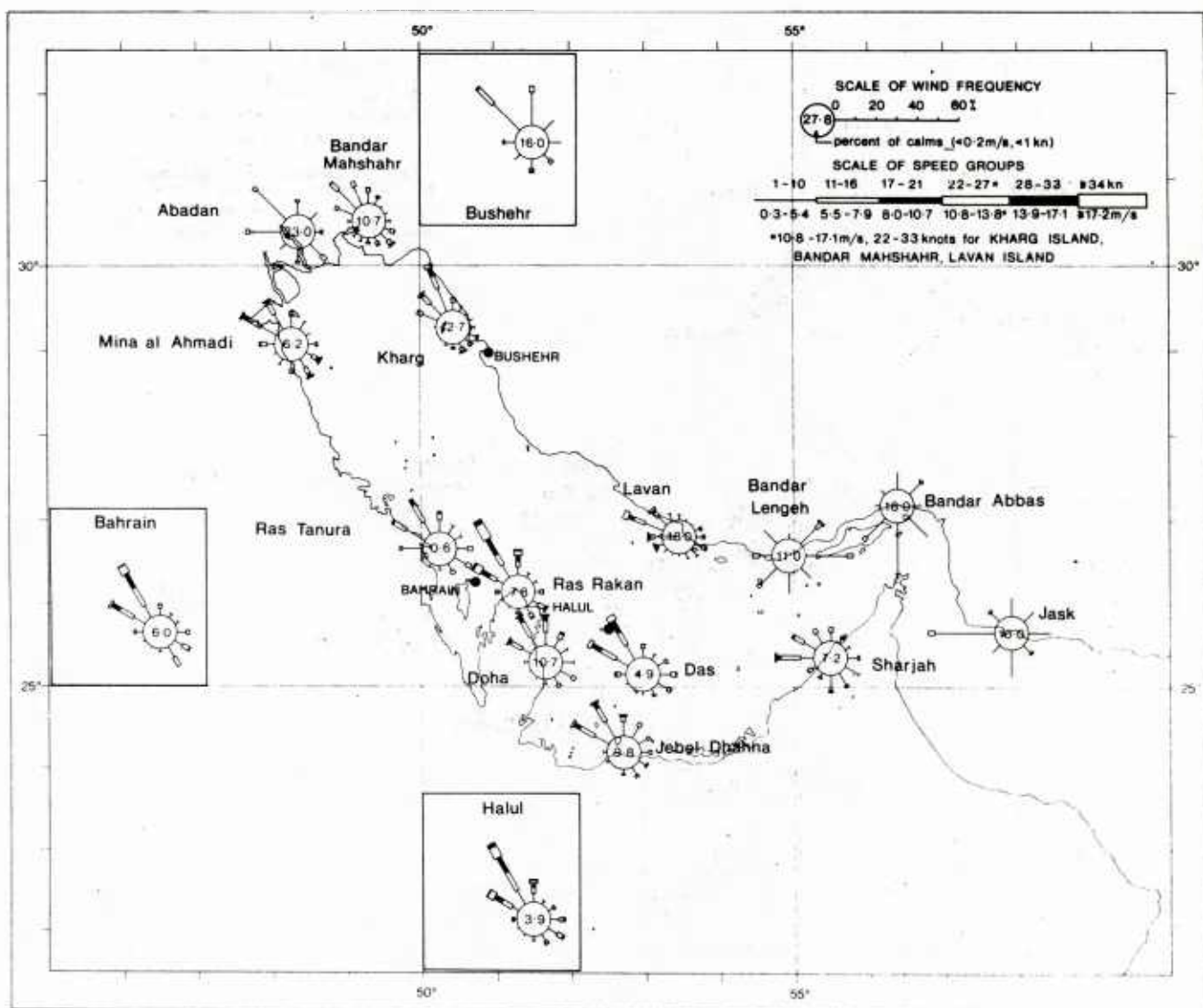


Figure C-4. Distribution of surface winds for February.

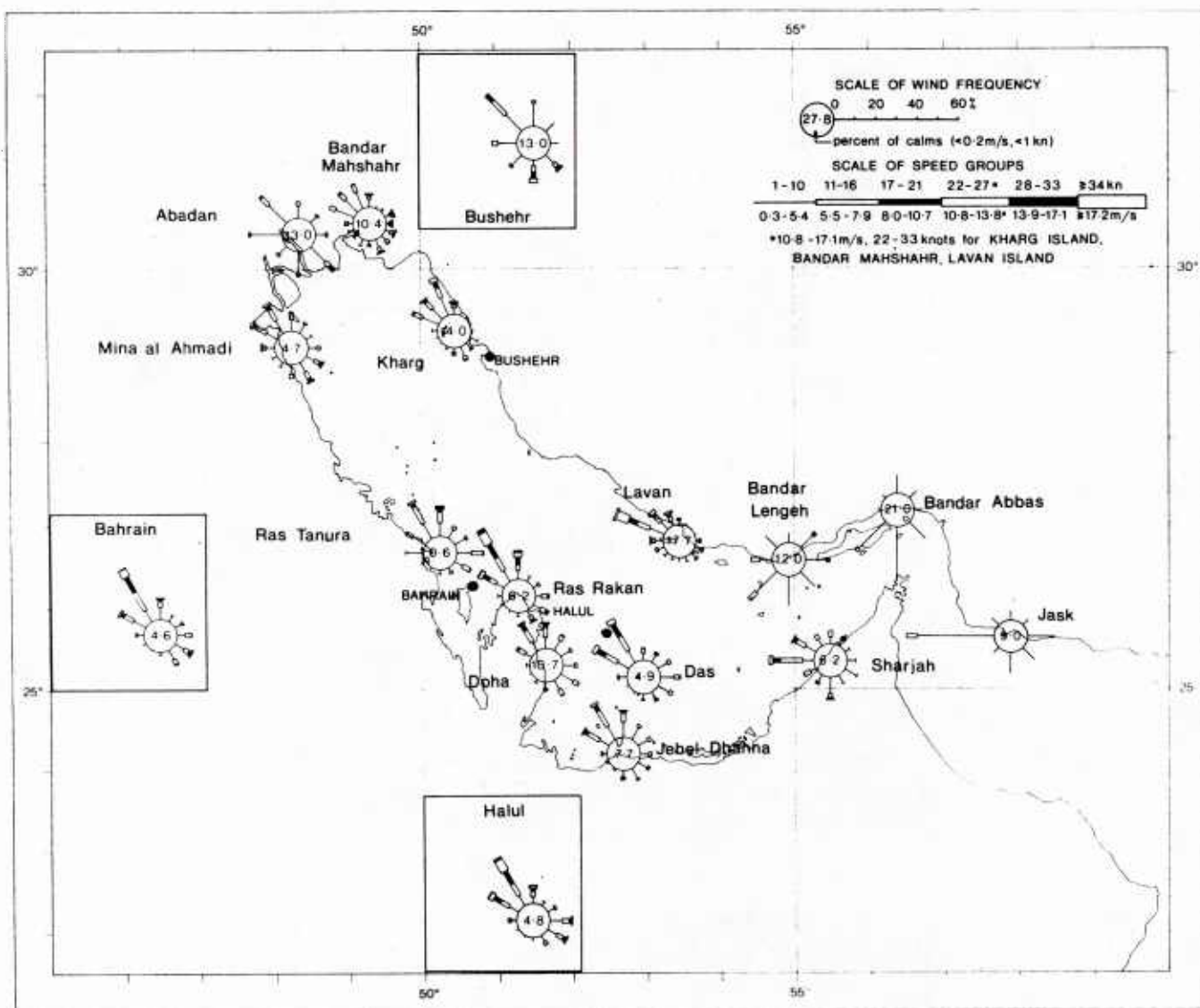


Figure C-5. Distribution of surface winds for March.

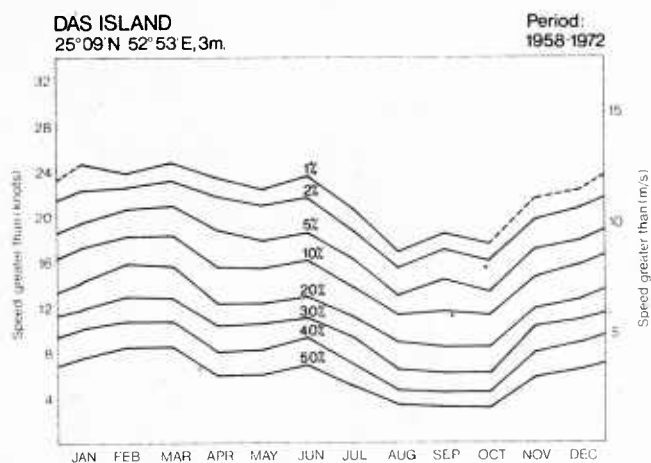
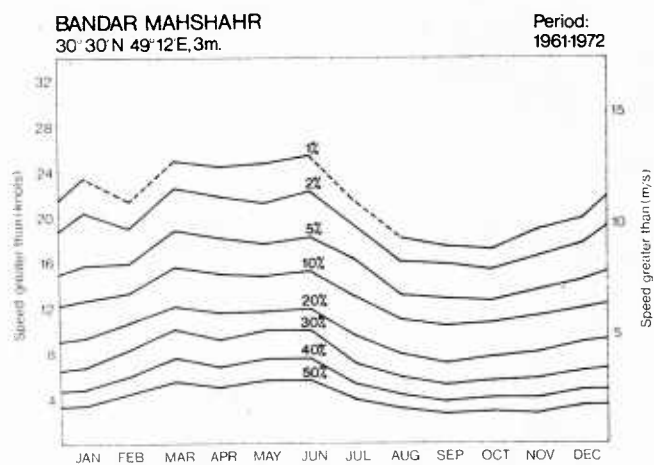
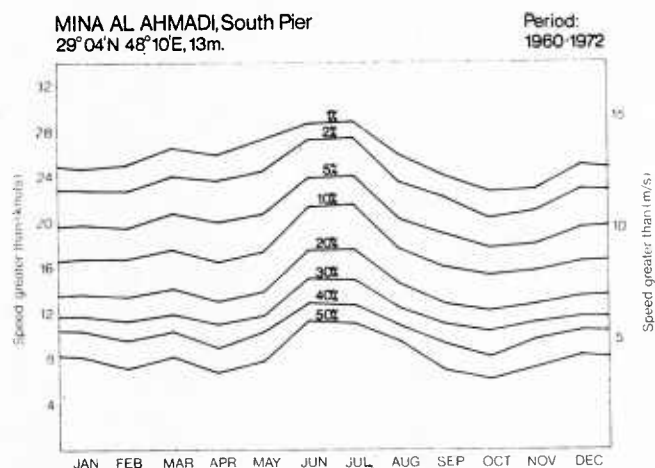
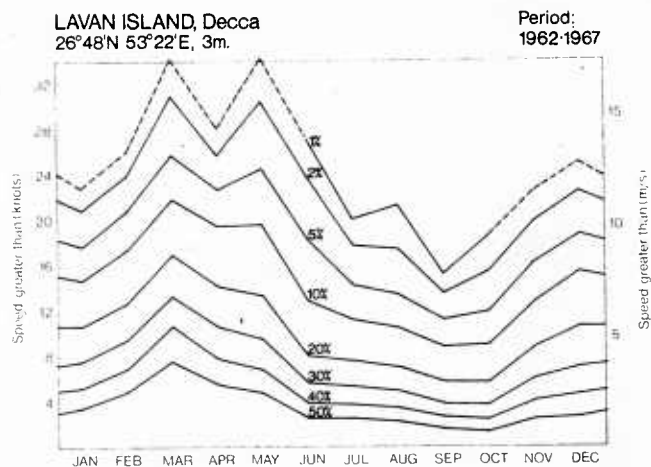
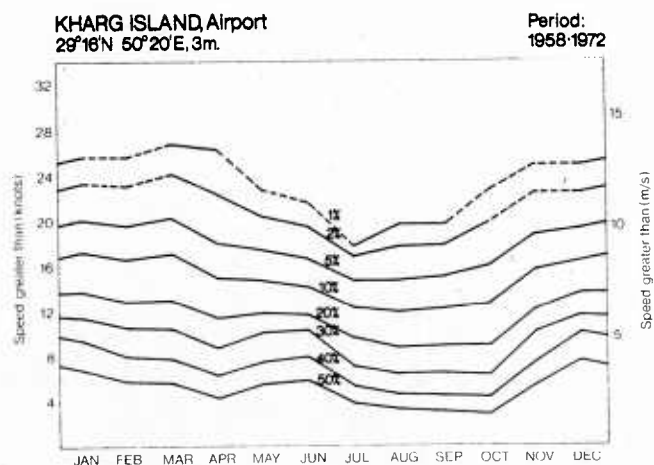
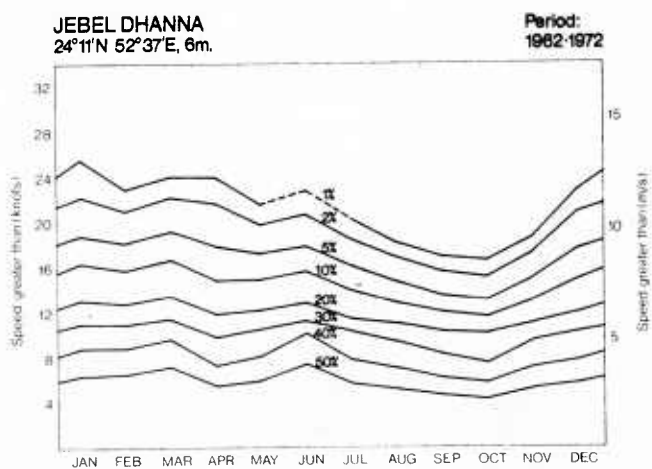


Figure C-6. Graphs of surface wind speed average exceedance at selected Persian Gulf locations.

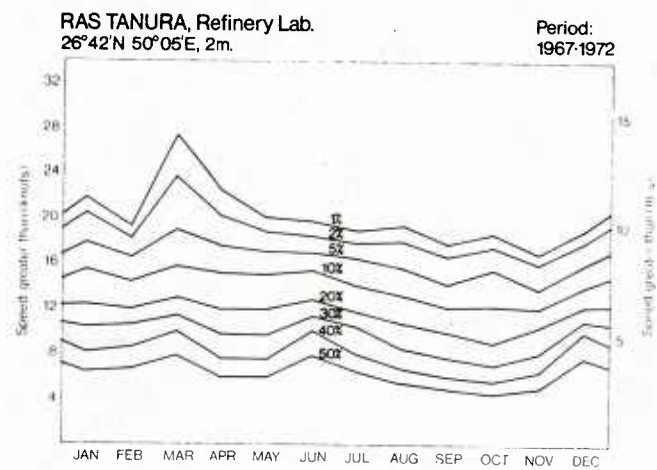
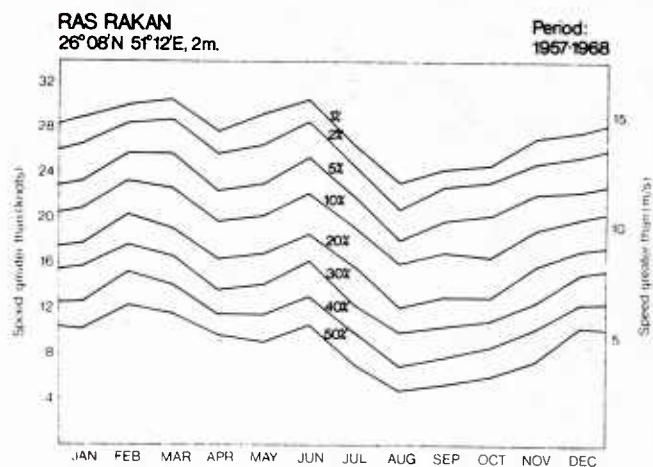
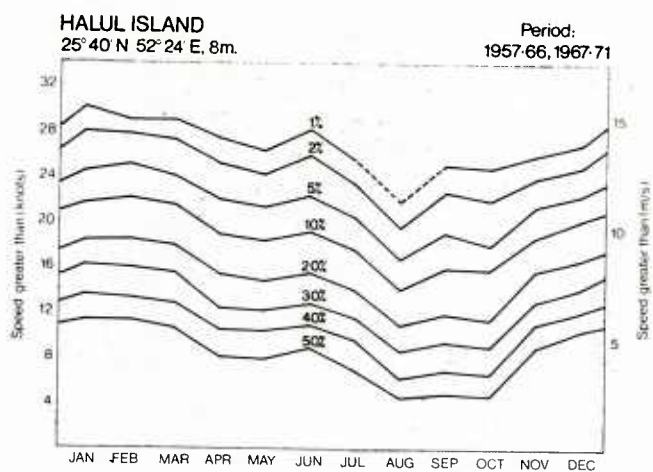
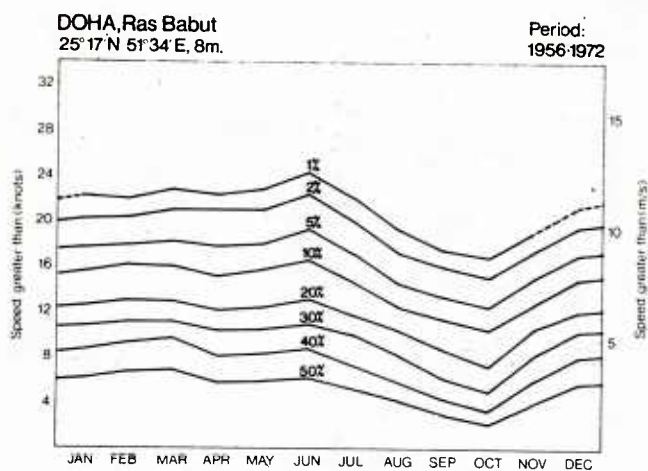


Figure C-6. Continued.

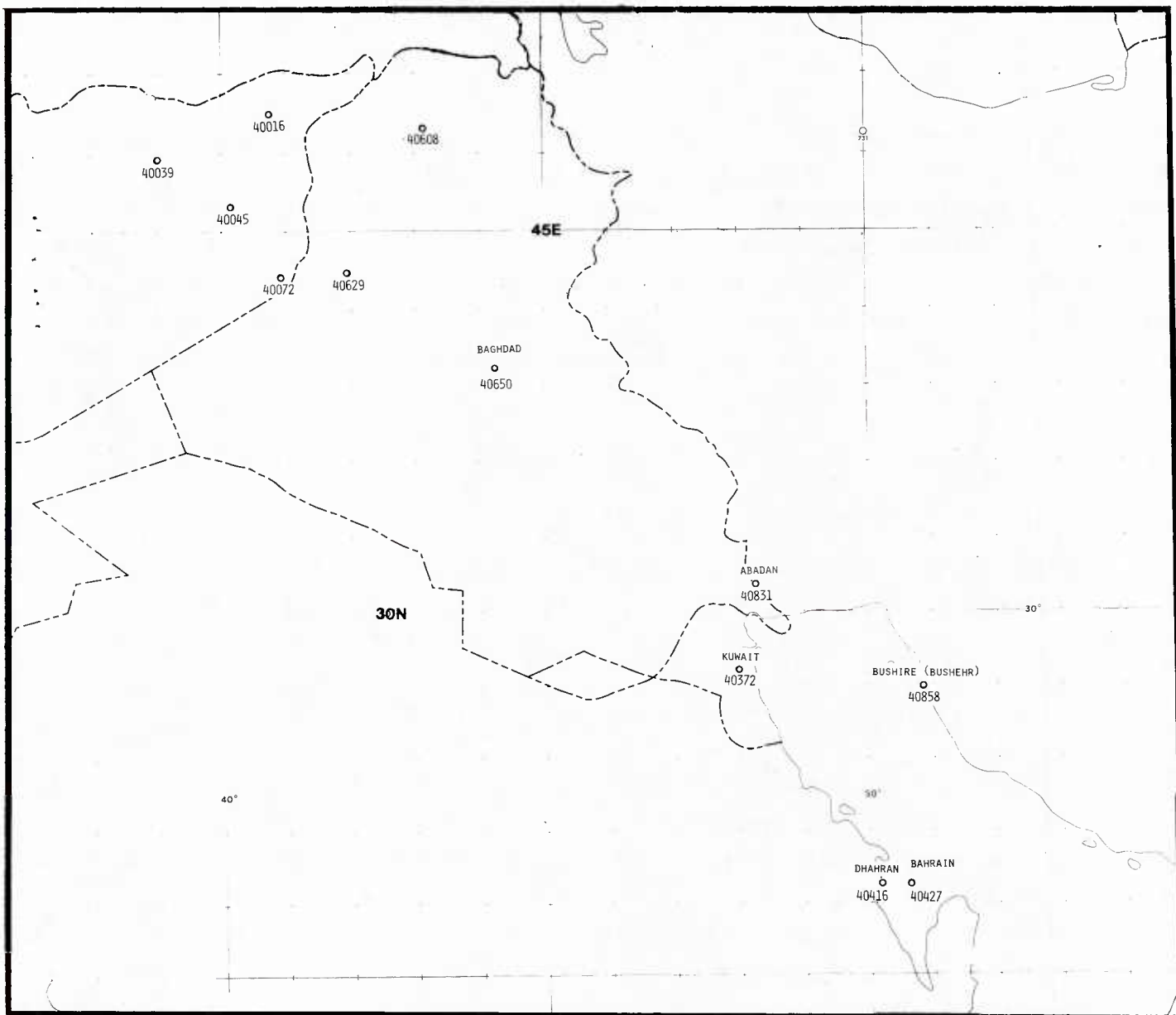


Figure D-1. Locations of stations referenced in text Para. D.1.1 (3).

APPENDIX D

FORECAST GUIDANCE

These suggestions for predicting certain conditions and characteristics of the winter shamal are largely "rules of thumb" culled by the author of this technical report from two years of experience as a meteorologist/forecaster in the Persian Gulf region. They represent, in large part, a distillation of the experience of forecaster colleagues in the Gulf. In two cases, however -- item (4), Para. D.1.1; and Para. D.2 -- the indicated procedures were suggested by research for this report and thus may require further tuning based on actual field experience.

D.1 RULE 1: ONSET

D.1.1 Midwinter - Mid-December through February

Although it is difficult to forecast with precision the time of a shamal's onset, favorable indications from any of the considerations listed below point to an onset. If all are favorable, occurrence over the entire Gulf is indicated.

(1) A cold upper-air long-wave trough with central temperature of at least -25°C at 500 mb, dips south of the Taurus Mountains of Turkey. This trough is often associated with a blocking high pressure ridge over central or eastern Europe; the ridge forces cold air south over the eastern Mediterranean-Lebanon-Syria area to "dig" the trough south of the Taurus Mountains and bring in the cold air.

(2) The long wave upper air trough tends to "hang back" over the eastern Mediterranean (see main text, Para. 3.3.4, and Figures 5a-e). From mid-December through February, the shorter waves that may move eastward from the long wave position (Para. 3.3.4) do not tend to produce the cyclogenesis in the lower Tigris-Euphrates valley/northern Gulf region which precedes most winter shamals. The movement eastward of the long wave trough itself, however, tends to produce this cyclogenesis. Thus, make the best possible prognosis of when the long wave trough will move eastward. Ignore the shorter waves which may move eastward from the long wave position.

(3) Plot consecutive Skew-T Log-P diagrams from station 40650 (Baghdad, Iraq), 40831 (Abadan, Iran), or 40372 (Kuwait); station locations are shown in Figure D-1. Analyze these plots for Lifting Condensation Level (LCL),

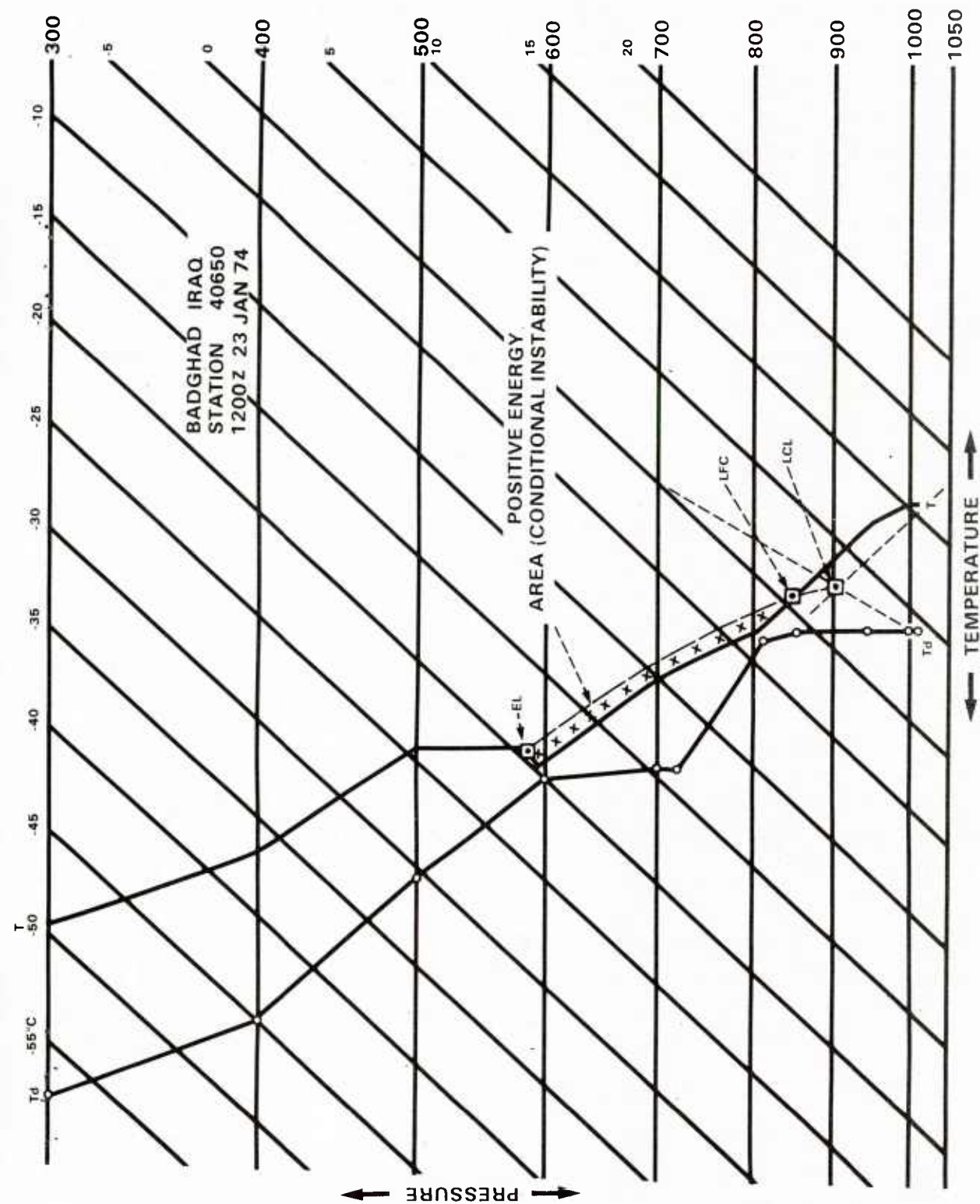


Figure D-2. Typical pre-shamal Skew-T Log-P diagram.

Convective Condensation Level (CCL), and Level of Free Convection (LFC).^{*} The Skew-T Log-P diagrams should be conditionally unstable (i.e., an LFC should exist) from 12 hr to 24 hr before onset of the shamal. Use the LCL to determine the LFC, as the air is to be orographically lifted (AWSM 105-124, pp 4-14). The conditional instability should increase somewhat on consecutive Skew-T Log-P diagrams as onset time approaches (i.e., the "positive energy area" above LFC should increase on successive Skew T's). Fig. D-2 shows a typical radiosonde ascent for Baghdad for 12Z 23 Jan 1974, with analyses of the LCL, LFC, and positive and negative energy areas.

(4) The average surface temperature contrast between stations in the upper Euphrates Valley and stations surrounding the northern and central Gulf should equal or exceed 12°C, during the period from mid-December through February. This surface temperature contrast should be determined by averaging daytime (12Z) and nighttime (00Z) surface temperatures to compensate for the effects of daytime heating and nocturnal cooling of the air in the lowest layers of the troposphere.

Obtain the required average surface temperatures by following these steps:

(a) Select from among the following groups a set of surface stations at 12Z to represent surface temperature reports from the upper Euphrates valley: 40016, 40039, 40045, 40072 in Syria; 40608 and 40629 in northern Iraq. Note that surface reports from stations in the Middle East are available somewhat sporadically, so use as many stations from those given above as are available.

From the stations selected, average the surface temperatures together to form T_{U12Z}

(b) Select a set of surface stations from 12Z from among the following to represent reports from the northern and central Gulf: 40372, 40831, 40858, 40416, and 40427. Again, use as many of these stations as are available.

From the stations selected, average the surface temperatures together to form T_{G12Z} . (Note the locations of the stations given in (a) and (b) above may be found in Figure D-1.)

(c) Repeat step (a), using surface data from 00Z, to form T_{U00Z} .

(d) Repeat step (b), using surface data from 00Z, to form T_{G00Z} .

^{*}See NAVEDTRA 10363-E, Aerographer's Mate 3 and 2 Rate Training Manual, pp. 236-238; NAVEDTRA 10362-B, Aerographer's Mate 1 and C Rate Training Manual, pp. 52-55; or AWSM 105-24/NAVAIR 50-1P-5, Use of Skew T, Log-P Diagram in Analysis and Forecasting, pp. 4-13, 14, 15, for determination of these quantities.

(e) Average the values for both regions over time, to compensate for daytime heating and nocturnal cooling of the air:

$$T_U = \frac{T_{U12Z} + T_{U00Z}}{2}$$

$$T_G = \frac{T_{G12Z} + T_{G00Z}}{2}$$

(f) The required temperature contrast thus becomes

$$T_G - T_U,$$

$$\text{and } T_G - T_U \geq 12^\circ\text{C}.$$

(5) From the prognoses of the upper air, determine when the long wave upper trough axis will lie just north of the Gulf. Since the shamal begins before the trough axis reaches this point, forecast the time of the onset of the shamal to coincide with the time when the upper trough axis is at the midway point (approximately 44°E) between the upper Euphrates valley (the Syria/Iraq border, longitude 41°E) and a position just north of the Gulf (longitude 48°E).

D.1.2 Late Fall - November through mid-December

Use the same rules as above, relaxing the surface temperature contrast and central 500 mb temperature criteria slightly. Forecast the shamal over the northern Gulf only.

D.2 RULE 2: ONSET INTENSITY (NOV-FEB)

(1) Use area average temperatures derived in Rule 1. Use the formula

$$C = 1/2 \sqrt{gh \frac{\Delta T}{\bar{T}}}$$

where C is the average wind speed in m/sec; g , acceleration due to gravity, is 9.8 m/sec^2 ; h is 2500 meters, the typical depth of the cold air mass; ΔT , in $^\circ\text{C}$, equals the difference between the temperatures at the upper Euphrates valley and the northern Gulf; and \bar{T} ($^\circ\text{C}$) is average of the two temperatures.

In computing form for onset wind speed, using the quantities derived for rule D.1.1 (4):

$$C \text{ (in kt)} \approx 156 \times \sqrt{\frac{T_G - T_U}{\frac{T_U + T_G + 273.16}{2}}}$$

where T_U is the average temperature ($^{\circ}\text{C}$) in the upper Euphrates valley and T_G is the average temperature ($^{\circ}\text{C}$) of the middle and northern Gulf area.

(2) Add 10 kt to the quantity C, derived in rule 2 (1), for average gusts.

(3) Add 15-20 kt to the quantity, C, derived in rule 2 (1) for peak gusts.

(4) The formula is based on conversion of potential energy in adjacent cold and warm air masses into kinetic energy as the cold air mass underruns the warm air.*

D.3 RULE 3: DURATION (NOV-FEB)

(1) If the upper air prog series (24, 36, 72 hr) and the forecaster's judgment indicate rapid movement of the long wave upper trough through the region without stalling over or near the Strait of Hormuz (in the vicinity of 26.5°N , 56.5°E), forecast 24-36 hr duration for the shamal from the time of onset.**

(2) If the upper air prog series and the forecaster's judgment indicate that the long wave upper trough will stall either over or near the Strait of Hormuz, or else move through the Persian Gulf region very slowly, forecast the shamal to last 3 to 5 days. Recheck the prog series every 12 hr to confirm the forecast, recalling that the 3-5 day extended shamal is a rare event.

(3) If the shamal is expected to last more than 2 days, forecast wind speeds of 35-45 kt in the southern Gulf, where the surface pressure gradient will be strongest.

D.4 RULE 4: CESSATION

This rule of thumb is for the 3-5 day shamal, which occurs from mid-December through February.

Check the upper air prog series and determine when the upper trough will move away to the east. Forecast the shamal to break by sunset of the day on which the trough moves away. If satellite images are available, they should be examined to see whether a convergence band off Oman is present in late morning images (see Case Studies 1 and 2, Appendices A and B respectively, Figures A-31, A-32, B-30 and B-35). If the convergence band is present,

*After Margules, suggested by Feteris (1973), and cited on p. 301 in Hess (1959).

**If the forecaster is using Fleet Numerical Weather Central (FNWC) prognoses, he should be aware that the FNWC upper air progs are pure persistence from the equator to about 10°N , that they are fully prognostic north of about 20°N , and that they are a blend of the two between 10°N and 20°N . As the southern part of the Persian Gulf lies north of 22.5°N latitude, the forecaster can be generally confident that the FNWC progs are fully prognostic in Gulf regions; this is the region, however, that borders the latitude where the progs begin to blend from prognostic to persistence.

forecast the shamal to end that evening. Forecast northwest winds 15-20 kt in the western Gulf that afternoon. Forecast local sea breezes, southeasterlies, or a combination in the eastern Gulf.

D.5 RULE 5: TYPICAL SEA HEIGHTS (NOV-FEB)

The sea heights given here are the significant heights, i.e., the average of the highest one-third observed.

When the cool shamal winds blow over the warm, shallow Persian Gulf, they raise a short-period, steep sea faster and higher than would a wind of similar strength over the open sea.

(1) If the initial wind forecast is for 30-40 kt, forecast:

(a) Combined sea height to rise to 10-12 ft, 12-24 hr after onset.

(b) Combined sea height to rise further 12-14 ft, 24-36 hr after onset, if the shamal persists that long.

(2) If the shamal persists for more than 36 hr, a rare event, increase wind forecast to 35 to 45 kt in the southern Gulf and increase combined sea heights in the southern Gulf to a maximum of 15-18 ft.

D.6 RULE 6: LATE-SEASON SPECIAL CASES

This rule of thumb addresses shamals that occasionally occur in late winter and into early spring. Sea heights (significant) given are the average of the highest one-third observed.

(1) In March, forecast 12-24 hr 30 kt northwesterlies with each vigorous 500 mb short wave passage (see Section 3.2^{*}). Forecast maximum combined sea height of 10-12 ft. Forecast the residual swell decay according to Rule 7 below.

(2) During the first half of April, the same rule applies, but limit the wind to 25-30 kt and forecast for the northern Gulf only. Forecast a maximum combined sea height of 8-10 ft. Forecast the residual swell decay according to Rule 7.

D.7 RULE 7: SWELL DECAY

(1) For the day following the break of 24-36 hr shamal:

(a) Forecast 2-4 ft swell if the maximum significant combined sea height was 10-12 ft during the shamal.

(b) Adjust this forecast upward or downward if higher or lower maximum significant combined sea heights occurred during the shamal.

*This is an exception to the guidance of Para. D.1.1 (2). In this situation the short waves are significant and should not be ignored.

(2) Following the break in the 3-5 day shamal, if 12-15 ft maximum significant combined seas occurred:

- (a) Forecast 6-8 ft swell on the day after the shamal breaks.
- (b) Forecast 3-5 ft swell on the second day after the shamal breaks.
- (c) Forecast 1-3 ft swell on the third day after the shamal breaks.

D.8 RULE 8: HIGHER-WINDS SPECIAL CASES

These modifications to previous guidance should be applied for those areas that experience higher than normal winds during shamal occurrences. See discussion in main text, Para. 3.6.1, and Figure 3-7.

(1) For the area east of the Qatar Peninsula:

- (a) Add 10-15 ft to wind speeds determined by rules 2, 3, or 5.
- (b) Add 2-4 ft to all combined sea or residual swell heights determined by rule 6.
- (c) Add an extra day of significant residual swell (2-4 ft significant swell height).

(2) For the area near Lavan Island, but only in March and early April:

- (a) Add 10 kt to wind speed determined by rule 5.
- (b) Add 2-4 ft to combined sea heights determined by rule 5 or residual swell determined by rule 6.
- (c) Add an extra day of significant residual swell (2-4 ft significant swell height).

D.9 RULE 9: THUNDERSTORMS, RAINSHOWERS

(1) Thunderstorms and rainshowers in conjunction with the shamal are more frequent in the northern Gulf than in the south.

(2) Subsidence in the lower troposphere behind cold fronts can quickly suppress convection behind the front.

(3) Include thunderstorms and rainshowers with each forecast of shamal onset for the northern Gulf. Forecast convective activity to precede cold frontal passage and onset of the shamal by 3-6 hr. Forecast the severest thunderstorm activity north of the subtropical jet axis; determine the axis from satellite images or upper air (200 mb) progs, as demonstrated in Case Study 1, Appendix A.

(4) Check satellite images, if available, for evidence of development or suppression of convection after frontal passage and modify the forecast accordingly.

D.10 RULE 10: REDUCED VISIBILITY IN BLOWING DUST

Visibility can be reduced during shamal occurrences, most severely in the northern Gulf area, by wind-blown dust drawn from the arid surface of the lower Tigris-Euphrates valley.

(1) For the first shamal of the season, forecast sharply reduced visibilities of one-eighth to one-quarter of a mile in blowing dust.

(2) Keep a record through the winter season of the interval between rainfalls over the lower Tigris-Euphrates valley region. The longer the interval since the previous rainfall, the more likely the soil surface will become dry and powdery, thus increasing the likelihood of blowing dust during shamals following such dry periods.

D.11 RULE 11: LOW LEVEL TURBULENCE

D.11.1 Prior to the Passage of the Cold Front

(1) If the maximum surface wind speed associated with the Kaus is expected to be at or near gale force, forecast light to moderate turbulence from the surface to 5000 ft in the center of the Gulf (the east-west speed shear zone), and from 3000 ft to 8000 ft over the eastern Gulf (the vertical speed shear zone).

(2) Forecast locally severe turbulence in and near organized convective cells at all levels of the troposphere in and near organized prefrontal lines of convective cells.

D.11.2 In Association with the Cold Front

(1) Forecast moderate to locally severe turbulence in and near convective cells imbedded in the cold front.

D.11.3 After the Cold Front has Passed Through the Gulf Region

(1) Forecast light to moderate turbulence in the lowest 3000-5000 ft of the atmosphere, in association with the gusty strong wind zone which extends from the frontal position back to the northwest.

(2) Use DMSP imagery to pinpoint the more severe occurrences of this sort of low level turbulence. The cloud pattern to look for is that of postfrontal cumulus caused by relatively cold air streaming over warmer Gulf waters. Upgrade the turbulence in these areas to moderate.

(3) Forecast moderate mechanical turbulence to occur in the area on the eastern side of the Gulf in the lee (to the west) of the Zagros Mountains, during the extended 3-5 day shamal.

Forecast the turbulence 1000-2000 ft below the mountain crest height to 3000-5000 ft above it; the general height range of the Zagros Mountains is 6000-9000 ft. A conservative estimate of the altitudes for the turbulence would

be 4000-11000 ft for mountain heights of approximately 6000 ft, and 7000-14000 ft for mountain heights of approximately 9000 ft.

(4) Forecast moderate to severe turbulence in the region downstream of mountainous areas which produce wave clouds. Forecasting an altitude for the turbulence is difficult because it is a function of local stability and other local effects such as the specific wind speed and direction, specific terrain configuration and vertical wind profile. A conservative estimate would be at least 2000-3000 ft below the crest of the mountains (although mountain wave turbulence can reach the ground) up to a maximum height of jet stream altitudes.

D.12 RULE 12: UPPER LEVEL TURBULENCE

(1) Forecast light to moderate turbulence at altitudes of 20,000-35,000 ft near the subtropical jet when it is present. The normal winter position of the jet is near the middle-to-southern Gulf.

(2) During winter shamal occurrences, broaden the turbulence area to include the region from just south of the subtropical jet to just north of the polar jet. (See Section 3.8, main text, and Figures 3-9 and 3-10.) Note that when the shamal occurs, the subtropical jet tends to be displaced southward by the intrusion of the polar jet south of the Taurus Mountains of Turkey to a position over Iraq, Syria, Iran, and northern Saudi Arabia.

(3) Forecast moderate to severe turbulence at 15,000-30,000 ft in the northern, polar-jet portion of the turbulence region (Figures 3-9, 3-10).

(4) Forecast moderate to severe turbulence at 20,000-35,000 ft in the southern, subtropical-jet portion of the turbulence region (Figures 3-9, 3-10).

(5) More detailed guidance for forecasting upper level turbulence is given in the technical publication NWRP 15-0568-137(II), 1968; Clear-Air Turbulence, Part II, A Survey of Contemporary Prediction Techniques and Recommended Operational Procedure.

(6) Rules D.11.1 (2), D.11.2 (1), and D.11.3 (4) also apply in forecasting regions of upper level turbulence.

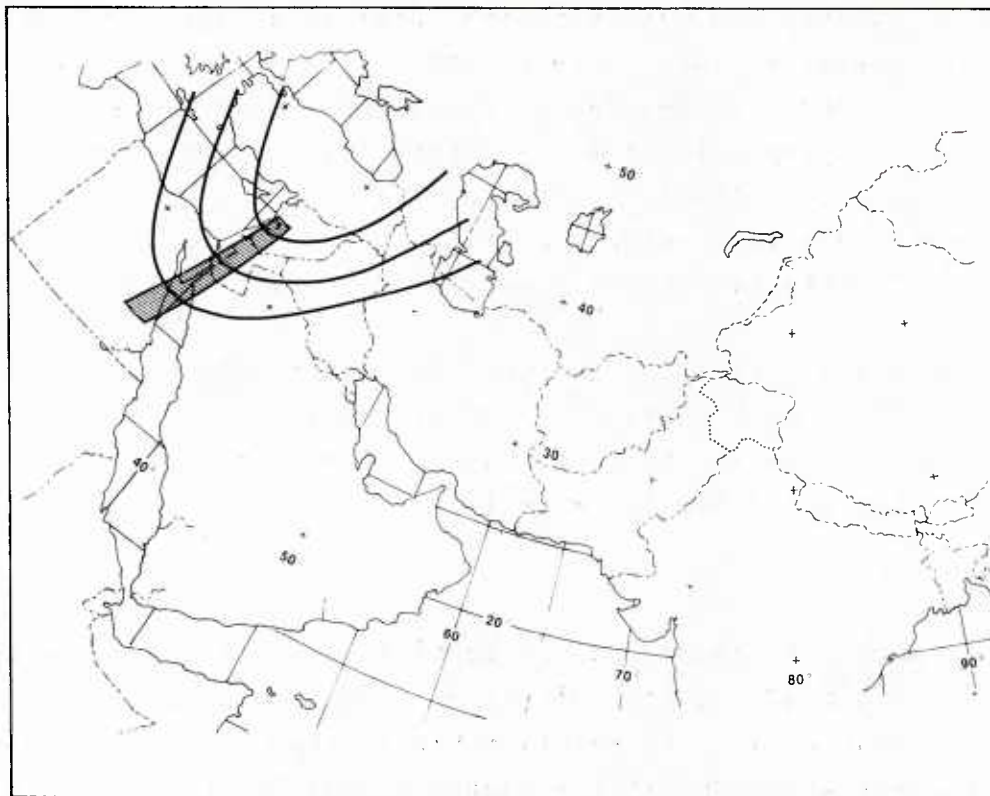


Figure 3-5d. Long wave position quasi-stationary near eastern Mediterranean coast: Trough axis re-established near eastern Mediterranean coast after short wave has moved away to the east.

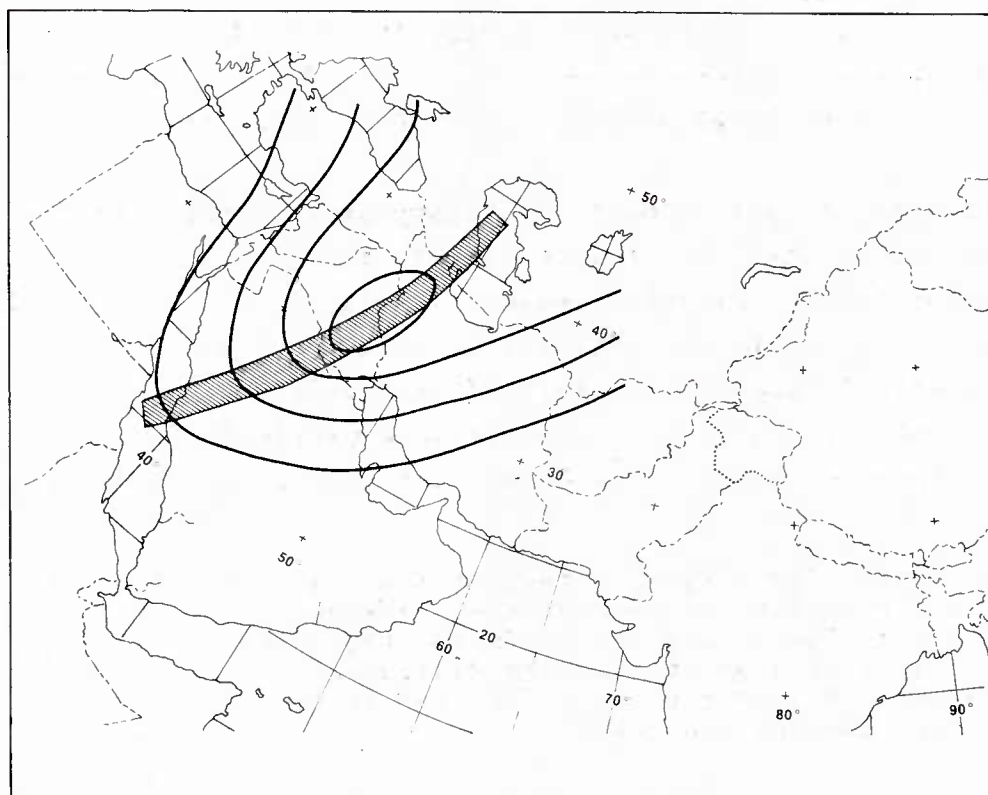


Figure 3-5e. Long wave position moves eastward, and shamal begins.

The dynamic significance of the situation is this: The shorter waves which move through the long wave position, usually as far north as depicted in Figures 3-5a-c, transport insufficient cold air in the lower layers of the troposphere to the south of the Taurus Mountains and into the upper Euphrates valley to cause cyclogenesis. This cyclogenesis, in turn, sets off the shamal. It appears that the full force of the strong cold advection behind the long-wave upper trough is required to bring sufficient cold air into the Tigris-Euphrates valley to set off the shamal from mid December through February.*

Given the situation just described, especially from December through February, forecasters must monitor the upper air flow very carefully to avoid forecasting the onset of a shamal too soon. (A forecast technique is outlined in Appendix D, Forecast Guidance, Rule 1.)

3.4 DURATION

Once the shamal has begun, it may subside 12-36 hr after the cold frontal passage (as in Case Study 1, Appendix A) or it may persist for 3-5 days (as in Case Study 2, Appendix B). The relationship between the surface and upper air patterns determines which duration sequence is most likely to occur.

If the long-wave upper trough moves away quickly to the east, shamal conditions will occur at and behind the cold front as it progresses down the Gulf; however, gale force northwesterlies will usually subside within 24 hr after frontal passage.

On the other hand, if the upper westerlies extend as far southward as 23°N to 28°N, and the upper trough becomes stationary for a time over or near the Strait of Hormuz, the shamal will continue until the upper trough moves away to the east.

When the upper trough becomes stationary over or near the Strait of Hormuz, subsidence occurs in the lower troposphere in the area south of the Taurus Mountains of Turkey (see synoptic sequence, Para. 3.1). Consequently, the surface pressure builds in the vicinity of northern Saudi Arabia. A surface low also is frequently induced in the Gulf of Oman by the same upper trough. This situation typically produces a 6-8 mb pressure gradient from the high over Saudi Arabia to the low over the Gulf of Oman. The Zagros Mountains, parallel to the

*On-going DMSP satellite imagery interpretations at NEPRF indicate the likelihood of a strong relationship between the breakdown of the blocking high pressure ridge over Europe and the eastward progression of the long-wave upper trough from a position over the Eastern Mediterranean Sea into the Persian Gulf region. Such movement, of course, is limited to the occurrence of the shamal from mid December through February.

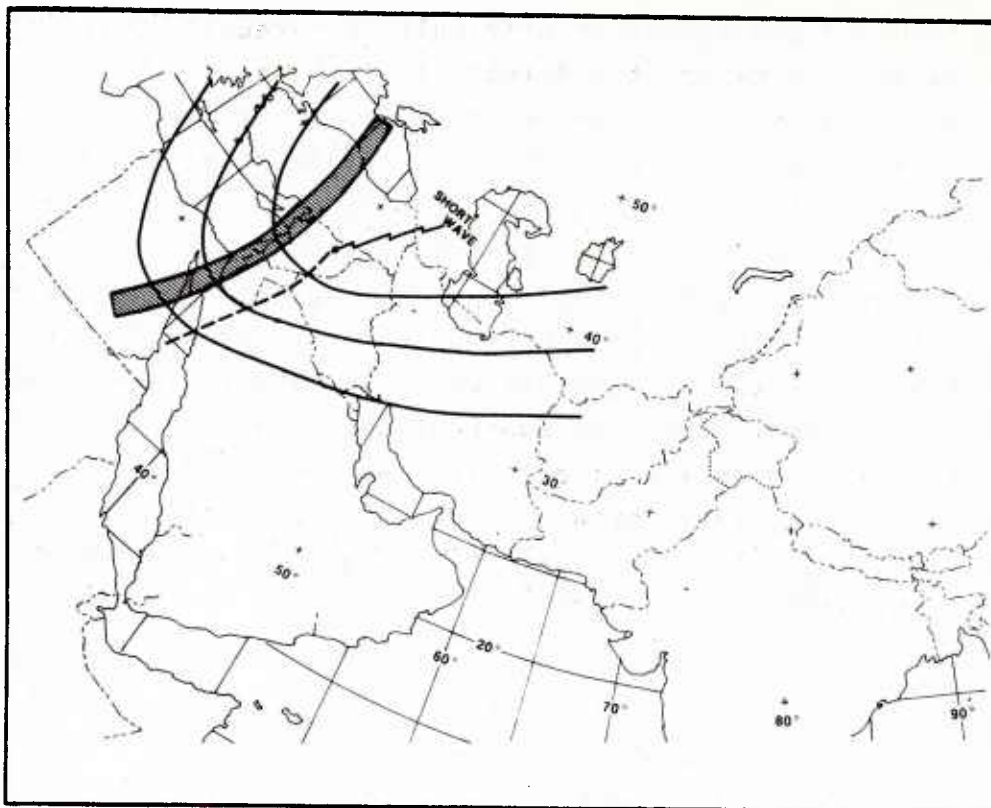


Figure 3-5b. Long wave position quasi-stationary near eastern Mediterranean coast: Short wave moves through long wave position, flattening long wave somewhat.

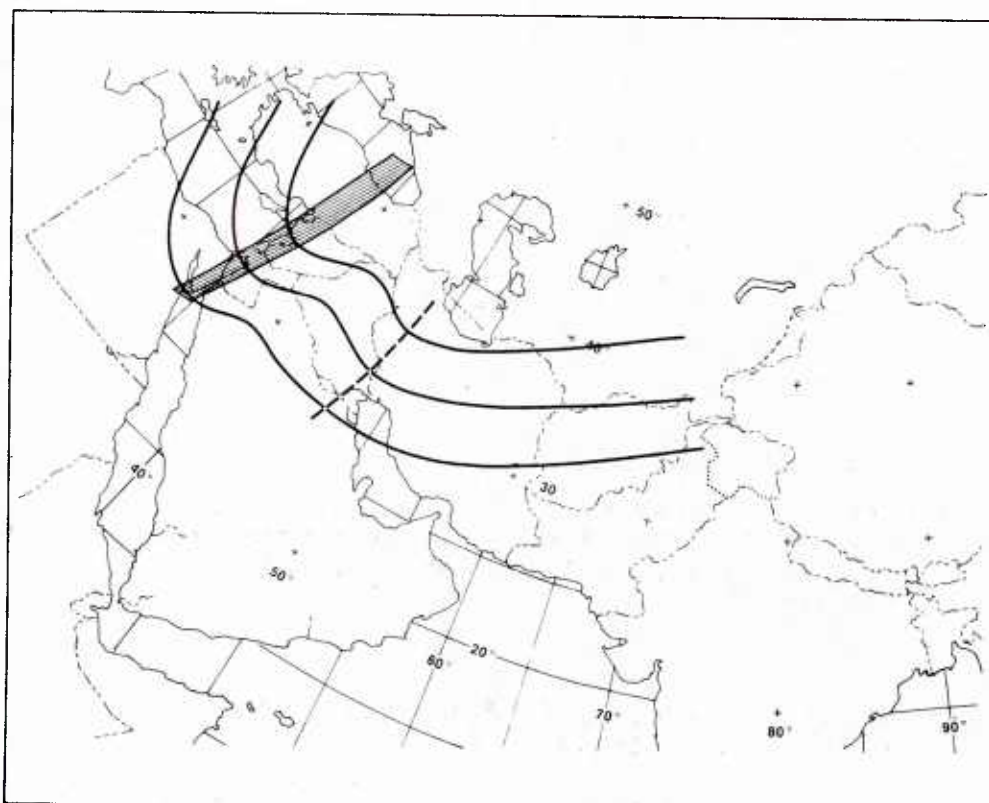


Figure 3-5c. Long wave position quasi-stationary near eastern Mediterranean coast: Short wave propagates eastward.

3.3.3 Difficulties in Forecasting Onset

The onset of the shamal is difficult to forecast, primarily because the upper air pattern involved is difficult to forecast. The chief difficulty lies in correctly forecasting the movement of upper air features from the eastern Mediterranean into the lower Tigris-Euphrates/northern Persian Gulf area. In the pre-shamal situation, a sharp, long-wave upper trough over the eastern Mediterranean will typically be located to the east of a blocking ridge over central or western Europe. Short waves moving through the long wave position often will flatten the base of the long wave trough and create the appearance that the long wave trough has begun to move eastward. Within a day or so however, it frequently becomes apparent that the long wave has remained stationary in the eastern Mediterranean near the Syria and Lebanon coasts, while the shorter waves have moved through. A few days later the long wave may actually move eastward, triggering a shamal. Figures 3-5a through 3-5e illustrate a typical sequence of this type.*

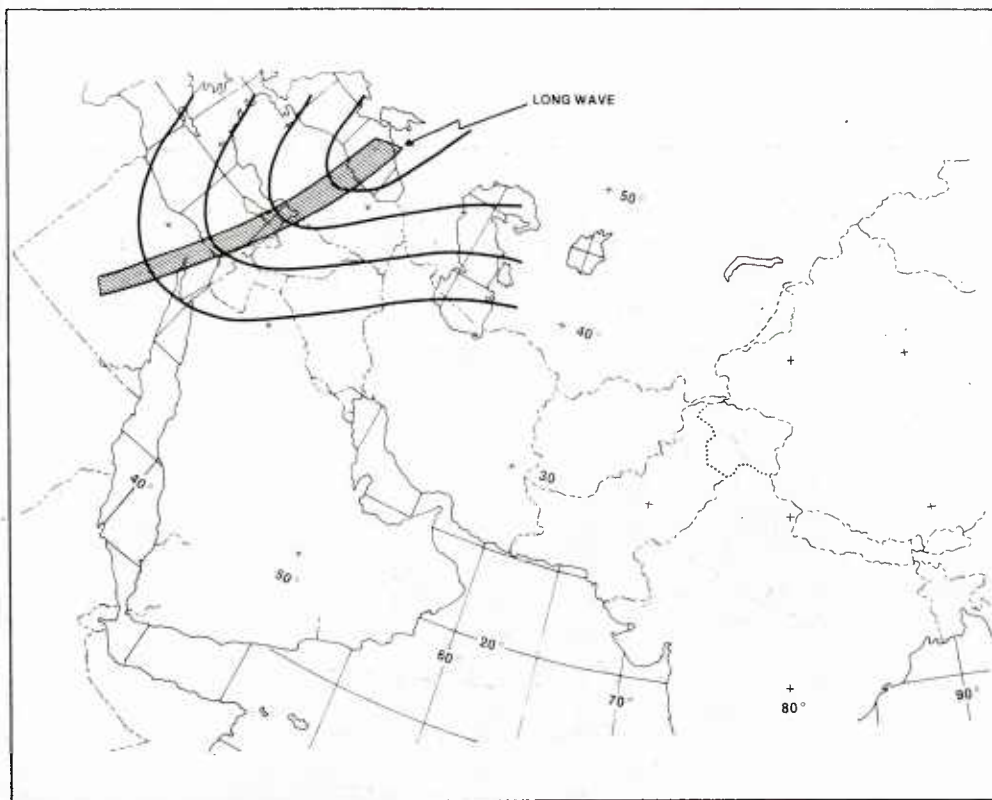


Figure 3-5a. Long wave position quasi-stationary near eastern Mediterranean coast: Long wave position initially in eastern Mediterranean near coast.

*A situation similar to this occurred in mid-January 1974, a few days prior to the onset of the shamal; see Appendix A, Figure A-1.

DUDLEY KNOX LIBRARY - RESEARCH REPORTS



5 6853 01078748 4

U189700